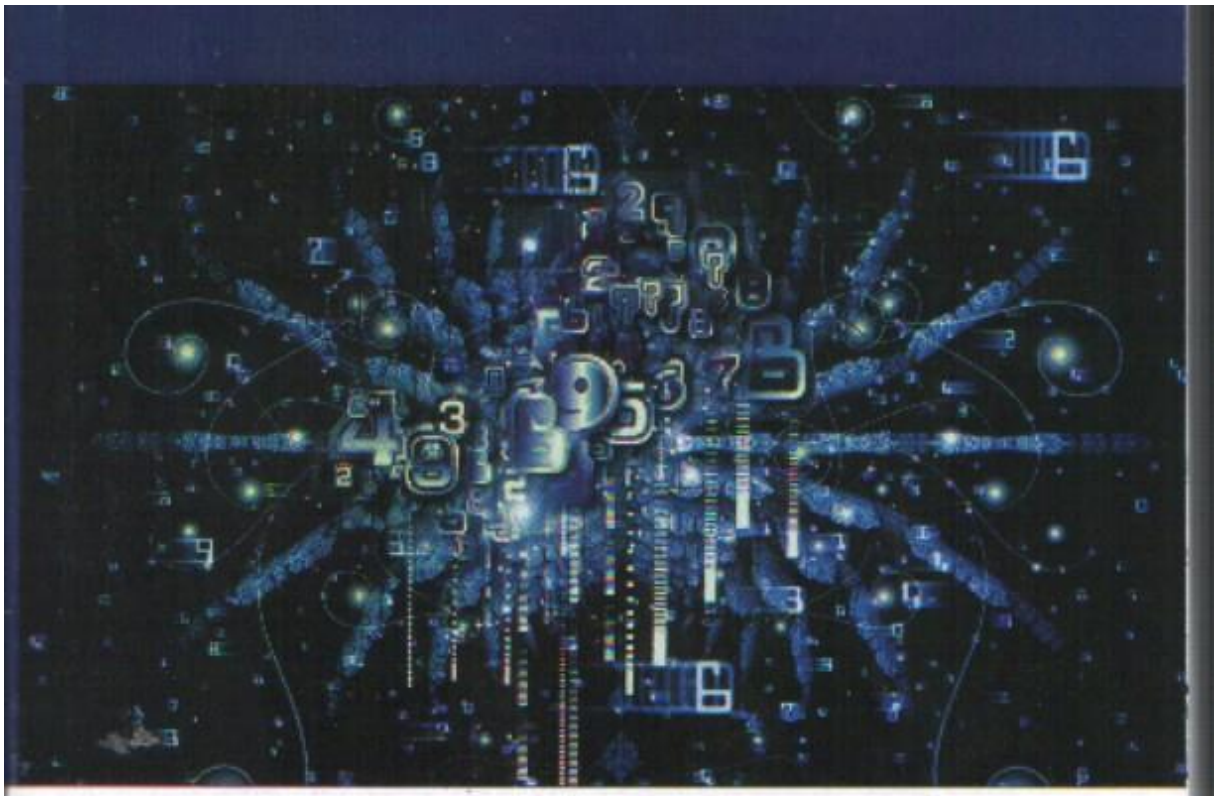

Vasiliy Zadorozhny
Sergey Fedosov
Alexandra Sergeeva

Polymer films and coatings deposited in vacuum

LAP LAMBERT Academic Publishing

V. G. Zadorozhny, S. N. Fedosov, A. E. Sergeeva

POLYMER FILMS AND COATINGS DEPOSITED BY USING ELECTRON AND ION TREATMENT

2019

The book contains information about modern achievements in the field of deposition of thin polymer films in a vacuum. The features of the effect of temperature, ultraviolet irradiation, electron flux, glow discharge on the process of thin polymer films formation are considered. Much attention is paid to the processes of evaporation and condensation of polymers in vacuum, as well as processes of structure formation, protective, dielectric and optical properties of the obtained films and coatings. The prospects for the use of thin polymer films in microelectronics, optics and precision engineering are discussed. The book can be useful to scientific and engineering staff, graduate students, students specializing in the physics and chemistry of polymers, thin-film technology and materials science.

CONTENT

FOREWORD

The purpose of this book is to summarize the results of research in the field of new technologies for producing thin polymer films and coatings in vacuum. This is due to the fact that at present microelectronics and optical mechanical engineering need new non-polar dielectrics for their application in capacitive elements of microwave circuits, electroacoustic transducers and optical elements.

It should be noted that a great number of new polymeric materials have been synthesized, which by their protective, dielectric and optical properties considerably exceed the traditional inorganic materials, such as silicon monoxide and dioxide, used in the above-mentioned branches of engineering.

Currently, various methods are proposed for deposition of polymer films in vacuum, such as polymerization of monomers on cooled substrates under action of the ultraviolet irradiation, an electron beam, and a glow discharge. All the above methods have one major drawback. In the obtained films, a non-polymerized monomer remains that leads to aging of the obtained films and coatings and to deterioration of their performance characteristics. In recent decades, new methods for producing thin polymer films have become actively used, such as sputtering of polymers in vacuum under the action of thermal, electron beam, ion beam, ion plasma, or laser sputtering.

The book reviews the current state of the polymer films and coatings deposition by using electron and ion treatment and summarizes results of the corresponding research carried out for a number of years at the Department of Physics and Materials Science of the Odessa National Academy of Food Technologies for the development of technology and study of the thin polymer films and coatings properties, mainly produced from polytetrafluoroethylene (PTFE), polychlortrifluoroethylene (PCTFE) and polyethylene (PE).

New technologies were developed during the recent years for producing thin polymer films from fluoropolymers under the action of thermal, electron-beam and gas-discharge sputtering of polymers in a vacuum. The result of these studies was the creation of new capacitive elements for microwave hybrid and planar circuits in radio electronics, electro-acoustic transducers based on electret polymer films (hearing aids, mini microphones), coatings to protect water-soluble crystals in optical quantum generators, polymer films for moisture protection of holograms used in the infrared range.

CHAPTER 1
METHODS OF MANUFACTURING AND PROPERTIES OF THIN POLYMER FILMS

The quality of films and coatings, as well as their fields of application in engineering, are determined by chemical, mechanical, electrophysical properties and stability of these properties. Polymer films and coatings in many cases have a number of advantages in comparison with films made from metal oxides and semiconductors, the deposition methods and properties of which were studied in sufficient detail [1,2].

In the present book we describe experimental and theoretical results on deposition of thin polymer films and coatings. The main polymers used for the deposition are: polytetrafluoroethylene (PTFE), polychlorotrifluoroethylene (PCTFE) and polyethylene (PE).

PTFE is a synthetic fluoropolymer of tetrafluoroethylene. PTFE is a high molecular weight compound consisting wholly of carbon and fluorine. Its chemical formula is $(C_2F_4)_n$. PTFE is hydrophobic: neither water nor water-containing substances wet PTFE. It has one of the lowest coefficients of friction of any solid.

PCTFE is a homopolymer of chlorotrifluoroethylene (CTFE). Chemical formula of PCTFE is $(C_2F_3Cl)_n$. The monomers of the PCFTE differs from that of PTFE structurally by having a chlorine atom replacing one of the fluorine atoms. This accounts for PCTFE to have less flexibility of chain and higher glass transition temperature. PTFE has a higher melting point and is more crystalline than PCTFE, but the latter is stronger and stiffer. Though PCTFE has excellent chemical resistance, it is still less than that of PTFE. PCTFE has lower viscosity, higher tensile strength and creep resistance than PTFE. PCTFE is injection-moldable and extrudable, whereas PTFE is not.

PE is the most common plastic. Many kinds of polyethylene are known, with most having the chemical formula $(C_2H_4)_n$. PE is usually a mixture of similar polymers of ethylene with various values of *n*. Polyethylene is a thermoplastic; however, it can become a thermoset plastic when modified (such as cross-linked polyethylene). It exists mostly in two modifications: high density polyethylene (HDPE) and low density polyethylene (LDPE).

The polymer chains of LDPE are highly branched compared to HDPE. The polymer chains in HDPE, on the other hand, are more linear. They pack closer

together, resulting in greater intermolecular forces and a more "crystalline" structure. HDPE has greater tensile strength than LDPE.

Some important properties of PCTFE, PTFE, HDPE and LDPE are presented in Table 1.1. The data have been taken from Goodfellow, one of the largest suppliers of materials for research and development.

Table 1.1

Comparison of some properties of PTFE, PCTFE, HDPE and LDPE [3]

	PTFE	**PCTFE**	**HDPE**	**LDPE**
Electrical Properties				
Dielectric constant (1 MHz)	2.0-2.1	2.24-2.8	2.3-2.4	2.2-2.35
Dielectric strength ($kV \cdot mm^{-1}$)	50-170	14	22	27
Dissipation factor (1 MHz)	$3\text{-}7 \cdot 10^{-4}$	0.01	$1\text{-}10 \cdot 10^{-4}$	$1\text{-}10 \cdot 10^{-4}$
Surface resistivity (Ω/sq)	10^{17}	10^{15}	10^{13}	10^{13}
Volume resistivity (Ω·cm)	$10^{18}\text{-}10^{19}$	10^{16}	$10^{15}\text{-}10^{18}$	$10^{15}\text{-}10^{18}$
Mechanical Properties				
Elongation at break (%)	400	80-250		400
Tensile modulus (GPa)	0.3-0.8	1.3-1.8	0.5-1.2	0.1-0.3
Tensile strength (MPa)	10-40	31-41	15-40	5-25
Physical Properties				
Density ($g \cdot cm^{-3}$)	2.2	2.12	0.95	0.92
Refractive index	1.38	1.435	1.54	1.51
Water absorption (%)	0.01	<0.01	<0.01	<0.015
Thermal Properties				
Coefficient of thermal expansion ($x10^{-6} \cdot K^{-1}$)	100-160	70	100-200	100-200
Lower working temperature (°C)	-260	-240		-60
Specific heat ($J \cdot K^{-1} \cdot kg^{-1}$)	1000	0.9	1900	≈2100
Thermal conductivity ($W \cdot m^{-1} \cdot K^{-1}$)	0.25	0.13	0.45-0.52	0.33
Upper working temperature (°C)	180-260	120-149	55-120	50-90

1.1 Evaporation of polymers

The first report on evaporation of PE is attributed to Madorsky [4] who pyrolysed a number of solid polymers at pressure of $1.33 \cdot 10^{-4}$ Pa within the temperature range 380-475 °C.

The pyrolysis was reported to lead to a wax-like deposit on a substrate, together with gaseous fractions and a solid residue. The evaporation of polymeric material is basically the evaporation of thermal degradation products. Considerable degradation occurs during evaporation of PE. Observation of the mass spectrum obtained from PTFE pyrolysed has shown a different pattern of degradation, but a thorough one nonetheless.

PTFE properties are derived mainly from the strong carbon-fluorine bond energy of 507 kJ/mol, compared with typical energies of 415 kJ/mol for C–H or 348 kJ/mol for C–C bonds. Slow decomposition of PTFE occurs above the application temperature of 260 °C. However, for a noticeable decomposition to occur, temperatures above 400°C are needed. The primary decomposition products are TFE and CF_2. Further products are formed by secondary reactions depending on temperature, reaction pressure and reaction atmosphere. The typical main products are TFE, HFP, cycle-perlluorobutane (c-C4Fs) and other fluorocarbons. The rate-determining step of the decomposition is the chain cleavage.

Decomposition involves the formation of free radicals due to random chain scission. Apart from the monomer and about 2.5% of C_3F_6, practically no other products were found during decomposition.

The substrate which receives a deposit during thermal evaporation of a polymer has a large number of degradation products incident on it, the properties of which are unlikely to have much similarity with those of the original polymer from which they came.

Post-deposition treatment and even treatment during deposition have been carried out in attempts to cause cross-linking between species arriving at the substrate, in order to produce a sort of polymeric material whose properties are as nearly as possible the same, or better, than those of the original material. White and Luff [5] have shown that ultraviolet irradiation of the substrate during and after deposition of PE caused cross-linking to occur, reduced crystallinity and improved the high temperature properties of the films.

Crystallinity of PE films can be improved by post-deposition annealing at the

temperature of 150 °C without previous irradiation. Infrared absorption spectra of both irradiated and annealed specimens have shown remarkable similarity to the spectrum of the original bulk polymer [6].

With the advent of the RF sputtering process, it became possible to produce thin films from insulators, including polymeric materials. Numerous articles and reviews on many aspects of the technique have appeared, including the excellent review by Jackson [7].

Unlike deposits produced by thermal evaporation, material released from a target by the RF sputtering process is subjected to a number of phenomena both during and after deposition has occurred.

For example, the time spent by the sputtered material within the RF glow discharge can cause it to be ionized and so alter the energy of impact at the substrate. At a chamber pressure of 0.13 Pa, at which the mean free path is of the order of 50 mm, sputtered material can travel from the target to the substrate without suffering energy loss, i.e. without undergoing collision with gas particles. At chamber pressure of 13 Pa, the passage of sputtered material to the substrate is essentially one of diffusion through the plasma. Loss of energy of the sputtered material leading to the increased possibility of being involved in collision reactions may modify it. So, the properties of the deposited film may be considerably different from those of the target material.

It appeared that sputtered material, leaving the target as neutral atoms, became ionized by the Penning ionization process. If an atom X is sputtered using argon ions, then it can also become ionized. In certain instances, the positive ion bombardment is sufficiently energetic to re-sputter material from the substrate.

The first report on RF sputtered PTFE appeared in 1967 [8] and was followed by a detailed description of the of sputtered PTFE films friction. The sputtering was initiated by the introduction of argon to the chamber, but as soon as the RF discharge became self-sustaining, the argon supply was cut off. Sputtering was then continued by means of C_2F_4 liberated from the target.

Decomposition products, in order of increasing concentration, consisted of CF_4, C_3F_8, C_3F_6, C_2F_6 and C_2F_4. C_2F_4 accounted for over 85% of the total decomposition products. The decomposition is described in terms of the formation of free-radical fragments which occurs by random cleavage of the polymer chain.

1.2 Radiation induced degradation of PTFE

Radiation induced degradation of PTFE was reviewed in detail in [9]. The radiation degradation of PTFE is characterized by a complex of parallel competitive and consecutive reactions. The high-energy radiation splits the C–C and C–F bonds stochastically. In an inert atmosphere (nitrogen or vacuum) double bonds are formed by the disproportionation of terminal radicals as well as by β-splitting of side radicals. Carbon radicals in fluoropolymers formed by radiolysis do not undergo disproportionation reactions because of the stability of the C–F bond. But, the thermal degradation of PTFE in inert atmosphere under autogenous pressure is known to result in a mixture of low-molecular perfluoroolefins and perfluoroparaffins. The scission of C–F bonds is unlikely in the thermal degradation because of the great difference in bond energy of C–F and C–C bonds. Therefore, the scission of C–C bonds is concluded to result in formation of unsaturated and saturated chain ends by disproportionation. Taking into account this fact, the disproportionation is assumed to be an important reaction also in the radiation-induced degradation of PTFE especially at higher temperatures under continuous irradiation [9]. A further indication of the scission of C–F bonds in secondary reactions is the fact that internal double bonds are formed in PTFE by irradiation in addition to terminal double bonds.

PTFE can be degraded by high-energy irradiation in the inert atmosphere to a mixture of low-molecular perfluoroolefins and perfluoroparaffins of different chain length without any residue. In irradiation process of PTFE in oxygen or in air, peroxy radicals are formed from side radicals that give acid fluoride groups under splitting of the C–C bonds, which can be easily hydrolyzed to carboxylic acid groups. The terminal radicals form carbonyl difluoride in the same way. The degradation of PTFE by high-energy irradiation with a high dose in presence of oxygen or air gives perfluorinated carboxylic acids, among other compounds. However, about 50% of the PTFE is converted into carbonyl difluoride [9].

High-energy electron beam or γ irradiation of virgin PTFE powders at relatively low doses (100–500 kGy) in the presence of air yield free-flowing PTFE micropowders with molecular weights significantly lower than in the case of normal PTFE [9].

It could be shown that the predominant process in radiation degradation of PTFE is the formation of COF, COOH and CF_3 end groups. The molar ratio of

CF_3 end groups to oxygen-containing groups (carbonyl end groups: COF and COOH groups) was found to depend on the irradiation dose and the irradiation conditions.

In the nineties of XX century, it was found that PTFE is cross-linked by high-energy irradiation in an oxygen-free atmosphere at approximately 340 ^oC, a temperature just above the melting point of PTFE.

An important difference in the spectra of specimens irradiated at room temperature and in molten state can be observed in the region of 1025-825 cm^{-1}. A new band appears at 985 cm^{-1} having a relatively high intensity compared with the other radiation-induced bands. The intensity of this band increases with increasing the dose. The concentration of CF_3 branches was found to be much higher during irradiation at elevated temperature than in case of the room temperature irradiation with the same dose [9]. The CF_3 and other branches are assumed to cause the reduced crystallinity indicated by the transparency of PTFE specimens irradiated in the molten state.

With increasing dose, the melting temperature and the crystallization temperature shift to lower temperatures [9]. The higher crystallinity is ascribed to lower molecular weight PTFE chains. It indicates that chain scission is the dominant process at the room temperature irradiation. On the other hand, the crystallization is assumed to be suppressed by $–CF_3$ side groups and branched structures upon irradiation at 385 ^oC.

Thus, it has been shown in [9] that the high-energy irradiation of PTFE with the high dose leads to complete degradation of the macromolecules to low-molecular compounds in presence of oxygen and subsequent hydrolysis to perfluorinated carboxylic acids, or in inert atmosphere to a mixture of perfluorinated olefins and paraffins. In the irradiation process in oxygen or air, peroxy radicals are formed from side radicals that give COF groups under splitting of C–C bonds which can be easily hydrolyzed to COOH groups. In inert atmosphere (nitrogen or vacuum), double bonds are formed by the disproportionation of terminal radicals, as well as by β-splitting of side-radicals. Virgin PTFE is disintegrated by the high-energy irradiation in air with a low dose into a micropowder modified with COF groups, which can subsequently be hydrolyzed to COOH groups.

The concentration of COOH groups increases and the molecular weight of PTFE decreases with increasing the irradiation dose. Homogeneous incorporation of the micropowder into other media or other polymers is possible,

making the special properties of PTFE, such as its particular release and lubricating properties and its chemical resistance effective in other materials. Irradiation of molten PTFE in inert atmosphere leads to the formation of internal and terminal double bonds as well as of CF_3 side groups. The concentration of all these groups increases with increasing irradiation dose. In the first step of the irradiation process, in addition to main-chain scission, the CF_3 side groups and long-chain branches are formed and in the second step after the formation of a sufficient quantity of side groups and branches, cross-links are formed.

1.3 RF plasma sputtering of PTFE

There is a short review on PTFE films prepared by plasma polymerization and by RF sputtering in [10]. Plasma polymerization is a popular technique for depositing certain polymer thin films. RF sputtering may also be employed for plasma polymerization with the principal difference being the introduction of fragmented polymer species (for the latter) rather than gaseous monomer species as found in the plasma. It is commercially desirable to replicate the bulk properties of certain polymer systems in the thin film form. The dielectric properties of PTFE films hold promise in electronic and electrical applications and for miniaturized device fabrication.

Comparison of PTFE films prepared by plasma polymerization and by RF sputtering has been carried out by Biederman *et al* [11]. Plasma polymerized TFE films were deposited with a continuous flow of CF_4 precursor and reacted in a microwave glow discharge [11]. RF sputtering of a PTFE target was carried out in pure Ar plasma. Alternatively, self-sustained glow discharge (SSGD) was initiated in Ar atmosphere, which was subsequently shut off and the plasma was sustained by fluorocarbon molecules.

Both methods resulted in film formation by the reaction of fragmented molecules of C_2F_4 in Ar, or fluorocarbon plasmas on their path to the substrate [11]. Optical examination revealed the transmission of sputtered PTFE-like films to be yellow, implying a fluorine deficiency, and plasma polymerized PTFE to be non-absorbing. In the infrared, both types of films appeared identical and sputtered PTFE absorbed UV and blue light. The refractive index was the same for both types of the films. Electron bombardment of the substrate during deposition aided in the polymerization process [11]. Biederman also reported that optical absorption properties are changed by altering the substrate bias, with

the bias deposited films being less absorbing to near UV radiation. Bias also resulted in a higher fluorine content in the sputtered films [11]. Electrical property measurements indicated that the sputtered PTFE and the bulk PTFE are similar, while sputtered PTFE and plasma polymerized PTFE are different [11].

Tibbit *et al*. also compared plasma polymerized PTFE and sputtered PTFE films [12]. They determined that 85 mol % of the decomposition products of PTFE in glow discharge were monomers of TFE, ensuring SSGD [12]. They inferred that ion, electron, and UV radiation processes occurred in the plasma promoted cross-linking and resputtering from the substrate [12]. Optical and electrical properties were found to be similar for both film types [12]. Travot *et al*. also examined fluorocarbon polymers prepared by sputtering [13]. The infrared absorption spectra were shown to be identical for the bulk foil and the sputtered PTFE films [13].

Marechel *et al*. carried out characterizations of RF sputtered PTFE films [14]. They prepared fluorocarbon films in Ar and Ar/C_3F_8 with continuous or self-sustained glow discharges. Mass spectroscopic analysis of the glow discharge revealed the presence of CF_4, C_2F_6, C_3F_8, C_3F_6, and C_2F_4 species, the latter is 85 mol% of the total glow discharge [14]. CF_4 added to the glow discharge resulted in only a slight increase in fluorine film content when mixed with Ar in the plasma. X-ray diffraction showed an amorphous structure for both plasma polymerized PTFE and sputtered PTFE films [14]. The F/C ratio was at a maximum value of 1.5 for films sputtered in pure Ar and decreased with increasing C_3F_8 content when added to the glow discharge. The F/C ratio increased with deposition at higher pressures. IR absorption spectra for bulk and sputtered PTFE were found to be identical [14].

Sujimoto *et al*. carried out RF sputtering of the PTFE target to form hard, lubricating and electrically conductive films [15].

Wydeven *et al*. studied the O(^3P) etching behavior in PTFE coating [16]. They carried out ion beam sputtering of PTFE and found F/C ratio of 1.7. They found that O(^3P) etched plasma polymerized PTFE film was more resistant than O(^3P) etched ion beam sputtered PTFE film. RF sputtered PTFE films exhibited more cross-linking than ion beam sputtered PTFE films, and were more similar to plasma polymerized PTFE films with respect to O(^3P) etching [16]. The F/C ratios decreased from 1.30 to 1.23 for plasma polymerized PTFE films after O(^3P) etching.

Ion beam sputtering of PTFE resulted in formation a film with combination

of bulk PTFE and plasma polymerized PTFE characteristics. ESCA analysis showed, for the C(1*s*) regions, no change for ion beam sputtered PTFE films after O(^3P) etching [16]. However, the O(1*s*) regions showed O_2 uptake. The F/C = 1.3 for plasma polymerized PTFE, whereas it was found to be equal to 1.73 for ion beam sputtered PTFE, and 2.0 for bulk PTFE after O(^3P) etching [16].

The following conclusions are made in [10]:

1. RF sputtered PTFE films possess similar attributes to bulk PTFE, and closely resemble plasma polymerized PTFE films. However, the film appears to damage readily under Ar bombardment being reduced predominantly to CF containing groupings.

2. RF sputtering of simple linear molecular chainlike polymers is a valid and viable method for producing thin films with properties closely resembling the parent polymer.

As mentioned in [17], the deposition of plasma polymers by means of RF sputtering of targets made of conventional polymers received considerable attention in the 1970s. The interest was particularly focused on PTFE. The motivation was apparently to prepare good dielectric films [18] and low friction coatings [19,20]. Optical applications were also considered [20].

Usually, PTFE was sputtered in argon. Also, the so called self-sputtering of PTFE was performed. In this case, argon was used only to initiate the discharge that continued in volatile fragments of PTFE when argon supply was shut off. Because sputtered PTFE films were found deficient in fluorine sputtering in a mixture of Ar and CF_4 was performed that increased the ratio F/C in prepared films [21].

At the beginning of the XXI century interest in RF sputtering of PTFE has been renewed as the obtained plasma polymer films are again in demand as protective, low friction and non-wettable coatings. Yamada *et al*. [22] sputtered PTFE films in Ar at $6.65 \cdot 10^{-1}$ Pa. At a constant power density 1.27 W/cm^2 the deposition rate for PTFE was $7 \cdot 10^{-2}$ μm/min. Sputtering targets were polymer sheets 50 μm thick bonded to copper backed plates. The tribological performance was examined. The friction coefficient was found to be about 0.3 and 0.2 for the film. Sputtered fluorocarbon films were worn away from the frictional tracks within a small number of passes. A very thin film was left on the track that served as a lubricant film. In the case of PTFE, polymer building groups were found: CF, C_2F_2, CF_3, C_2F_4.

Authors of [17] attempted to prepare fluorocarbon plasma polymers by means of RF (13.56 MHz) self-sputtering of PTFE targets (78 mm in diameter) [23]. A parallel plate electrode system with the magnetron facing down the substrate positioned 100 mm away from the substrate was applied. The pumping system consisted of diffusion and rotary pumps. First, conditions were determined for self-sputtering mode for the deposition apparatus in the case of balanced magnetron. When one gradually increases the power and relates to its each value the extinguishing pressure (i.e. pressure value at which the discharge switches off after the cut off of Ar supply), one can find for a given target size (geometrical configuration) and effective pumping speed in the deposition chamber, the threshold power for self-sputtering. In case of [17], it was 220 W and a deposition rate related to the power unit was 0.15 nm/min·W. During sputtering the deposition rate decreases (by 30% within 40 min) due to the build-up of an altered layer on the target surface enriched by carbon. F/C ratio in the erosion track is 0.7 while in the center of the target it is 1.3. The SEM micrographs of the cross-section of the films deposited at various substrate temperatures showed columnar structure at low temperature, while amorphous structure was apparent at high temperatures [24]. The morphology of the film changed from amorphous-continuous at higher positive temperatures, while below the room temperature a closely packed fibrillar structure appeared. Columnar structures are clearly apparent at negative temperatures. Based on the measurements, a hypothetical model of the fluorocarbon films was presented.

In the unbalanced magnetron deposition, it was found in [17] by Langmuir probe measurements that the floating substrate can be bombarded with positive ions which in the central region may have maximum energy 10-30 eV (radial distance from the axis of the magnetron up to 20 mm) while further from the axis (20-40 mm) the maximum energy is less (about 5-20 eV). Therefore, the deposition rate is very low or even negative (etching) in the central region than in longer radial distances. The C/F ratio as measured by ESCA is low (2) in the center; however, it is high (4) between 20-40 mm of the radial distance from the axis. The films deposited were rather hard and therefore may be called as hard plasma fluorocarbon polymers.

It was concluded in [17] that deposition of plasma polymers using RF sputtering of polymer targets is a promising process. Gaseous organic fragments as precursors for plasma polymerization process are emitted and fragmented from the conventional polymer target. No gaseous or liquid precursors are

needed. In the case of fluorocarbon films various applications were proposed. These included a low friction coating, protective and non-wettable films and barrier coatings. Optical properties of the films were considered, e.g. to use films as a quarter wavelength antireflective coating on glass. Electrical properties of the films were also investigated with the aim of using them as a dielectric film.

1.4 RF magnetron sputtering

A short review of preparing PTFE thin films on different substrates using gas phase processing techniques was presented in [25]. One of the impressive techniques for fluoropolymer thin films preparation is radio frequency (RF) plasma sputtering of a PTFE target.

Fluoropolymer films deposited using plasma sputtering system have shown many advantageous, such as high thermal stability, low dynamic friction coefficient, chemical inertness, low dielectric constant, bio-compatibility, and high hydrophobicity [26]. In order to control the deposition mechanism and the subsequent polymer structure and to increase the hydrophobicity of the surface, parameters including process pressure, flow rate, carrier gas type, power, treatment time, and reactor geometry have been studied mostly focused on flat sheet surfaces, such as silicon wafers [26]. For examples, Zhang *et al*. [26] studied the effect of sputtering gas using Ar, CF_4, H_2, N_2, and O_2 on the dielectric constant and chemical composition and molecular structure of the sputter-deposited polymer films from a PTFE target. The CF_4 plasma had the highest fluorine content while H_2 plasma gave rise to a polyethylene-like film with very low F content and the O_2 plasma gave no deposition on the surface. The dielectric constants of the deposited polymer film were increased in the following order by changing the type of the gas: CF_4\Ar\$N_2$\$H_2$.

Stelmashuk *et al*. [27] has found that the static contact angle and fluorine concentration of the deposited films by RF sputtering of PTFE are increased as the argon pressure augmented up to 70 Pa. Despite the fact that long substrate–target distances in combination with high deposition pressures (20–100 Pa) in RF sputtering lead to low deposition rates, Drabik *et al.* [28] found that at pressures higher than 40 Pa and for the target–substrate distance longer than 25 cm, fluorocarbon plasma polymers similar to the structure and chemical composition of conventional PTFE could be deposited.

Later, Kylian *et al*. [29] reported that under elevated pressure and longer target–substrate distances, the deposited fluorocarbon polymer by means of RF magnetron sputtering of PTFE target in argon is composed of longer fluorocarbon chains. In another study, Suzuki *et al*. [30] found that cross-linking in the deposited fluorocarbon films and correspondingly its adhesion strength to the Si substrate are enhanced by increasing the substrate temperature in the range of -5 to 200 °C.

The study in [29] deals with the treatment of hydrophilic-based PES membranes by PTFE plasma sputtering for applying in membrane distillation. The research aimed to understand the influences of RF power, gas pressure, and target–substrate distance on the properties of the plasma and deposited polymer.

PTFE sputtering in [25] was performed using the experimental set-up consisting of a cylindrical magnetron sputtering plasma reactor operated at a frequency of 13.56 MHz using a balanced magnetron cathode. The pumping system includes a turbo molecular pump and a mechanical pump for backing the turbo. The background pressure was about $7.9 \cdot 10^{-4}$ Pa, while the total working pressure was adjusted between 0.4 and 2.7 Pa. A PTFE disk was used as the sputtering target for deposition of all films in argon gas atmosphere. The RF power delivered by the generator was in the range of 15-100 W. The distance between substrate holder and the target was adjustable between 3 and 15 mm.

XPS spectra showed that the chemical structure of the films in [25] changed with the PTFE sputtering conditions. Considering obtained data the coatings prepared at higher pressures or target–substrate distances exhibited higher values of F/C ratio. In addition, a pronounced decrease in F/C was observed at higher powers. Lower F/C indicated that the coating consisted of highly crosslinked unsaturated structures. At constant pressure, increasing the power resulted in increase of the mean kinetic energy of the ions bombarding the target and thus increased the fragmentation of the polymeric target and consequently the kinetic energy of the fragments bombarding the substrate surface. Since the formation of unsaturated crosslinked components requires higher momentum transfer level supplied by the high-energy ions, the proportion of the crosslinked molecules will be increased by increasing the power. Increasing pressure or target–substrate distance tends to reduce the energy of the plasma ions. The latter will sputter fragments with higher molecular weights and would decrease the kinetic energy of the species bombarding the film which is growing on the substrate favoring for a mostly linear structure (high F/C, and CF_2 and CF_3

moieties) and less crosslinked deposited films [25].

Fluorocarbon polymer thin films were prepared in [31] by using a RF sputtering apparatus with the PTFE target. The RF sputtering apparatus was equipped with a magnetic field beneath the PTFE target. The PTFE target and substrates were equipped onto down and upper electrodes, respectively. The distance between the upper electrode and top surface of the PTFE target was 40 mm. Floating potentials of substrates in the RF sputtering without magnetic field and with weak, strong and unbalanced magnetic fields were -28, -44, -63 and -63 V, and ion current at the region I were 15, 48, 121 and 705 mA, respectively. Further, the ion current at the surface of the substrate in these magnetron sputtering systems slightly decreased with increase of distance from the middle of substrate.

Fluorocarbon polymer thin films were deposited in [31] with a PTFE target by three different types of RF magnetron sputtering systems with a strong, a weak and an unbalanced magnetic fields and RF sputtering. Friction coefficient of polymer thin film prepared by RF magnetron sputtering systems with weak magnetic field showed lowest, and that with strong magnetic field showed highest of all the thin films. Wear durability of polymer thin films prepared by RF magnetron sputtering systems with strong and unbalanced magnetic fields was higher than that prepared by RF magnetron sputtering system with weak magnetic field and RF sputtering. Both of the adhesion strength and shear stress of polymer thin films prepared with RF sputtering (without magnetron) were slightly higher than those prepared by magnetron sputtering systems.

The coatings were prepared in [28] by means of RF magnetron sputtering of PTFE target (diameter 81 mm, thickness 5 mm) using argon as a working gas (deposition pressure ranged from 5 Pa to 85 Pa). A water cooled magnetron operated at the frequency of 13.56 MHz and was mounted inside the cylindrical plasma reactor (0.05 m^3) from the top. All the thin films were prepared under constant power of 200 W, delivered to the magnetron and under constant Ar flow rate of 7 cm^3/s.

The RF magnetron sputtering of PTFE using balanced magnetron was utilized to prepare fluorocarbon plasma polymer films of different chemical compositions and surface roughness depending on deposition process parameters, especially on the Ar working gas pressure and the distance between the target and the substrate [28]. It was shown that, at Ar pressure higher than40 Pa, the chemical structure of the films change from highly disordered and rather

cross-linked fluorocarbon plasma polymer with C/F ratio of about 1.5 to more PTFE-resembling film with C/F ratio of about 1.9 when the target – substrate distance is increased from 14 cm to more than 20 cm. Even at this unusually large distance for RF sputtering from a 3-inch target, the deposition rate was relatively high: about 2 nm/min. It was shown that certain granular objects were developed in the film that provided sufficient roughness for super-hydrophobicity and slippery character of the films. This property was stable even after 12 months of storage in the open air.

Usually the researchers used the RF sputtering of PTFE in Ar or in an RF plasma composed of polymer fragments that is called 'self-sputtering'. In this case argon is introduced into the sputtering chamber to initiate the discharge. The argon is shut off after a time and the discharge continues in its own PTFE vapors.

Morrison and Robertson [18] used a grid instead of the anode. The substrates were placed behind it to prevent an excessive bombardment of the growing films as this bombardment was blamed for high dielectric losses of the resulting films.

Harrop and Harrop [19] and Biederman *et al*. [20] were interested in the static friction of the sputtered films on steel and glass. PTFE sputtered films were found to be deficient in fluorine (F). Sputtering in an Ar-CF_4 mixture [21] led to increasing of F content. Recently the interest in sputtering of PTFE was renewed as these sputtered films are promising for application as protective, low friction and non-wettable coatings. Sputtering of hydrocarbon polymers like PE is infrequent.

For the sputtering of films in [23], a parallel plate electrode system was used with an RF planar magnetron (78 mm in diameter) facing down with the substrate placed 100 mm from the magnetron. A balanced planar magnetron was used for sputtering PTFE A conventional pumping system, composed of diffusion and rotary pumps, was used. The absolute pressure was measured and argon was introduced through a needle valve. RF power (13.56 MHz) was delivered to the magnetron electrode via a match box from one terminal of the power supply, while the other was grounded as well as the stainless steel chamber of the sputtering system. The films deposited on Si substrates were studied by an electron scanning microscope.

Authors of [23] determined conditions for the self-sputtering. At a certain power, the Ar flow was gradually closed until the discharge switched off and the value of pressure was recorded. The threshold power for self-sputtering was

about 220 W for PTFE. Typical deposition rate was 0.15 nm/(min·W) for PTFE. The deposition rate increased with increasing power. The decrease of argon pressure from 10 Pa to 0.1 Pa was accompanied with increase of the deposition rate. During sputtering the deposition rate decreased due to appearance of an altered layer enriched by carbon. Within 40 min this decrease in the deposition rate was about 30%. An XPS analysis showed that the positive ion bombardment of the target, especially in the areas of the erosion track, increased the concentration of carbon. For the PTFE target the F/C ratio in the erosion track was 0.7 while in the centre of the target it was 1.3. The PTFE films seem to be amorphous with some features of densely packed 'fibres' perpendicular to the substrate.

The spectra of sputtered PTFE films differ from bulk (conventional) PTFE. The bands due to C–F and C–C stretching are observed in the spectral range between 1100 and 1300 cm^{-1} (doublet with maxima at 1152 and 1207 cm^{-1} for the bulk PTFE.

The main development described in [32] consists of combining magnetron sputtering with a Nd:YAG laser to provide additional properties to the deposited thin films. The combination of both of these techniques has been revealed as an innovative methodology by the complementary effects able to respond to all the technical requirements of the desired ultrathin film properties. Plasma sputter-deposited fluoropolymers have been deposited on PET substrates by this innovative Nd:YAG laser-assisted magnetron sputtering technique from a PTFE target.

Laser irradiation of the substrate, occurring directly in the deposition chamber simultaneous to the first step of the deposition process, exhibits the advantage of inducing a micropatterning of the polymer surface by a photoablation process and then affords a high control of the roughness and microstructure. Deposition parameters of the fluoropolymer thin film have been optimized to obtain the maximum F/C atomic ratio to optimally functionalize the structure with fluoro groups; the F/C ratio was evaluated by X-ray photoelectron spectroscopy.

Finally, the combination of the optimized sputtering parameters and the Nd:YAG laser treatment of the PET substrates led to superhydrophobic surfaces with a high water contact angle ($\theta = 160^{o}$). The films' morphology and topography were studied by scanning electron microscopy and atomic force microscopy, respectively.

Deposition of organic fluorocarbon thin films by radio frequency (RF) magnetron sputtering from a polymeric solid PTFE target on diversified substrates received considerable attention and has been extensively studied by Biederman *et al*. [23,33] and more recently by Zhang *et al*. [26]. Magnetron sputtering still represents the most promising way to obtain dense ultrathin organic films. The advantage of this pure physical process concerns its high-energy environment, which induces strong bond formation between the thin coating species and the polymeric substrate, leading to a high adherence and a perfect homogeneity of the organic coating.

Two basic approaches can be considered to increase the surface hydrophobicity: (i) the decrease of the surface energy by modifying the surface chemistry and (ii) the increase of the surface roughness, leading to the improvement of the effective surface area. The combination of both approaches can lead to superhydrophobicity properties [36-38].

All films in [32] have been processed in a custom-made high-vacuum reactor, equipped with an RF unbalanced planar magnetron. A dual flange has been especially developed to directly focus a pulsed Nd:YAG laser beam (266 nm and 10 Hz) on the sample polymer surface without affecting the deposition process. The angle of the laser flange can be adjusted to improve focusing accuracy. A 2.54 cm pristine PTFE (99%) disk (0.64 cm thick) was used as a target and backside-bonded to a conductive elastomer disk and fixed on the magnetron head.

Substrates have been fixed on a rotary sample holder with a substrate/target distance of 100 mm. The vacuum chamber was initially pumped down to a pressure below $1.33 \cdot 10^{-5}$ Pa. Sputtering gas was then introduced into the chamber to the working pressure by a leak valve at a constant flow rate.

Laser and magnetron devices have been switched on simultaneously, and the laser was stopped after 5 s and only sputtering of PTFE occurred. A top-hat beam shaper optic has been used to collimate the Gaussian incident beam. This shaper, associated with the optical pathway necessary to focus the laser beam in the deposition chamber, finally applied a 10 mm^2 uniform intensity well-defined spot on the PET substrate.

A significant advantage of such a method is due to the versatility of the laser treatment, which represents an interesting combination with the magnetron sputtering deposition technique and allows one to foresee a good potential with numerous other substrates.

1.5 Evaporation of PTFE by electron bombardment

In [39] the results of depositing PTFE by means of an electron gun are described. It is believed that the basic mechanism for the deposition of the films is analogous to those of some of the previously described techniques, i.e. depolymerization and evaporation of the bulk material by heating through bombardment with high energy electrons, and repolymerization of the gaseous products on the substrate through bombardment by stray electrons. The electrical properties of this deposited material have been investigated [39] and compared with those reported by other workers.

Before starting the evaporation, the vacuum system was pumped down to a pressure of about $7 \cdot 10^{-4}$ Pa with an oil diffusion pump [39]. The PTFE was placed on a water-cooled copper crucible between the two poles of a magnet. The tungsten filament of the electron gun, which was at a potential of -4 kV relative to the crucible, was heated, resulting in the emission of electrons. A cathode shield at the same potential as the filament prevented the electrons going straight to the anode and the magnetic field focused the electrons towards the crucible. Bombardment of the PTFE surface with 4 keV electrons caused melting of the polymer on the spot where the electrons were focused [39]. An electron current of about 5-10 mA resulted in the liberation of a large amount of gas so that the pressure rose to about 0.133 Pa. During the process a light blue to green glow discharge was observed on the anode and a polymer layer was formed on the substrate. The substrate was fixed in a metal holder at anode potential and at the distance of 30 cm from the evaporation source.

By hand regulation of the filament current, the deposition rate could be adjusted from a few Å per second up to 70 Å/sec [39]. At higher rates pressure runaway occurred because of the limited pumping power of the 1500 l/see oil diffusion pump. With the aid of a feedback system, the filament current could be regulated so that the evaporation rate stayed constant to within 10%. In some cases, however, high voltage sparks disturbed the automatic system and caused irregularities in the rate.

A metal mask with a thickness of 25 μm was placed between the evaporation source and the substrate at a distance of roughly 20 μm from the glass substrate. The deposited polymer films had no sharply defined edges. This indicates that no "straight-on evaporation" took place from the evaporation source to the substrate. It is important that the mask-substrate distance be kept small, for

otherwise definition of the edges would be even worse.

A number of workers have studied the thermal depolymerization of PTFE. All investigators found large amounts of the monomer C_2F_4 in the gaseous products of depolymerization both by resistive heating in a metal boat and by heating in a glow discharge. The gaseous products formed by ion bombardment in RF sputtering unit are also believed to consist for the major part of C_2F_4. In the technique used in [39], the PTFE bulk material was bombarded with electrons and so only a small area was heated to its melting temperature. No detectable amount of C_2F_4 was found by mass spectroscopy of the gaseous products during the evaporation. large peaks of CF, CF_2, CF_4 and C_2F_2 were found instead [39].

The polymerization of monomer gases has been studied by several workers. The polymerization occurs in a glow discharge or by high energy radiation or by electron bombardment of the substrate. The light gas discharge established on the anode is not believed to give a strong enough radiation to cause repolymerization on the substrate. It is believed instead that electron bombardment of the substrate is responsible for the repolymerization of the monomer gas. Electrons ejected by the filament are attracted by the substrate, which are at +4 kV relative to the filament.

Since the filament-substrate distance was about 30 cm, most of the electrons go straight to the substrate or the crystal without any collision and arrive there each with energy of 4 keV. This energy is certainly high enough for polymerization to occur because other workers have polymerized monomer gases by means of bombardment by electrons with energy of a few hundred electron volts. Examination of the deposited material has been carried out using double-beam infrared absorption spectroscopy [39].

The 400-1500 cm^{-1} spectrum had the same shape as the absorption spectrum of PTFE. Therefore, it was suggested that the polymer film deposited on the substrate consisted of chains having a very similar structure to PTFE. Comparison of both spectra led to identification of most of the peaks.

There were, however, some additional peaks assigned to C–F stretching vibration and CF_3 vibration respectively [39]. The C–F stretching vibration only appears if chain branching is present. The CF_3 are the chain end groups. The presence of them indicated that there were many chain ends meaning that the chain lengths were short or that many chain branching occurred. Electron bombardment of the substrate during the growth of the polymer film may be

responsible for the chain branching.

From the infrared absorption data it was concluded that the deposited film is similar to PTFE. The chains are probably shorter and chain branching occurs. The polymer was in an amorphous state.

Capacitors were formed with a PTFE deposited film as a dielectric [39]. The first examination of the capacitors was a check for short circuit. None of the measured samples showed electrical connection between the electrodes indicating that the thin polymer films were free of pinholes. The real and the imaginary parts of the admittance of the thin film capacitors were measured with a hand regulated double transformer bridge [39]. These results were converted into the permittivity ε and the loss factor $\tan\delta$. Measurements made a few minutes after the evaporation of the plastic gave loss factors of the order of 0.02. After one day this value had decreased to a few tenths of a percent. The capacitance also decreased during this time, by 5 to 10%. This was probably due to further polymerization of the freshly deposited plastic film, leading to decrease in the film disorder. After a further day's aging, the $\tan\delta$ and permittivity values remained constant.

The DC leakage current was very small and difficult to measure; 10 V DC applied to a dielectric of 550 Å caused a current of about 1 pA. The breakdown field strength was $2 \cdot 10^6$ V/cm.

The change of the capacitance as a function of temperature was measured [39]. Below the T_g temperature, the capacitor has a negative temperature coefficient of capacitance. As long as the temperature was below melting point T_m the capacitance change was reversible, but once the temperature rises above T_m the capacitance starts increasing rapidly in an irreversible way.

Thus, in [39] it was possible to evaporate PTFE using an electron-gun evaporation unit. The dielectric formed on the substrate was pinhole-free, free from mobile ions and has good dielectric behavior at both low and high frequencies. The permittivity varies from 2 up to 2.9 for samples evaporated at different rates. No correlation between the evaporation rate and the value of the permittivity has been found. $\tan\delta$ varied from 0.22 to 0.62%. From the localization of the absorption peaks in the infrared spectrum it was concluded that the evaporated fluorocarbon polymer had a structure similar to PTFE but the polymer chains were shorter and branched. The deposited plastic had an amorphous structure.

1.6. UV polymerization

White [40] was the first to apply the photolysis method for producing thin dielectric films used as a dielectric layer in film capacitors. As a result of irradiating a metal film with UV light in butadiene vapor, a thin polybutadiene film was formed on the substrate. It was shown that a significant role in the polymerization is played by the wavelength of ultraviolet light. At a wavelength of less than 0.26 μm, the reaction proceeds in the gas phase, and for polymerization on the surface of the substrate, radiation with wavelengths of 0.26-0.32 μm is necessary. Thus, for the implementation of surface polymerization only, it is necessary to filter out a part of the spectrum with a wavelength of less than 0.26 μm. The photon energy in this case reaches 4-5 eV. This energy is sufficient for the homolytic decomposition of the chemical bond and the creation of conditions for the polymerization process to proceed on the substrate by a free-radical mechanism. The radicals that cause the reaction arise either as a result of the primary act of molecules dissociation, or as a result of secondary processes. Molecules containing double bonds are most suitable for photolysis. They are polymerized by a free-radical mechanism, combining in a head-to-tail pattern with the formation of thin coatings.

It was found in [41] that with the pressure in the reaction chamber of the order of 500-1300 Pa, a wavelength of UV light of 0.2-0.4 μm and a substrate temperature of -196 °C, the growth rate of the films did not exceed several angstroms per minute and obeyed the following law:

$$v = A \cdot \exp \frac{\Delta E_a}{RT}, \tag{1.1}$$

where A is the pre-exponential factor; ΔE_a is the activation energy; R is the universal gas constant; T is the temperature.

In the general case, the photolysis process on the substrate surface can be divided into several stages:

1) Adsorption of molecules on a substrate at low temperatures;

2) Activation of molecules under the influence of UV irradiation;

3) The interaction of the active radical with the adsorbed molecule on the surface of the substrate leading to an increase in the length of the polymer chain, while maintaining the active center at the end of the chain, which is transmitted through it;

4) Interaction of two active sites leading to the formation of cross-linking.

The limiting stage of the polymerization process is the adsorption of the monomer on the substrate. The growth rate of the films decreases with time, apparently due to an increase in the absorption of light by the film. Photons with a relatively low energy do not lead to the destruction of films in the process of polymerization, so the films have the same properties as massive polymers.

The work [42] presents the results of studies of the dielectric properties of some polymers obtained by the method of polymerization under the action of UV irradiation. It is shown that if the monomer contains one functional group (usually a double bond), then the structure of the films obtained by UV irradiation is the same as that of the corresponding bulk polymers. It is noted that the use of a polyfunctional monomer leads to the formation of a three-dimensional structure as a result of the cross-links formation. Such films are highly stable at elevated temperatures. This method has not found wide application in technology due to low film growth rates.

1.7 Polymerization from the vapor phase under action of electron beam

As mentioned in [43], thin and ultrathin polymer films (TPF) on solid substrates are becoming more widely used in science and technology. The areas of their use include microelectronics (polymer resists in the manufacture of integrated circuits, dielectric, protective and other functional layers), sensor technologies, nonlinear optics, etc. A relatively new, very promising direction of TPF deposition is the polymerization of monomers directly on the surface of solid substrates. In recent years, there has been a sharp surge in research in this area, and many studies have used methods of controlled "living", including radical polymerization, initiated on the surface of a solid substrate, allowing to obtain polymer layers with a given molecular weight and polydispersity of macromolecules.

In [43], the processes of TPF deposition by the method of polymerization from the vapor phase under the action of an electron beam at an electron energy in a beam of 1-100 keV (E-VDP method) are considered.

Among the features of this method, the absence of organic solvents can be noted; the possibility of applying a polymer layer selectively (on those parts of the substrate surface that are exposed by the initiating beam); wide possibilities of automatic control of the parameters of the electron beam and, accordingly, the deposition rate, topology, and properties of the forming polymer layers.

Applied tasks, which can be efficiently solved by E-VDP processes, should be divided into two main areas [43]: applying solid polymer layers on substrates with desired properties and drawing lines (or points) on a given program to obtain an image of a lithographic mask or other functional layers, as well as images in information recording systems.

The main task is to identify technological advantages over traditional methods of applying PF, in particular solution ones. Using the E-VDP method, PF can be obtained from those polymers for which solution deposition methods are not applicable, for example, from PTFE [43]. At the same time, PF based on PTFE, which has a unique set of properties and, in particular, combines extremely low dielectric constant (ε = 1.9-2.0) with high chemical and heat resistance, are of considerable practical interest, for example, to obtain interlayer insulation in multilayer microelectronics products and in some other areas.

The application of TPF obtained by electron beam evaporation with VDP initiated by UV light was studied in a series of studies. TPF were obtained using UV initiation on the basis of a number of vinyl and diene monomers (acrylonitrile, styrene, MMA, tetrafluoroethylene (TFE), ethylene, butadiene, and others). The growth rate of the films usually did not exceed 10-50 nm/min. The film thickness was 100-1000 nm. It was found that for most systems, a decrease in the growth rate of films with increasing substrate temperature is characteristic, which is associated with the adsorption polymerization mechanism. At acceptable growth rates for most systems, a very strong heating of the substrates is also characteristic, reaching several hundred degrees. Accordingly, without special cooling of the substrates, the growth rate of the films was usually low. Thin (about 50 nm) continuous films with good insulating properties were obtained from mixtures of some vinyl and diene monomers. The dielectric constant of the films and the breakdown voltage were usually close to the values of these parameters for block polymers.

The disadvantage of the processes of obtaining VDP initiated by UV light, in addition to the above-mentioned strong heating of the substrates and the relatively low growth rate of the films, is also an extremely low absorption of light energy in the working polymerization zone. Even with the highest extinction coefficients of monomers (and polymers) of the order of 10^3-10^4 l/mol·cm and the thickness of the forming polymer layer 10^2-10^3 nm, the useful absorption of the incident light flux does not exceed a few hundredths of a percent.

The authors of [43] believe that the use of an electron beam for initiating VDP opens up new possibilities for the synthesis of a TPF, both in the form of continuous films and during the application of high-resolution images.

The TPF was obtained in [43] by conducting the process in a metal vacuum cell placed directly into the chamber of a scanning electron microscope. Electrons (with energy of 20 or 40 keV) were introduced into the cell through a thin (0.5 μm) polymer membrane with a size in the form of a diverging beam. The experimental conditions provided an effective charge drain from the surface of the plate on which a polymer film was applied. The plate was pumped out (in a vacuum of 10^{-2} Pa) and polymerization was carried out at room temperature.

Monomer vapors were introduced into the cell from a tank with a liquid monomer whose temperature was below room temperature. The vapor pressure of the monomer (133–$3.99 \cdot 10^3$ Pa) and the current in the electron beam (1–6 μA) remained constant during the experiment. The polymer layer on the plate was formed as a spot with a diameter of 4-5 or 8-10 mm, depending on the distance between the plate and the membrane. In the central part of the spot with a diameter of 2-3 mm, the density of the flux of incident radiation was maximal and was distributed fairly uniformly (in various experiments it was 0.5-10 W/cm^2). In the peripheral ring, the radiation flux density smoothly changed from the minimum at the edge of the spot to the maximum at the border with its central part. Such experimental conditions made it possible to obtain information on the nature of the polymerization and the structure of the polymer layer at different doses of radiation and, respectively, at different stages of the process of forming a polymer film in the same experiment [43].

At the end of irradiation, the plate with the polymer film formed on it was taken out of the cell and placed again in an electron microscope to study the film structure and determine its thickness. Plates of various materials were used as substrates.

Using the methods discussed above, TPF were obtained from various polymers, including PTFE with a thickness of 0.1-10 μm on various solid surfaces. In the overwhelming majority of experiments, applied TPF were solid, fairly uniform polymer films. During the deposition, vapor pressure was $9.3 \cdot 10^2$ Pa, current in the beam was 6 μA, electron energy 20 keV, film thickness 0.85 μm, average film growth rate was 6.7 nm/μA·min.

Deposition rate increases with increasing vapor pressure of the monomer and the electron flux density in the beam and weakly depends on the nature of the

substrate. It was found that the studied processes are characterized by the presence of an initial part of auto-acceleration [43].

It can be assumed that, under the studied conditions, polymerization is initiated mainly by radical centers and proceeds via an adsorption (sorption) mechanism. For the adsorption mechanism of polymerization, attachment to the growing active center of the monomer molecules previously adsorbed on the surface is observed on the surface. An alternative to the adsorption is the so-called percussion mechanism, when the monomer molecule joins the active center during a collision directly from the gas phase.

The predominantly radical nature of the active sites of polymerization is indicated by the inhibitory effect of oxygen, as well as the effective polymerization of TFE, which, as is known, is polymerized only by a radical mechanism.

It should be emphasized [43] that with increasing monomer vapor pressure over a certain limiting P_{vr}, a polymer that directly forms in the gas phase and settles to the surface in the form of spherical globules, the size of which varies from a few tenths of a micron to a few microns, makes a significant contribution to the formation of films on the surface. The values of P_{vr} are determined by a number of factors, in particular, the nature of the monomer, the height of the gas phase layer above the plate on which the polymer film is formed, the duration of polymerization, etc. and is usually $(2\text{-}4)\cdot10^3$ Pa.

For the PTFE films deposited by the E-VDP method, IR spectra were measured [43]. In the transmission spectra, a broad band is seen in the region of 1150–1350 cm^{-1} with a maximum of 1230–1250 cm^{-1}, corresponding to the stretching vibrations of C–F bonds in the CF_2 groups of the polymer, whose intensity increases with increasing polymerization time and a corresponding increase in the thickness of the polymer film.

In the IR spectra, a band of 980 cm^{-1} is also noticeable, which corresponds to the stretching vibrations of the C–F bonds in the CF_3 groups of the polymer [43]. In the PTFE samples with M = 10^6-10^7 amu, the 980 cm^{-1} band is usually not observed. Its presence in the IR spectra indicates a low molecular mass of the resulting polymer with CF_3 end groups. This conclusion is confirmed by independent experiments on training the resulting PTFE films at elevated temperatures in a vacuum. It turned out that already at 300 °C the polymer almost completely evaporates from the substrate.

The absence of bands characteristic of the amorphous polymer phase (778

cm^{-1}) in the IR spectra of PTFE films indicates a high degree of crystallinity of PTFE.

The value of the specific volume resistance of the films calculated from the current-voltage characteristics was ~ 10^{16} Ω·cm, which is close to the values of ρ for block PTFE (10^{16}-10^{17} Ω·cm).

Thus, in [43], a "dry" one-step method was proposed for applying thin polymer layers on substrates of various natures directly from the monomer. The chemical composition and properties of these layers are mainly determined by the choice of monomer. In this case, of course, one should take into account possible changes in the properties of the layers under the influence of the radiolysis to which they are subjected during the deposition process.

A PTFE layer as a continuous spot of ≈10 mm in diameter, whose thickness was maximal in its central part (≈700 nm) and gradually decreased to the periphery, was formed through the electron-beam vapor deposition polymerization of TFE on a silicon substrate [44]. The structure of the polymer layer obtained was studied using scanning-force microscopy, electron microscopy, IR spectroscopy, and other techniques. The average degree of polymerization of the polymer produced did not exceed a few tens. It was assumed that polymer chains are arranged primarily normal to the substrate surface forming disc- and ribbon-like mesomorphic entities with a minimal size of ≈15 nm. This value corresponds to the length of an oligomeric PTFE macromolecule with a degree of polymerization of ≈30. The original mesomorphic structure of the layer in question was metastable, as the formation of local crystalline regions takes place after several months' storage at room temperature [44].

The structure features and properties of TPL formed from TFE vapor at different electron beam current densities were found to be different strongly [45]. In 1-10 μA/cm^2 range, the low molecular mass PTFE films with tape and disk supramolecular structures formed. These films are low thermally stable (to 250-300 °C) because of sublimation under heating. Macromolecules in these films are regulated (mesomorphic state). The polymer chain axes are oriented perpendicularly toward substrate surface. In 10^2-10^3 μA/cm^2 field the films with high thermostability (400-450 °C) are formed. These films are probably crosslinked. In 10^4-10^6 μA/cm^2 field the amorphous, strongly crosslinked, high thermostable, high uniform films are formed. The observed differences of structure and properties of films deposited by E-VDP method are caused

probably by different balance of chain polymerization and polyrecombination mechanisms in the film deposition processes. In highest current density range the polyrecombination mechanism predominates. In low current density the main mechanism of deposition is the radical-chain polymerization. The results obtained show great possibilities of controlled change of properties of E-VDP films deposited from the same precursor [45].

As noted in [46], low-*k* dielectric thin films and technology of their deposition is highly necessary for the semiconductor industry for the next generation of microchips. PTFE is the best suitable material due to its excellent dielectric properties and stability. PTFE films can serve as dielectric, barrier and protective coatings in organic light emitting devices (OLED) and organic field effect transistors (OFET) [47]. The most promising use of PTFE is its application in the novel advanced research branch – plastic electronics on flexible polymer substrate. However, deposition of PTFE thin film is a difficult problem due to it is insolubility with any solvent. One way to deposit perfluoropolymer film is by plasma polymerization of various perfluoromonomers [48]. Films deposited by means of plasma polymerization are highly cross-linked and have no linear macrochains at all.

PTFE films have been deposited onto polycarbonate (PC) substrates from the products of PTFE evaporation, activated by a cloud of accelerated electrons [46]. A 40.68 MHz glow discharge was used during the deposition process. The use of the low power plasma during film growth led to the formation of PTFE films with modified structure. Films are amorphous and contain more cross-links, but in general, the structure of their macromolecules is still linear. An increase of RF power leads to the formation of films with large amount of double bonds and enhanced internal stresses [46].

Deposition of PTFE on PC without plasma treatment led to the formation of PTFE clusters up to 50 nm in diameter. The RMS roughness of the films, deposited without plasma, was about 4 nm, while the films deposited with plasma treatment had a roughness of 1.5 nm. The use of plasma has an additional effect if a PTFE coating is deposited on the PC substrate with submicrometer-sized steps. Without plasma the steps retain rectangular shape. Deposited with the RF-discharge the PTFE layers resemble plasma-polymerised films [46]. Under certain conditions the deposited films can fill trenches in the substrate like a wetting liquid, while under other conditions they avoid trenches and grow in between them.

Gritsenko proposed film deposition from the products of PTFE thermal evaporation, activated by a cloud of accelerated electrons [49,50]. Under this action, the composition of the destruction products was changed. The concentration of the CF_3 and C_3F_5 fragments correlates well with film deposition rate. So the suggestion was made, i.e., these fragments are responsible for the film growth [51]. Although the origin of the transformations is still not clear, this mechanism of PTFE deposit growth was later confirmed by Wijesundara and co-authors [52]. Further modification of PTFE film properties can be done by non-selfsustained RF discharge [46,50].

Films were deposited by evaporating bulk PTFE in vacuum and activating vapor using an electron cloud. Additional activation of both vapors and substrate surface was done using RF discharge. The discharge frequency of 40.68 MHz was chosen as it is suitable for PTFE vacuum deposition conditions. The higher the frequency, the higher electron concentration will be, and thus the lower their energy will be [51]. Such conditions are favorable for polymerization. The method was described in detail elsewhere [50]. This method allows tuning of the PTFE film structure. Bare DVD polycarbonate (PC) disc was used as a model of plastic micropatterned (period is 800 nm) surface. Gold films were deposited using a tantalum boat.

It was found [46] that plasma treatment does not significantly influence film growth rate, if substrate was placed between RF electrodes. Film grown between RF electrodes have a C1s main peak at 293.2 eV attributed to CF_2–CF_2 groups. Other peaks, related to end groups or cross-links, were present but at minor percentages. Oxygen was at less than 1%. The chemical composition of the surface of the films was like that of bulk PTFE. However, an increase of discharge power to 70 W led to the formation of classic plasma-polymerized deposit. When a substrate was placed onto the RF electrode, film growth rate decreased proportionately to RF power. The sputtering of growing film was already not small at 20 W. At 70 W no film growth was detected at all.

Therefore, at the same period, the thickness of the film deposited with RF plasma was thinner compared to the film deposited without plasma. For all three spectra bands located near the next wavelengths: 526, 555, 640, 729, 1151, and 1213 cm^{-1} were attributed to PTFE conformation [53]. The band near 980 cm^{-1} was assigned to $–CF_3$ groups, 1352 cm^{-1} to –CfC– groups. Increase of RF discharge power leads to 980 and 1352 cm^{-1} bands relative intensity growth and therefore, increase of concentration of $–CF_3$ and –CfC– groups. The relative

intensities of the 555, 625, 777 and 1150 cm^{-1} bands decreased. On the other hand, relative intensities of the 530, 703, 737, 738 and 1260 cm^{-1} bands increased. The content of the crystal phase decreased, while the content of the amorphous phase increased. The quantity of $–CF_2–$ groups decreased.

The film deposited without plasma contains some quantity of the crystal phase, while films deposited with plasma are completely amorphous. The next conclusions have to be made for additional activation by RF discharge: 1) films deposited with RF plasma on electrode have the structure like that of plasma-polymerized films; 2) films deposited with low RF power between electrodes have a mainly linear structure close to that of bulk PTFE with minimal concentration of double bonds and branches.

Authors of [46] found that vapor treatment with low power RF discharge allows for deposition of smooth PTFE film on plastic substrate. Film grown on Au surface was smooth. Its surface roughness was about 2 nm. Deposition of PTFE on PC surface without plasma treatment led to formation of large flat clusters up to 50 nm in diameter and film average roughness was more than 4 nm, while film deposited with plasma treatment had an average roughness of 1.5 nm.

It appeared that RF plasma deposited films (between electrodes) is more hard and rigid. This is the confirmation of the cross-linked film structure as compared with structure of the film, deposited without plasma. The smooth PTFE film can be formed on bare DVD steps only with plasma discharge. At some plasma conditions, polymer film fills trench like wetting liquid, while without plasma it grows in the middle of the trench, repelled from the walls. The obtained results [46] show the promising direction for obtaining the dielectric and protective coatings on the micro-patterned plastic substrate. In general, the PTFE film grown with low power RF plasma shows the covering ability on micro-relief plastic substrate like the covering ability of the PPX-N coating.

Thus, it was shown in [46] that variations in power of RF plasma during PTFE evaporation in vacuum allow for obtaining films with structures ranging from classic plasma deposits to one like bulk PTFE. The properties of covered film surface strongly influence relief of the PTFE. Variations in deposition conditions lead to tuning of the mechanism of coverage of sub-micrometer-sized steps on plastic surface. The PTFE coating can be close to conformal, wetting or anti-wetting. The developed method can be used for the technology of OLED, OFET and other organic functional multi-layered systems.

Despite a large number of studies on the production of thin polymer films under the action of an electron beam, there is still no consensus on the mechanism of their formation. Most authors believe that the main role in the formation of thin polymer films is played by processes occurring on the surface of the cooled substrate. This is obvious, since the polymerization under the action of the electron beam occurs at pressures of 10^{-2}-10^{-4} Pa. In this case, the probability of electron collision with monomer molecules in the gas phase is very small. Molecules on the substrate are activated by the interaction of electrons with monomer molecules. Film growth occurs due to the subsequent interaction of two activated molecules of the initial substance (initial period), or an activated center on the surface of the formed polymer and the activated monomer molecule. In contrast to photolysis, the electron energy is sufficiently large to ionize the monomer molecules. Therefore, polymerization of any organic monomer is possible provided it is adsorbed onto a cooled substrate.

The main question, to which researchers still do not have a single answer, is the question of what is the mechanism of polymerization: either ionic, or radical. Christie [42] developed a phenomenological theory of the formation of polymer films and obtained a formula for the growth rate of films, which in the unsteady case has the form

$$v = \frac{\sigma \cdot P}{1 + \dfrac{1}{j \cdot \tau \cdot Q}} \left\{ 1 - k \cdot \exp\left[-\left(Q \cdot \tau \cdot j + \frac{t}{\tau} \right) \right] \right\}, \qquad (1.2)$$

where Q is the cross section of polymerization, σ is the surface density of adsorbed molecules (the number of molecules per unit of surface area and per unit of time), j is the current density of electrons (the number of electrons per unit of surface area and per unit of time), P is the average volume of one molecule, τ is the lifetime of the adsorbed molecule on the surface, t is the polymerization time, k is a constant.

To clarify the mechanism of polymerization under the action of an electron beam, it is of interest to study the formation of films from vacuum oil and acetylene at low electron energies (0-20 eV). It has been established that the cross section and rate of polymerization substantially depend on the electron energy, and this dependence is non-linear. It was also shown that electrons with energies below 2.5 eV do not cause polymerization on the substrate, and with increase in the electron energy above 2.5 eV, increase in the polymerization cross section (Q) is observed, and at 3 eV it reaches the first maximum value of

$3.1 \cdot 10^{-16}$ cm^2. At an electron energy of the order of 10.0-10.5 eV, the second maximum of the polymerization cross section appears equal to $8 \cdot 10^{-16}$ cm^2. In addition, if the electron energy increases to 11 eV, a negative charge monotonously increases on the film surface. The charge on the surface decreases with a further increase in the electron energy. The maximum with a threshold of 2.5 eV in the energy dependence of the film growth rate is associated with the decay of a molecule that is in a vibrationally excited state, into which the molecule passes when the electron is captured. The resulting radicals initiate polymerization according to this scheme:

$$P + e^- \rightarrow P^- \rightarrow P^*_{osc} + e^-, \tag{1.3}$$

$$P^*_{osc} \rightarrow R' + R'', \tag{1.4}$$

where P is a polymer molecule, P^- is a polymer with a negative charge localized on the surface of a carbon atom, e^- is an electron, P^*_{osc} is a polymer molecule in a vibrationally excited state, R' and R'' are free radicals.

The origin of the second maximum is explained by the resonant formation of radicals and ions during dissociation and reducing interaction of molecules that are in new excited states. In addition, at these energies, direct non-resonant ionization of molecules by electrons begins, which also causes ionic polymerization.

$$\begin{aligned} &P + e^- \rightarrow p^* + e^- \\ &p^* \rightarrow R' + R'' \end{aligned}, \tag{1.5}$$

$$\begin{aligned} &P + e^- \rightarrow p^* + e^- \rightarrow P^+ + 2e^- \\ &P + e^- \rightarrow P^+ + 2e^- \end{aligned}, \tag{1.6}$$

P^* is a polymer molecule in the excited state, P^+ is a polymer molecule with a positive charge localized on the surface carbon atom.

1.8. Glow Discharge polymerization

Polymerization in a glow discharge occurs much faster than in case of the electron irradiation in high vacuum. This is due to the high density of the glow discharge current and the high pressure in the reaction chamber.

Goodman [54] believes that the growth of films consists of two processes: polymerization and destruction. Polymerization occurs due to ionized particles that lose their charge and stick to the surface, while falling on it. However, such

a model cannot explain the temperature dependence of the growth rate. Therefore, it was not adopted to explain polymerization processes in the glow discharge, although the processes of ion capture and sputtering (destruction) can play a certain role.

Denaro [55] believes that radicals on the surface can be formed due to the dissociation of molecules excited by collisions with electrons or by dissociation of excited molecules that have arisen during the recombination of ions with electrons. The radicals formed on the surface initiate the polymerization according to the radical type. Having considered theoretically the polymerization process, the author [55] obtained the dependence of the growth rate on pressure and energy of the glowing charge in the following form:

$$v = k'''W^n \frac{p}{p + 2A}, \tag{1.7}$$

where v is the growth rate, W is the specific power of the discharge (W/cm^2); p is pressure (Pa); n, k''', A are constants.

The obtained experimental data are in good agreement with the theoretical data that, in author's opinion, confirms the mechanism proposed by him. In this paper was proposed the following chain of chemical reactions:

I. $\dot{R}_n + M \xrightarrow{k_1} \dot{R}_{n+1}$ is the chain growth reaction; M is an adsorbed molecule; R is a radical.

II. $\dot{R}_n + \dot{R}_m \xrightarrow{k_2} P_{m+n}$ is the reaction of disproportionation or recombination of radicals.

III. $\dot{R}_n \rightarrow \dot{R}'_n$ is the reaction of radical capture on traps in the film.

During polymerization by the glow discharge with a frequency in the MHz range, the ions do not reach the surface of the electrodes and do not participate in the polymerization process. Therefore, it is assumed that the formation of radicals in the film occurs due to the bombardment of the latter by electrons:

$$p^+ + e^- \rightarrow P^* \rightarrow 2R. \tag{1.8}$$

In this case, the growth rate of the films is described by the following expression:

$$v = \frac{p(k'W^2 + k''W)}{p + A + \sqrt{A^2 + B(k'W^2 + k''W)}}, \tag{1.9}$$

where p is the pressure in the gas phase (Pa); W is the discharge power density (W/cm^2), k', k'', A, B are constants.

When comparing the experimental data with the theoretical ones it was concluded that one radical was formed in the glow discharge on the substrate surface for every 20 polymer molecules that agrees well with the experimental data on measuring of the free radicals concentration in the films.

The authors of [55] investigated the polymerization of more than 50 monomers based on hydrocarbons. In all cases, thin films were formed on the cathode, the anode, as well as on the walls of the reaction chamber.

Da Silva [56] showed when studying the polymerization of butadiene and vinyl chloride that with a gas pressure of 100 Pa, a glow discharge current of 70-90 mA and a voltage of the discharge burning of 100-150 V, the deposition rate was 0.2 $\mu m \cdot min^{-1}$ for butadiene and 0.18 μm/min for vinyl chloride.

Many authors, for example, in [57], report on the use of microwave discharge for polymerization of various organic monomers. The main direction of work in this area is to increase the stability of films, because they are quickly aged meaning that the characteristics of the devices in which such films are used are not stable.

The authors of [58] investigated the magnetic properties of thin (up to 10 μm) polymer films synthesized from 1-amino-9,10-anthraquinone (*AAQ*) in a DC glow discharge. The films obtained at the cathode had a specific conductivity of $\sigma = (10^{-2}\text{-}10^{-3})$ $1/(\Omega \cdot m)$ in the direction perpendicular to the film plane, which is unusually high for samples obtained in plasma.

In contrast to the monomer, the polymer film obtained by the polymerization of *AAQ* at the cathode, considering its magnetic properties, was a diamagnetic with a noticeable contribution of the ferromagnetic state. The total mass of the polymer film sample in these experiments was several milligrams.

For ferromagnetism of the polymer, the saturation field of ~ 80-160 kA/m is characteristic. Paramagnetic properties are associated with the presence of free radicals that always present in polymer films synthesized in plasma [59].

According to the electrical properties of the film synthesized in plasma from *AAQ*, they are anisotropic [58]. It was found that along with the anisotropy of the electrical properties there is a non-uniformity of the magnetic properties of the films. The high sensitivity of the measuring instruments made it possible to reduce the mass of the studied films by an order of magnitude (up to several

tenths of mg) and then in different film samples, along with ferromagnetism, areas with a predominance of diamagnetic properties were found.

The observed nonlinearities of magnetic curves in fields <80 kA/m are very stable. They persist after exposure to large magnetic fields up to 480 kA/m and do not collapse, if the direction of the magnetic field changes to the opposite.

Thus, in the films obtained by the method of polymerization in a DC discharge at the cathode, along with the high electrical conductivity, unusual magnetic properties were detected. In the samples, a significant contribution of the ferromagnetic state was observed, as well as inhomogeneity of the magnetic properties of the film was found. a sharp deviation of the magnetic curves from linearity was found in fields less than 80 kA/m in samples with mass of several tenths of a milligram.

The authors of [58] investigated the plasma polymerization of 1-amino-9,10-anthraquinone (*AAQ*). They suggested that a polyaniline-type polymer containing functional groups in the side chain could be obtained from this compound.

Films produced at the cathode and anode differed significantly in their electrical properties. For the film on the anode, the conductivity value was ~ 10^{-14} 1/(Ω·m) at 20 °C, typical for dielectrics synthesized in plasma [60,61]. The film deposited on the cathode had $\sigma = 10^{-3}$-10^{-2} 1/(Ω·m), i.e. 11-12 orders of magnitude higher, and this value was maintained after heating to 300 °C.

While measuring the conductivity of films of different thickness deposited on the cathode, it was found that in the range of 1-9 μm the electrical resistance was almost independent of the film thickness. This is due to the fact that the main part of the sample resistance falls on a thin surface layer. The surface conductivity of the film deposited on the cathode turned out to be $3.7 \cdot 10^{-14}$ 1/(Ω·m), i.e. typical for dielectrics. The results obtained suggest a pronounced anisotropy of the electrical properties of the film deposited on the cathode.

Since the polymer deposited on the cathode has semiconducting properties, it can be assumed that it contains poly-conjugated chains. One can imagine two mechanisms for the formation of a poly-conjugated chain from *AAQ*: the first is the poly-condensation of amino groups with carbonyl groups of *AAQ*, the second is oxidative polycondensation involving amino groups, i.e. a process similar to the electrochemical polymerization of aniline [62]. If the formation of *PPAAQ* occurred by the first mechanism, the content of oxygen atoms in the polymer should decrease that was not confirmed by the measured data.

Therefore, it is more likely that the second mechanism is valid in which poly-conjugated chains are formed by attaching a radical cation to the carbon atom of the aromatic ring at position 4.

Thus, polymer films with semiconducting properties were obtained from 1-amino-9,10-anthraquinone in a DC discharge at the cathode, apparently due to the presence of a conjugated cyclic structure in them.

It is known [63] that polymers synthesized by plasma polymerization of organic compounds of various classes are, as a rule, good dielectrics with electrical conductivity of $\sigma = 10^{-10}$ 10^{-14} 1/(Ω·m). High dielectric characteristics of such films, as well as features of the method, which makes it possible to obtain polymers in the form of thin films and coatings without the use of solvents, determined their use in microelectronics in the 70-80 s of the last century. It was also shown that by polymerization of thiophene and its derivatives, 2-vinyl thiophene and α-difluoro-chlorovinyl thiophene in a 1 kHz plasma, it is possible to synthesize polymers with semiconducting properties ($\sigma = 10^{-8}$ 1/(Ω·m)) [62] .

Interest in the production of polymer films in plasma from such compounds as aniline, pyrrole, pyridine, thiophene, the chemical and electrochemical polymerization of which leads to the formation of poly-conjugated polymers, appeared in the early 90s, when such polymers from aniline, pyrrole and their derivatives started to be widely used in practice. The polymers thus synthesized, for example, polyaniline (PA), were doped in various ways (using iodine, HCl, sulfonic acids, etc.), converted to the oxidized salt form. As a result, the electrical conductivity of the PA significantly increased and ranged from 10^{-5} to 10 1/(Ω·m).

An example of electrochemical synthesis is the preparation of polypyrrole in an aqueous electrolyte solution (p-toluenesulfonate and Na sulfate) [64]. The process was carried out at 20 °C in a three-chamber electrochemical cell. Films with a thickness of 1000 μm had conductivity up to 10^3 1/(Ω·m). In some cases, electrochemical synthesis was carried out in organic solvents, for example, in acetonitrile.

However, both of these methods have significant drawbacks: they are used to synthesize powdered polymer, which must be separated from the solution, cleaned, and then obtained by spin-coating. By electrochemical method film of the polymer can be obtained directly on the electrode, which in turn imposes appropriate restrictions.

Most of the research on the production of semiconducting polymers in plasma was carried out in a high-frequency discharge. Aniline, pyrrole and their derivatives, thiophene, 3-methylthiophene, and 1-benzothiophene were used as starting materials. Polymers were obtained on substrates of various natures in the form of thin films up to 10 μm thick. Using electron microscopy, it was shown that films synthesized in plasma from aniline had a smooth homogeneous surface, whereas on the surface of similar films obtained by the electrochemical method, the inclusion of powder particles was observed [65].

Using chemical analysis, it was found that the polymer obtained in plasma substantially retained the original cyclic and heterocyclic structures [65,66]. In some cases, there was a partial disclosure, transformation into aliphatic structures and oxidation. Studies using IR spectroscopy confirmed this data [65,66]. Comparison of the composition and structure of films synthesized in plasma and films obtained by electrochemical means showed that they differ only slightly. It should be noted that during the electrochemical polymerization only oligomers are formed (n = 3-7), whereas during the plasma method, polymers with a high degree of conjugation in the polymer chain are formed.

Polyaniline (*PA*) films obtained by polymerization in plasma are thermally stable to ~ 200 °C, and their conductivity does not decrease after heating. In contrast, heating of PA synthesized chemically in air to 180 °C led to decrease in conductivity 3-5 orders of magnitude [67].

The films synthesized in plasma had semiconducting properties, and their electrical conductivity was 10^{-1}-10^{-3} 1/(Ω·m) [64-68]. Doping of such films with iodine and *HC1*, as well as change in humidity, led to increase in conductivity up to 10^{-2}-10^{3} 1/(Ω·m).

Semiconducting films based on 1-amino-9,10-anthraquinone were obtained in a DC discharge [69]. Polymer films of black color with a metallic luster with a thickness of 1-9 μ, insoluble in basic organic solvents, acids and alkalis, were deposited on the cathode. The conductivity of the film had a pronounced anisotropy. Surface conductivity was $3.7 \cdot 10^{-14}$ 1/Ω, which corresponded to the conductivity of the dielectric. The volume conductivity was 10^{-3}-10^{-2} 1/(Ω·m), as in semiconductors. The films were also characterized by a high thermal stability of electrical conductivity up to 300 °C. The content of C, N and O did not differ much from the original substance. Doping of such films with iodine increased their conductivity up to 1-0.1 1/(Ω·m).

In the DC discharge at the cathode, semiconducting polymer films were obtained based on 3-methoxythiophene [70]. Using IR spectroscopy, it was shown that thiophenic cycles are the main structural units in the polymer. It was established that the polymer based on 3-methoxythiophene has its own p-type conductivity with the activation energy of 0.045 eV. The polymer's electrical conductivity at 20 °C was 10^{-6} $\Omega^{-1}\cdot m^{-1}$, and doping with iodine led to its increase to 0.1 1/(Ω·m).

A distinctive feature of the poly-conjugated structures synthesis in the DC discharge was that in all cases the conductive film grown only on the cathode. The discharge was maintained during the film thickness growing on the electrode up to 10 μm. Apparently, the growth of the polymer chain was carried out through the formation of a cation-radical and its selective attachment to the chain in positions with high electron density.

Of great interest is the practical use of polymer semiconductors. Some of them, for example, polyaniline (PA), are produced by the industry in large volumes, since, compared with inorganic semiconductors, they are much cheaper, and are used in various electronic and optoelectronic devices as semiconducting, transport, electroluminescent and photovoltaic cells. The deposition of a poly-conjugated polymer by the method of polymerization in plasma allows obtaining thin semiconducting layers with a thickness from 0.001 to 1 μm using a relatively simple technology. In the future, the method can be used to form micron and nanoscale semiconducting structures, which are currently obtained by using complex and expensive technologies for plasma chemical deposition, etching and doping. The high thermal stability of n – Si – p structures obtained on the basis of polymer semiconductors synthesized in plasma (Fig. 1.1) will make it possible to create electron microstructures with higher nominal powers and to reduce the demands on the rate of heat removal from conducting nanoscale channels.

Interesting from a practical point of view is the conductivity anisotropy of a polymer synthesized in plasma from 1-amino-9,10-anthraquinone [69].

The polymer had conductive properties in the direction perpendicular to the surface of the film, and dielectric properties in the direction parallel to the surface. This was probably due to the fact that the semiconducting film consisted of macromolecules whose chains were oriented perpendicular to its surface. As a result, high conductivity along the chain of poly-conjugation and low conductivity in the orthogonal direction were observed. The movement of

charges can be accomplished only by jumping onto neighboring macromolecules. The resulting anisotropy allows the use of such films as a thermally stable structure to create high-resolution sensor arrays, nanoscale structures with isolated p-n junctions and logic elements based on them consisting of controlled molecular channels with electron or hole conductivity.

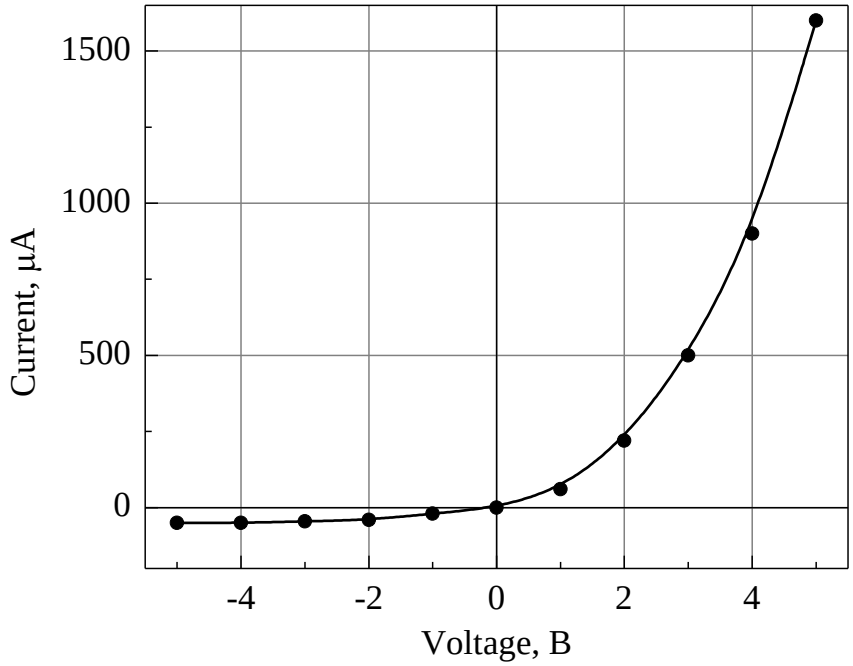

Fig. 1.1. Volt-ampere characteristic of the *p-n* transistor in the *n-Si/p-polymer* structure synthesized from anthracene in plasma at 20 °C

At present, polymer semiconductors are used in practice in gas sensors as materials whose conductivity is highly dependent on the atomic and molecular composition of the external medium. Synthesis in plasma of new thin semiconducting polymer layers and nanostructures with high conductivity anisotropy will allow the development of a new class of position-sensitive sensor devices.

Another promising direction in the use of thin polymer films obtained in plasma can be the manufacture of luminescent and electroluminescent, as well as photosensitive transport layers from 10 to 1000 nm thick, used in optoelectronic devices designed to transmit, receive and display information. The use of plasma-chemical technology will make it possible to obtain not only uniform functional polymer layers, but also to form complex micron and nanoscale optoelectronic structures having a specific set of electrical, optical, and electro-optical properties.

1.9. Production of films and coatings by decomposition and condensation of polymers in vacuum

The need for microelectronics in thin films and coatings has led to a significant number of studies on the preparation and investigation of properties of thin dielectric films based on metal oxides and semiconductors like silicon monoxide [69]. However, many authors note that in these films large internal stresses arise, which lead to their cracking.

In order to find a suitable material for the manufacture of thin films, in which there would be no internal stresses, experiments have been carried out in recent decades on the evaporation of solid polymers in a vacuum.

Heating of polymers in vacuum accompanied by evaporation of volatile products is not a surface phenomenon, as in the case of inorganic substances evaporation. In this case, evaporation is due to the formation of molecules capable of evaporation and molecular fragments in the entire volume of the polymer sample. Decomposition and evaporation of 25-50 mg of polystyrene in vacuum at a pressure of 0.001 Pa at a temperature of 375 °C takes about 30 minutes, and for evaporation of the same amount of non-polymeric material by ordinary evaporation at the same temperature it will take a fraction of a second.

The nature of the decomposition of various polymers is different. The decomposition products in vacuum are monomers, dimers, trimers and longer fragments of macromolecules. In polystyrene in the first stage of destruction, which corresponds to 5-10 % of mass loss, there is a rapid decrease in the average molecular weight; then the process slows dramatically. The rapid initial decrease in average molecular weight is partly due to the thermal breaks of weak bonds in the polymer chain. One of the reasons leading to the formation of such bonds is impurities, especially oxygen. With further destruction of polystyrene, the decrease in the average molecular weight caused by random breaks is balanced by the disappearance of shorter chains. The nature of the destruction is determined by the structure of the linear chains of the polymer under study. Thus, the splitting of polystyrene molecules may be accompanied by intra- or intermolecular transfer of a hydrogen atom [4]. With the decomposition of polystyrene molecules, the monomer content is about 40 %. The remaining 60 % are dimers, trimers and longer fragments of macromolecules [4].

Studies of the polyethylene thermal destruction in a vacuum of 10^{-4} Pa by the mass spectrometry method shows that it decomposes with the formation of a

series of hydrocarbons, both saturated and unsaturated, with molecular weights from 16 to 1200 [5].

The largest peaks in the spectrum of polyethylene fall on the region *m/e* = 42-43, 53-58; 67-71, 81-94, 86-100 with the most intense peak at *m/e* = 43, which corresponds to the ion $C_3H^+_7$. The mass range from 110 to 142 includes groups of peaks with very low intensity.

In the area of masses more than 142, separate broad peaks with mass numbers 156, 170, 184, 198 were observed. Peaks with mass numbers 92, 94, 122 and 137 could not be attributed to individual atomic groups, although, as indicated in [5], they apparently correspond to fragmented degradation products. Low-molecular decomposition products of C_2H_4, CH_4, C_3H_8, C_2H_6 hydrocarbons were absent in the spectrum. This was probably due to the lack of sufficient energy to break the carbon bond and to break up the molecule into shorter fragments.

The nature of the decomposition of PTFE in a vacuum of 10^{-4} Pa at a temperature of 500 °C is significantly different from the decomposition of the polyethylene molecules [5]. The largest molecule was C_3F_6, but in small quantities. None of the fluorocarbons CF_4, C_2F_4 or C_3F_8, as well as free fluorine, was detected. It is interesting to note that in the course of the experiment, not a single HF group was found being consistent with the results described in.

These data refer to the evaporation of polymers at 300-500 °C. The nature of decomposition changes with increase of temperature. At 800-1200 °C, the rate of destruction significantly increases, but the rate of temperature rise in the evaporator is limited due to the low thermal conductivity of polymers. As a consequence, the evaporation of the main mass of the polymer does not occur at a constant temperature, but during its increase. In addition, during thermal heating, the lower layers are always heated to higher temperatures, and the resulting decomposition products diffuse through a thin layer of the melt, and this changes their composition and shape.

The increase in temperature also leads to a change in the decomposition products. On the one hand, the decomposition rate increases at high temperatures that should lead to decrease in the size of evaporating fragments. On the other hand, the heat energy of molecules increases and accordingly the probability of evaporation of larger fragments also increases. The ratio of the number of long and short fragments in pairs depends on which of the two trends prevails. In the study of the destruction of PTFE at 1200 °C, the yield of

monomer fell to 75 %. At the same time, a fraction of larger non-volatile at room temperature fragments appeared. It is therefore advisable to investigate the process of thermal destruction when the sample is heated from above (radiant energy flux, electron beam). In this case, the decomposition of polymers would be carried out on the surface, and many side reactions would be minimized. However, there are no works in this direction.

An attempt was made in [71] to create a mathematical model of the process of polymers evaporation. The following idealized problem was considered. The polymer in the form of a film of thickness l consists of a low molecular weight fraction with an initial concentration of Q_o and a high molecular weight fraction. The evaporation rate is limited by the diffusion processes of the low molecular weight fraction (its concentration Q_τ on the surface is 0). Under these conditions, the value of Q_τ after the expiration of time τ can be calculated by the following formula:

$$\frac{Q_\tau}{Q_o} = 1 - \frac{8}{\pi^2}\left(e^{-y} + \frac{1}{9}e^{-9y} + \frac{1}{25}e^{-25y} + \ldots\right), \qquad (1.10)$$

where $y = \frac{D\tau\pi^2}{4l^2}$; D is the diffusion coefficient of the low molecular weight fraction.

The process of evaporation of polyethylene in vacuum is described in detail by Luff and White [5]. From the plot of film growth rate versus temperature, the authors determined the activation energy, which turned out to be 338 kJ/mol. This indicates that the evaporation process follows the Langmuir law:

$$v = p \cdot A\sqrt{\frac{M}{2\pi RT}}, \qquad (1.11)$$

where v is the evaporation rate of the substance from the evaporator at temperature T, p is the vapor pressure at T, R is the universal gas constant, M is the molecular weight, A is the correction factor.

Calculations of the molecular mass M of the obtained film yielded $M \approx$ 300,000 [5]. This is the minimum value, if the correction factor $A = 1$. However, the molecular weight of the original polyethylene was only 200,000 amu.

The most important processes determining the kinetics of polymer coatings growth on the surface of the substrate during evaporation and condensation of polymers in a vacuum are the adsorption of atomic and molecular particles of the gas stream, the chemical interaction between the adsorbed molecular fragments (polymerization) and their fixation on the surface, the thermal

desorption of the low molecular weight adsorption component phase, ion-stimulated polymerization and ion sputtering of the film as a result of exposure to ionized particles of the gaseous stream [72]. In some cases, chemically active low molecular weight compounds, such as oxygen, which may not be the products of polymer sputtering, have a significant effect on the growth rate of the films and their properties. So, when carrying out the process of coating in an oxygen-containing medium, their chemical composition changes and, consequently, the kinetics of the polymerization process also changes [73].

The modeling of growth processes of polymer coatings from the active gas phase was considered in detail by Rogachev [74]. The author has established the main kinetic patterns of growth of the polymer phase under conditions of exposure of volatile products of polymers dispersion containing active particles, ions and high-energy molecular fragments.

In the general case, when a constant mass flow j_p interacts with the substrate surface for time t, the mass of adsorbed low molecular weight fragments m_n + m_p, which undergo subsequent desorption or polymerization, and the mass of the polymer phase m_p are related to each other as

$$j_n \cdot t = m_n + m_p + m_o, \tag{1.12}$$

where m_o is the mass of a substance that has passed into the gas phase as a result of thermal desorption or ion etching.

Using the basic principles of chemical kinetics and the theory of thermal desorption, the mass change of low molecular weight adsorbed particles, as well as the polymerized part of the coating and the adsorbed particles in isothermal conditions correspond to the following expression

$$\begin{aligned}
\frac{dm_n}{dt} &= -K_{1,n} f_1(C_x, C_n) - \frac{m_n}{\tau_2} - S_p \beta_u j_n \Theta_n - K_{2,n} f_2(C_u, C_p) + \beta_o j_n, \\
\frac{dm_p}{dt} &= (1-\beta_o) j + K_{1,n} f_1(C_x, C_n) + K_{2,n} f_2(C_n, C_p), \\
\frac{dm_o}{dt} &= \frac{m_p}{\tau_2} + S_p \beta_u j_n \Theta_n,
\end{aligned} \tag{1.13}$$

where $K_{1,n}$ and $K_{2,n}$ are the polymerization rate constants, respectively, under the action of the active residual gas (oxygen) and active volatile fragments of macromolecules; $f_1(C_x,C_u)$, $f_2\ (C_n,C_p)$ are kinetic functions; C_k, C_f, C_p are concentrations of active residual gases, active molecular fragments and low molecular weight degradation products of the original polymer; S_p is the

effective ion sputtering coefficient; Θ_n is the degree of filling the surface with low molecular weight sputtering products (it is believed that only these products are etched by the charged particles of the gas stream); β_o is the fraction of low molecular weight particles in the mass flow j_n; β_i is the degree of ionization of the flow; τ is the average lifetime of the fragments in the adsorbed state.

The values of C_k, C_f, C_p, and Θ_n change in a generally complicated way in the process of the coating growth. At the same time, it is possible to make a number of sufficiently substantiated simplifying assumptions that allow one to obtain an analytical solution of the system of equations (1.13) and to evaluate the nature of the influence of individual physicochemical processes on the growth kinetics of the polymer coating. Based on the results of mass spectrometric analysis of the products of dispersion and the data of calculating the pressure generated by the products of laser dispersion [75], it can be assumed that the proportion of high molecular weight particles in the mass flow j_n is small, i.e. the process of formation of the polymer phase occurs almost from low molecular weight products. Then, $\beta_o = 1$ and the degree of filling the surface with low molecular weight particles $\beta_n = 1$. Since the flow of active residual gases is not directed, as a result of their interaction on the surface of the substrate, their regeneration is observed. Provided that their mass in the adsorbed state is much smaller than the mass of gases in the reaction chamber, we can assume the formation of an equilibrium surface concentration of the active gas, t. e. to assume that C_x = const. In addition, it is quite reasonable to take $C_H = K_{0,1}m_n$. Taking into account these assumptions, we consider two most common cases that are realized during the formation of polymer coatings: the growth of the polymer phase at the initial stages of formation and the growth of the film in the later stages.

In the first case, the main parameter determining the growth kinetics of the polymer phase is the concentration of active molecular fragments, the proportion of which in the flow falling on the surface of the substrate is y_{ak}. Then, neglecting the processes of regeneration of active radicals (during radical polymerization) or ions (during ionic polymerization), their concentration at the initial stage linearly increases with time $C_p = y_{ak}j_nt$.

The main difficulty in analyzing the polymerization processes is the choice of the kinetic function. In order to universalize the description of chemical reactions, the author accepted that:

$$f_2(C_n, C_p) = A^o\gamma_{ak}j_nt + B^o\gamma_{ak}^2j_n^2t^2, \qquad (1.14)$$

The process of chemical interaction of active residual gases with products of destruction is described by a kinetic function of the first order

$$f_1(C_x, C_n) = K_{0,2} m_n , \tag{1.15}$$

The result of solving equations (1.13) with the selected kinetic functions (1.14) and (1.15) under initial conditions $m_n(0) = 0$; $m_p(0) = 0$; $m_0(0) = 0$ has the form:

$$\begin{aligned} m_H &= \frac{a}{a^0}\left[\exp(-\alpha_0 t) - 1\right] + \left[1 - \alpha_0 t - \exp(-\alpha_0 t)\right]\left(\frac{b^0}{a_0^2} - \frac{2d^0}{a_0^3}\right) - \frac{t^2 d^0}{a_0}, \\ m_n &= (1-\beta_0)\, j_n t - \frac{b^0 t^2}{2} - \frac{t^3 d^0}{3}, \qquad m_0 = j_n t - m_H - m_n, \end{aligned} \tag{1.16}$$

where $a^0 = (S_p \beta_i \Theta_n - \beta_0) \cdot j_n$; $b^0 = A^0 K_{2,n} \gamma_{ak} j_p$; $d^0 = K_{2,n} B^0 \gamma^2_{ak} \gamma^2_n$.

Analysis of expressions (1.16) shows that the nature of the kinetics of change in the mass of the polymer phase is determined by the values of the parameters A^0 and B^0. Thus, at $B^0 < 0$, auto-retardation of polymerization processes is described, when the resulting polymerization products slow down the interaction of active particles with low molecular weight particles.

In the later stages of growth, an equilibrium concentration of C_p is established in the coating. This process is due to the fact that the probability of chain termination increases with increasing concentration. At some values of C_p, equilibrium is established between the processes of generation of active particles due to their receipt from the gas phase and the processes of recombination or disproportionation. Therefore, as a kinetic function one can take the expression

$$f_2(C_n, C_p) = A_1^o m_n + B_1^o m_n^o , \tag{1.17}$$

To describe the chemical interaction of active particles of residual gases with molecular fragments, the following kinetic function was used.

$$f_1(C_x, C_n) = (A_2^o m_n + B_2^o m_n^2) C_x \tag{1.18}$$

Then, for this case, the solutions of equations (1.13) are the following relations

$$\begin{aligned} m_n &= \frac{d_1[\exp(2k_3\delta t)]}{1 - \frac{d_1}{d_2}[\exp(2k_3\delta t)]}; \quad m_p = j_n t - m_n - m_o, \\ m_o &= S_p \beta_n j_n \Theta_n t - \frac{d_2}{2k_3\delta}\ln[d_2 - d_1\exp(2k_3\delta t)] - d_1 d_2 \int_0^{t_1} \frac{dt}{d_2 - d_1\exp(2k_3\delta t)}, \end{aligned} \tag{1.19}$$

where $K_3 = \sqrt{\frac{a^o}{\delta} - \frac{l_3^2}{4\delta}}$; $l_3 = K_{1,n} A_2^0 C_k + \frac{1}{\tau_2} + K_{2,n} A_1^0$;

$\delta = K_{1,n} B_2^0 C_x + K_{2,n} B_1^0$; $d_1 = k_3 - \frac{l_3}{2\delta}$; $d_2 = k_3 + \frac{l_3}{2\delta}$

The growth rate of the polymer phase

$$v_p = \frac{dm_p}{dt} = j_n + \frac{a^o}{l_3 \tau_2} - S_p \beta_n j_n \Theta_n + a^o \left(1 - \frac{1}{l_3 \tau_2}\right) \exp(-l_3 t) \qquad (1.20)$$

The mass of the coating $M = m_n + m_p$ in the process of growth changes in accordance with the expression:

$$M = j_n + \frac{a^o}{l_3 \tau_2} - S_p \beta_u j_n \Theta_n + \frac{a^o}{l_3^2 \tau_2} [\exp(-l_3 t) - 1], \qquad (1.21)$$

and $M = m_p$ for sufficiently large deposition times. From the obtained relations it follows that ion sputtering has the most significant effect on the coating thickness at the initial stages of growth. The coating is not formed at the values of the effective sputtering coefficient $S_p \geq \frac{\beta_o - l_3 \tau_2}{\beta_u \Theta_n (l_3 \tau_2 - 1)}$. This conclusion agrees qualitatively with the results of [76].

The analysis shows that there is no linear relationship between the values of M and j_u in the general case. It is possible only with certain values of the kinetic parameters b^0, d^0 and during the course of the first-order polymerization reaction. In this connection, it should be noted that the method for assessing the character of the spatial distribution of particles in the flow through the thickness of the deposited polymer coating adopted in papers [77,78] is erroneous.

An important consequence arising from the considered model is the incompleteness of the growth of the coating upon the termination of the flow of particles onto the surface of the substrate. It can be shown that post-polymerization processes are described by such equations

$$\begin{aligned} m_n &= \frac{l_3 m_{n,0} \exp(-l_3 t)}{l_3 + m_{n,0} d^o [1 - \exp(-l_3 t)]}; \\ m_o &= \frac{1}{d^o \tau_2} \ln\left\{1 + \frac{m_{n,0} d^o}{l_3} [1 - \exp(-l_3 t)]\right\}; \\ m_n &= m_{p,o} - m_{n,0} - m_0 - m_n \end{aligned} \qquad (1.22)$$

As can be seen from (1.22), at the initial stages of coating treatment, its mass decreases linearly with time and then stabilizes. In this case, the change in the

mass of the coating occurs due to decrease in the number of non-polymerized low molecular weight fragments and increase in the polymer phase. The maximum weight loss of the coating is $\Delta M_{\max} = \frac{m_{n,0}}{\tau_2 l_3}$. The mass of desorbed particles and particles that entered into the reaction on the substrate surface at all stages of the coating growth (at any *t* values) is redistributed in accordance with the following expression

$$\frac{\Delta m_o}{\Delta m_n} = \frac{1}{\tau_2 (k_{1,n} A_2^0 C_x + K_{2,n} A_1^2}, \tag{1.23}$$

Note that the experimental registration of changes in the mass of the coating is not difficult. Therefore, the obtained relations can be successfully used to determine the basic kinetic parameters. So, by carrying out a graphical differentiation of the kinetic mass change curve, we get

$$\tau_2 = -m_{n,0}\left(\frac{dM}{dt}\right)^{-1}; \quad l_3 = \frac{1}{\Delta M_{\max}}\frac{dM}{dt}, \tag{1.24}$$

Thus, on the basis of experimental data on the change in the mass of the coating, it is possible to determine the values of the kinetic parameters, knowledge of which is necessary for calculating the technological regimes of the polymer films formation with desired properties.

As mentioned above, the evaporation of polymers is not a purely superficial process. Fragments capable of evaporation result from the destruction in the entire volume of the sample, and the rate of evaporation depends on the rate of diffusion of the fragments to the surface. In the process of decomposition and diffusion, secondary reactions may occur, which lead to the fact that the composition of the evaporated products is different from the composition of the products of the initial decomposition. In mass spectrometry studies, samples with a mass of several tenths of a milligram are studied, and thus the influence of secondary processes is minimized [50]. However, when polymer coatings are deposited by evaporation in vacuum, the weight of the polymer loaded into the evaporator will exceed the mass of the samples studied in mass spectrometers. The nature of evaporation in these cases will be different. Namely, when heated in the evaporator, a thin layer of molten polymer is formed. Considering that the heat is supplied from below, the polymer begins to spray out of the evaporator with intensive evaporation [79]. This leads to unproductive losses of the evaporated material and to the deterioration of the quality of the coatings due to

the fact that some sprayed droplets reach the substrate and are deposited on it, contributing to the formation of pores and film heterogeneities.

The reason for this phenomenon during the evaporation of polymers is associated with their low thermal conductivity. The temperature of the polymer at the bottom of the evaporator is higher than at the surface. In the case of polymers, not all of the heat entering the evaporator goes to evaporate the material; part of it is absorbed in the volume of the polymer during the destruction. In the layers adjacent to the bottom of the crucible, boiling begins earlier than on the surface, which leads to splashing of the polymer.

In work [80], to eliminate the splashing phenomenon, it is proposed to cover the evaporator with a grid-shaped cover with very small holes. The latter limit the possibility of large droplets falling on the substrate. It is also recommended to carry out the evaporation of polyethylene very slowly at a temperature not exceeding 350 °C. In this case, although the spattering disappears, the productivity of the process decreases, and the quality of the coatings becomes low.

A successful solution to the problem is a discrete method for the evaporation of polymers [81]. In this case, conditions are provided under which the polymer powder is fed into the evaporator with the speed of its evaporation. The device proposed in [81] is presented in Fig. 1.2.

The device consists of a drive, a flat polished disc, a molybdenum scraper and a guide tray. When the disk is rotating, the drive of which is made on the basis of a stepper motor, the previously out-pulverized fine powder flows from the hopper to the surface of the disk and with the help of a scraper is sent to the tray and then to the evaporator. It should be noted that the radiation from the evaporator can heat the powder so much that it will sinter during its movement along the tray. This leads to the formation of large lumps that fall into the evaporator and violate the mode of evaporation. Lumps can also clog the tray. To prevent this phenomenon, it is necessary to cool the tray with running water and use screens. At the same time, the presence time of the polymer powder in the evaporator is minimal that prevents thermal oxidative degradation of the original substance. In addition, no polymer melt is formed in the evaporator, and the film growth rate is rather high. The authors [81] obtained coatings of PCTFE, polycaproamide, PE with a growth rate of 1 μm/min, and PP with a growth rate of 0.5 μm/min.

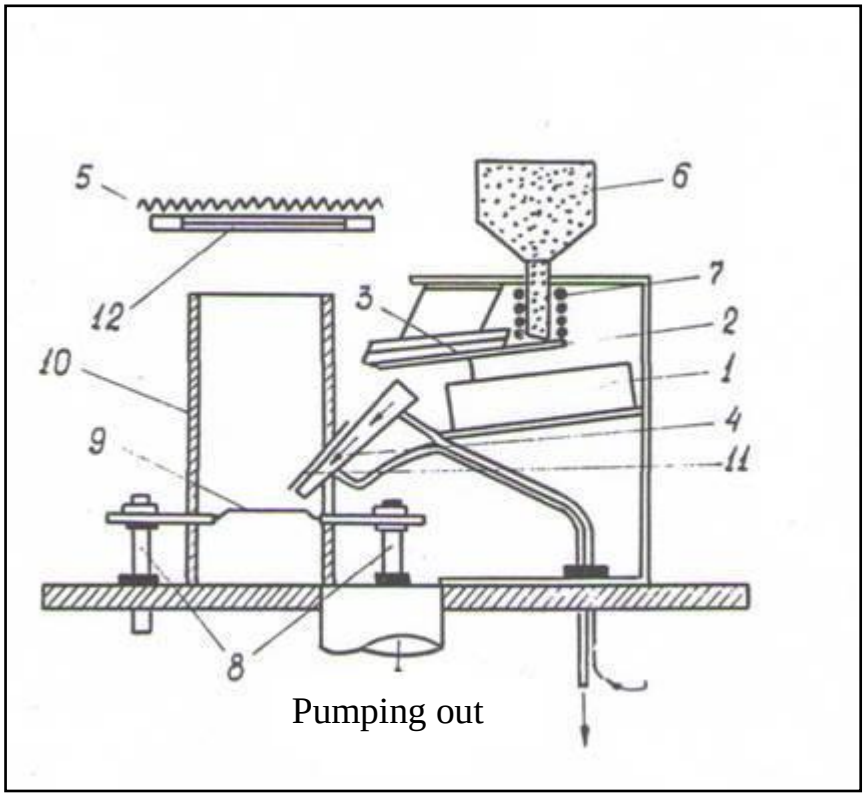

Fig. 1.2. Schematic view of the apparatus for "explosive" decomposition of polymers. 1 - electric drive of the disk; 2 - feed disc; 3 - molybdenum scraper; 4 - tray; 5 - substrate heater; 6 - bunker; 7 - powder heater; 8 - current leads; 9 - evaporator; 10 - screen; 11 - tray screen; 12 - substrate.

Madorsky [4] determined the average molecular weight of the condensates while evaporating polyethylene under vacuum at a pressure of 10^{-4} Pa. It was equal to 692. He excluded sprinkling during evaporation and found that when 77 % of the original polyethylene are decomposed at 400 °C for 75 min, the evaporation rate fell. The rate of polyethylene evaporation obtained in [41] during evaporation of 100 mg of the polymer from a steel evaporator was 6 times greater than that of Madorsky [4]. The rate remained constant until all the matter had evaporated. The high evaporation rate can be explained by the fact that the evaporation process is macroscopic in nature. When the temperature of the evaporator rises above 350 °C, the intensive boiling of the polyethylene causes the emission of macroscopic particles of massive polyethylene, giving them sufficient energy to reach the substrate. The ejected particles had a spherical shape with a diameter from 1 to 500 μm [41]. Since each macroscopic particle may contain several polymer molecules, the average molecular weight obtained by the authors from the Langmuir equation was higher than the molecular weight of the original polymer. High evaporation rates are also associated with this.

To test this theory, in work [82] they proposed to cover the evaporator with a quartz fibrous lid, which made it possible to continue the evaporation of molecules and prevented the direct emission of macroscopic particles. The evaporation rate was reduced 5 times at the evaporator temperature of 340-400 °C. Thus, the macroscopic evaporation process was the main mechanism with the uncovered evaporator.

The most successful solution to the problem of the evaporation of polymers was proposed in the U.S. patent [83] where it was proposed to supply heat to the surface of evaporation from above using an electron beam from an electron beam gun. The electron beam, bombarding the surface of the polymer, heats it to temperatures at which evaporation occurs. In this case, the temperature of the polymer decreases with increasing depth of the layer. Due to poor thermal conductivity, the bulk of the polymer remains cold. The layers adjacent to the surface are heated. Macromolecules are decomposed into fragments and evaporated. With such evaporation, the amount of polymer charged to the evaporator is almost unlimited. Another advantage of the electron beam heating is that accelerated electrons break some of the chemical bonds inside the polymer macromolecules. This should lead to increase in the fraction of fragments that evaporate and condense on the substrate. For comparison, the authors of [83] produced the evaporation of polyethylene in two ways: the usual one by the thermal heating and by the electron-beam heating. In the first case, uneven brown degradation products of polyethylene were condensed on the substrate, while in the second, a homogeneous transparent coating was formed, the analysis of which showed that the substrate had the same material that was in the evaporator.

In work [69], the evaporation of polytrifluorochloroethylene (PCTFE) was investigated under the action of thermal and electron beam heating. In the first case, it was found that macroscopic evaporation takes place. A non-uniform coating was obtained on the substrate, the molecular weight of which, according to viscometry data, did not differ from the molecular weight of the initial PCTFE. In the case of the electron beam decomposition, evaporation depended on the power of the electron beam. At low decomposition powers, splashing was not observed, however, an increase in the power of the electron beam to 60 W/cm^2 led to a strong heating of the polymer substance in the evaporator, and evaporation began to follow the spray mechanism. In the case of PCTFE, not all the material was decomposed into fragments. Considering a significant yield of

monomer (about 25 %), it can be assumed that some chain breaks during the decomposition of PCTFE leading to the formation of free radicals, which break up along a chain mechanism with the formation of the monomer:

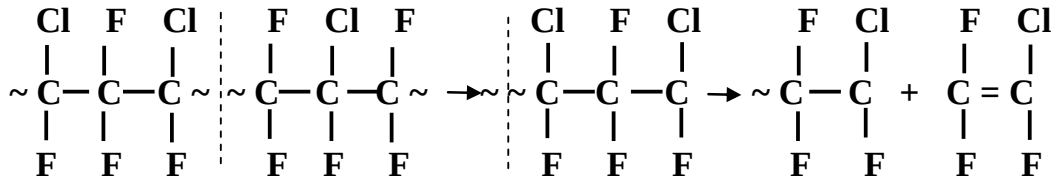

Other chain breaks are accompanied by the transfer of a chlorine atom to the break point and lead to the formation of polymer fragments with one saturated and one unsaturated group at the ends of the chains:

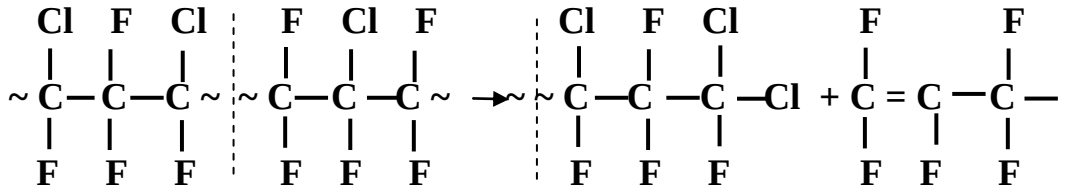

When studying the decomposition of polymers in vacuum, evaporation products are divided into three fractions depending on the condensation temperature [50]: the first one, which does not condense at liquid nitrogen temperature; the second, which condenses at liquid nitrogen temperature, but does not condense at room temperature; and the third, condensing at room temperature, but volatile at evaporation temperature. Sometimes the fraction volatile at room temperature was divided into two: the fraction volatile at -80 °C (and condensing at -190 °C) and the fraction condensing at -80 °C.

From the point of view of obtaining coatings in vacuum, the fraction condensing at room temperature is of interest, since cooling the substrates to temperatures below room temperature significantly complicates the process, as well as increases its cost and degrades the quality of the coatings. Studies have shown that this fraction contains the longest of the evaporated fragments. Therefore, the decomposition conditions should be chosen in such a way that a significant part of the fragments are present in the vapors, since the monomers do not condense at room temperature.

In [69], it was shown that the production of coatings from polyethylene decomposing under the action of thermal heating into fragments with molecular masses from 16 to 1200 is more promising than from PTFE, whose product at 500 °C is monomer. Apparently, the above statement is not quite reasonable. As

mentioned above, with an increase in the decomposition temperature of PTFE to 1200 °C, the proportion of the volatile fraction containing long fragments of PTFE begins to increase.

In a number of works, the structure and properties of films were investigated depending on the conditions of their deposition. The process of formation and the structure of the films obtained were studied in [82]. Films produced by the "spatter" mechanism, with thicknesses less than 0.2 μm, had a polycrystalline structure. Increase in thickness to 0.3 μm led to a change in supra-molecular formations. They became amorphous. The hardness of the films was low and they were easily dissolved in toluene. After annealing at 150 °C for 3-5 hours, the structure, regardless of the film thickness, became single-crystal and became identical to that of polyethylene crystals grown from solution. After annealing, the hardness of the coatings increased, and the solubility in toluene decreased. To increase the degree of polymerization in the condensation process, the substrate was illuminated with UV light. The structure of the films became amorphous, the hardness of the coatings increased greatly, and they became insoluble in toluene. This is apparently due to the occurrence of cross-links and the formation of three-dimensional network structures. The properties of the films obtained at decomposition temperatures not higher than 350 °C (no splashing was observed) turned out to be significantly different. They had an amorphous structure, but after annealing, under the same conditions they became polycrystalline. *UV* irradiation during growth led to the appearance of an amorphous structure. The micro-hardness of the coatings was low even after annealing and exposure to UV light. The films were soluble in toluene after annealing and irradiation with UV light.

Annealing of coatings in vacuum causes decrease in their thickness. This is due to the evaporation of low molecular weight fractions contained in the films, which was confirmed by mass spectrometric studies. In non-annealed films, the internal stresses were of the order of $32 \cdot 10^5$ N/m^2. At film thicknesses of more than 1 μm, these stresses do not change with time. With a thickness of 0.1-1 μm, the stresses immediately after deposition have the same magnitude, but they decrease to zero with time depending on the thickness of the films.

The following film deposition mode is recommended: evaporation at the temperature of 400 °C (accompanied by micro outliers) and subsequent annealing at 150 °C for 5 hours.

Due to the fact that fluoropolymers are currently the best dielectrics, many researchers are working on the production of films and coatings of these materials.

An attempt was made to obtain thin coatings of fluoropolymers by cathode sputtering of solid polymers in an inert gas atmosphere [69]. Two sputtering schemes were used: diode and triode ones. The cathode was a disk made of PCTFE or PTFE with a diameter of 130 mm and a thickness of 5 mm. The substrate was at a distance of 25 mm from the cathode. The plasma was ignited at a pressure of 1 Pa. At the beginning of sputtering, the pressure in the chamber increased and after a few minutes stabilized (2.5 Pa at a power of 6 W/cm^2). The growth rate of the coatings was 30-50 μm/h with a power of 5-6 W/cm^2.

The antifriction properties of the obtained coatings were investigated. It was established that the coefficient of friction of the coatings did not differ from the coefficient of friction of the original substance. In particular, at a sliding speed of 0.17 mm/s, the friction coefficient was $k = 0.08$.

Electron diffraction and X-ray diffraction analyzes of the films showed that they are amorphous. However, their heat treatment in a hydrogen environment at 350-380 °C led to the appearance of ordered structures.

Studies using a special microprobe showed that free fluorine was not formed during the decomposition of the fluoropolymer. Studies of infrared spectra of the films showed that they are very different from the original massive fluoropolymer. Thus, the films had crosslinks, contained $C = C$ double bonds and CH_3 groups. They had a high concentration of $C = O$ and OH groups, which indicated the presence of oxygen in them. Heat treatment in vacuum at a temperature of 350 °C led to decrease in the oxygen content in the films. The films contained a large number of pores. The dielectric characteristics at a frequency of 1 kHz were as follows: $\varepsilon = 2$; $\tan\delta = 2 \cdot 10^{-3}$ (for the starting PTFE, $\tan\delta = 2 \cdot 10^{-5}$).

Film properties have improved when using a cylindrical diode circuit. It was possible to increase the deposition rate of PCTFE to 1 μm/min. The properties of PCTFE films approached the properties of the starting polymer. A detailed study of the technology of obtaining coatings from PCTFE was carried out in [69]. The evaporation of PCTFE was carried out by both thermal and electron beam heating. During the thermal decomposition of PCTFE, in the temperature range of 300-450 °C, a high decomposition rate was initially observed, which

decreased after a few minutes and became constant. At temperatures above 450 °C, the decomposition rate did not change with time.

The residual pressure in the chamber during thermal decomposition up to 400 °C varied slightly and did not exceed $3 \cdot 10^{-2}$ Pa. Increase in the heating temperature to 470-500 °C led to increase in pressure to 0.1 Pa. To eliminate the splashing phenomenon, discrete decomposition of PCTFE was applied. At the same time, polymeric powder of PCTFE was fed into the evaporator continuously in small portions, and the melt practically was not formed. At the evaporator temperature of 450 °C and an area of 4 x 5 cm^2, the growth rate of PCTFE films reached 4-5 μm/min, and in the case of evaporation from a filled evaporator, the growth rate did not exceed 0.5 μm/min.

With the decomposition of PCTFE by the electron beam, with an increase in the current density at a constant accelerating voltage, the growth rate of the films initially increased, and then reaching a maximum began to decrease. It was found that the current density decreased with increasing voltage, at which the maximum film growth rate was achieved. The growth rate of films obtained by evaporating the starting material by the method of electron beam heating reached 3-5 μm/min with the evaporator-to-substrate distance of 10 cm.

It is known that during the evaporation of metals, the quality of films and coatings significantly depends on the temperature of the substrate at which condensation takes place. This turns out to be significant during the deposition of polymer coatings too.

For example, the dependence of the molecular weight of the obtained coatings of PCTFE on the condensation temperature was studied in [69]. It has been established that increase in the condensation temperature leads to a significant increase in the molecular weight of the films and an improvement in their physic-chemical properties. At low condensation temperatures, although the lifetime of the radicals is large, their mobility is significantly reduced. The molecular mass of such condensates (the coating has a gel-like appearance) was 5000 (medium-viscosity) and 300 (number-average).

Increase in the substrate temperature (condensation) leads to increase in the mobility of macro-radicals that should lead to increase in the molecular weight. So, at condensation temperatures of 200 °C, it reaches: 140,000 (medium-viscosity) and 50,600 (number average). This decreases the polydispersity of the films and improves their physical and chemical properties.

1.10 PTFE thin films deposited by vacuum evaporation

In preparing polymer films for practical electronic applications a number of physical and chemical techniques may be employed, including vacuum evaporation, either thermal or electron beam. In view of the cost and simplicity, the deposition of polymers was studied in [84] such as PE and PP by thermal vacuum evaporation and have been able to show that although some degradation of the starting polymeric material takes place during the evaporation, nevertheless the deposited layers are still effectively insulators and such properties as the permittivity of the deposited material are similar to the value for the starting material. The authors of [84] also prepared films by vacuum evaporation of PTFE as a starting material to study the structure and some of the physical properties of the deposited layers, and to compare their properties with those of other polymers.

A standard evaporating apparatus was used and the samples were deposited under high vacuum on glass slides, some with metal electrodes for electrical measurements. The vacuum reached was of the order of $1.33 \cdot 10^{-4}$ Pa and a liquid nitrogen trap was used. PTFE shrinks on heating so a spring system was used to exert a mechanical pressure on the PTFE surface to the molybdenum boat during the thermal evaporation process. The original material was in granular form, the grain size being of the order of 200 μm.

PTFE films with Cu or Al electrodes have similar electrical properties [84]. Films 50 nm thick measured at both DC and AC had very low resistance, while films thicker than 100 nm were more resistive, having a typical resistance value of 50 Ω corresponding to a resistivity of $3.5 \cdot 10^5$ Ω·cm. Annealing the samples in a vacuum reduced their effective resistance, probably as a result of morphological changes.

It was concluded in [84] that PTFE films prepared by thermal vacuum evaporation were not suitable for applications in electronics where high resistances are needed. Nevertheless, the work has shown the types of changes which may occur when the films are formed and throw some light on the way in which monomers may assemble on the substrate in such a way that they form molecules with variations in molecular weight, and these in turn form highly crystalline complex chains situated in a liquid of lower molecular weight. Closer examination, however, shows [84] that these apparent amorphous regions are themselves made up of low molecular weight islands surrounded by a wall or perhaps by ropes of polymer chains, linearly aligned. The high electrical

conductivity must arise from free carbon in the deposited films. The constancy of the infrared absorption spectrum suggests that the strongly bound CF_2 groups retain their composition through the evaporation and deposition processes so that there will be little, if any, free fluorine in the deposited films. The breaking down of the polymer structure on heating in a vacuum probably takes place in an analogous way to step-wise polymerization where strain rupture occurs randomly along the chain, leaving fragments several times the monomeric size, or to chain polymerization where the successive release of monomer units from a chain end in a stripping reaction are involved. It is preferable that the latter process should be the main degradation process since the random process could in principle release such units as CF and CF_3, rather than the basic CF_2, units.

There are only a few reports on the PTFE thin films prepared by a vacuum evaporation. We have shown [85] that the vacuum evaporation technique can be used to produce thin polymer electrets. Thin films (2-7 μm) of PE and PTFE were deposited by the electron-beam method. The secondary polymerization was activated either thermally (5-200 °C) or by electron irradiation (0.6 keV). It was found that the electron irradiation of PE and PTFE films defects acted as shallow traps, while the deep trapping of injected charge carriers took place at cross-links.

Elemental composition and chemical structure of the PTFE thin film prepared by the vacuum evaporation were similar to the pristine PTFE compared to those by the RF sputtering [86]. In addition, transparency of the PTFE thin films prepared by the vacuum evaporation was quite different, which depended on the deposition conditions, i.e., pressure during the deposition and temperatures of the basket [86]. In this paper, we elucidate a relationship between the molecular structure and transparency of the PTFE thin film prepared by the vacuum evaporation.

In [87] the PTFE thin films were deposited onto a glass slide substrate by using a heat resistance type vacuum evaporation apparatus. Gap distance between the basket and substrate was 40 or 70 mm. Back pressure was $1.3 \cdot 10^{-2}$ Pa, and pressures during the deposition of the transparent and white colored PTFE thin films were maintained at $1.3 \cdot 10^{-1}$ and 67 Pa, respectively. PTFE pellets, whose weight is 1 g, were used as the deposition material. They were heated in a tungsten basket coated with alumina, and the temperature of the pellets in the basket was monitored with a Pt–Rh thermocouple. Temperature of the basket depends on an electric current, and it was maintained at 15 or 20 A.

The transparent PTFE thin film prepared by the vacuum evaporation at 15A heating, 70mm gap distance has microcrystalline structure. The sputtered PTFE thin film prepared by the RF sputtering was transparent, whose structure was amorphous [88]. These results indicate that the crystal structure decreases the transparency of the PTFE thin films.

It is already reported that PTFE polymer chains break into fragments when the material is heated to its sublimation temperature, and low molecular weight fluorocarbon are deposited. The primary decomposition products are TFE and CF_2. Moreover, it is well known that lower molecular weight polymers indicate lower melting points, e.g., there is a significant reduction in melting point with low molecular weight. Polymer chains are broken into the fragments and evaporated by the heating into the vacuum chamber, and some of the fragments are repolymerized.

These results suggest that molecular weight of the PTFE thin film prepared by the heat-resistance type of vacuum evaporation is lower than that of the pristine PTFE. It is considered that the lower molecular weight of the PTFE thin film enhances the reduction of the crystal structure and leads to amorphous structure, and enhances the expression of the transparency.

Chemical structure of the PTFE thin film prepared by the vacuum evaporation in [87] was similar to that of the pristine PTFE. However, the crystallinity of the transparent vacuum evaporated PTFE thin film was different from that of the white vacuum evaporated PTFE thin film. The crystal structure is one of the factors that affect the transparency of the PTFE thin film.

Melting point of the transparent PTFE thin film prepared by the vacuum evaporation can be observed at lower temperature than that of the white PTFE thin film prepared by the vacuum evaporation. This result suggests that molecular weight of the PTFE thin film affects the transparency. It is considered that the lower molecular weight of the PTFE thin film enhances the reduction of the crystal structure and leads to the expression of the transparency.

1.11 Pulsed electron beam deposition

Recent research has demonstrated that PTFE coatings can be successfully deposited by means of pulsed laser deposition (PLD). The majority of studies confirmed that the chemical composition of the materials remained the same after deposition. Although the PLD technique is well known and useful for obtaining PTFE films, pulsed electron beam deposition (PED) can be a

promising alternative to this end [89]. This is an advanced technique and the newest in film coating manufacturing that enables the deposition of very thin films with a well-controlled stoichiometry [90]. So far, PTFE coatings deposited by the PED technique have not been extensively studied. As yet, only a few attempts have been made [90,91]. Chandra and co-workers [90] only concentrated in their work on the crystallinity of PTFE films. Other properties of the coatings were not studied. Henda and co-workers [91] prepared PTFE films on glass and silicon substrates. The process conditions (background gas – argon, nitrogen; gas pressure, substrate temperature, discharge voltage) were widely varied. However, despite the extensive work carried out by the authors it is difficult to directly correlate the film properties and the deposition parameters. This may be attributable to the fact that too many parameters were changed simultaneously.

In [89] extended research on the deposition of PTFE thin films by the PED technique has been carried out. The aim was to clarify the influence of changes in the gas pressure on film thickness, chemical structure and coating morphology. The studies in particular were focused on the preservation of the chemical structure and hydrophobic properties of the material after the deposition process. [89] is the first work that shows the results of both *SFE* (surface free energy) and *WCA* (water contact angle) measurements for PTFE coatings obtained by PED methods.

In the experiments [89], PTFE coatings were deposited by means of a PED system. The setup consisted of a vacuum chamber and a pulsed electron source. PTFE coatings were obtained on monocrystalline Si (100) substrates, 10 x 10 mm in size. A 99% purity PTFE bulk disk was used as a target for the PED deposition. The chamber was evacuated to 0.1 mPa using nitrogen as the background gas. The PTFE film deposition took place at pressures of 0.4, 0.67, 0.93 and 1.46 Pa at room temperature. The deposition time was the same for all coatings, corresponding to 5000 pulses. The distance between the target and substrate was set at 80 mm. The electron source was operated at 12 kV with a repetition rate of 5 Hz.

Measurements with the profilometer indicated that the thickness of the coatings decreases linearly from about 200 nm to above 100 nm as the deposition pressure increased. The coatings deposited at 0.4, 0.67 and 0.93 Pa show a similar surface topography. A grain-like structure and a few small spikes were observed. The highest points on the film surface were probably droplets.

The coating obtained at 1.46 Pa was different from the others: the number of spikes was greater and there were more uneven regions. This observation correlated well with the arithmetic average roughness results.

The roughness of the film deposited at 1.46 Pa was much higher than those depicted at the lower nitrogen pressures. An increase of gas pressure reduced the mean free path of both electrons and polymer species ablated from the target. This led to a decrease in the effective electron energy deposited in the target. Therefore, there was a growing tendency for melting the polymer target instead of ablating it and, as a consequence, a larger number of droplets were formed.

The Si substrate showed only one weak peak at approximately 610 cm^{-1}. The two characteristic peaks at 1201 cm^{-1} and 1150 cm^{-1}, seen in the spectrum of the PTFE target, were attributed to asymmetric and symmetric -CF_2- stretching vibrations. A third, weaker peak observed at 642 cm^{-1} corresponded to the -CF_2- wagging vibrations. All the PTFE coating spectra had characteristic -CF_2- stretching peaks at approximately 1220 cm^{-1} and 1154 cm^{-1}. The intensity of stretching peaks increased with larger coating thickness, which was a result of the fact that the coating thickness was smaller than the material thickness analyzed by the FT-IR detector.

In summary, it was stated in [89] that the FT-IR spectra analysis of the coatings did not indicate any major chemical differences compared to the target material. Notwithstanding, some differences were observed between the spectra obtained for the PTFE coatings and that of the target material. The -CF_2- wagging peak of the coatings was shifted towards lower wave numbers in comparison to the position of the same peak registered for the target material.

The surface free energy of the films was calculated according to the Owen-Wendt model [92] using the contact angle of de-ionized water and diiodomethane. The *SFE* values obtained are in the range of 14.9 mJ/m^2 to 19.3 mJ/m^2 for the PTFE coatings. This was comparable to the value of 16.04 mJ/m^2 obtained for bulk PTFE. The most important result was that the obtained *SFE* values were low, and that the PTFE coatings retained a non-adhesive character. Moreover, the nearly constant *SFE* values were additional evidence of the presence of a stable chemical PTFE structure in the coatings.

Pulsed electron deposition (PED) has been a promising alternative to PLD in thin film coating applications [93,94]. PED is conceptually similar to PLD except that a short pulse (~100 ns) of energetic electrons replaces a short pulse of photons to ablate material from a target. Due to a short penetration depth (~1

μm) of the electron beam into the target, rapid non-equilibrium heating results, leading to the formation of a highly forward directed, stoichiometric plasma plume, which in turn facilitates stoichiometric preservation of the target composition in the deposited film under optimal process conditions. Compared to lasers with similar power densities (~10^8 W/cm^2), advantages of electron beam sources include higher electrical efficiency (30%), the ability to process materials that are transparent or highly reflective to laser light, and lower capital costs [94]. Nearly all solid-state materials with varying complexity can be deposited in thin film form with PED. Recently, Chandra and Manoharan [90] have investigated the fabrication of PTFE films by PED under argon as the background gas. Thin films have been obtained under a constant gas pressure of $6.7 \cdot 10^{-1}$ Pa, room temperature, and constant discharge voltage.

In [91], authors report on the preparation of PTFE by channel spark PED technique on glass and silicon substrates. PTFE thin films have been deposited under a wide range of process conditions, namely, background gas, temperature, pressure, and discharge voltage. The chemical composition and wetting properties of the deposited films are investigated.

The PTFE thin films were deposited in a pulsed electron ablation system with pulse duration of 100 ns. The pulsed electron beam source based on channel-spark discharge geometry consists of a trigger, a hollow cathode, and a dielectric capillary tube. A two-inch diameter PTFE rod was cut into ¼—inch thick targets, and glass microscope slides were cut into ½×½ inch^2 substrates. The electron pulse energy was varied from 10 to16 kV with fixed pulse frequency of 1 Hz and a constant number of 600 electron pulses throughout the experiments. Prior to film deposition experiments the deposition chamber was evacuated to $6.6 \cdot 10^{-4}$ Pa before admitting the background gas into the chamber at a specific pressure for deposition. The gas pressure was varied from $133.32 \cdot 10^{-3}$ Pa to $799.93 \cdot 10^{-3}$ Pa. The distance between the target and electron gun ceramic tube tip was kept at 15 mm whereas the target to substrate distance was kept at 80 mm. Prior to deposition the target was pre-ablated by the electron beam over 1200 pulses at 1 Hz and 10 kV. The operating conditions of PED system were varied to determine their effect on the wettability of the film produced.

The deposited films were characterized using Attenuated Total Reflection Fourier Transform Infrared (ATR-FTIR) spectroscopy. The spectra were collected using infrared microscope with a liquid nitrogen cooled mercury

cadmium telluride detector and an ATR objective equipped with a germanium crystal. Each spectrum was the result of 100 scans collected at a resolution of 4 cm^{-1}. All spectra were collected with an air background and were corrected for CO_2 and H_2O with the atmospheric compensation function of the software. Static angle goniometry was used to assess film hydrophobicity by measuring the contact angle between a drop of de-ionized water and the film surface under various process conditions.

The FTIR spectrum of the PTFE target material has two strong vibrational bands at approximately 1154 cm^{-1} and 1210 cm^{-1} that are ascribable to the -CF_2- symmetric and asymmetric stretching vibrations of the PTFE molecule [19,20]. A third weaker peak assigned to the -CF_2- wagging of the PTFE molecule is also observed at approximately 644 cm^{-1}. Upon comparison to the PTFE target material, the deposited film also has two absorption bands at approximately 1154 cm^{-1} and 1210 cm^{-1}. This confirms that PTFE is present on the glass surface and that, overall, its chemical structure is similar to PTFE target material. A new band was also observed at approximately 1259 cm^{-1}. This peak has been attributed to overlapping CF, CF_2 and CF_3 vibrational modes and may be due to the presence of cross-linked or unsaturated species [10,20]. AFM topographic images show that the films are composed of clusters or particulates of pyramidal shape and of varying size. Overall, particulate size seems to increase with pressure, to decrease then increase with discharge power, and to increase with temperature. The measured contact angle for water is about 110° for bulk PTFE, whereas the contact angle for bare glass and silicon substrates is around 32° and 43°, respectively.

PTFE films were obtained under argon and nitrogen at a constant discharge voltage and for different gas pressures as a function of deposition pressure and background gas. The contact angle data indicate an overall decrease (increase) in contact angle (in solid–liquid area) as the pressure increases for both gasses. For any given pressure the contact angle is higher for films deposited under nitrogen as such films have a higher roughness, according to reflectance data.

Finally, the effect of the deposition temperature on film wettability has been assessed. For PTFE films deposited on glass and silicon (100) substrates, the contact angle decreases as the deposition temperature of the films increases. From an inspection of AFM images films deposited at higher temperatures than RT present pinholes. The size of particulates is smallest at RT, while at higher temperatures the particulates size is somewhat higher at 100 °C than 300 °C, but

the surface density of the particulates seems to be larger at 300 °C than at 100 °C. Also, both thickness and roughness of the films obtained at 300 °C are lower than those of films deposited at 100 °C and RT as per reflectometry measurements.

Thin films of PTFE were deposited in [90] by pulsed electron deposition (PED) technique. The PED gun used in the experiment is a commercial source. The following deposition parameters have been employed: 5-20 kV charging potential, 5-30 mTorr (Ar) of background gas pressure required for focused beam propagation, beam energy of 0.2-0.8 J (energy variation < 20%), pulse duration 100 ns, maximum power density $1.3 \cdot 10^8$ W/cm^2, beam cross-section of about $6 \cdot 10^{-2}$ cm^2. The repetition rate of the pulses can be adjusted up to 10 Hz.

In PED, the pulse energy increases strongly and arises approximately linearly with the voltage, when operating at 12-15 kV with the beam cross-section of about 9 mm^2, the power density at the target is about 6-7 J/cm^2.

During deposition, the chamber pressure was maintained at 0.665 Pa by controlled flow of Argon. The substrate temperature was kept at 300 K during deposition. In order to stabilize the working conditions of the source and to clean the target surface, the target was preablated by electron beam while masking the substrate for 20 min at 1 Hz. For film deposition, the electron beam operating at 1 Hz was made incident onto a rotating target of PTFE at an incident angle of 45^o.

The ablated material was allowed to condense on glass substrate positioned in front of the target, typically 8 cm away. The discharge voltage was kept at 12 kV. The deposited films were characterized by scanning electron microscopy (SEM), transmission electron microscopy (TEM), X-ray diffraction and Fourier Transform infrared (FTIR) spectroscopy. An analysis of the processing parameter in comparison to pulse laser deposition, sputtering and evaporation techniques is listed in Table 1.2 [90].

The transmission electron microscopy (TEM) image of the RT fabricated (20 Å thick) film on carbon coated copper grid shows crystalline nature. Infrared spectra show one to one correspondence between PED ablated film and the PTFE bulk target. The asymmetrical and symmetrical –CF_2– stretching modes were observed at 1220 and 1156 cm^{-1}, respectively. The –CF_2– wagging and bending modes occur at 644 and 512 cm^{-1}, respectively. X-ray diffraction patterns of the film deposited at room temperature (RT) show oriented film along (100) plane of hexagonal structure and the crystalline nature is retained up

to 300 ^{o}C on vacuum annealing. The room temperature fabricated film shows smooth and pin hole free surface whereas post-annealing brings discontinuity, roughness and pin holes [90].

Table 1.2.

Some processing of PED method in comparison to other deposition techniques

Parameter	PLD	PED	Sputtering	Evaporation
Energy/pulse	1 J	0.7 J	–	–
Pulse width	20-30 ns	100 ns	–	–
Efficiency of energy conversion	3% (electrical optical)	25% (electrical optical)	–	–
Pulse repetition rate	1-200 Hz	1-10 Hz	–	–
Optimum growth rate	0.7 Å/pulse	0.3 Å/pulse	1-5 Å/s	1000 Å/s
Band gap of materials	Critical	Not critical	Not critical	Not critical
Surface roughness	Very smooth	Comparable to PLD	Comparable to PLD	Very rough surface
Stoichiometry of the film	Good	Good	Poor	Very poor
Background pressure	Any pressure	0.665-3.99 Pa	2.66-66.5 Pa	<0.133 Pa

1.12 Ionization-assisted deposition (IAD) method

In many cases, thin films prepared by solution methods suffer from the residual solvent or impurities present in the solvent. The solution methods are not suitable for preparing multilayered structures, because the solvent damages the underlying layer. As the film thickness goes down to the nanometer range, it becomes more difficult to prepare uniform thin films from solution. With this respect, the physical deposition method seems to have an advantage in fabricating high-purity thin films and their stacked structures. In [97] the

ionization-assisted deposition (IAD) method analyzed. It is relatively easy to prepare thin films of low molecular weight organic materials by this method. The IAD method has advantages in controlling film properties through refinement of the deposition conditions. Such features are also attractive for the preparation of polymeric thin films. Since polymers do not evaporate in general, a special approach is required for their deposition. It was found that IAD provides some novel features, such as enhanced reactivity and controlled dipole orientation, which are not available by the conventional vacuum evaporation method. The applications of these films include electrical insulators, piezoelectric or non-linear optical devices, and light emitting diodes.

The ions can be incorporated in film formation in various ways, including inert gas ion bombardment, mass-selected ion beam, glow discharge, etc. Ionization assisted deposition (IAD) is one of the simplest extensions of the conventional vacuum evaporation method. The film material is evaporated in the same manner as in the conventional evaporation process. The IAD is distinguished by the electron impact ionization source placed above the evaporation source and also by the ion acceleration voltage applied between the ionizer and the substrate. The ionizer consists of a hot-cathode filament and a box-shaped anode grid. The ion concentration, typically 1 to 0.1% of the depositing material, can be controlled by the electron emission current. The anode voltage V_e is normally set between 50 to 100 V. Higher V_e is favorable for larger electron emission, but complicates the ionization process due to molecular fragmentation. The ion energy, around several hundred eV, is determined by the ion acceleration voltage V_a. The deposition is made at high-vacuum so as not to cause any unwanted discharge or plasma in the vacuum chamber. The IAD method can be used to prepare films of low-molecular weight organic materials that can be evaporated in vacuum. On the other hand, polymers do not evaporate in general, and need special measures to be deposited by physical methods. There exist some polymeric materials that have low molecular weight and weak intermolecular interactions and can be forced to evaporate with accompanying chain scission. This category of polymers includes PE and PTFE.

The practical method of depositing polymers is to evaporate low-molecular weight source materials and polymerize them on the substrate surface. There might be two kinds of reactions [97]. One method is to co-deposit two monomers and polymerize them by stepwise reaction, such as polycondensation or polyaddition. The other scheme uses a chain reaction, such as vinyl

polymerization or ring-opening polymerization. For this purpose, the source material needs to be activated by some means to produce the reactive species such as radicals or ions. Polymeric film can be synthesized from single source material by selecting an appropriate molecule.

The most straightforward method of depositing polymer thin films is simply to force it to evaporate by elevating the temperature, followed by condensation of the vapor on the substrate. This method can be applied for low-molecular weight polymers that have relatively small intermolecular interactions. PE is the simplest polymer that falls in this category. However, the usable molecular weight of the source material is limited to several thousands, and the deposited film has the molecular weight of around 1000 because chain scission takes place concurrently with the evaporation. On the other hand, it has an advantage that the molecular weight dispersion of the film is narrow, which is favorable for controlling the film properties. The PE film has excellent electrical insulation. The capacitance voltage measurement of a PE/silicon MIS diode shows that the PE-semiconductor interface state can be reduced by depositing the film under an appropriate ion acceleration voltage [97].

PTFE is another simple but useful polymer that can be directly evaporated to form thin films. PTFE has remarkable chemical and thermal stability. Therefore, it is difficult to form thin films by the conventional wet process due to the lack of an appropriate solvent. Physical vapor deposition would make it possible to utilize its unique chemical and physical properties for thin film devices. PTFE in the molecular weight range of several thousand was deposited by IAD. The deposited film has uniaxial crystal orientation with the molecular chain lying in parallel with the substrate surface. The PTFE film is useful as a low-dielectric constant material and low-loss thin insulating layer. IAD method is also effective in reducing the pinhole density. As a consequence, the IAD film retains its insulation capability down to lower film thickness compared to the vacuum-deposited film [97].

Thin films of PTFE (mean molecular weight of source material 8500) were deposited in [98] by ionization-assisted deposition (IAD) method at different ion acceleration voltages V_a on substrates kept at room temperature. The molecular chains in the film were found to be oriented in parallel with the substrate, and the film has preferential crystal orientation to (100) plane. Although the ion acceleration did not give significant influence on the film orientation and chemical structure, IAD was effective to improve the surface smoothness. The

Cu decoration test revealed that the pinhole density in the film is reduced and the insulating capability is improved by depositing the film at V_a = 500 V. The result of dielectric loss measurement for A1/PTFE/A1 capacitors was in consistency. However, excessive ion acceleration deteriorated the insulating property, probably due to the dielectric breakdown that occurred in the course of deposition.

1.13 Ion beam assisted deposition

Ion beam sputtering deposition (IBSD) and ion beam assisted deposition (IBAD) are promising techniques for obtaining PTFE films of high quality. In IBSD and IBAD, the many experimental parameters are most independent of each other and all easy to control.

Deposition temperature can be as low as the ambient temperature. This greatly enlarges the choice of film and substrate materials. Film structure and property can also be easily tailored by adjusting the energy, dose and species of a second bombarding ion beam. IBSD and IBAD have been widely used in preparing thin films of many inorganic materials. In [99] IBSD and IBAD are employed to prepare thin films of PTFE.

PTFE thin films were prepared in an ion beam deposition system with its base vacuum of $2 \cdot 10^{-4}$ Pa. Films were deposited at a pressure of $1.5 \cdot 10^{-4}$ Pa. Commercial PTFE was used as the target. Two groups of thin films were deposited by IBSD and IBAD, respectively. IBSD thin films were prepared by singular sputtering of PTFE target. Sputtering energy varied from 700 to 1500 eV and sputtering current was fixed at 40 mA [99]. IBAD thin films were prepared by sputtering of PTFE together with a simultaneous Ar^+ beam bombardment of the growing film. Sputtering was performed by a 1000 eV, 40 mA, Ar^+ beam. Bombarding energy varied in the range of 200-1500 eV while bombarding current was always kept at 20 mA. Silicon and glass were used as substrates. During the deposition, substrates were water-cooled to maintain at room temperature.

For thin films prepared by IBSD [99], the IR spectra were almost identical and all very similar to the spectrum of original PTFE. The absorption band around 1200 cm^{-1} is strong. Peaks at 1220 and 1150 cm^{-1} can be attributed to C-F asymmetric and symmetric stretching vibrations in CF_2 groups which are characteristic of high molecular weight PTFE. So, thin films prepared by IBSD

may be structurally quite similar to the PTFE target material. There is a trend for the C-F band to broaden and shift toward lower wave number as the sputtering energy is decreasing. This indicates that sputtering at higher energy is favorable for obtaining polymeric PTFE thin films [99]. For thin films prepared by IBAD, the IR spectra were quite different. Absorption band around 1200 cm^{-1} seriously debates in comparison with those of IBSD films. This indicates that the films experienced serious defluorination under Ar^+ bombardment. As the bombarding energy increased from 200 to 1000 eV, the defluorinating effect was aggravated.

Films prepared by IBAD were all amorphous [99]. But films prepared by IBSD showed a certain degree of crystallization. So, IBSD films had a structure more similar to that of the target material. The integrity of polymer molecule was better than that prepared by IBAD. This is easy to understand because ion beam bombardment caused defluorination and irradiation damage in the film.

Polymers usually have a mean molecule weight of tens of thousands or greater. In addition, molecules are tangled with each other even for the simplest structure $(CH_2)_n$. It is hard to imagine that a polymer molecule can be completely sputtered by the incident ions. So, the sputtering deposition of polymers cannot be simply taken as atomic collisions and removal. A possible comprehension is to take it as a sequential process of decomposition and polymerization [99]. In the case of PTFE, the target material was first destroyed into CF_x or larger fragments by energetic ions. Then, these fragments were deposited onto the growing film surface. Since the incident fragments and the growing film surface both had dangling bonds, they were thus combined. As a result, the incident fragments extended the molecule chain length and the polymer molecules were thus "reconstructed". It should be noted that motivation energy was needed in the "reconstruction". The sputtered fragments by ion beam sputtering possess a few electron-volt energy which is higher than that in other processes, such as PECVD or RF sputtering. Higher energy is favorable to drive the fragments onto the growing surface and to combine with the already-exit chains. This can also explain why the films prepared by IBSD had some crystallization but RF sputtered PTFE films were amorphous [99]. No matter what the mechanism might be, it is true that polymers can be sputtering deposited into thin films, as demonstrated above by PTFE. The significance is that it provided possibility and convenience to make ultra thin films of polymers on various substrates and to prepare various composites of polymers with other materials.

1.14 Pulsed laser deposition of PTFE

A short review of the PTFE films deposition was presented in [100]. Due to remarkable processing difficulties, the development of reliable techniques for the formation of thin PTFE films is a technologically challenging task. The high melting temperature and the very high melt viscosity, as well as its insolubility rule out conventional processing routes. However, during the past years several techniques for thin-film formation have been developed, for example, RF- and ion-beam sputtering, electron-beam and ionization-assisted evaporation, plasma polymerization, and thermal chemical-vapor deposition.

One reason for the often reported poor electrical properties seems to be the more or less gradual deviation of the chemical structure of fluorocarbon films from conventional PTFE. These deviations are, for example, due to impurity contamination, extensive lowering of the molecular weight, oxidation, and fluorine deficiency.

A rather novel technique in the field of polymer thin-film formation is the technique of pulsed laser deposition (PLD) [101]. The application of this well-established procedure also to weak-absorbing materials like PTFE has been demonstrated by employing either bulk targets or pressed-powder targets. The investigation of the ablation products within the laser-induced plasma plume showed that the predominant species generated by laser ablation from bulk targets are CF_2, C_2F_4, and C_3F_6 radicals [102]. Repolymerization of these low molecular fragments has been suggested to be initiated by CF_3 and C_2F_5 radicals readily available within the plume.

The bulk-PLD process appears to be related to plasma-polymerization (PP) [103] as in the PP technique where similar radicals are involved in the repolymerization process. Therefore, the question arises whether this comparable film-forming mechanism will also lead to similar film properties. In particular, it is of special interest to clarify whether the radical fragments of the PLD films can trigger any substantial film-oxidation as observable in plasma-polymerized PTFE-like thin films (P-PTFE films) [104]. Film formation in PLD–PTFE from pressed powder targets (P-PLD–PTFE) is based on the laser-assisted transport of grains from the target to the heated substrate surface and the subsequent melting and crystallization of the material [105]. PLD films prepared by this technique are pinhole-free, with a distinct spherulitic, highly crystalline surface morphology. To get more comparable evidence about the PTFE-like nature of the films, it is desirable to look for the well-documented structural

PTFE phase and glass transitions in the deposited films.

Glass-like and structural first-order phase transitions were investigated in PTFE foils and PTFE-like films prepared by pulsed-laser deposition (PLD) and plasma polymerization (PP) in [100].

For comparison with the PP and different PLD films, PTFE films (thickness 25 μm) have been used, metallized with two Al-electrodes (100-nm thickness, 15-mm diameter) for dielectric measurements. KrF-laser radiation (wavelength 248 nm, fluence 0.5–6 J/cm^2, pulse duration 25 ns, repetition rate 1–10 Hz) has been used. Targets from polished pellets cut from a 13-mm diameter PTFE rod and pressed PTFE powder have been employed [100].

All PLD films were deposited at a substrate temperature of 355 °C within an Ar-atmosphere of 300 Pa on a Si-substrate partly metallized with a 100-nm thick Al-electrode for dielectric investigations. A smooth pinhole-free film was obtained from the powder target by annealing the film up to 500°C followed by cooling, both at a rate of 10°C per minute. Crystallization occurs within a temperature interval between 310 and 280°C; therefore, in this temperature region cooling was slowed down to 2°C/min to enhance the degree of crystallinity [100].

No annealing was done with the bulk-target film, as the films thermally degrade at high temperatures due to the evaporation of low-weight molecular fragments. Plasma polymerization was performed in a capacitively coupled 13.56 MHz radiofrequency RF plasma reactor [100]. The cyclic compound octafluorocyclobutane (C_4F_8) was used as feed gas for producing the radicals responsible for polymerization. C_4F_8 plasma contains large amounts of CF, CF_2, and CF_3 radicals, and is known to provide films with a large F/C ratio around 1.7. Films with thicknesses in the range of 1-4 μm were deposited on silicon substrates that were partly metallized with 25 μm Au and 25 μm Cu bottom electrodes for dielectric measurements. During film deposition the reactor pressure was adjusted between 20 and 70 mbar. Films were deposited under different RF power conditions in the range between 10 to 70 W. Deposition rates were on the order of 10–20 nm/min. On top of the PP films 100 nm-thick Al electrodes were evaporated [100].

Dielectric dilatometry and infrared spectroscopy enabled a structural comparison of conventional PTFE foils and PTFE-like films prepared by pulsed-laser deposition and plasma polymerization [100]. The promising features of PLD–PTFE films from pressed-sintered powder targets and their structural

similarity to conventional PTFE make these films interesting for possible new applications in electret devices. Furthermore, dielectric dilatometry proved to be an elegant means for investigating volumetric transitions in thin nonpolar polymer films.

PTFE has a variety of practical applications as a thin film in many fields, including microelectronics, bioscience, and display industry. Pulsed laser deposition (PLD) has been used to ablate PTFE and to deposit thin films [106]. PTFE films deposited by PLD consist of four major particles ranging from nano- to microscale in diameter. Because PTFE adheres poorly with other substrates, RF magnetron sputtering has been used to enhance adhesion, depositing a titanium thin film as a buffer layer between the glass and the PTFE. However, both CVD and RF-magnetron sputtering are expensive techniques for fabricating PTFE films without substantially compromising their chemical integrity. In [106] transparent, superhydrophobic PTFE thin films were successfully produced using PLD with various deposition times at room temperature. This technique produced thin films with low surface energy and nano-microstructural features in a single step.

The PTFE thin films exhibited a very high contact angle and low contact angle hysteresis (CAH). In addition, the films showed very good transparency in the visible (VIS) and near-infrared (NIR) region. These results suggest that the films will have many potential applications, including industrial, solar cell panel, and telecommunication device coatings.

PTFE thin films were successfully deposited in [106] on a glass substrate using pulsed laser deposition with deposition times ranging from 30-120 minutes.

The surface roughness of the films increased as deposition time increased, with micro/nanoscale roughness developing when deposition time increased over 60 minutes. This roughness made the surface superhydrophobic, having a contact angle of about 151.6^{o}. UV-VIS spectroscopic analysis of the PTFE films revealed that they were highly transparent, up to 90% in visible and near infrared ranges. Furthermore, when the deposition time was increased which increased the films' thickness the films were able to absorb 80%–90% of ultraviolet light in the wavelength range 300 nm. The researchers analyzed the PTFE films with an x-ray photoelectron spectrometer to find the chemical and elemental composition of their surfaces. Atomic force microscopy was used to determine the effect of surface roughness on hydrophobicity. These films have

many potential practical uses, from self-cleaning materials to solar cell panel coatings. Additionally, the low dielectric properties of PTFE make it ideal for communication antenna coatings and similar applications.

A KrF excimer laser with a laser wavelength of 284 nm, repetition rate of 10 Hz, pulse duration of 20 ns, energy density around 1.3 J/cm^2 per pulse, and spot size of ~5 mm^2 on the PTFE target was used for the deposition process [106]. The PTFE target, which was 50.8 mm in diameter and 3.18 mm thick, and glass substrate were mounted 7.5 cm away from each other. A turbo-molecular pump was used to evacuate the chamber to a pressure of $1.6 \cdot 10^{-7}$ Pa. The pulsed laser was directed through a focal lens to ablate the PTFE target and collect evaporated species on the glass substrate for different lengths of time — 30, 45, 60, 90, and 120 minutes — to produce different thicknesses of films. All film deposition was done under the same conditions at room temperature.

Superhydrophobic PTFE thin films were successfully deposited in [107] on glass substrates by PLD. A KrF excimer laser (λ = 248 nm) with laser pulse duration of about 25 ns at a repetition rate of 10 Hz was used in the sample fabrication. The laser fluence used throughout the deposition was about 1 J/cm^2. The deposition process was carried out at room temperature in vacuum at a pressure of about 1.33 Pa.

The distance between the glass substrates and the mounted PTFE bulk target was kept at 30 mm. Infrared absorption spectra of the deposited PTFE films were measured with a Fourier transform infrared (FTIR) spectrometer. The surface morphology of the prepared samples was inspected by a scanning electron microscope (SEM). Atomic Force Microscope (AFM) was used to examine the surface morphology and the surface roughness of the PTFE thin film deposited on glass substrates. The contact angle was measured using a standard automated contact angle goniometer with deionized water.

A large contact angle of about 170^o and low sliding angle was achieved. The surface morphology shows that the surface roughness increased with the number of laser pulses.

The water contact angle was related to the surface roughness. This result indicates that nano-scale surface roughness is important in producing superhydrophobic surface, since it will increase the volume of trapping air to achieve a large contact angle and low sliding angle with low contact angle hysteresis.

The described study provides a convenient one-step dry method to produce a

superhydrophobic surface with good self-cleaning properties.

PTFE films were deposited in [108] on cotton fabrics by PLD technique using a KrF 248 nm excimer laser at a repetition rate of 10 Hz. The laser energy density used throughout the experiment was fixed at 1 J/cm^2. Deposition was performed in a vacuum chamber that was evacuated to a pressure of 2.66 Pa. The deposition time was about 3 min. The fabric substrate was mounted on a holder inside the PLD chamber and placed 30 mm in front of the target.

The structure and morphology of the coatings were investigated by scanning electron microscopy (SEM) equipped with an energy dispersive X-ray system (EDX) operating at 20 kV. Fourier Transform Infra-Red spectrometry (FTIR) was performed. The water contact angle was measured using a contact angle meter. The contact angle was determined 60 s after the water drop was placed on the substrate.

Thus, nanostructured PTFE films were deposited on cellulosic cotton fabrics by a relatively low energy density PLD technique. The PTFE film coating renders cotton superhydrophobic with a water contact angle of 151^o.

PTFE thin films were prepared in [109] from pressed powder pellets via pulsed laser deposition by using ArF (193 nm) excimer laser. The irradiated area was 0.87 mm^2, and the repetition rate was 2 Hz. Films were deposited on KBr (for IR spectroscopy) and glass substrates placed onto a heatable holder. The applied laser fluences were in the 1.6–10 J/cm^2 range, FWHM = 20 ns. The substrate temperature was varied between 27 °C and 250 °C and post-annealing of the films was carried out in air at temperatures between 320 °C and 500 °C. Films deposited at 250 °C substrate temperature were found to be stoichiometric while those prepared at lower temperatures were fluorine deficient. Morphological analyses proved that the film thickness did not significantly depend on the substrate temperature and the post annealing at 500 °C resulted in a thickness reduction of approximately 50%.

It was demonstrated that the films prepared at 8.2 J/cm^2 fluence and annealed at 500 °C followed by cooling at 1°C/min rate were compact, pinhole-free layers. The adherence of films to the substrates was determined by tensile strength measurements. Tensile strength values up to 2.4 MPa were obtained. These properties are of great significance when PTFE films are fabricated for the purpose of protecting coatings.

Thin films of crystalline PTFE were prepared by pulsed-laser deposition [105] using 248 nm UV-excimer-laser radiation (fluence ϕ = 0.5-6 J/cm^2, pulse

duration 2.5 ns, repetition rate l-10 Hz. The laser spot size on the rotating PTFE target was 1 mm^2. Deposition was carried out in flowing argon at a pressure of 10 to 100 Pa. Pressed powder pellets and bulk PTFE have been employed as target material. The films were analyzed by means of optical polarization microscopy, stylus profilometry, capacity measurements, XRD, and IR spectroscopy. The effect of substrate temperature on the morphology and crystallinity of the films was studied.

Films deposited from pressed powder targets at sufficiently high T, consist mainly of spherulite-like microcrystallites [105]. These films are continuous, pinhole-free, well adherent to the substrate, and have a composition which is similar to that of the target material. It is suggested that film formation is based on laser-assisted material transfer with subsequent melting and crystallization [105]. They are superior to films deposited from PTFF bulk targets, cut from a solid rod, with respect to film morphology, deposition rate, film cohesion, and optical and electrical properties.

Deposition rates up to 160 A/s were obtained by PLD from the powder targets at a laser-repetition rate of 4 Hz. This deposition rate is much higher than that obtained by other techniques, except films deposited by synchrotron radiation, where a comparable rate was obtained [105].

At sufficiently high T, films are formed via melting and crystallization of laser transferred PTFE grains on the heated substrate. These films are continuous with a smooth surface and high transparency for non-polarized visible light. They are well adherend and pass the ‘Scotch tape test’.

Post-annealing of these films improves the morphology, and favors spherulitic growth up to lateral dimensions of several 100 pm. The dielectric constant of these films is l-5. The dielectric strength $(l\text{-}3)\cdot 10^5$ V/cm, and the resistivity up to 10^{12} Ω·m. With the polished PTFE targets, laser irradiation results in rapid depolymerization and ejection of low molecular weight fragments that repolymerizes on the substrate. The films are quite rough, show many particulates, and are opaque for visible light. In the ‘Scotch tape test’ the films show cohesion failure. The deposition rates are much lower than in the case of films deposited from powder targets. The electrical resistivity of the films is lower [105].

Films of PTFE were deposited in [110] by laser ablation. The deposition was carried out in a vacuum chamber with a background pressure of $1.33\cdot 10^{-5}$ Pa. The targets were prepared by pressing Teflon powder in pellets. The targets

were ablated using the fourth harmonic line (266 nm) of a Nd-YAG laser. The beam was directed into the chamber by a pair of plane mirrors and focused onto the target by a lens placed at the entrance of the vacuum chamber. The photon fluence was varied between 0.5 and 2 J/cm^2 in 10 ns pulse by changing the spot size at the target at constant deposition rate. Films were deposited in argon or CF, atmospheres at pressures ranging from 6.65 to 33.3 Pa.

The films were found to be stoichiometric with the correct optical properties. Authors of [110] suggested that UV absorption onsets the pyrolitic decomposition of PTFE leading to a monomer that subsequently repolymerizes onto a substrate. The interaction between a high energy laser pulse and a solid results in a fairly uncontrolled breakup of crystalliner structure with the expulsion of its fragments at high velocities. Consequently, it has been the general consent, that UV photoablation of organics is better suited for material removal than for material deposition. Nevertheless, the studies reported in [110] show that UV laser ablation can also be a useful tool for the deposition of thin polymer films. Upon UV absorption organic molecules are excited into such a high electronic state that it may result either in direct bond dissociation [ablative photodecomposition (APD)] or in rapid conversion to vibrational energy with considerable heating of the solid. It is the current belief,' that the ablation of organics occurs via APD.

It is believed in [110] that the deposition of PTFE by laser ablation is a thermally driven process. Although bond dissociation can be either thermally or photoinduced, chain cleavage in a media held at elevated temperatures onsets the pyrolitic decomposition of PTFE. This depolymerization reaction leads to monomer as the primary ablation product that ejected explosively from the target reaches a substrate where repolymerization occurs. The film composition was that of PTFE indicating that one can transfer matter from the target onto a substrate with the appropriate stoichiometry.

It can be assumed that the thermal decomposition of PTFE follows first order kinetics with monomer as the only important product at elevated temperatures. Vacuum pyrolysis of PTFE occurs via random cleavage, depropagation, and termination by disproportionation. Since the heat penetration depth is about 700 A, all the energy is essentially trapped within a light absorption depth during the laser pulse. A thermal time constant of 10^{-7}-10^{-8} s suggests that the exposed area is intensely heated during the short laser pulse with negligible diffusion of heat outside the laser exposed region.

Once a radical is formed, either by a thermally or photoinduced process, it is feasible for it to travel down the polymer chain leading to its unzippering dissociating about 10^5 bonds in the thermal time constant of PTFE. Therefore, a thermal route to decomposition would lead to the formation of an ablation plume composed primarily of monomer and not of random polymer fragments, as it would be expected from an ablative photodecomposition. The monomer, ejected at high kinetic energies, repolymerizes onto the substrate where the thin film is formed.

Thus, it has been shown in [110] that laser ablation can be used to deposit PTFE films. The photon energy initially absorbed as electronic excitation is rapidly converted to vibrational heating of the solid. The intense local heating results in the rapid depolymerization of the polymer chains. Then the explosive evaporation of monomers and low molecular weight fragments occurs. The monomers and the low molecular weight fragments arrive at the substrate where repolymerization takes place. This model suggests that UV ablation of PTFE is a thermally driven process.

1.15 Hot filament chemical vapor deposition

Frictional characteristics of PTFE films deposited by a hot filament chemical vapor deposition (HFCVD) method was investigated in [111]. PTFE films were deposited on glass substrates to thickness of 300 nm, 5 μm, and 10 μm.

Hot filament chemical vapor deposition (HFCVD) with the precursor hexafluoropropylene oxide (HFPO) enables polymerization of PTFE thin films [112,114] HFCVD contrasts with plasma enhanced CVD (PECVD) wherein PECVD fully functional linear polymers are not produced because the high-energy plasma environment results in nonselective chemistries leading to cross-linked networks. PECVD is capable of producing PTFE-like films, but these differ stoichiometrically from bulk PTFE. Further, when PECVD films are examined under X-ray photoelectron spectroscopy (XPS), a high concentration of dangling bonds is detected [112].

The presence of the dangling bonds is detrimental because it will lead to structural damage that will reduce the material's lifespan and result in inferior dielectric properties [112]. HFCVD allows for fine control over precursor reaction pathways and is capable of producing films spectroscopically indistinguishable from bulk PTFE. PTFE films deposited by HFCVD transpire

when the decomposition of hexafluoropropylene oxide gas occurs over a hot filament. The temperature of the HFPO gas and the substrate are controlled independently during the HFCVD method. This control allows for the thin PTFE film to be deposited on inorganic substrates [113], as well as temperature-sensitive substrate materials, because the substrate can be maintained at room temperature.

The PTFE film deposited by the HFCVD method is crystalline, with a lattice structure resembling that of bulk PTFE above 19 ^{o}C. X-ray diffraction (XRD) patterns show evidence of an increase in crystallinity, with the HFCVD film showing a characteristic peak at 18 ^{o}C representing the (100) plane of the hexagonal structure of crystalline PTFE above 19 ^{o}C [114].

1.16. Initiated chemical vapor deposition of PTFE electret

The technique of initiated chemical vapor deposition (iCVD) was evaluated for electret applications for the first time in [115]. PTFE is well known for its outstanding performance as a real charge electret material. For next-generation electret devices, a fluoropolymer thin film deposition technique is highly demanded to enable device miniaturization, precise fluoropolymer thin film control, as well as the integration into state-of-the-art industrial microelectronic processing lines.

Particularly for PTFE electrets, high quality PTFE thin films are needed. Nevertheless corona-charged PTFE thin films deposited, e.g. by RF sputtering show significant differences in charge storage and electrical properties compared to commercial PTFE, due to deviations from the original PTFE structure. PTFE thin films prepared by plasma polymerization suffer often from C=O group formation due to oxidation which increases also the dissipation factor of the film and consequently impairs the electret properties. Promising PTFE film fabrication approaches with pulsed laser deposition (PLD) are not suitable for large-area deposition.

The mentioned problems were solved in [115] by using PTFE thin films synthesized via initiated chemical vapor deposition (iCVD). This technique is known to preserve the original polymer functionality and to maintain a low substrate temperature, due to its mild deposition conditions, allowing thus the deposition on flexible organic substrates.

The iCVD process is already well established for PTFE thin film deposition

[116-118]. The technique does not involve any organic solvents, because the thin film is directly polymerized by a free radical polymerization on a substrate, which is cooled to room temperature. An initiator provides CF_3 end groups, preventing polar group formation at dangling bonds, and increases thus the dielectric performance regarding, e.g. dissipation factors. It furthermore increases the deposition rate significantly. Rates of several µm/h were reported for iCVD PTFE [116,118], so that the demanded film thickness of typically 10 µm for stable polymer electrets is easily obtained. The CVD-typical conformal growth enables furthermore smooth film surfaces and easy scale-up of the process to larger dimension substrates, making it interesting for industrial applications.

In [115] 13 µm iCVD PTFE films were grown on 0.5 mm aluminum. Perfluorobutanesulfonyl flouride (PFBSF, 95%) was mixed with hexafluoropropylene oxide (HFPO, 97%) at a ratio of 1/5. PFBSF was kept at room temperature and the PFBSF vapor was delivered through a leak valve to the reactor. The filament power of 50 W was applied during the deposition using a Nickel Chromium filament array. The pressure of 50 Pa inside the reactor was controlled. A point-to-plane DC corona discharge setup was operated at V_{tip} = -6.5 kV tip potential and used to irradiate the samples with ions in order to fabricate electrets.

The resulting surface charge of the electret (σ_s) after the ion irradiation generates an internal electric field (E_{in}) and an external electric field (E_{ex}) in the vicinity of a counter electrode. The initial value of σ_s is limited by the corona parameters and dielectric strength of the material [115]. Non charged iCVD PTFE films deposited on C-Si were used for the chemical characterization. The similarity of iCVD PTFE films to commercial PTFE is reported by many authors [117,119]. Also the X-ray photoelectron spectroscopy (XPS) and Raman spectroscopy conducted for this study confirmed the similarity of iCVD PTFE thin films to commercial bulk PTFE. The XPS spectrum showed a C1s peak around 292 eV, which can be assigned to the carbon in the backbone of the molecule.

The peak around 690 eV was identified as the primary F1s peak for the fluorine atoms, bound to the carbon backbone, while the peaks in the region between 800 eV and 900 eV can be associated with the Auger peak for fluorine. Recorded Raman spectra of iCVD PTFE thin films and bulk PTFE showed identical bands [115]. The 520 cm^{-1} band appears only in the iCVD PTFE thin

film spectrum. Other than that, the two spectra for bulk PTFE and iCVD PTFE showed excellent agreement and the obtained PTFE thin films seemed to be identical to commercial bulk PTFE.

The dielectric properties of the iCVD deposited films were determined by the impedance, measured in a thin film capacitor arrangement [115]. The relative permittivity was determined to $\varepsilon = 2.1$, which is typically reported for PTFE. The dissipation factor was calculated for commercial PTFE and iCVD PTFE from the impedance data [115]. No difference between iCVD PTFE and commercial PTFE was found. This confirmed that iCVD PTFE did not only resemble commercial PTFE with regard to chemical properties, but further on with regard to the dielectric properties.

Due to the CF_3 end-groups, the dissipation factor was much lower as typically observed in plasma polymerized PTFE thin films, because polar C=O group formation can be excluded [115].

The thermal charge stability of the iCVD PTFE thin film electrets was compared to conventional spin coated PTFE thin film. The measurement showed that fluoropolymers, like iCVD PTFE and initial PTFE, are superior to non-fluoropolymers [115]. The iCVD PTFE thin films showed even higher charge stability compared to conventional PTFE thin films. The activation energy of the traps was estimated to $E_a = 1.163$ eV. The iCVD technique enables furthermore to tune these properties by a change in the deposition parameters. They have a direct influence on the underlying free radical polymerization and hence the resulting structural properties, like molecular weight and crystallinity of the PTFE thin film [115].

The iCVD enables a direct control of the charge trapping behavior in the polymer film via the deposition parameters. This might be used to tune the charge trapping of the electret layer in e.g. electret memristors or similar applications. The presented results show that the iCVD technique is well applicable for the production of PTFE thin films for electret applications thanks to their excellent resemblance to commercial PTFE with regard to chemical and dielectric properties.

The mild deposition conditions enable furthermore the deposition on temperature sensitive substrates like flexible organic substrates for next generation organic electret devices.

CHAPTER 2
INVESTIGATION OF DECOMPOSITION AND CONDENSATION PROCESSES OF POLYMERS IN A VACUUM

2.1. Evaporation and condensation of polymers using an electron beam gun

Author of [69] for the first time used an electron-beam gun for evaporating polymers in a vacuum and for polymerization of decomposition products on the substrate where thin polymer films have been deposited.

Polytetrafluoroethylene (PTFE) was chosen as the starting material, as a representative of fluorine-containing polymers. PTFE is a non-polar polymer dielectric with good dielectric, mechanical, and optical properties, as well as high chemical resistance to acids, alkalis, and oxidants. It is most successfully applied where a combination of high heat resistance with good protective properties is required. Recently, PTFE has also found application in space technology.

For evaporation, powdered PTFE grade B was used. Substrates were steel, copper, aluminum, tin, glass-ceramics, and other materials used in electronic equipment. To study the modes of obtaining polymer films in vacuum and to carry out research, the authors developed and manufactured a vacuum unit, the block diagram of which is shown in Fig. 2.1.

The installation consisted of a vacuum unit, a mechanical pump, a vacuum-wire system and switching equipment, which provided the necessary sequence of operations. The chamber was made of stainless steel in the form of a parallelepiped with a volume of 0.15 m^3. There were vacuum-sealed inlets for two high-voltage electron guns with a linear vertical cathode, inlets for a substrate thermal heater, rated for current up to 1000 A, a thermocouple, a high-voltage input for supplying voltage to the substrate, and a high-voltage input for creating glow discharge. Electron-beam guns and a square-shaped crucible with dimensions of 2×2 cm^2 were placed inside the vacuum chamber, into which the evaporated substance was loaded. The crucible was covered from above with a grounded grid with either small (0.5 mm), or large (1.5 mm) cells. A substrate and a heater were also placed in the vacuum chamber. The evacuation system was provided for obtaining and maintaining a working vacuum from 0.01 to 0.05 mPa in the chamber.

The applied voltage was intended to power the mechanical pump, the heater, the cathode filament, and the diffusion pump heater. The main elements of the

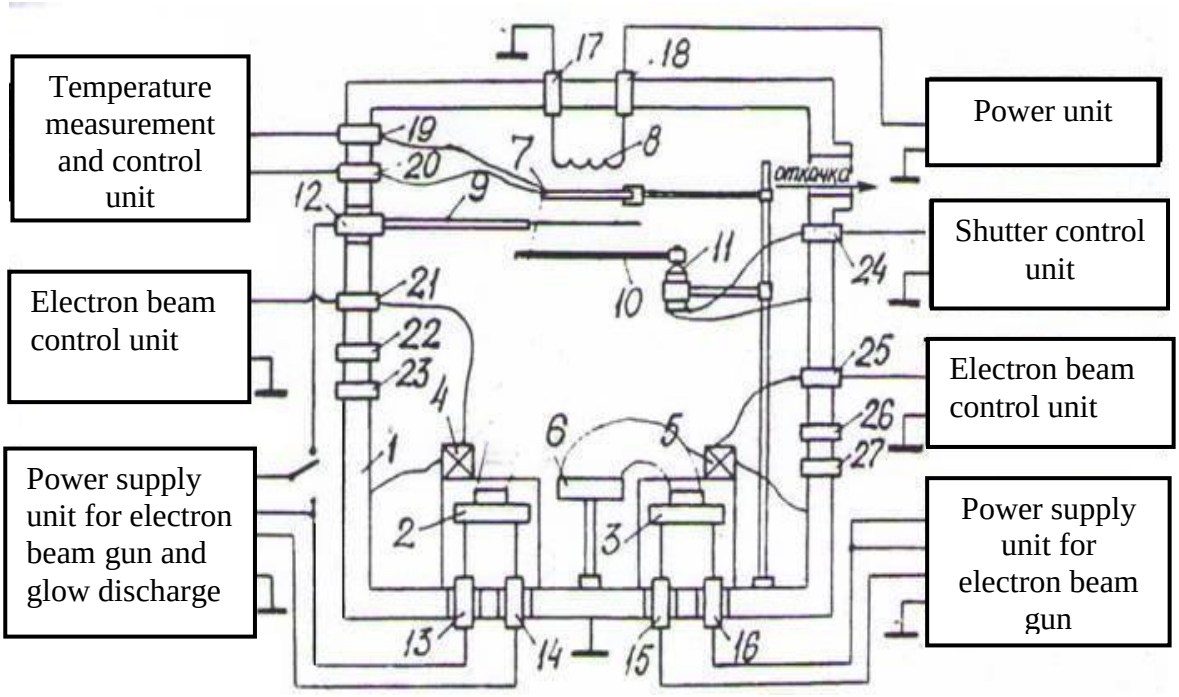

Fig. 2.1. The block diagram of the installation for production of polymer films from PTFE in a vacuum. 1 – vacuum chamber; 2,3 – electron beam guns; 4,5 – coils of electromagnets; 6 – crucible with evaporated substance; 7 – substrate; 8 - resistive heater; 9 – glow discharge electrode; 10 – damper; 11 – electric motor; 12-16 – high-voltage feedthroughs; 17-27 – leads.

unit were power transformers and voltage regulators. Voltage to create a constant electric field, in which the substrate was placed, was supplied through the high-voltage inlets from universal power sources.

The high-voltage unit was designed to power the electron-beam guns. The corresponding block diagram is shown in Fig. 2.2.

A glow discharge was used in a number of experiments to treat the substrate surface before depositing the films. The scheme for producing the glow discharge consisted of a high-voltage transformer and a rectifier. To monitor and control the temperature regime during production of films, a DC potentiometer and chromel-copel, chromel-alumel or copper-constantan thermocouples were used. The control unit was necessary to monitor the operation of all installation systems and consisted of measuring instruments, alarm devices and interlocking circuits.

The decomposition of PTFE was carried out under the action of the electron irradiation. For this purpose, an electron-beam gun was designed, description of

which is given in [69]. The tungsten filament of the cathode resistively heated to 2500 °C served as a source of electrons, which, by using an electrode system,

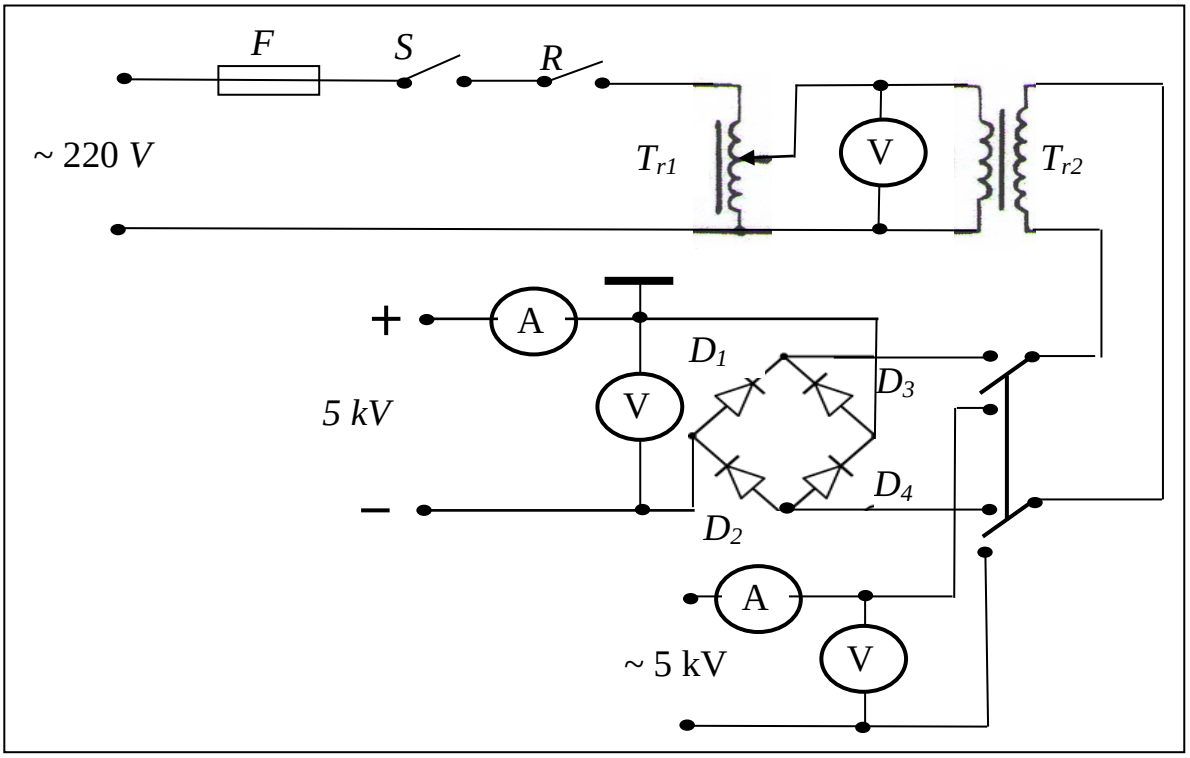

Fig. 2.2. Schematic diagram of the electron-beam gun and the glow discharge powering. *F*– fuse; *S* – magnetic starter; *R* – blocking relay; T_{r1} – autotransformer; *V* – voltmeter; T_{r2} – high voltage transformer; *D1-D4* – rectifier diodes; *A* – milliammeter.

formed the electron beam. The deflecting system directed the beam to the appropriate part of the crucible. To initiate polymerization on the substrate by electrons, the second similar gun was used. The guns were mounted on the flanges of the chamber. To prevent overheating of the anode, a water cooling system was provided during operation. In order to ensure the safety of work on the installation, the anode of the electron-beam gun was grounded, and the negative potential of up to 10 kV was applied to the cathode.

When studying the effect of the degree of surface cleaning on porosity and adhesion of films, the following types of surface pretreatment were used:

1) Rinsing the surface with ethyl alcohol;

2) Chemical cleaning of the surface in a solution containing 20 g/l of Na_3PO_4, 25 g/l of NaOH, 25 g/l of Na_2CO_3 at 90 °C for 20 min. Then the samples were washed in distilled water and dried. In the case of using thin steel sheets as substrates, the samples were washed, etched in 5% H_2SO_4 solution,

washed in distilled water, neutralized in 5% NaOH solution, washed again and dried.

3) Heating the steel substrate with a passing current at pressure of 6.7 mPa to 600 °C for 2-3 min followed by cooling the sample in vacuum immediately before deposition of the coating.

4) Surface treatment by glow discharge. The schematic diagram used to obtain the glow discharge is shown in Fig. 2.2. When processing in the DC glow discharge, the samples were placed in front of aluminum electrodes on the cathode or in the dark cathode space. The mutual arrangement of elements inside the chamber during the processing by the glow discharge is shown in Fig. 2.3.

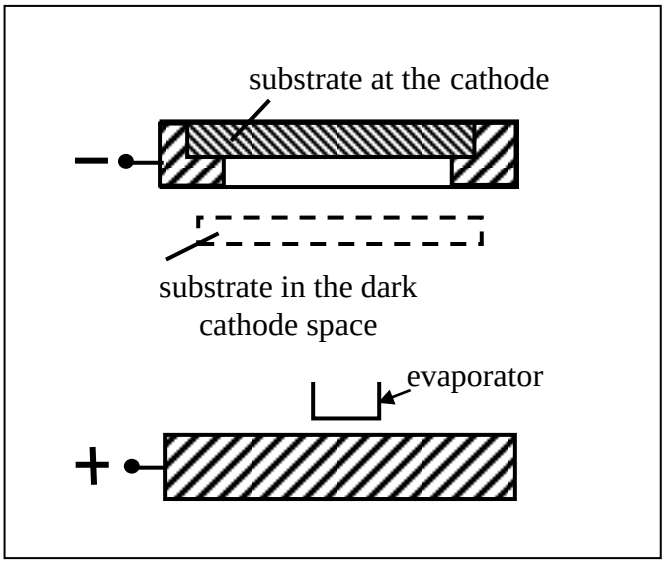

Fig. 2.3. Mutual arrangement of intracameral elements during the sample processing in a glow discharge.

It is known that the quality of cleaning by glow discharge depends mainly on two parameters: the current density of the discharge and the processing time. In our studies, the current density varied from 0.1 to 2.0 mA/cm^2, the processing time was 3-30 s. Working pressure was 1.0-10 Pa.

2.2. The mechanism of fluoropolymers destruction

Fluoropolymers containing C–F bonds, such as PTFE, have a high heat resistance, they are chemically resistant in various corrosive environments, are not wetted and do not swell in solutions.

When the temperature rises to 400-500 °C, PTFE begins to decompose with the formation of low molecular weight fragments. In early studies [120], deep decomposition of PTFE under the action of irradiation was observed, and recently it was decomposed by the action of fast electrons [84], which was not expected due to the high chemical and thermal stability of PTFE. Under the influence of radiation, PTFE is decomposed without structuring. PTFE was studied by a number of researchers [4,121].

In principle, the result of radiation exposure to organic compounds is not so much dependent on the nature of the radiation (α-particles, photons, X-rays, fast electrons), but on the electrons released by these particles as they pass through matter.

In accordance with the main mechanism of action, high-energy electrons cause ionization and excitation of molecules to higher energy states. The decomposition of excited molecules and the recombination of ions lead to the formation of new molecules and free radicals. The following chain mechanism is applied to all polymers that decompose to monomer, dimer, trimer and other oligomers, the formation of which occurs as a result of breaking the main chain [120]:

Initiation:

$$Q_n \rightarrow R_i + R_{n-1} \qquad 2k_1 n Q_n$$

Growth:

$$R_n \rightarrow R_{n-1} + M \qquad k_2 R_n$$

Transmission (intermolecular)

$$R_n + Q_m \rightarrow Q_n + Q_{m-e} + R_e \qquad k_3 R_n m Q_m$$

Breakage:

Disproportionation

$$R_i + R_j \rightarrow Q_i + Q_j \qquad 2k_{4d} R^2$$

Recombination

$$R_i + R_j \rightarrow Q_{i+j} \qquad 2k_{4c} R^2$$

In the above scheme, Q_n is the molar concentration of polymer molecules containing n units in the chain, R_i is the molar concentration of radicals in the sample, which have i monomer units, M is the molar concentration of monomer, and k is the reaction rate constant.

The rate of thermal destruction was studied by a number of researchers [69,120]. However, there were no papers devoted to the study of the depolymerization of PTFE subjected to radiation.

It can be assumed that some bonds break in the macromolecule chain when exposed to fast electrons, in addition to heating. The process begins with free radical initiation followed by a rapid stage of chain disintegration of the polymer into monomer units from the free radical end of the polymer chain. In this case, fragments larger than monomer fall into the composition of the gas phase. The carbon–fluorine bond breaking energy is higher than the carbon–carbon bond breaking energy [4]. Therefore, when the chain is broken, no fluorine atom transfer occurs. Breakage of the polymer chain during destruction leads to the appearance of free radicals capable of chain decomposition with the formation of monomer. In accordance with the mechanism of the polymers destruction, the reaction of chain destruction in PTFE can be written in the following form:

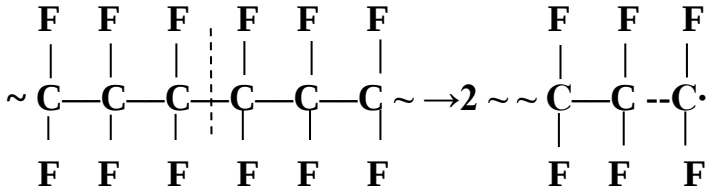

and further

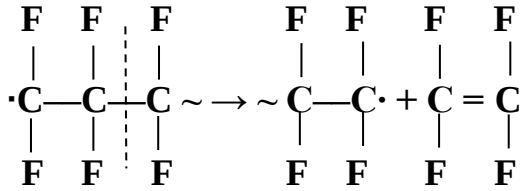

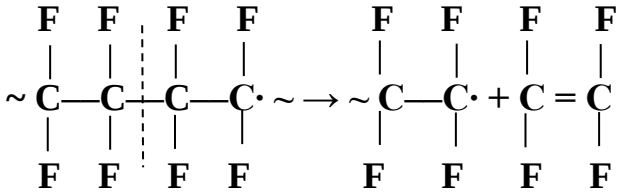

etc.

The initiation of the PTFE destruction process may occur due to the breaking of carbon–carbon bonds or some other weak bonds in the macromolecule itself or at its ends. Weak ties disappear in the first stage of the destruction. After this,

the breaks of the carbon–carbon bonds of the chain occur mainly due to the thermal motion of the macromolecules. These breaks occur randomly.

The main effects that occur in PTFE under the influence of high-energy radiation are the breaking of the main chains and the formation of free radicals, double bonds, cross bridges, and end bonds. Effects that alter the molecular weight distribution include the breakage of the main chain, the transverse and the terminal crosslinking.

As shown above, when the main chain is broken, the polymer molecule is divided into two smaller molecules that lead to a change in the molecular mass distribution of the polymer. It is highly doubtful that the probability of breaking a bond belonging to a monomer unit located near the end of the molecule will differ from the probability of breaking the bonds in the rest of the molecule. If rupture of the main chain is more likely in the immediate vicinity of the end of the molecule than in any other part of it, then smaller molecules should be easier destructed compared to larger molecules. Consequently, the smaller the molecular weight of PTFE, the greater the breaks number in the main chain. However, for PTFE such data is not available [122,123]. According to the authors of [124], this may be due to the following: since PTFE consists of molecules whose degree of polymerization is very high, even if several monomer units at the end of the molecule are more susceptible to breaking the main chain, such a terminal effect should not be detected due to the fact that the rest of the molecule behaves the same way.

The main assumption of theoretical considerations of polymer degradation is the constancy of the probability of breaking the main chain regardless of the position of the break point in the polymer molecule. If necessary, this assumption can be easily discarded [124], but it provides information about the main circuit breaks.

It follows from the above that in the theory of the polymers degradation it can be assumed that the probability of rupture of each monomer unit under the action of radiation is the same.

Consider the statistical theory of polymer destruction under the following assumptions [124]: all polymer molecules are linear, each monomer unit undergoes a gap with the same probability, the average molecular weight is quite large, and the total number of main chain breaks is significantly less than the total number of monomer units.

The equation expressing the change in the molecular mass distribution of linear molecules experiencing breaks in the main chain is:

$$\frac{\delta\omega(p,y)}{\delta y} = -p\omega(p,y) + 2p\int \frac{\omega(l,y)}{l}dl \qquad (2.1)$$

where $y = \int_0^t r dt$, t is time, p is the degree of polymerization of the polymer molecule, r is the rupture probability of the monomer unit per unit of time, $\omega(p,y)$ is the mass fraction of polymer molecules having p monomer units. Integration is carried out over all values of p.

The first member of the right-hand side of (2.1) corresponds to decrease in the number of molecules having p monomer units due to breaks in the main chain, and the last term corresponds to increase in the number of molecules having p structural units due to breaks in molecules containing p monomer units.

The value of y, equal to the number of breaks of the main chain per monomer unit, is called the density of the main chain breaks. We can assume that $y=r\cdot t$, since r does not depend on t.

The solution of equation (2.1) is

$$\omega(p,y) = \left[\omega(p,0) + p\cdot y\int_p^\infty \frac{2+yl-yp}{l}\omega(l,0)dl\right]\exp(-py) \qquad (2.2)$$

where $\omega(p,0)$ is the initial mass fraction.

From this solution one can get information about the degradation of the polymer. For calculating the average molecular weight, it is convenient to use the following expression:

$$f_i(y) = \int_0^\infty p^{i-j}\omega(p,y)dp, \qquad (j = 1,2,3,\ldots) \qquad (2.3)$$

which is called the j-M moment of the molecular mass distribution. It is also necessary to take into account that cross-linking and end stitching of the polymer material occuring during destruction.

From the point of view of obtaining polymer films and coatings, electron-beam decomposition of a polymer in vacuum is more promising than thermal decomposition for the following reasons: heat is supplied to the outer surface of the polymer material and the local micro parts of the molten material are heated, in which active fragments are formed. They are immediately evaporated from the surface of the material not participating in the diffusion process. In addition,

there is no loss of activity, and their number increases due to decrease in the reaction rate of the chain decay. Being reactive, these fragments can participate in the process of the secondary polymerization on the substrate and to form a polymer coating.

2.3. Effect of deposition and condensation conditions on the growth rate of PTFE films

The method of electronic initiation of polymerization allows us to effectively control the parameters of the deposition process and, therefore, to directionally change properties of the films. However, the advantages of this method can be realized only if a strictly constant flow of the original substance molecules is provided [69].

The main deposition parameters on which the growth rate, as well as structure and properties of the PTFE films depend are pressure and composition of residual gases in the reaction chamber, the decomposition rate and, accordingly, the energy of the electron beam decomposing the polymer, the distance from the source to the substrate, the angle between the normal to the evaporator and the direction to the substrate, the current density of electrons on the substrate and their energy.

The effect of pressure and composition of the residual gases in the reaction chamber, as well as the distance from the evaporator to the substrate, the angle between the normal to the evaporator and the direction to the substrate on the growth rate, structure and properties of PTFE films during thermal initiation of secondary polymerization condensing on the substrate fragments were investigated in the work [69].

Disadvantages of the thermal initiation are the low growth rate of the film (around 0.5 μm/min), since the substrate heating to 200-250 °C required for polymerization during the deposition of PTFE fragments leads to re-evaporation of low molecular weight fragments. Therefore, a low utilization factor of PTFE is obtained. Energy is also required for heating the substrate by passing current or by radiation (10 V, 200 A). On this basis, it is desirable to initiate the secondary polymerization reactions on the substrate at room temperature. This is possible, if the substrate is irradiated by either UV light, or electrons, or it is placed in a glow discharge.

In [69], the substrate was illuminated with 400 W and 1000 W mercury lamps. Evaporation was carried out at different distances between the evaporator and the substrate (5 cm, 10 cm, 20 cm) that provided a different rate of deposition of fragments on the substrate (inversely proportional to the square of the distance between the evaporator and the substrate). As shown by studies of the films, the desired result of UV irradiation was not obtained, because low molecular weight porous films were formed.

As shown below, the minimum energy of the electrons bombarding the substrate, at which the secondary polymerization reactions are initiated, is 30-50 eV. The same energy is obviously necessary to initiate ultraviolet polymerization. This corresponds to a wavelength of UV light of about 0.03 μm or less. In the spectrum of used mercury lamps, unfortunately, there was no UV light with wavelengths of 0.03 μm.

The possibility of initiating polymerization reactions on a substrate by a glow discharge was also investigated. A glow discharge occurs at a pressure of the order of hundreds of Pa and disappears at the pressure of 0.1 Pa. During the operation of the electron beam gun, breakdowns occur at such pressure. This leads to significant interruptions in evaporation of the PTFE, since the electron beam gun does not work most of the time, the mean free path of the fragments at glow discharge pressures is $\lambda \sim 6$ cm, i.e. it is shorter than the distance between the evaporator and the substrate (10 cm). This increases the likelihood of collision of oxygen with active fragments leading to their fragmentation. This also results in significant decrease of the films growth rate (to 0.05 μm/min), while presence of oxygen in the films significantly increases.

Due to the drawbacks of the thermal treatment, the ultraviolet irradiation and initiation of secondary polymerization reactions on a substrate by a glow discharge, the authors of [69] proposed a method of initiating secondary polymerization reactions of active fragments on the substrate by irradiation (bombardment) of electrons. Its essence is that a beam of electrons created by a gun irradiates (bombards) the substrate. The electrons bombarding the substrate, initiate the reactions of the secondary polymerization of the fragments. The decomposition and evaporation of PTFE is produced by an electron beam created by the second electron beam gun. The main advantage of this method is the high film growth rate, the ability to precisely control the parameters of the technological process (electron energy, electron current density), low energy

losses, and the higher utilization rate of the polymer material than in the case of other initiation methods.

A study was conducted of the effect of the decomposition rate, as well as the power of the electron beam decomposing the polymer, the current density of the electrons irradiating the substrate, and their energy on the growth rate of the PTFE films. Since the active fragments mass decreases with increasing power of the electron beam [69], which produces heating and decomposition of PTFE, the condensation rate depends on the decomposition rate and, consequently, on the rate of PTFE evaporation.

It was found that during decomposition of PTFE by heating it with an electron beam, the evaporation rate decreases by a factor of 1.5 in 1.5 minutes with the evaporation power of 30 W/cm^2. This is obviously connected with the charging of the upper layers of the evaporating PTFE. When this happens, defocusing of the electron beam bombarding the evaporator occurs. As a result, the degree of PTFE destruction decreases and, accordingly, the number of active fragments evaporating from the surface decreases, which leads to decrease in the film growth rate. Therefore it is necessary to reduce the charge on the PTFE surface. To drain the charge from PTFE loaded into a crucible with dimensions of 2 x 2 cm^2, the crucible was covered first with a large cell (1.5 mm) grid and then with a small (0.5 mm) one. The grid was grounded. The power (accelerating voltage and current) of the electron beam which decomposed the polymer was varied in the process of evaporation.

To compare the rates of evaporation and film growth, PTFE was evaporated under identical conditions without a grid. Data on the evaporation rates of PTFE and film growth at various powers (accelerating voltages and current densities are given in Table 2.1). It follows from the table that presence of the grid increases the rate of evaporation, and the growth rate of films also increases. However, it should, be noted that as PTFE evaporates, its surface ceases to be in a contact with the grid, and the grid action becomes ineffective. Moreover, it starts to screen the electron beam irradiating PTFE.

It should be noted that the most effective grid effect is observed at the accelerating voltage of about 2 kV and the current density of 10 mA/cm^2. More efficient, as one would expect, is a grid with a small cells, since it removes charges from the larger surface of the PTFE. At the same time, the shielding effect of the grid with a large cell is more pronounced affecting the application of thick coatings. However, industrial electronics are more interested in

obtaining thin polymer films and coatings with a thickness of 0.2-4 μm. Therefore, the screening effect is insignificant with this technology.

From Table 2.1 it also follows that as the power of the electron beam increases (due to increase of current density up to 25 mA/cm^2), the effect of the grid on removing the charge from the surface decreases and the rate of evaporation decreases and the film growth rate decreases as well. This is due to the fact that the grid with the used mesh size (0.5 mm) does not remove the entire charge, and its shielding effect is more pronounced.

Table 2.1

The ratio of the film growth rate under various modes of deposition of PTFE through the grids to the growth rate without grids (V_c/V)

Accelerating voltage of the electron beam, U (kV)	1.0	1.5	2.0	2.5	1.0	1.5	2.0	2.5
Electron beam current density j (mA/cm^2)	V_c/V (grid with small cells)				V_c/V (grid with large cells)			
10	–	4.5	4.1	2.0	–	3.5	3.2	1.5
15	3.7	3.6	3.6	1.1	3.0	1.6	1.5	1.0
20	1.2	1.3	1.3	0.8	1.2	1.4	1.3	0.8
25	0.8	1.3	1.3	0.7	0.8	1.1	1.0	0.6

The active fragments of PTFE evaporated from the surface under the action of electron-beam heating are deposited on the substrate, condensed on it, and participated in the secondary polymerization reactions under the action of electrons leading to the formation of the PTFE film. When fragments hit the substrate, they can either immediately be fixed on the surface of the substrate, or migrate along it. They can also re-evaporate from the substrate surface, if they have enough energy.

Polymerization caused by irradiation (fast electrons) at ordinary temperatures always proceeds by the radical mechanism [69]. The action of all types of radiation, ultimately, is reduced to the interaction of charged particles with electrons of the matter. It can be assumed that a fast electron loses energy in portions of different size while moving through a substance, as a result of interaction with the electrons of the substance. These losses in most cases are 20–50 eV in liquids and solids [69]. It follows from the Heisenberg uncertainty principle that the lost energy ΔE cannot be localized on a single molecule, but should cause a collective excitation of a certain region, i.e. delocalized arousal

occurs [69]. The value of λ in this region can be found from the following relationship:

$$\lambda = \frac{h\nu}{\Delta E},$$

where h is Planck's constant; v is the electron velocity. It is known that $v = 10^8$ m/s for fast electrons and, therefore, $\lambda \approx 0.02$ μm. Areas, in which the energy of a fast particle is dissipated, are called "spurs". The path of a fast electron through the substance (track) is a sequence of spurs separated from each other at a distance of about 1 μm.

At present, little is known about properties of the collective excitation occurring in spurs at the first moment after the formation of a track. It can be assumed that processes occur in the first 10^{-14} s leading to the formation of secondary electrons with low energy and radical cations. Having lost energy, the secondary electron turns into a thermal electron at the end of the path.

During the time of the order of 10^{-14}-10^{-13} s, various processes involving thermal electrons, radical cations and excited molecules develop and partially end in spurs. These processes either compete with each other, or quickly follow one another. In contrast to the first stage of the spur life, all these processes are associated with oscillations of nuclei, elementary displacements of nuclei, rupture and formation of chemical bonds. The processes occurring in the spurs at this stage can be divided into processes involving thermal electrons and primary cation-radicals and into processes involving excited molecules.

All the considered processes ultimately lead to the formation of a radical, i.e. the longest living particles. Reactions involving radicals are the third stage of the process. The formation of radicals cannot occur for the time less than 10^{-13}-10^{-12} s from the moment of spur's formation.

It is important to know for polymerization what proportion of the radicals that have arisen will react with each other and what proportion can be used for other reactions, for example, to initiate polymerization. If particles (radical precursors) have a long lifespan, then they have time to diffuse far beyond the original spur, and the radicals formed from them are dispersed in a large volume that reduces probability of recombination of the primary radicals.

The mechanism of this process as applied to the formation of a polymer film on the surface can be represented qualitatively as follows. In the case of an inelastic collision of electrons with condensed fragments, electron levels are excited in the latter leading to dissociation of molecules into fragments (ions and

radicals). Fragments with kinetic energy sufficient to overcome the bonding force with the surface are re-evaporated. Fragments that did not receive sufficient kinetic energy during the decay of fragments remain on the surface. They can react with each other or with fragments condensing on the surface of the substrate that leads to formation of a polymer film on the substrate. Thus, the polymerization rate and the film growth rate will significantly depend on the current density (concentration of the bombarding electrons) and on the accelerating voltage (electron energy).

In this regard, the authors of [69] investigated the effect of the current density of electrons bombarding the substrate and the accelerating voltage (electron energy) for various modes of polymer decomposition (PTFE) on the film growth rate. Fig. 2.4-2.7 shows dependences of the deposition rate of the polymer coating on the current density of electrons bombarding the substrate at various electron energies and different decomposition modes of PTFE.

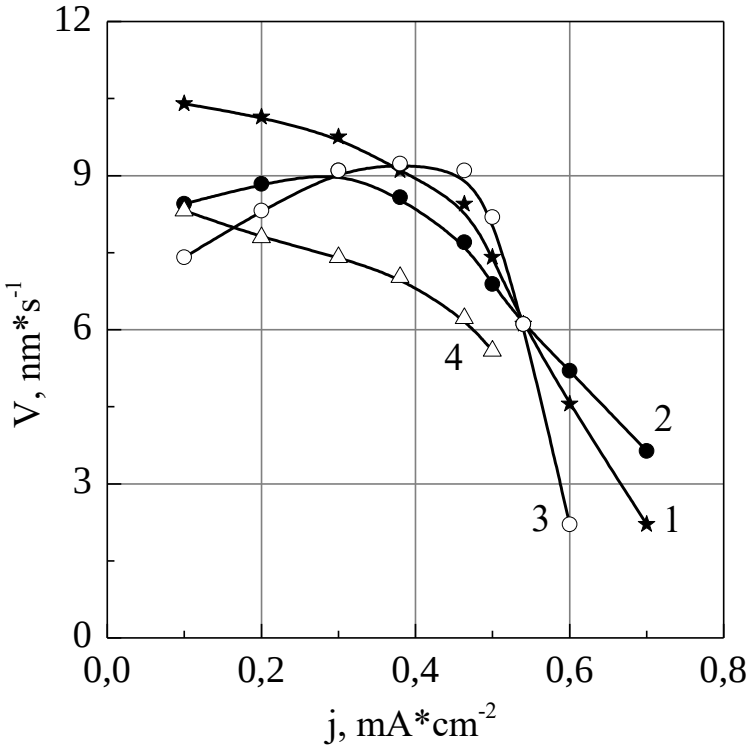

Fig. 2.4. Dependence of the PTFE film growth rate (V) on the current density (J) of electrons irradiating the substrate at various energies (E) of electrons: 1 – 300 eV; 2 – 400 eV; 3 – 500 eV; 4 – 700 eV. Specific power (P_2) of the electron beam is 20 W/cm^2 (1 kV and 20 mA/cm^2).

It follows from presented plots that the film growth rate decreases from 15 to 1.5 nm/s with increasing the electron current density. This, obviously, may be due to the increasing role of the destruction process taking place along with the

polymerization process. The destruction leads to the decomposition of the polymer material to low molecular weight fractions and monomer that evaporates from the surface of the substrate, so the film thickness decreases. The destruction of the films with increasing the electron current density is indicated by studies carried out by methods of the electron paramagnetic resonance and the infrared spectroscopy.

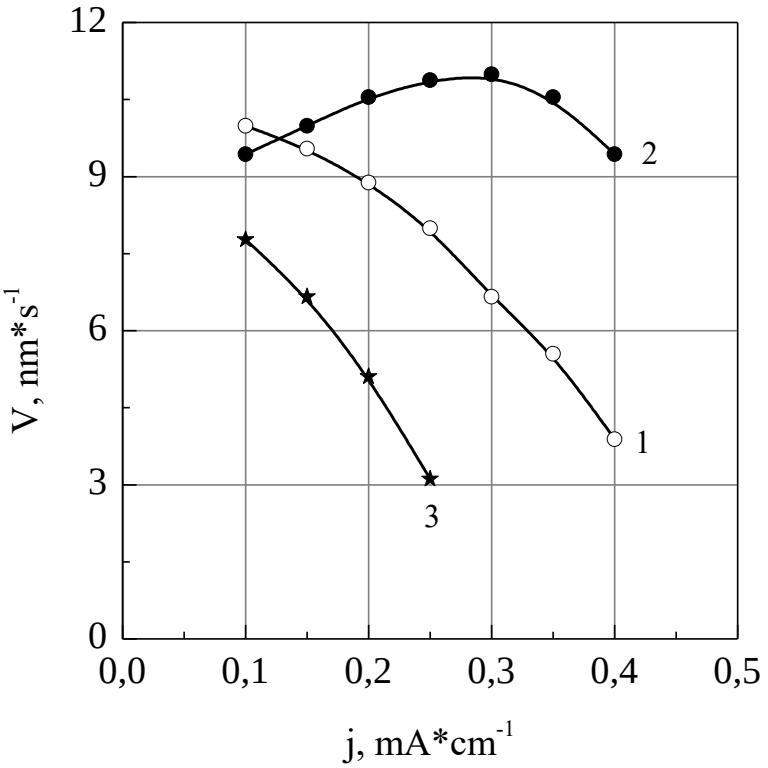

Fig. 2.5. Dependence of the PTFE film growth rate (*V*) on the current density (*j*) of electrons irradiating the substrate at various energies (*E*) of electrons: 1 – 300 eV; 2 – 500 eV; 3 – 700 eV; Specific power of the electron beam is 20 W/cm^2 (2 kV and 10 mA/cm^2).

The film deposition rate increases with decrease of the electron current density to 15 nm/s at the beam power of 60 W/cm^2. This occurs due to the slowing down of polymerization and destruction processes. The degree of polymerization, and hence the molecular weight are reduced that is confirmed by the infrared spectroscopy, the differential thermal analysis and the thermo gravimetric analysis. The slowing down of the destruction process leads to decrease in the proportion of monomers, dimers, and trimers in the film meaning that the re-evaporation of the active fragments from the crucible decreases.

It follows from the graphs in Fig. 2.4-2.7 that the same film growth rate can be achieved with a small accelerating voltage (electron energy) and with the higher current density of electrons on the substrate. This is due to the fact that electrons with low energy are involved in the smaller number of acts of initiation the secondary polymerization reactions of PTFE active fragments. However, increase in the current density leads to increase in the number of polymerization events. This compensates decrease in their energy and, ultimately, the degree of polymerization is almost the same.

Fig. 2.4-2.5 shows dependence of the film growth rate on the electron current density at the power of the PTFE electron beam decomposition equal to 20 W/cm^2. It can be assumed that the number of electrons initiating the polymerization at the low current density is insufficient for a given number of active fragments deposited on the substrate (dimers, trimers, etc.). However, as follows from the graphs in Fig. 2.6-2.7, the same degree of polymerization can be achieved at the lower current density with increase in the energy of electrons bombarding the substrate. This is probably due to the fact that electrons with

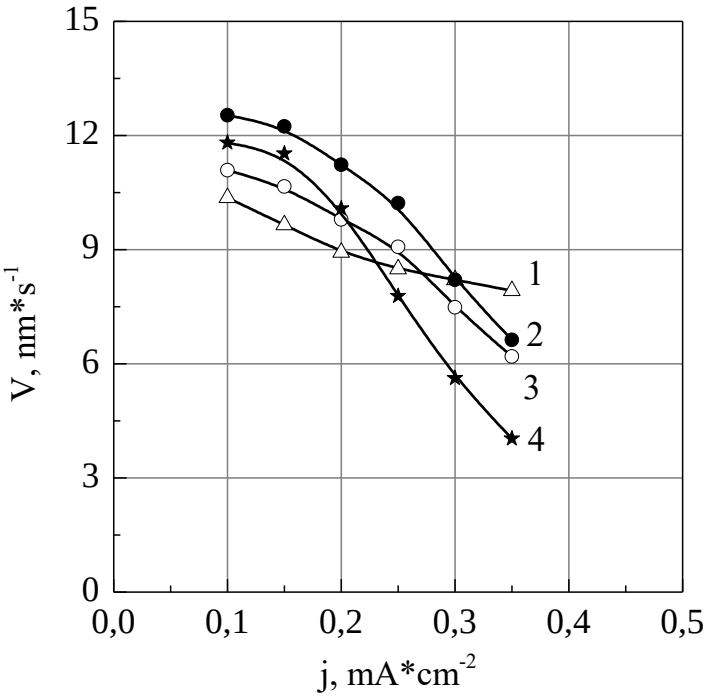

Fig.2.6. Dependence of the PTFE film growth rate (*V*) on the current density (*j*) of electrons irradiating the substrate at energies (*E*): 1– 300 eV; 2 – 400 eV; 3 – 500 eV; 4 - 600 eV. Specific power of the electron beam is 20 W/cm^2 (2 kV and 20 mA/cm^2).

high energy cause a large number of initiating acts in a larger volume of the

deposited fragments. The resulting radicals recombine to a lesser extent, thereby promoting the polymerization.

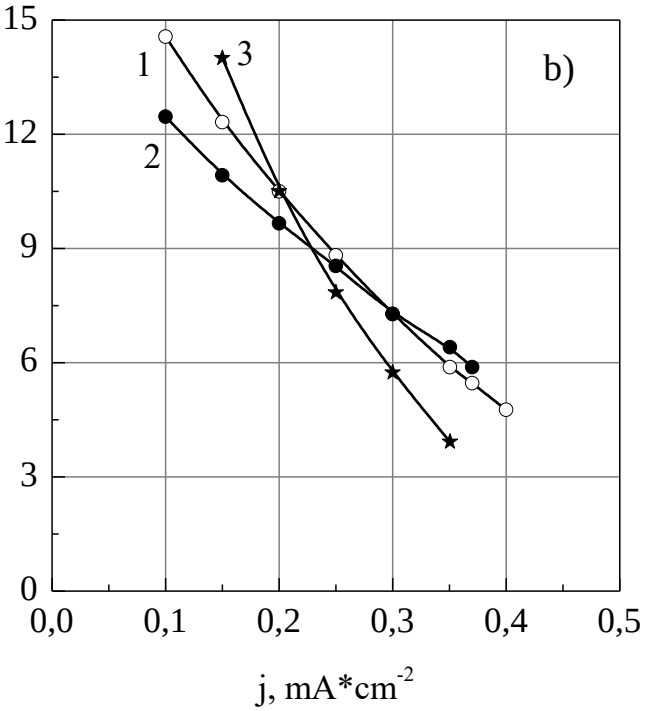

Fig. 2.7. Dependence of the PTFE film growth rate (*V*) on the current density (*j*) of electrons irradiating the substrate at energies (*E*): 1 –300 eV; 2 – 500 eV; 3 – 700 eV; Specific power of the electron beam is 60 W/cm^2 (3 kV and 20 mA/cm^2)

The growth rate and formation of the polymer film V first slightly decreases to 6 nm/s and then increases to 15 nm/s with increase in the power of decomposition from 20 to 35 W/cm^2. It can be assumed that this is due to the fact that if the power of the electron beam increases, two opposite processes compete. On the one hand, the decomposition of the polymer leads to a deeper destruction of the polymer material (the proportion of monomers in the total number of evaporating fragments increases) and the molecular weight of the fragments shifts towards smaller values. However, the number of fragments reaching the substrate increases, because the total number of evaporating active fragments increases.

2.4. The utilization rate of the polymer material during the deposition of coatings in a vacuum

As noted above, the process of destruction proceeds during the deposition of fragments on a substrate along with the polymerization. As a result, some of the

fragments, after being decomposed into low molecular weight fractions and monomer, are re-evaporated from the surface and disappeared. Thus, not all the polymeric material decomposed by the action of the electron beam on the active fragments, but only a part of it, participates in formation of the polymer coating (film).

An important characteristic of this technology is the utilization rate of a polymeric material determined using the procedure given in [69] and calculated as $k_u = M/M_0$. Here M_0 is the mass of the evaporated polymer; M is the mass of fragments condensed on the hemisphere with the center at the evaporator position. Thus, $M = m\pi R^2$, where m is the amount of substance condensing on the surface unit of the hemisphere at $\varphi = 0$, and φ is the angle between the

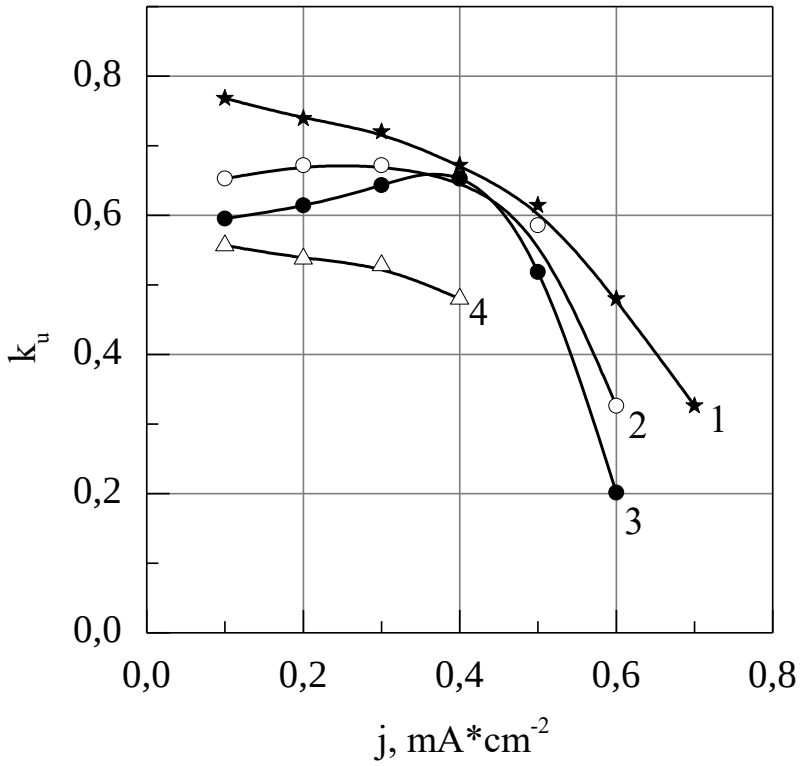

Fig. 2.8. Dependence of the utilization factor (k_u) of PTFE on the current density (j) of electrons irradiating the substrate at various energies (E) of electrons: 1 – 300 eV; 2 – 400 eV; 3 – 500 eV; 4 – 700 eV; Specific power of the electron beam is 20 W/cm^2 (1 kV and 20 mA/cm^2); Specific power of the electron beam is 20 W/cm^2 (1 kV and 20 mA/cm^2).

normal to the evaporator and the direction to the substrate; R is the distance between the evaporator and the substrate (hemisphere radius).

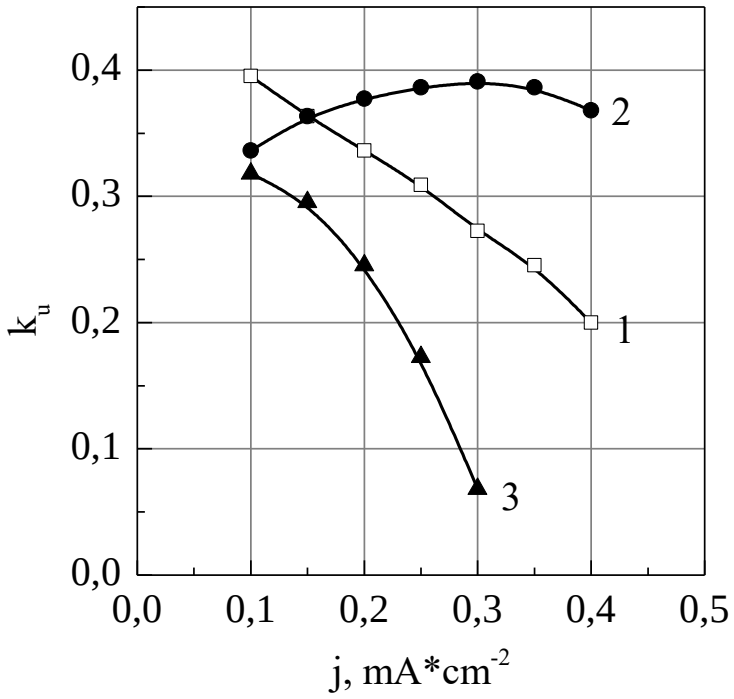

Fig. 2.9 Dependence of the utilization factor (k_u) of PTFE on the current density (j) of electrons irradiating the substrate at various energies (E) of electrons: 1 – 300 eV; 2 – 500 eV; 3 – 700 eV. Specific power of the electron beam is 20 W/cm^2 (2kV and 10 mA/cm^2).

Therefore, it is advisable to investigate the effect of the power of the electron beam decomposing the polymer, the current density and the energy of the electrons bombarding the substrate on the utilization rate of the polymer material. It is also interesting to compare the values of the coefficient of using the polymeric material (PTFE) while producing films by thermal initiation and by electronic initiation of the secondary polymerization reactions.

Data indicating the dependence of the utilization rate of the polymer material on the decomposition mode (electron beam power) and deposition conditions (substrate temperature, current density of electrons bombarding the substrate), respectively, in thermal and electronic ways of initiating secondary polymerization reactions of active fragments condensing on a substrate, are shown in Fig. 2.8-2.12.

It follows from the figures that the utilization rate of the polymer material (PTFE) with the electronic initiation of polymerization is higher than with the thermal one and reaches a value of 0.75 versus 0.7.

It should be noted that this utilization rate of the polymer material can be

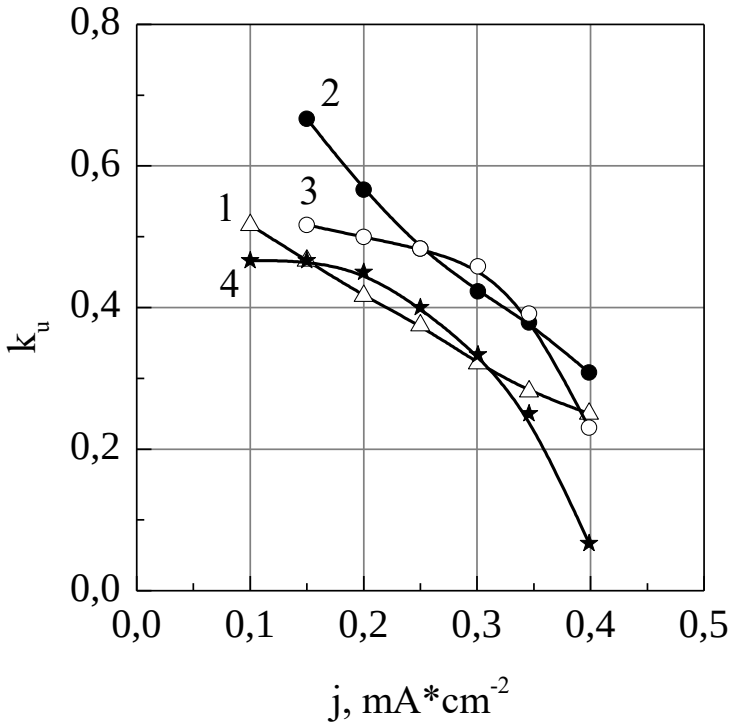

Fig. 2.10 Dependence of the utilization factor (k_u) of PTFE on the current density (j) of electrons irradiating the substrate at various energies (E) of electrons: 1 – 300 eV; 2 – 400 eV; 3– 500 eV; 4 – 600 eV; Specific power of the electron beam is 40 W/cm^2 (2 kV and 20 mA/cm^2).

achieved if the temperature of the substrate during thermal initiation of the secondary polymerization reactions does not exceed 50 °C. However, the film has low molecular weight under these conditions. Moreover, it is porous, it has poor adhesion to the substrate, it has poor dielectric properties, and it rapidly ages. The improvement of the above properties is noticeable at the condensation temperature (substrate) of 250 °C. But under such conditions of deposition the utilization rate of the polymer material (PTFE) decreases and reaches a value of 0.2 if the power of the electron beam decomposing the polymer is 100 W/cm^2.

At the same time, the films obtained by electronically initiating the secondary polymerization reactions of the PTFE active fragments on the substrate have good dielectric properties, low porosity, good adhesion, as will be shown in Section 3, with the utilization rate of the polymer material (PTFE) about 0.6. As follows from Fig. 2.10, this coefficient of using the polymer material is achieved if the power of the electron beam decomposing PTFE is

about 40 W/cm^2, the electron energy is 350-450 eV, and the electron current density is 0.2-0.25 mA/cm^2.

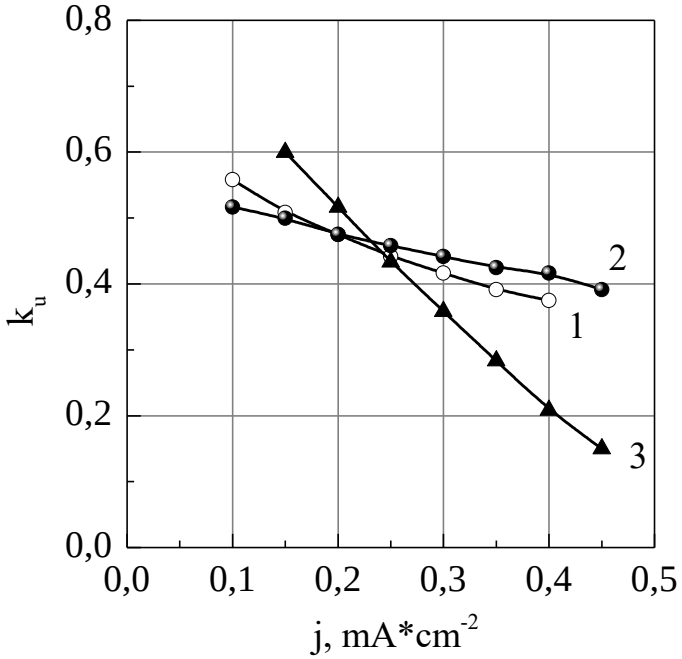

Fig. 2.11 Dependence of the utilization factor (k_u) of PTFE on the current density (j) of electrons irradiating the substrate at various energies (E) of electrons: 1 – 300 eV; 2 – 500 eV; 3 – 700 eV. Specific power of the electron beam is 60 W/cm^2 (3 kV and 20 mA/cm^2).

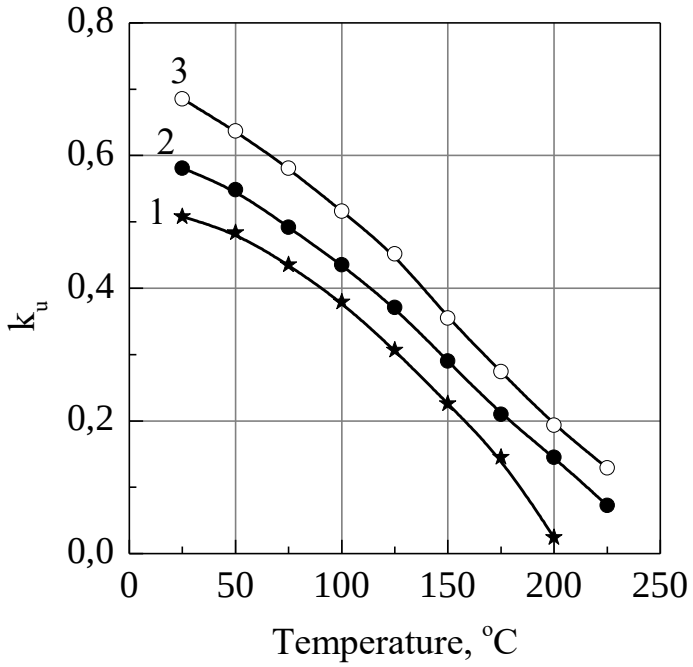

Fig.2.12 Dependence of the utilization factor (k_u) of PTFE on the condensation temperature (substrate) (T_c) at various specific power (P) of the electron beam: 1 – 10 W/cm^2; 2 – 30 W/cm^2; 3 – 100 W/cm^2.

CHAPTER 3
POLYMERS DECOMPOSITION AND CONDENSATION PROCESSES BY MEANS OF A GAS-DISCHARGE ELECTRON-BEAM GUN WITH A HOLLOW CATHODE

3.1. Installation, materials, in-chamber devices, systems and methods for controlling the deposition process

Serial equipment can be successfully used in installations for the deposition of polymer coatings in vacuum currently used for thermal evaporation of metals and dielectrics. Methods for producing thin polymer coatings from monomer are described in [125,126]. The initial product is supplied in the vapor-gas state to the vacuum chamber and a certain pressure is maintained by injecting inert gas.

The disadvantage of this technique is the requirement of continuous supply of thoroughly cleaned monomer with a constant speed from the external tank into the working chamber. The presence of a vessel with a gaseous monomer under high pressure, especially with a fluorine-containing substance, dramatically increases the risk of fire and explosion during operation. It is difficult to implement automatic modes of operation in installations of this kind. The distance between working electrodes does not exceed 15-30 mm that imposes strict requirements on the dimensions of the processed samples. Increase in the inter-electrode distance leads to increase in the ignition voltage of the glow discharge, and hence the increase in probability of the electrical breakdown of the film. The utilization rate of the original substance is extremely low. The main disadvantage due to which this method did not go beyond the scope of laboratory research is the low deposition rate (a few μm/min) and instability of parameters.

A method [69] is also known, in which the initial polymer is placed in a crucible and heated by the resistive or the electron-beam method. Polymer molecules are degraded into active fragments, some of which condense on a substrate located above the crucible. To obtain coatings from fluorine-containing polymers with good physicochemical and adhesive properties, it is necessary to heat the substrate to 150 °C for PCTFE and to 250 °C for PTFE. Heating the substrate causes re-evaporation of a part of the condensed fragments and dramatically lowers the coating formation rate.

To eliminate these shortcomings, the author of [69] proposed an installation whose structural block diagram is shown in Fig. 3.1. In addition to those shown in the diagram, eight electric vacuum feedthroughs were placed in the chamber walls allowing thermal evaporation and automation of the process. The starting material in the form of polymer powder, a solid piece, or pellets was placed in a crucible, and then it was decomposed by the resistive or the electron beam heating method. The decomposition products were condensed on the surface of the substrate treated with a high-frequency glow discharge. If in [127] the discharge was ignited between two plane-parallel electrodes, in a new system created by us, one electrode was the element to be coated and the second electrode was the wall of the vacuum chamber. To construct the electron beam gun under conditions of a glow discharge (1-20 Pa), the author of [69] used a gas discharge electron beam gun (GDEBG) with a hollow cathode.

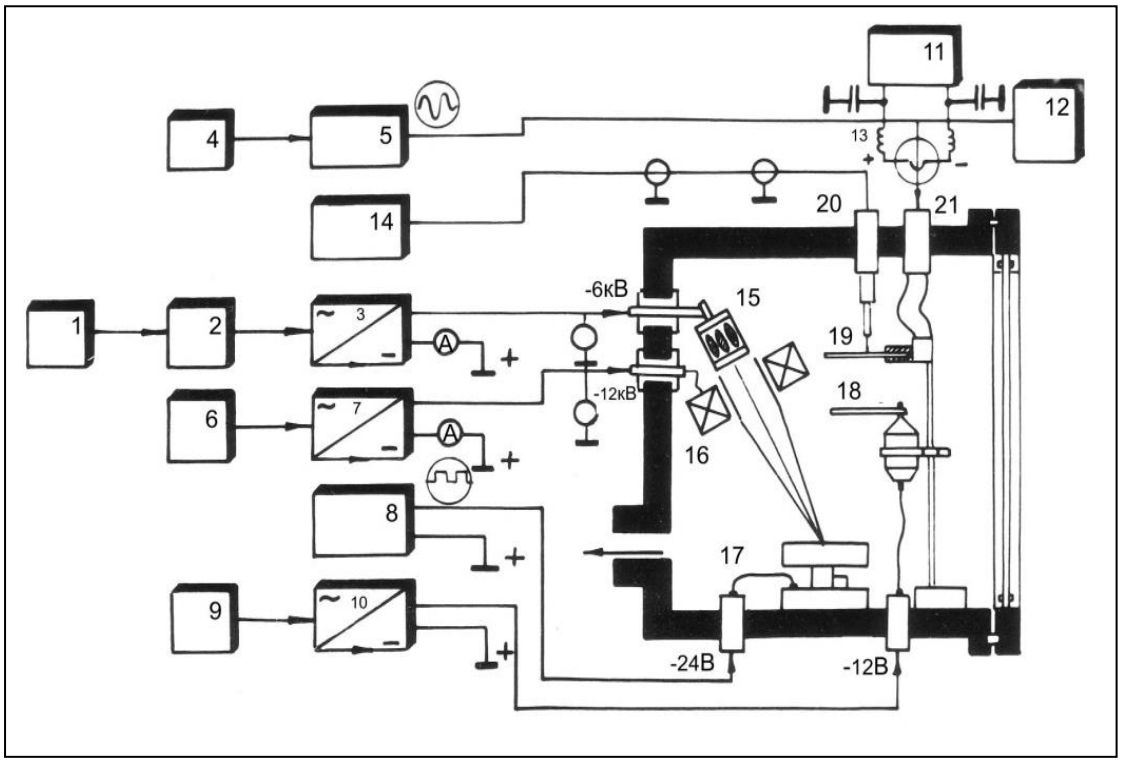

Fig. 3.1. Structural block diagram of the installation for gas discharge deposition of fluoropolymers

The pilot plant was operating with the voltage regulator 1 and the step-up transformer 2. The voltage of 0-9 kV was taken from the high-voltage rectifier 3, the positive output pole of which was grounded through a ammeter and fed to the hollow cathode of the gas-discharge gun 15. When the independent high-voltage glow occurred, the DC discharge beam of accelerated electrons fell on the rotating crucible 17 with the source material through the focusing

electromagnetic lens 16. By using a coaxial cable, the sinusoidal voltage from the high-frequency oscillator 4 was supplied via wattmeter 5 to the oscilloscope 12 and through a contactless vacuum thermal converter 13 to the substrate 19. The thermocouple ends of the thermal converter were connected to the millivoltmeter. The high-frequency voltage on the substrate 19 was measured by the voltmeter 15. The RF power supplied to the load was measured by the method described below.

The system of vacuum pumping of the working chamber is shown in Fig. 3.2. The vacuum chamber 1 was pre-evacuated to a pressure of 1.2 Pa through

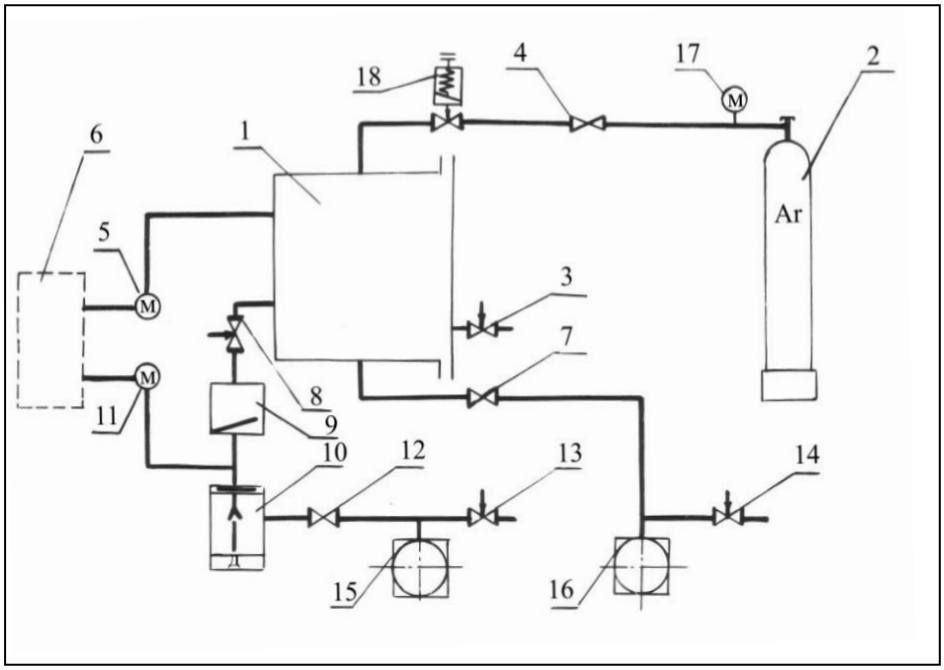

Fig. 3.2. Scheme of the vacuum part of the pilot plant.

the valve 7 by means of the separate mechanical vacuum pump 16. High vacuum pumping to pressure of 1 mPa was carried out through the valve 8 and the vacuum valve 9 by a steam-oil diffusion pump 10, the outlet of which was connected through the valve 12 to the mechanical vacuum pump 15. Flushing the volume of the chamber before sputtering and setting the working pressure of 3-10 Pa was achieved by argon inlet with the impurity concentration not more than 0.1% of the total volume through the needle leak valve 18 and the air reducer 4. Pressure in the cylinder 2 was monitored by the pressure gauge 17. Pressure gauges 5 and 11 were used to control pressure in different parts of the vacuum line, the output signals of which were fed to the pressure control unit 6. Air was let into the vacuum chamber before it was opened through the leak valve 3. Air was let into mechanical vacuum pumps 15 and 16 through leak valves 13 and 14 after completion of work. The vacuum chamber was made in

the form of a non-magnetic stainless steel cube. The volume of the chamber was 100 liters. The pumping speed of the vacuum system was 500 l/s.

Two types of the starting material decomposition were tested during operation: the thermal one and the electron-beam one. The thermal evaporation was carried out using resistive heating of the metal crucible with passing electric current of 10-150 A. The crucible was made of tantalum foil in the form of a boat, in which the initial polymer was loaded.

More difficult was the problem of electron-beam sputtering of fluoro-polymers under low pressure conditions. Creation of the electron beam by using conventional electron-beam guns with a heated cathode (EBGHC) [128] was extremely difficult in conditions of the glow discharge. This was due to the fact that for the normal operation of the EBGHC. It was necessary to use an additional system of vacuum rarefaction providing differential pumping of the EBGHC. Otherwise, at pressures of 0.8-12 Pa, electrical breakdown occurs between the elements of the gun. Focusing and controlling the electron beam without using the differentiated pumping was impracticable, since the hot cathode quickly failed. Therefore, the gas-discharge electron-beam gun (GDEBG) with a hollow cathode was used to form the electron beam. Such electron emitters are also called cold cathode guns. The electric power supply circuit of the GDEBG is shown in Fig. 3.3

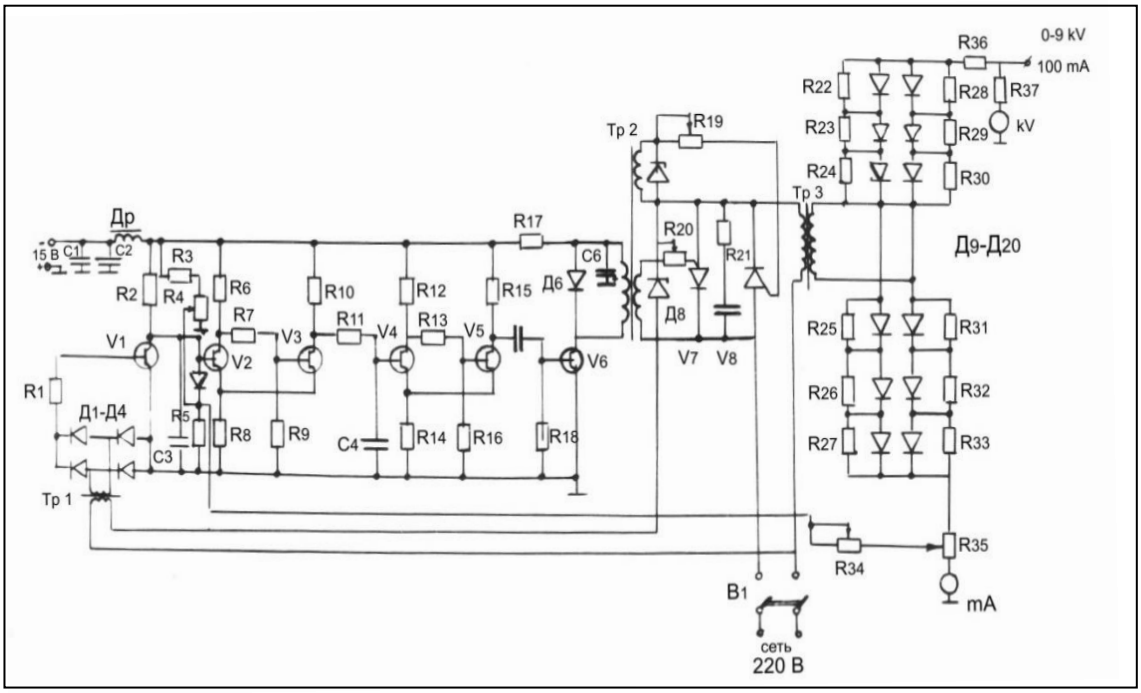

Fig. 3.3. Circuit diagram of the power supply for the gas discharge gun

An electromagnetic water cooled lens was used to control the electron beam and to change its specific power. The location of the in-chamber devices is shown in Fig. 3.4.

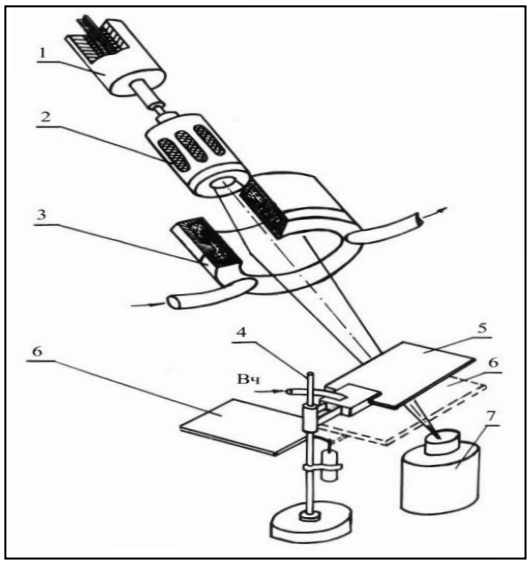

Fig. 3.4. Location of in-chamber devices: 1 – high-voltage feedthrough; 2 – hollow cathode; 3 – electromagnetic lens; 4 – tripod; 5 – substrate; 6 – semi-automatic shutter; 7 – rotating crucible.

It was found in the course of operation that the electron beam method is preferable to resistive heating for evaporation of fluoropolymers. In order to ensure the advantages of the electron-beam decomposition of the substance [129,130], a gun similar to that described in [131] was used. In the process of searching for the most efficient design, it was necessary to determine the effect of pressure in the chamber, the accelerating voltage, the relative position of the intra-chamber devices, and the shape of the cathode on the formation and intensity of the directional electron beam.

When the accelerating voltage is applied to the cathode of the gun, the electric discharge occurs at a certain pressure in the vacuum chamber characterized by the small current value and the high burning voltage. Such a discharge is called a high-voltage glow discharge. The following dependence recommended by Moly and Litton in [131] was used as a calculation formula for determining the current-voltage characteristic of the desired cathode geometry:

$$I_n = 7200\left(\frac{V}{120}\right)^{4{,}8p^{-h}}, \qquad (3.1)$$

where I_n is the discharge current, A; V is the accelerating voltage, kV; p is pressure, (mm Hg)·10^{-3}. h is a dimensionless quantity, the value of which correlates with the values of permeability (the ratio of the area occupied by the holes to the total area) used for the cathode of the grid.

Fig. 3.5 shows dependences of the discharge current (curves 1 and 2) and the current of the electron beam (curve 3) on the accelerating voltage at the permeability of the cathode wall of 30% and pressure of 9.8 Pa. The curve 1 is calculated by the formula (3.1), while the curve 2 is experimentally obtained for

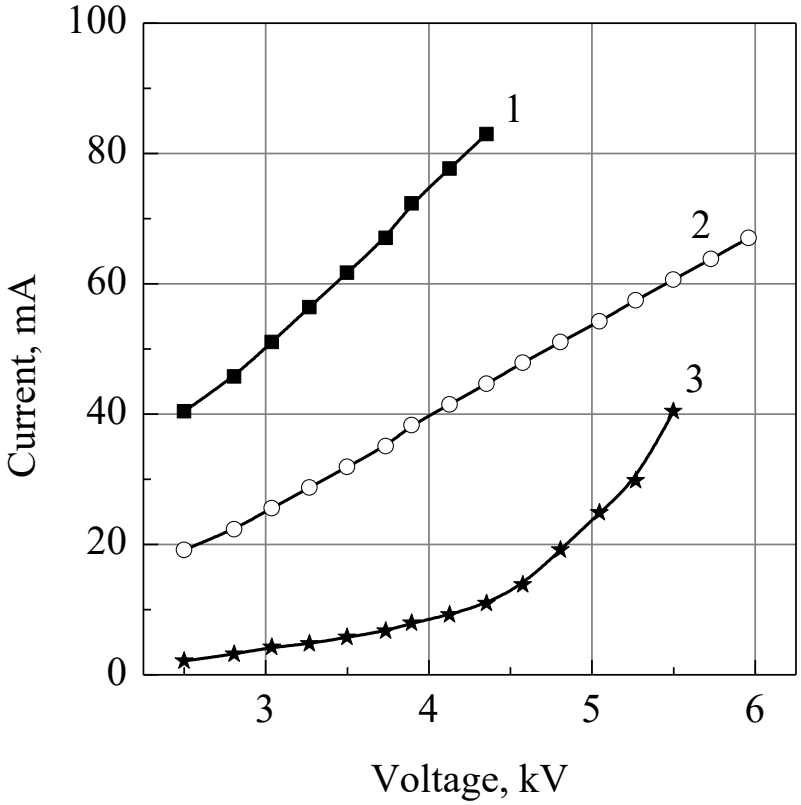

Fig. 3.5. Volt-ampere characteristic of the gas-discharge hollow-cathode electron-beam gun. Pressure is 10 Pa. 1 – calculated discharge current curve; 2 – experimental dependence of the discharge current; 3 – experimental values of the beam current

the used cathode.

Comparison of dependences 1 and 2 shows that the discharge current used in the cathode experiment is 1.9 times smaller than the current calculated by the formula (3.1). This can be explained by the fact that a spherical mesh cathode with a diameter of $5 \cdot 10^{-2}$ m was used in the works of Moly. Curve 3 was obtained experimentally by the method [132] using the Faraday cup according to the scheme shown in Fig. 3.6.

It was necessary to choose the shape of the cathode that ensures the maximal long-focus of the gun. Four types of focusing cathode electrodes were

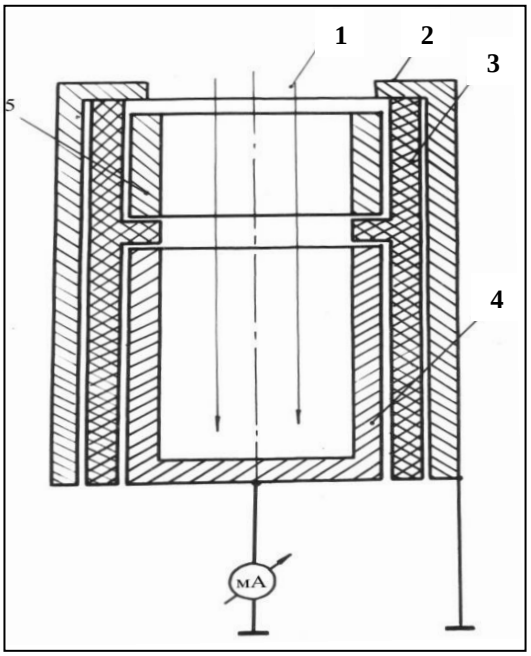

Fig. 3.6. Electron beam current measurement circuit: 1 – electron beam; 2 – screen; 3 – insulator; 4 – electrode with floating potential; 5 – Faraday's cylinder.

manufactured and tested. We have established that the maximum distance of 300 mm from the slice of the electromagnetic lens gives the electrode that satisfies the following relation:

$$0{,}3 < \frac{D-L}{d} = 0{,}5 \qquad (3.2)$$

and designated as the unit 4 in Fig. 3.7 and 3.8.

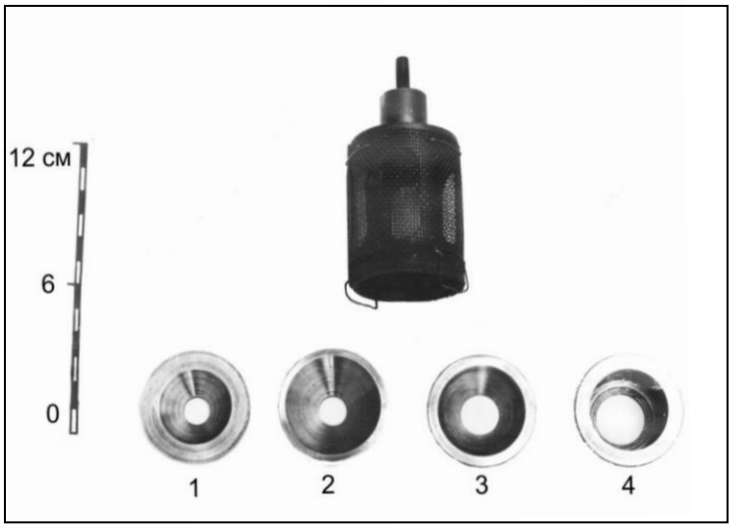

Fig. 3.7. Hollow mesh cathode with a set of interchangeable focusing electrodes

In this case, the conical part of the inner surface of the electrode 4 does not

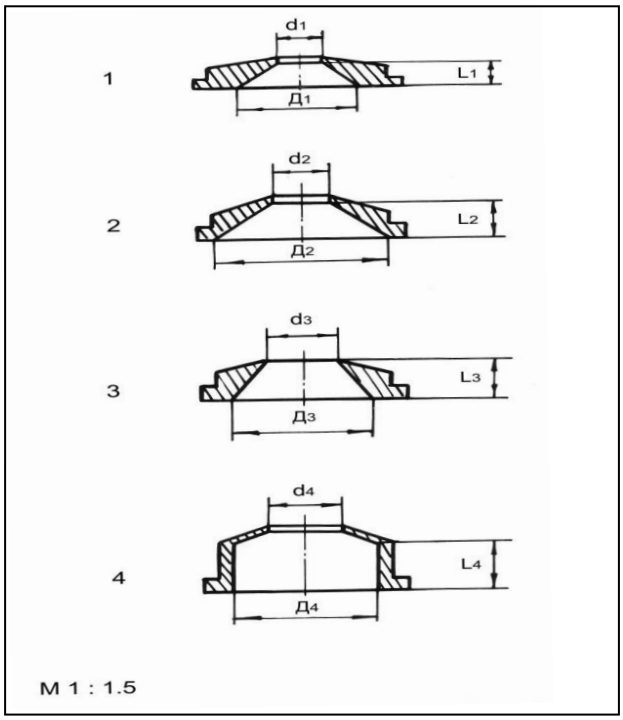

Fig. 3.8. Diagram of internal sections of replaceable electrodes

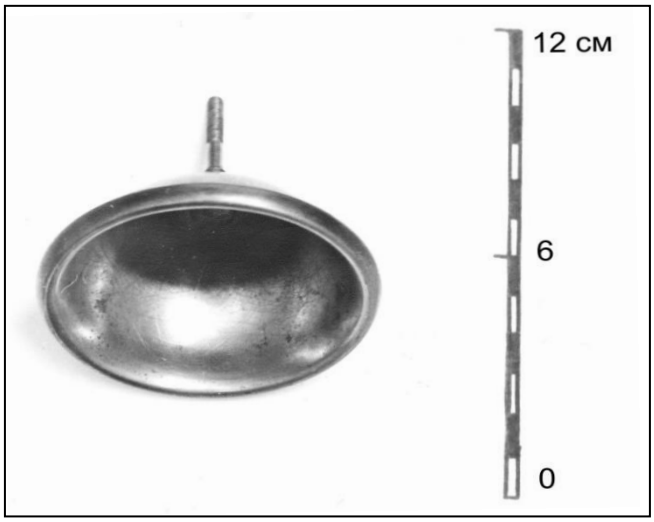

Fig. 3.9. Hemispherical hollow cathode

have a significant effect on the focal length, and d = 0.6 D. Here d is the inner diameter (mm), D is the diameter of the outlet (mm), L is the depth of the cathode electrode (mm). Electron-beam gun with a mesh hollow cathode creates increased ionization of residual gases in the working chamber.

Due to the fact that a part of the electrons from the inner plasma of the cathode are pulled out through the mesh openings [133], there is the increased bombardment of ions and electrons of the vacuum chamber adjacent to the gun.

This leads to a partial sputtering of the intra-chamber units. Therefore, a continuous hemispherical hollow cathode was used in separate experiments, as shown in Fig. 3.9. It was simpler to manufacture the cathode, but this required an additional grounded shield.

A comparison of the design features of the created gun with those already used shows that the developed gun is simpler to manufacture and it does not require differentiated pumping. In cases where the polymer deposition was preceded by the deposition of a metal or another polymer, the continuous hemispherical electrode was used. In this case, the coating was not contaminated by material deposited on the walls of the chamber. The developed design of the gun provided a fairly wide range of changes in the power of the electron beam when the pressure in the vacuum chamber changed. Pressure adjustment was carried out by using a specially designed needle leak valve. The dependence of the gun power on the pressure is shown in Fig. 3.10

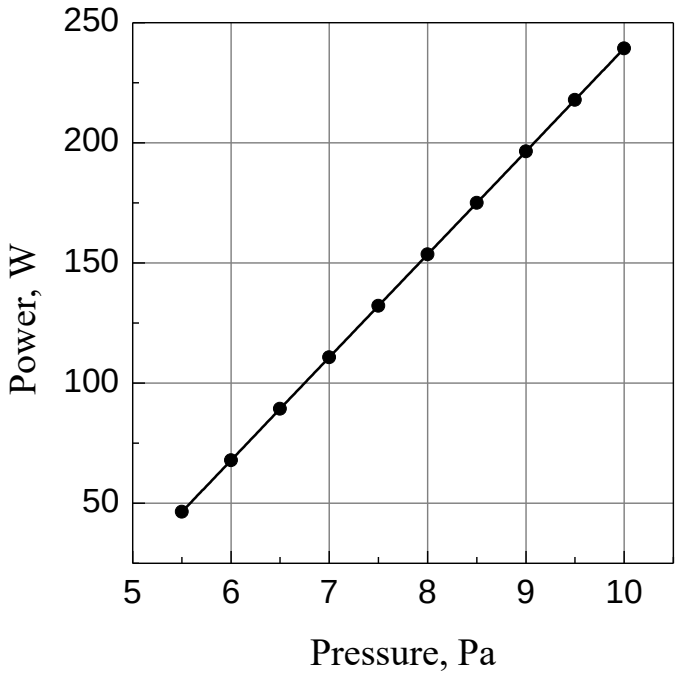

Fig. 3.10. Dependence of the gas discharge gun power on pressure.

It was also established in the course of the research that it was necessary to smoothly increase the specific power of the electron beam on the surface of the evaporated substance in order to prevent abrupt gas emission during the evaporation of fluoropolymers.

This cannot be achieved by changing the pressure in the chamber, since the focusing of the beam deteriorates. To ensure the stable process of PCTFE and

PTFE evaporation, the specific power of the electron beam on the polymer surface can be changed by changing the focal length of the magnetic lens. For this purpose, an electromagnetic water-cooled lens was made allowing reducing the diameter of the focal spot to 5 mm or less.

Characteristics of the created electron beam gun presented in Fig. 3.5-3.10 show that the effective electron-beam evaporator was designed to operate at high pressure (0.8-12 Pa) with the following parameters:

1. Accelerating voltage is 4-8 kV;
2. The beam current is up to 50 mA;
3. The discharge current is 100 mA;
4. The winding current of the electromagnetic lens is 0.5-2 A;
5. The number of ampere-turns of the lens is 2000;
6. The permeability of the hollow cathode is 30 %;
7. The diameter of the cylindrical cathode is 45 mm;
8. The diameter of the hemispherical cathode is 68 mm;
9. The diameter of the focused beam at a distance of 200 mm from the slice of the electromagnetic lens is 5 mm;
10. Pressure in the working chamber is 0.8-10 Pa;
11. Time of continuous operation of the gun with water-cooled lenses is 8-10 hours;
12. The service life of the cathode is more than 15 000 hours;

Fragments of molecules with a relatively small molecular weight are formed during the evaporation of polymers [69]. To obtain a high-quality coating, it is necessary that secondary polymerization of condensed fragments takes place on the substrate. As the initiator of the secondary polymerization can be heating, ultraviolet radiation, or bombardment with charged particles. In the present work, the coating was deposited on the substrate at room temperature. The secondary polymerization was stimulated by the bombardment of the substrate by accelerated charged particles (ions and electrons) of the low-temperature plasma of the high-frequency glow discharge. As noted in [41], it is better to carry out the polymerization of monomers by the high-frequency glow discharge. When polymerization is in the high-frequency discharge in the reaction chamber, it is necessary to create the smaller vapor pressure than in the case of the DC discharge. This improves reproducibility of the process, and the likelihood of contamination is reduced. It should be noted that the high-frequency discharge eliminates electrical breakdowns in the formed film and

makes it possible to carry out continuous operation. In the DC discharge, the process stops after deposition of a polymer film of a certain thickness due to electrical shielding of the substrate [134]. In the high-frequency processing, it is possible to use both metallic and dielectric substrates. The generator was made on two lamps for the formation of high-frequency sinusoidal oscillations (Fig. 3.11) with the following parameters:

1. The maximum oscillatory power is 80 W with the anode voltage of 600 V.
2. Working frequency is 13.56 MHz.

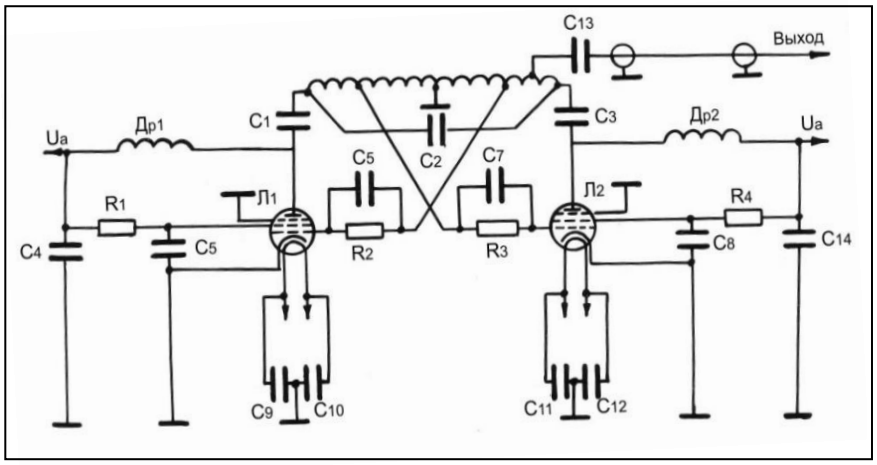

Fig. 3.11 Electrical circuit of the high-frequency generator: L_1, L_2 – lamps, C_1, C_3 – capacitors 100 pF, C_2 – 20 pF, C_4-C_{12}, C_{14} – 1000 pF, C_{13} – 2000 pF, R_1, R_4 – resistors 51 kΩ, R_2, R_3 – 10 kΩ, D_{p1} , D_{p2} – 100 μH chokes.

Fluoropolymer coatings were deposited on glass, as well as on plates of this material with copper, chromium, nickel, aluminum or resistive composition deposited in a vacuum. The size of the cell plates was 60 x 48 x 0.5 mm. A 50 μm thick copper foil was used as the substrate. Powdered PTFE and PCTFE were evaporated from the crucible.

The coating occurred as follows. The working chamber was pumped out to a pressure of 10^{-3} Pa. Then argon was injected into the chamber by using the needle leak valve, and pressure increased to 5-12 Pa.

Accelerating voltage was applied to the hollow cathode of the gas-discharge gun, and the high-voltage glow discharge was ignited. The sinusoidal voltage of 40–250 V with frequency of 13.56 MHz was supplied from the high-frequency generator after the gun was turned on. Non-independent glow high-frequency discharge was ignited on the substrate. The surface of the substrate was cleaned of impurities within two minutes. Then the voltage of high-frequency oscillations was reduced to a value that provided a high-quality coating. The power supply circuit of the electromagnetic lens was turned on, and the electron

beam was formed at the closed position of the shutter. Then the shutter was opened and the stopwatch was turned on. The process of sputtering of the starting material began. As it evaporated, the rotating crucible was rotated with the help of a remote control bringing a new portion of the sputtered substance under the electron beam. At the end of the sputtering, high-voltage and high-frequency discharges were turned on, the power of the electromagnetic lens was turned off, and the chamber continued to be pumped out for 30 seconds. Then the shutter of the steam-oil pump was closed, atmospheric air was let into the chamber, and the shutter was brought to its initial “closed” position. The manufactured sample was removed, the next one was placed, and the cycle was repeated.

Fig. 3.12. Gas discharge electron beam gun.

The possibility of stabilizing the main parameters determining the coating deposition process (pressure, evaporation rate, electron beam power, and high-frequency power delivered to the discharge) was tested. Since the instruments used to measure pressure and high-frequency power do not provide the required speed, the following technique was applied:

a) Stabilization of the beam power.

The pressure in the working chamber uniquely determines the value of the high-voltage discharge current at a certain voltage on the hollow cathode. Therefore, stabilization of the beam power is not difficult. The selected value of the discharge current was maintained by a needle leak detector and by adjustment of the power supply unit of the electron gun.

b) Stabilization of the evaporation rate.

To stabilize the evaporation rate, quartz thickness meters, ionization sensors, or micro-weighing devices are commonly used. With pressure less than 2-10 Pa, the constant sputtering rate can be achieved by stabilizing the operating mode of the electron-beam evaporator. In the case of evaporation at pressures higher than 1 Pa, this is difficult to perform, since the focusing of the beam is strongly influenced by the evaporation process itself and depends on slight pressure changes. Measuring of the beam diameter is associated with great technical difficulties. It was noticed that increase in the evaporation rate causes increase in the supply current of the anodes of the generator lamps. It is possible to provide the constant current consumed by the high-frequency generator by using the electromagnetic lens controlling the beam current density and, therefore, the evaporation rate and pressure.

The author of [69] used manual stabilization, but in the case of application an automatic leak valve, the automatic stabilization of pressure is possible. A signal proportional to the current consumed by the high-frequency generator can be used for automatic stabilization of the evaporation rate (current control of the electromagnetic lens winding).

Direct measurement of the power of the high-frequency discharge is difficult, especially when working with an unmatched load. The method of gas discharge polymer deposition is characterized by the change in impedance of the load in the process of production. Despite the variety of methods for measuring high-frequency power, they all used converting the electromagnetic oscillations

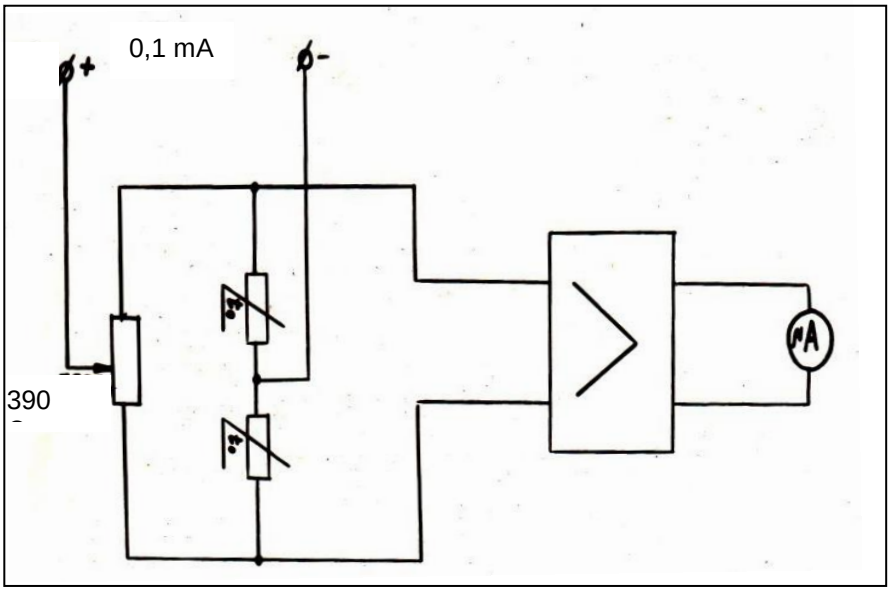

Fig. 3.13. Diagram of the thermistor bridge to determine the dissipation power of the high-frequency generator.

energy in another type of energy available for measurement, such as thermal energy, mechanical one, etc.

We measured the oscillatory power of the generator and the power dissipated by the anodes of the lamps. The dissipated power has been determined from the thermal radiation of the anodes using a thermistor bridge and taking into account the ambient temperature. The circuit of the thermistor bridge is shown in Fig. 3.13.

One of the thermistors was installed between the cylinders of the generator tubes opposite to anodes and was used to measure the heat flux of the anodes. The second thermistor was fixed on the generator case and compensated the electrical signal caused by changing of ambient temperature. Previously, the dependence of the microammeter readings connected to the output of the thermistor bridge amplifier (with grounded control stacks of lamps) on the

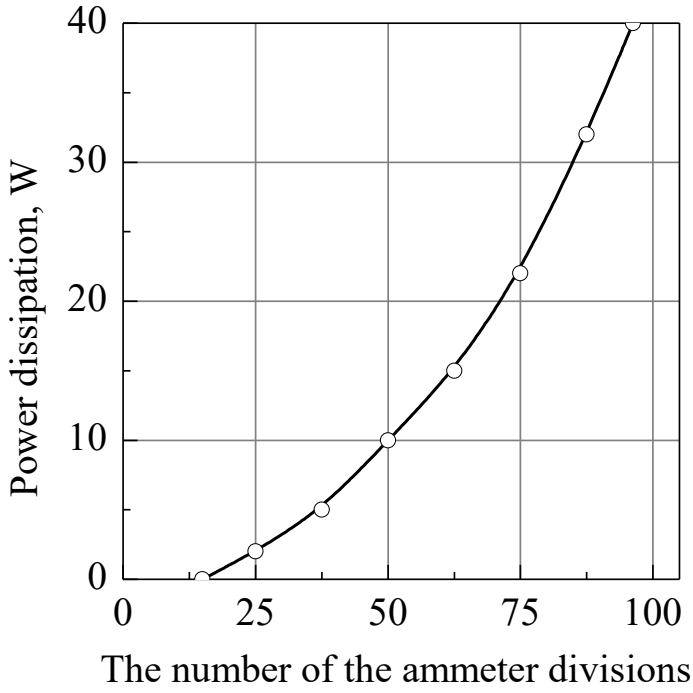

Fig. 3.14. Dependence of the power dissipated by anodes on the ammeter readings.

power dissipated by the anodes was removed. In this case, the dissipated power was equal to the power consumption from the anode power supply. The resulting dependence is shown in Fig. 3.14. It was used to determine the vibrational power equal to

$$P_{osc} = P_{con} - P_{dis}, \tag{3.3}$$

where P_{con} is the consumed power when the generator is loaded by the discharge resistance, W; P_{osc} is the power delivered to the load, W; P_{dis} is the dissipation power determined by the graph in Fig. 3.14.

Additionally, a non-contact vacuum thermocouple with a millivoltmeter and a voltmeter was used, since the error in power measurements increases at low powers (5-7 W). Graduation of the thermocouple with the ammeter with a direct current in the range of 0-0.5 A was performed beforehand.

Since standing waves occur with the incompletely matched load, the voltage at the point where voltmeter's probe is turned on is different from the voltage across the discharge gap. In our case, it is not possible to achieve matching of the voltmeter impedances and the load, since the discharge impedance varies during deposition of the coating. To obtain reliable values of the high-frequency voltage, it is necessary to connect a voltmeter directly to the electrode of the high-frequency discharge. The measuring part of this voltmeter $C_1 – C_3$; $R_1 – R_3$; $D_1 – D_3$ was managed to be placed directly in the working chamber. The length of the connecting line was less than 20 mm.

The largest error in measuring of the standing wave ratio is

$$\varepsilon = (k-1)\sin\frac{2\pi l}{\lambda}\cdot 100\%, \tag{3.4}$$

where ε is the largest relative measurement error, %; k is the standing wave factor; l is the electrical length between the switching point of the voltmeter and the point of the load connection, m; λ is the wavelength, at which the

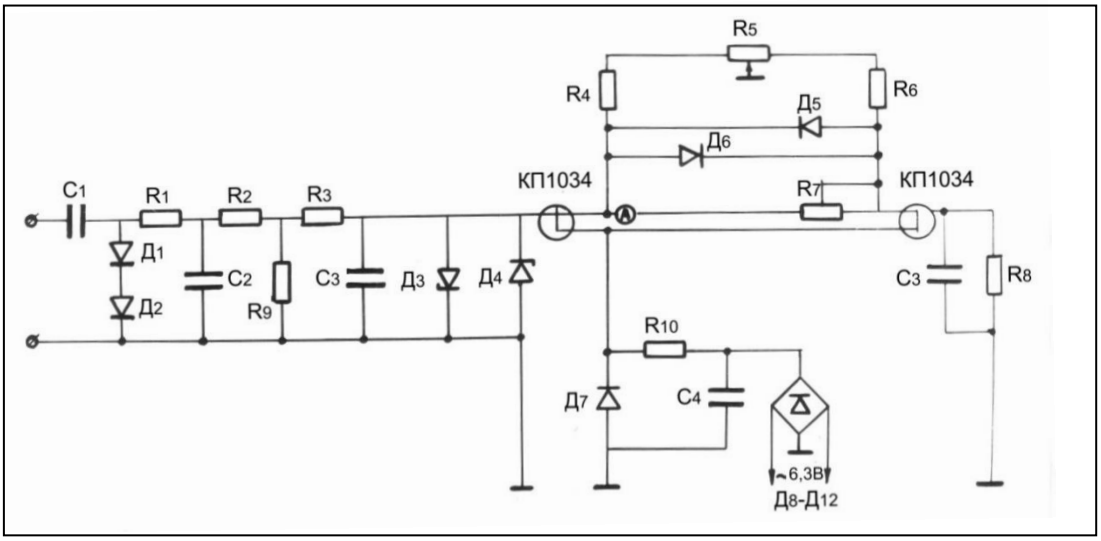

Fig. 3.15. Voltmeter circuit for measuring high frequency voltage.

measurement is performed, m. The voltmeter was manufactured to measure the RF voltage according to the scheme shown in Fig. 3.15.

3.2. Formation of coatings during the pyrolysis of polymers in vacuum under argon. Influence of the parameters of the gas-discharge electron-beam gun on the decomposition process

The authors of [134] noted that thin polymer films can be obtained in glow-discharge plasma from pyrolysis products of the original polymer supplied to the working chamber from outside. The PCTFE monomer coatings in the discharge are not formed. It was necessary to find out the possibility of the formation of PCTFE films from the pyrolysis products of the original polymer. The author of [69] carried out deposition of coatings by the method of the electron beam evaporation using the gas-discharge electron-beam gun in argon atmosphere. To improve the properties of coatings, the substrate was treated in high-frequency glow discharge. We studied the effect of high-frequency discharge and substrate heating on films obtained by resistive evaporation in argon atmosphere.

To do this, thermal decomposition of PCTFE and PTFE was carried out directly in the vacuum chamber at the argon pressure of 10-20 Pa. The starting material in the form of powder was loaded into a tantalum crucible heated by passing current to the required temperature. The temperature was controlled by the chromel-copel thermocouple welded to the crucible bottom. Decomposition of PTFE occurred at the crucible temperature of 600-800 °C. In the case of resistive heating, PTFE material does not melt and it becomes covered with black bloom in a few seconds. The material migrates along the crucible bottom at these temperatures. Formation of the coating took place on the substrate (copper-coated plate) placed at a height of 180 mm above the crucible. The substrate temperature was controlled by a chromel-copel or a chromel-alumel thermocouple. The tantalum foil heater was placed above the substrate for radiation heating.

In the process of PTFE decomposition, the substrate was heated by radiation from the crucible to the temperature of 45 °C. Under these conditions, fine powder is formed on the substrate in 1800 seconds, weakly adhering to the surface of the substrate. The maximal rate of the coating formation was 10-13 kg/m^{2}s (0.5 Å/s). The micrograph of the obtained coating is shown in Fig. 3.16.

The pressure of argon was 10-20 Pa at the substrate temperature of 45 °C. Fluoropolymer coating consisted of individual volumetric aggregates of up to 1 μm in size and having the irregular geometric shape. Black spots at the image corresponded to the precipitated particles of the fluorocarbon coating after treatment by technical gold.

Increase in the substrate temperature to 100-110 °C resulted in the complete absence of the coating on the substrate. A high-frequency voltage of 100 V was applied to the substrate in the following experiments, since the high-frequency discharge did not ignite at lower voltage. The coating was formed in 30 min at the rate of 0.7 Å/s at the substrate temperature of 45 °C with simultaneous treatment with high-frequency discharge. The coating was firmly attached to the surface of the substrate and did not crumble.

a) 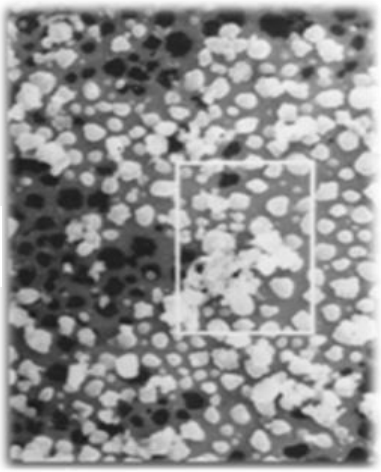 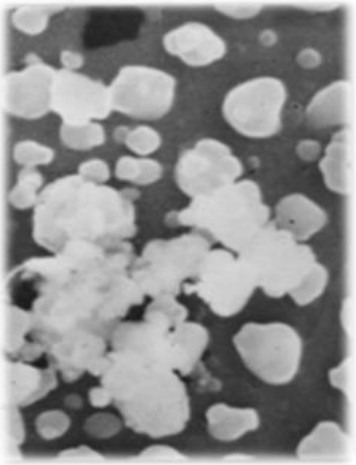 b)

Fig. 3.16. Micrograph of a fluorocarbon coating obtained by the thermal decomposition of PTFE.

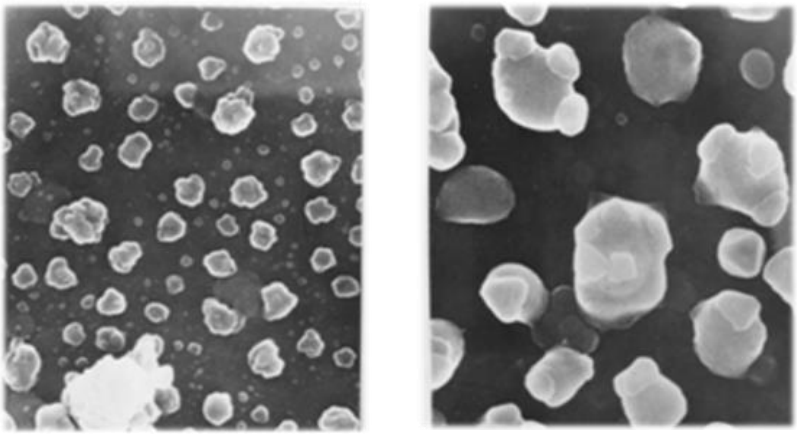

а) б)

Fig. 3.17. Micrograph of the coating from the products of the thermal decomposition of PTFE.Argon pressure is 10-20 Pa; substrate temperature is 45 °C, high-frequency voltage is 100 V. a) – 600^x, b) – 2300^x

It can be seen in photos Fig. 3.17 that the discharge treatment leads to unification of individual primary structural elements with the formation of agglomerates of the correct hemispherical shape with the average size of up to 20 μm. This can be explained by the fact that the treatment increases activity and mobility of the polymer chain fragments.

During the pyrolysis of PCTFE in argon atmosphere at a pressure of 10-20 Pa, the starting material was heated to the decomposition temperature of 450-470 °C. The crucible-substrate distance was 180 mm. At such a distance from the crucible, the temperature of the substrate from the radiation of the crucible rose to 27-35 °C. Under these conditions, a low molecular weight adhesive film of thermal decomposition products was formed on the substrate surface. Increase in the substrate temperature to 60 °C caused the coating to cease to be sticky, but its transparency deteriorated sharply, and the coating acquired the light brown color. Increase in the substrate temperature to 90 °C caused the coating to darken to dark brown. At temperatures above 90 °C, condensation on the substrate was disrupted. A photograph of the coating surface obtained at the condensation temperature of 70 °C is shown in Fig. 3.18.

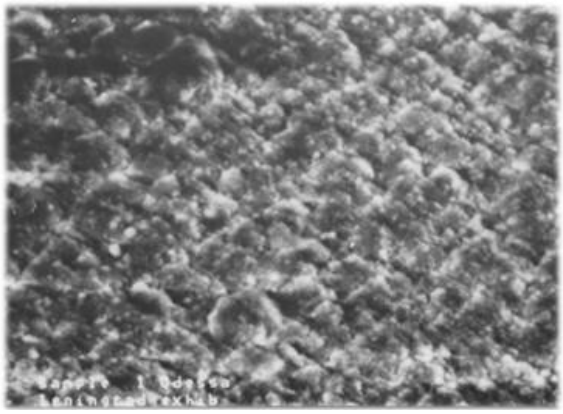

Fig. 3.18. Micrograph of a PTFCE coating obtained in an argon atmosphere at pressures of 10-20 Pa by pyrolysis of the starting material. The substrate temperature is 70 °C.

The deposition rate on the unheated substrate (30 °C) was 7 Å/s. When the high-frequency voltage with amplitude of 100 V was applied to the substrate, a transparent non-adhesive coating of the droplet structure was formed (Fig. 3.19).

The difference from the results obtained earlier [69] during the deposition of coatings by decomposition of PCTFE and PTFE by the thermal heating method at pressures greater than 0.1 Pa can be explained as follows.

As noted in [4], pyrolysis in inert atmosphere slows down the process of removing volatile products and increases the likelihood of secondary reactions

between decomposition products. In addition, at pressure of 10-20 Pa, the mean free path of the active fragments is two orders of magnitude shorter than at pressure of 0.1 Pa. This leads to increase in sputtering of pyrolysis products on inert gas molecules. A smaller number of active fragments are involved in the formation of coatings on the substrate, and they have less energy. This leads to decrease in the growth rate of coatings and to deterioration of their quality.

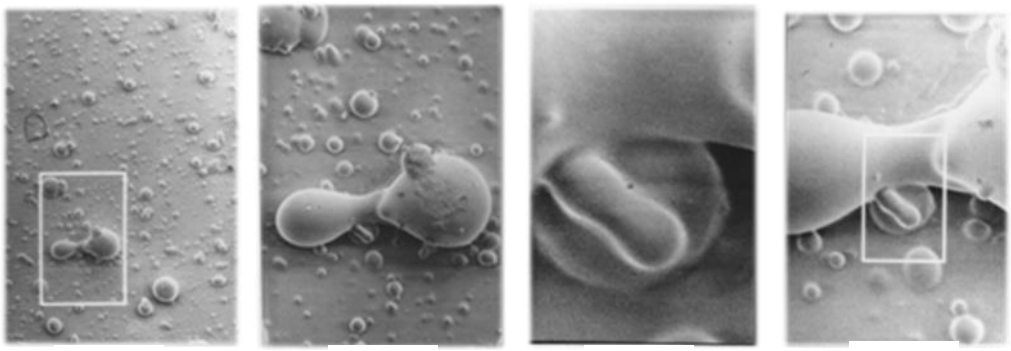

a) b) c) d)

Fig. 3.19. Micrograph of a PTFE coating obtained in an argon atmosphere (pressure 10-20 Pa) by pyrolysis of the starting material. The substrate was treated with glow HF discharge (T_{subs} = 30 °C); a – 80^x; b – 250^x; c – 530^x; d – 1600^x.

The disadvantages of resistive evaporation should also include the lack of possibility of ignition of high-frequency discharge at voltage less than 100 V that significantly narrows the range of pressures and voltages at which high-frequency glow discharge exists. Thus, resistive evaporation does not ensure the production of high-quality coatings from decomposition products of the initial fluorine-containing polymers.

It has been established [69] that the efficiency of electron-beam evaporators is significantly higher than that of thermal, induction, and high-frequency atomizers. In the implementation of electron-beam heating of fluoropolymers, we used the gas-discharge electron-beam gun (GDEBG), which allowed formation of the electron beam under conditions of 0.8-12 Pa pressure and effectively control the sputtering process. In addition, it is possible to ignite glow discharge on the substrate at lower voltages (up to 10 V) due to the powerful ionization of the working gas, and also to directly heat the surface of the evaporated substance. In this case, energy is supplied from above, but not from the bottom of the crucible, and the formed active fragments immediately evaporate, not participating in the diffusion process. In addition to the heating, electrons bombarding materials have a selective effect on the evaporated

substance (destroy the weakest chemical bonds) that leads to increase in the molecular weight of the polymer chain volatile fragments. Finally, directional evaporation of the polymer chain fragments can be carried out with the electron-beam evaporation that increases the condensate growth rate. For comparison, it should be noted that the polymer coating with equal probability and thickness covers all intra-chamber devices during the polymerization of the gaseous monomer. To obtain the increased deposition rate, it is necessary to apply substrate cooling [41].

The gas-discharge gun differs from the electronic evaporator with a heated cathode by its simplicity of manufacturing and durability. Glowed cathodes fail after 200-250 hours of operation, while the hollow cathode can work for more than 15 000 hours. In addition, with each replacement of the cathode, it is necessary to perform its adjustment that requires highly skilled service personnel and takes additional time.

The specificity of the fluoropolymers electron bombardment is that the object being processed acquires an induced surface charge. This charge must be removed from the surface, otherwise it is charged negatively, the beam will be defocused, and sputtering will slow down. In our studies, the electron beam was reflected from the target surface when PCTFE and PTFE were evaporated at pressures of 0.8-12 Pa (beam current density was less than 10-15 A/m^2 and an accelerating voltage of 2-7 kV). The increase in accelerating voltage led to the disruption of the gun operation. The high-voltage glow discharge was transformed into the arc. The sputtering process began if the treatment of the target with the above parameters was carried out continuously for 35-40 minutes for PTFE and 20-25 minutes for PCTFE. This phenomenon is explained by the fact that irradiation with low-energy primary electrons (2-3 keV) leads to elastic interaction. It follows from the laws of energy and momentum conservation that in the case of the elastic interaction of an electron with a fixed atom, the maximum value of the transmitted kinetic energy is determined by the mass ratio of the interacting particles and cannot exceed fractions of a percent of the initial energy of the electron.

Indeed, in each event of the elastic scattering, the primary electron loses energy in discrete portions, which is accompanied by increase in the internal energy of the solid, that is, energy of thermal fluctuations. As a result, the thermal energy increases with prolonged exposure to values leading to destruction of the polymer. Such a long heating before sputtering, of course,

does not meet the requirements of manufacturability. Increasing the accelerating voltage leads to the disruption of the gun operation with the formation of the arc. Therefore, an attempt was made to speed up the sputtering process by increasing the current density, and therefore, by changing the power density of the primary beam.

As the results of our experiments show, if the current density of the beam increases, interaction of the primary electrons with the polymer surface begins, at which not only the direction of their movement changes, but also the energy, that is, deceleration occurs. The main cause of the deceleration of the primary electrons in a solid is inelastic interaction processes, as the result of which the electrons completely lose their energy. Some fraction of this energy is carried away from the sample by electrons, photons and atomic particles emitted from the surface, and the remaining part is absorbed by the substance and, ultimately, is converted into heat. As with other methods of heating, this heat should be removed from the irradiated area due to the thermal radiation of the surface and the thermal conductivity of the material. The thermal conductivity of fluoropolymers is low (0.25 and 0.23 W/(m·K) for PTFE and PTTFE, respectively). Therefore, increase in the electron beam density leads to local heating. Increase in the temperature of the limited area, in turn, stimulates the following processes: structural phase transitions, annealing of defects, diffusion, recrystallization, melting, desorption, and evaporation from the surface of atomic particles, thermoelectronic emission, etc.

An important feature of the electron-beam heating is that it is possible to achieve a high concentration of the thermal energy bulk density at the relatively low total beam power. This allows, if necessary, to localize the processes in the limited sample area selected by the operator. In the present work, the change in the energy of the primary electrons beam was achieved by means of additional focusing by the electromagnetic lens. The change in evaporation area ranged from $2 \cdot 10^3$ mm^2 to 15 mm^2. The evaporation area was understood to be the area illuminated by the beam when it hits the grounded metal plate located at the same distance as the crucible with the material to be evaporated. This value is slightly different from the actual one.

The path traversed by a primary electron to the complete loss of its energy is far from rectilinear. In practice, they try to determine the penetration depth of electrons defined as the projection of the path to the normal to the surface. It is clear that the difference between average values of the penetration depth and the

length of the path is the greater, the more “broken” is the path of the electrons movement in the polymer. The path length depends on the initial electron energy. At the surface where the velocity of the primary electrons is still high, the probability of energy loss is smaller than at the end of the run. That is, the maximum of the spatial distribution of the specific energy released in the sample is located not on the surface, but in the bulk of the substance. This feature distinguishes electron bombardment from other methods of the energy transfer to a solid (for example, from laser irradiation).

A degree of the gas ionization under the action of primary electrons increases at high electron beam densities. In this case, a luminous region with a height of 10-15 mm is clearly visible above the evaporation zone. This is the ionic shell formed by the action of reflected primary electrons and emitted secondary electrons.

Dependence of the evaporation rate of PCTFE and PTFE on the power density of the gun is shown in Fig. 3.20. The required energy density was provided by focusing the electromagnetic lens.

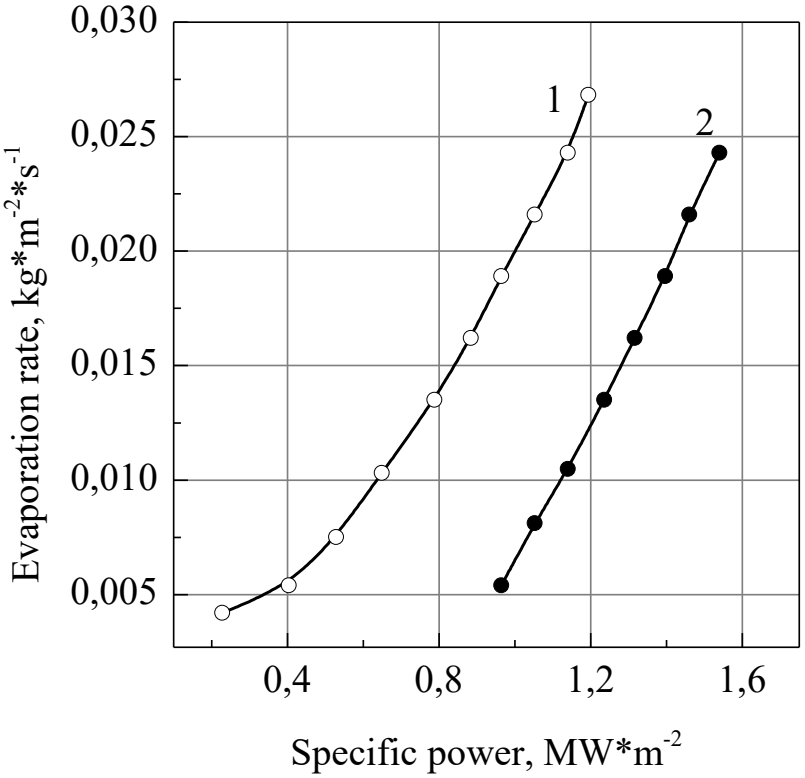

Fig. 3.20. Dependence of the evaporation rate of the fluoropolymer on the specific power of the gas-discharge electron-beam gun. Substrate to crucible distance is 160 mm; pressure is 8 Pa. 1– PCTFE; 2 – PTFE. The substrate was not treated by high-frequency discharge.

Analysis of the dependences shown in Fig. 3.20-3.21 confirms the high efficiency of the gas electron beam gun when working with fluoropolymers. The rate of the starting materials evaporation was not limited by the characteristics of the gun, but depended on capabilities of the vacuum system.

Dependence of the evaporation rate of PCTFE and PTFE on the lens winding current is shown in Fig. 3.21. As already mentioned, a coarse adjustment of the gun power (and hence the evaporation rate) can be carried out by changing the pressure in the vacuum chamber.

Smooth adjustment of these values is carried out by focusing the electron beam with the electromagnetic lens. It is seen from Fig. 3.21 that the

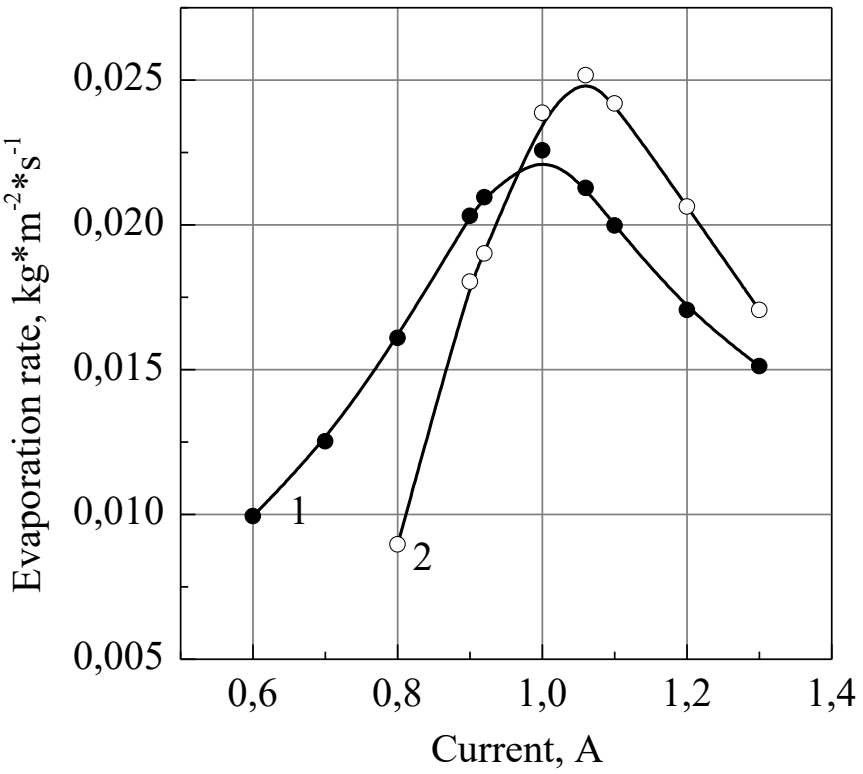

Fig. 3.21. Dependence of the evaporation rate on the winding current of the electromagnetic lens. Pressure is 8 Pa; 1 – PCTFE; 2 – PTFE. The distance "crucible – lens" is 300 mm.

dependence of the evaporation rate on the winding current of the lens has an extremum for PCTFE and PTFE. This is understandable, since increase in the lens winding current contributes to release of the electron beam power at the lowest possible evaporation area. When maximizing the evaporation rate, a further increase in the winding current leads not to increase, but to decrease the focal length and to “refocusing” mode that reduces the evaporation rate. The maximum density of the electron beam is in this case not on the surface of the

polymer, but higher. The gentler character of the ascending part of the curve and the lower extremum value for PCTFE is explained by the fact that it is less thermally resistant than PTFE.

Dependence of the diameter of the focal spot on the evaporation surface from the current through the winding of the electromagnetic lens is shown in Fig. 3.22. When sputtering the original polymer with the gun power more than 40 W for PCTFE and 110 W for PTFE, it is not possible to obtain the evaporation zone diameter less than 10 mm. This is due to the fact that under intense evaporation regimes (high specific power), the beam electrons are scattered on the gas cloud of degradation products.

It is seen from the graphs in Fig. 3.22 that the diameter of the focal spot in the evaporation zone increases with increasing accelerating voltage. This requires increase in the winding current of the focusing lens.

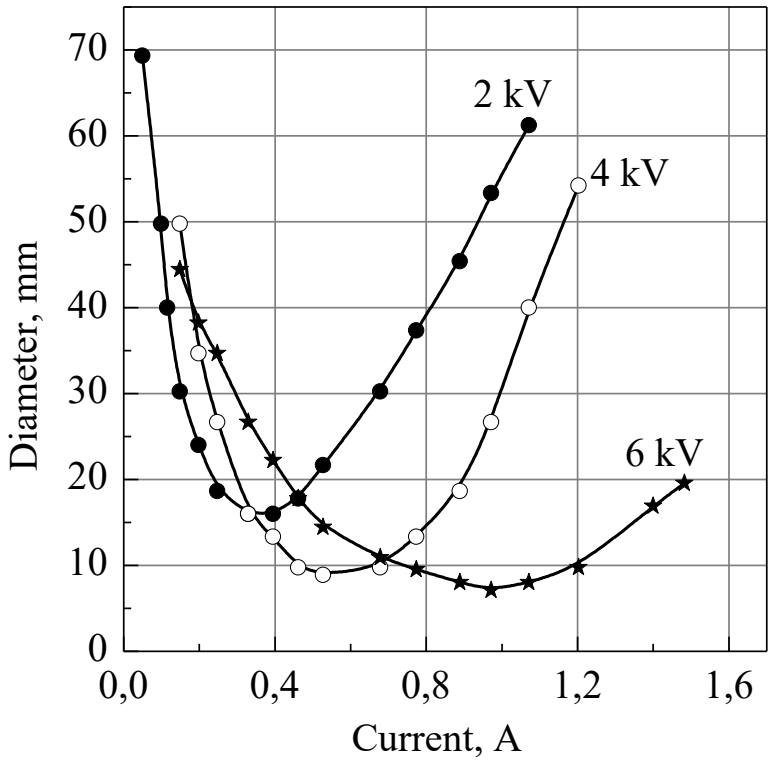

Fig. 3.22. Dependence of the diameter of the focal spot on the current of the electromagnetic lens without evaporation. The beam current is 45 mA.

When the initial polymer is irradiated with a beam of accelerated electrons, their energy (1-7 keV) is spent on ionization and excitation of atoms, as well as on heating the surface layer with the thickness approximately equal to the penetration depth of the electron into the polymer. In our case, according to literature data, this layer is equal approximately to 10-100 Å [135]. In contrast to

the thermal heating, a large number of ionized fragments of low molecular weight macromolecules capable of reacting with each other, that is, recombining, are formed during the electron beam heating.

For PTFE, the C–C bond break is most likely, since its strength is 86 kcal/mol, while the strength of the C–F bond is 108 kcal/mol. Breaking of the chain leads to formation of two radicals. After recombination, two fragments of the molecule are formed. This process continues until fragments of the molecules capable for evaporation are formed. Radicals that did not have time to be neutralized, break up along the chain mechanism with the formation of a monomer.

Unlike PTFE, PCTFE evaporates from the surface of the liquid phase formed by the molten polymer. Melt mixing occurs in the process of heating. Evaporation of macromolecular fragments of the original polymer occurs from the surface of the liquid phase due to thermal heating. Up to 25% of the monomer is released [136] during PCTFE pyrolysis in the temperature range of 350-450 °C.

The characteristic evaporation time of a polymer layer λ was calculated for comparison of the electron-beam sputtering in argon with evaporation in vacuum [69] (λ is the mean free path in a polymer of the electron with energy of 2.5-7 keV). It was assumed that all the electron beam energy is released in a layer of thickness λ, and the stationary mode of evaporation was considered. Given the made assumptions, the decomposition time of the polymer layer with thickness λ is equal to:

$$\tau = \frac{t \cdot S \cdot \lambda \cdot \rho}{\Delta m}, \tag{3.5}$$

where t is the time of the polymer surface irradiation, s; S is the area of the focal spot on the evaporation surface, m^2; ρ is the original substance density, kg/m^3; λ is the penetration depth of electrons into the polymer, m; Δm is the initial substance mass loss during the time t, kg.

According to the formula (3.5), τ values were calculated for layers of 10 and 100 Å thick for PTFE evaporation. The parameters of the two modes and the results of the calculations are given in Table. 3.1. Since PTFE was not melted even at the maximum gun power, mass transfer and heat transfer between the polymer layers were not taken into account. Then the values τ_1 and τ_2 will characterize the decomposition rate.

$$v = \frac{100}{\tau}, \text{ (\%/s)} \qquad (3.6)$$

where v is the decomposition rate in weight percent of mass loss per second.

Table 3.1

Calculation of decomposition time τ_1 and τ_2 for PTFE

Experimental conditions	Release, V	Beam power, W	The area of the focal spot, $S \cdot 10^{-5}$, m^2	Exposure time, s
Mode I	$7 \cdot 10^3$	70	7.85	300
Mode II	$2.5 \cdot 10^3$	30	2.00	300
Experimental conditions	Mass loss, Δm 10^{-4}, kg	Electron penetration depth $\lambda \cdot 10^{-4}$, m	Decomposition time $\tau \cdot 10^{-4}$, s	
Mode I	1.178	100	4.2	
Mode II	1.403	10	0.09	

In order to ensure the similar decomposition rate using pyrolysis, it is necessary to maintain the decomposition temperature estimated by extrapolation of the decomposition rate temperature dependence. We obtained values of the required temperatures in the range from 1080 to 1280 K. The monomer yield is 70-80% under these temperatures. It is significantly higher than that with the electron beam decomposition (less than 40%) [69]. Such an estimation cannot be made for PCTFE, since there is the convective mass transfer, so the volume of the liquid phase in the crucible is 3-4 orders of magnitude larger than the volume, in which the electron energy completely dissipates.

To compare the evaporation process at pressure of less than 10 Pa and in argon (1-10 Pa), the dependences of specific evaporation energies during the PTFE decomposition were obtained (Fig. 3.23). Here, the specific energy of evaporation W was understood as the value calculated by the formula:

$$W = \frac{\mathrm{P}}{\mathrm{v_e} \cdot \mathrm{S}}, \qquad (3.7)$$

where P is the power of the beam, W; v_e is the evaporation rate, kg/m^{2}s; S is the evaporation area, m^2, W is the beam energy required for evaporation of a unit mass of the initial substance under these conditions.

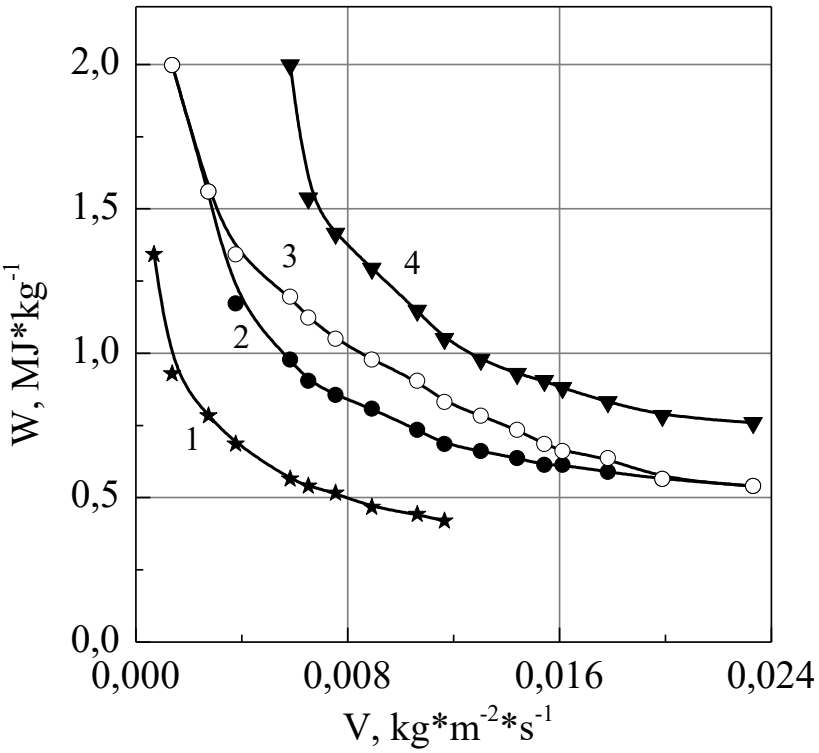

Fig. 3.23. Dependence of the evaporation specific energy on the decomposition rate of PCTFE and PTFE. 1,2 – at pressure of 10^{-2} Pa; 3.4 – at a pressure of 0.8-12 Pa; 1,4 – PTFE; 2,3 – PCTFE.

Curve 1 in Fig. 3.23 is based on the results of experiments PTFE evaporation in the entire pressure range (0.8-12 Pa) [69]. In this case, the points belonging to different pressures lie in the same vertical segment. A comparison shows that during evaporation in the inert gas medium, the significantly higher electron beam power is required to achieve the same evaporation rate as compared to evaporating in a vacuum. Such a difference can apparently be explained by dispersion of evaporated fragments on the way to the substrate, as well as by the loss of the gun power part during ionization of the working gas.

Comparison of curves 2 and 3 (PCTFE) in Fig. 3.23 shows that the differences between them are much smaller than those of similar curves during evaporation of PTFE. This testifies in favor of the fact that the release of active fragments occurs in the entire volume of the polymer melt during PCTFE evaporation, both in low and in high vacuum, and the effect of reactions occurring in the surface layer is insignificant.

Dependences of the coating deposition main parameters (decomposition rate and growth rate) on the pressure of inert gas in the working chamber were studied. The results of the experiments are shown in Tables 3.2 and 3.3. The

obtained data (Table 3.2) show a monotonic decrease in the evaporation rate of PCTFE and PTFE with increase of pressure from 1 to 12 Pa.

Table.3.2.

Evaporation rate and the evaporation specific energy at different pressure in the working chamber (the gun power is 0.9 MW/m^2; the substrate is not treated by discharge)

Pressure, Pa	Material			
	PCTFE		PTFE	
	Evaporation rate V_e 10^2, kg/m^{2}s	Specific energy $W \cdot 10^6$, J/kg	Evaporation rate V_e 10^2, kg/m^{2}s	Specific energy $W \cdot 10^6$, J/kg
1	1.85	59.9	0.87	103.8
6	1.45	62.1	0.75	120.0
12	1.27	71.1	0.63	142.1

Table 3.3.

Dependence of the growth rate V_p 10^{-8} m/s on the pressure in the working chamber (the power of the gun is 0.9 MW/m^2; the substrate is not treated by discharge; distance ''crucible-substrate'' is 0.1 m)

Pressure, Pa	Material	
	PCTFE	PTFE
1	4.03	2.00
6	3.08	1.57
12	2.58	1.43

With increasing pressure, the conditions for removal of volatile degradation products from the evaporation zone deteriorate, and the secondary decomposition reactions of these products are possible.

Decrease in the growth rate of PCTFE and PTFE films (Table 3.3) with increasing pressure from 1 to 12 Pa occurs to the greater extent than decrease in the evaporation rate. This can be explained by the influence of the scattering

factor (decrease in the mean free path) during the passage of macromolecular fragments between crucible and substrate.

Sputtering and deposition rates of PCTFE and PTFE on the untreated substrate were investigated depending on the accelerating voltage of the gun at various beam current densities and at the constant pressure of 8.7 Pa. Results of

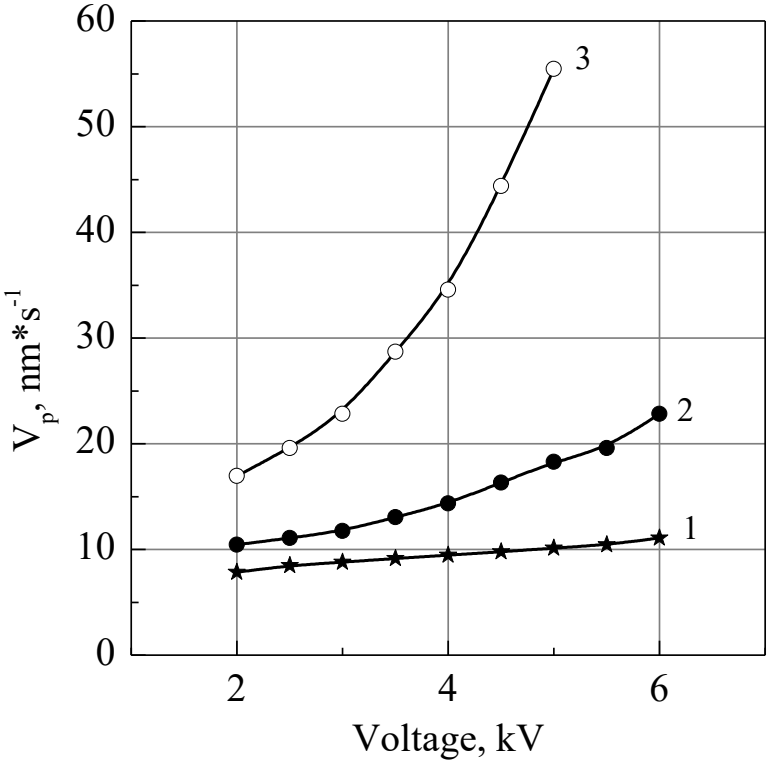

Fig. 3.24. Dependence of the decomposition rate of PTFE on the accelerating voltage at different current densities of the electron beam. 1 – 60 A/m^2; 2 – 110 A/m^2; 3 – 250 A/m^2. The pressure in the chamber is 8.7 Pa.

the experiments are presented in Figs. 3.24-3.27. As shown in [69], with the electron beam evaporation of PCTFE at pressure of 10 Pa for accelerating voltages in the range of 1.5-3.0 kV, current densities exist that ensure the maximum deposition rates. With increasing the accelerating voltage under these conditions, the maximum growth rate of PCTFE coatings shifted to the region of low beam current densities.

In our experiment, the used current densities did not lead to evaporation, characterized by an extremum of the growth rate. Such a difference can be explained by the fact that the accelerating voltages used in [69] (1.0–3.0 kV) are not acceptable for operation of tour gun. Stable decomposition of the original substance is possible starting with accelerating voltages greater than 3.0 kV.

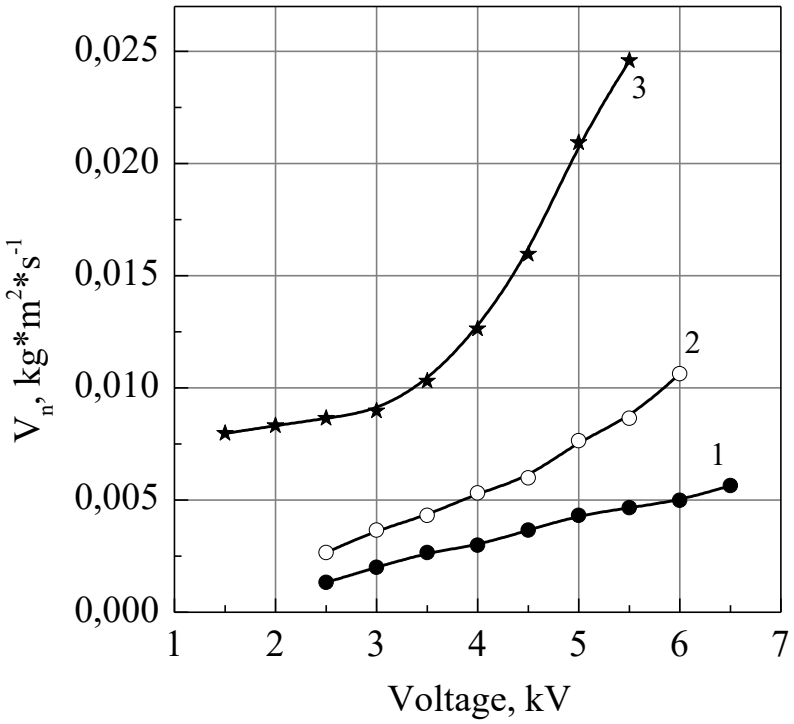

Fig. 3.25. Dependence of the growth rate of PTFE coatings on a substrate that is not treated by the discharge on the accelerating voltage at different current densities of the electron beam. 1 – 60 A/m^2; 2 – 110 A/m^2; 3 – 250 A/m^2. The pressure in the chamber is 8.7 Pa, the "crucible – substrate" distance is 100 mm.

In addition, a complex interaction of the degradation products and the plasma cloud above the evaporation surface occurs at pressures of 8-9 Pa. The growth rate at the current density of 250 A/m^2 with increasing accelerating voltage is determined by the increase in the sputtering rate.

At the current density of 60 A/m^2, the growth rate with increasing accelerating voltage from 2 to 6 kV grows much slower than the decomposition rate.

This can be explained by fragmentation of the polymer chain fragments in the plasma and by decrease in the number of fraction fragments reaching the substrate and condensing on it at temperatures of 25-27 °C. When the beam current density is 110 A/m^2, the above factors simultaneously affect the dependence $V_p = f(U_{sc})$.

The main difference between the PTFE decomposition process and PCTFE degradation is that no molten layer forms on the evaporation surface of PTFE under any experimental conditions.

Analysis of the curves shown in Fig. 3.26, shows that the main factor affecting the rate of decomposition is the specific power of the beam, that is the power of the beam per unit area of evaporation.

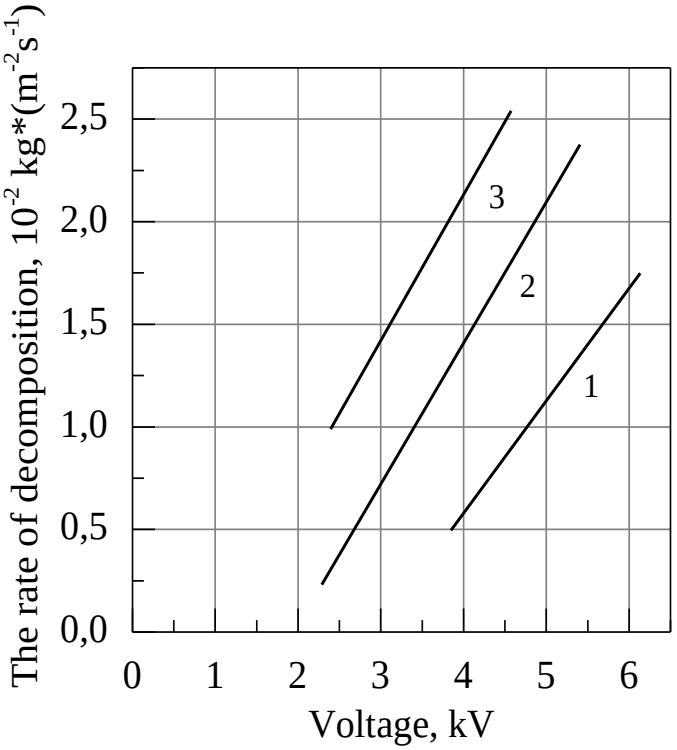

Fig. 3.26. Dependence of the decomposition rate of PTFE on the accelerating voltage at different current densities of the electron beam. 1 – 100 A/m^2; 2 – 300 A/m^2; 3 – 470 A/m^2. The pressure in the chamber is 8.7 Pa, the "crucible–substrate" distance is 100 mm.

With increasing voltages of 2-6 kV, changing of the beam current density (230-470 A/m^2) has the stronger effect on the growth rate of the coatings than on the sputtering rate. This can be explained by the fact that reducing the current density of the beam from 320 to 230 A/m^2 makes it necessary to increase the accelerating voltage to maintain the constant specific power of the electron beam on the evaporation surface. Such compensation leads to penetration of electrons to the greater depth. The volume of material, in which the destruction process takes place with the constant area of evaporation, increases. Since, the evaporation rates with different accelerating voltages at the constant specific power of the beam differ only slightly, the time spent by the polymer chain fragments in the decomposition volume at low current densities of the beam is greater. The yield of the volatile fraction not capable of condensation at temperatures of 25-27 °C, increases. At beam current densities of 470 and 320

A/m^2 and the specific power more than 1.2 MW/m^2, the growth rate of the PTFE coating is approximately the same at identical specific powers. This can be explained by the fact that at such high decomposition rate (1.52 kg/m^{2}s) and current density greater than or 320 A/m^2, the residence time of the polymer chain fragments in the destruction volume becomes quite small and it has slight effect on the release of volatile fractions that can condense at room temperature.

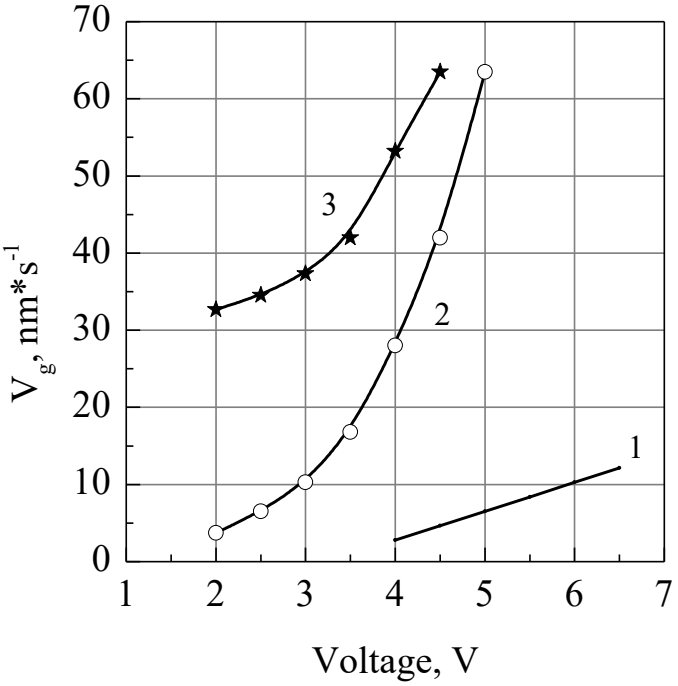

Fig. 3.27. Dependence of the growth rate of PTFE coatings on a substrate that is not treated by the discharge on the accelerating voltage at different current densities of the electron beam. 1 – 230 A/m^2; 2 – 300 A/m^2; 3 – 600 A/m^2. The pressure in the chamber is 8.7 Pa. The crucible–substrate distance is 100 mm.

3.3. Effect of deposition conditions on the utilization rate of the original polymeric substance

An important characteristic of the vacuum evaporation process of a substance is the angular distribution of vapor [137]. In our experiment, the distribution of polymer chain fragments (capable of condensation at room temperature) during the electron beam sputtering was studied. For this purpose, flat samples of equal area were placed at the same distance from the crucible at angles of 0°, 10°, 30°, 70° and 90° to the surface of the evaporated substance. The process took place at pressure of 3.7-4 Pa; the “crucible-substrate” distance was 70, 100, 150, 210 mm; the evaporation rate was from 0.011 to 0.015 kg/m^{2}s; the evaporation area was $5\cdot10^{-5}$ m^2; evaporation materials were PCTFE and PTFE; the evaporation

time was 1200 seconds. Rotation of the crucible was used at a speed of $3 \cdot 10^{-3}$ rev/s to exclude the shielding effect of the hole on the evaporated material surface.

The experiment was carried out on substrates untreated by the discharge. Since it was found that precipitation occurs not only on the front side facing the crucible, but also on the back side, two substrates were fixed, tightly lying one on top of the other. The ratio of polymer mass deposited on the front and back sides was 5:1 and it varied by no more than 10% depending on the specific conditions of the experiment. As the result, the ratio was determined, where *Φ(L)* is the mass of the substance deposited on the substrate located at an angle *L* to the normal to the evaporation surface, so *Φ(0)* corresponds to *L*=0.

Fig. 3.28 shows dependence of the relation on different angles. Experimental results are shown in curve 3. Differences between PCTFE and PTFE evaporation patterns were not observed. The resulting dependence (curve 3) was approximated by a function of the cos(*nL*) form where *n* = 2.8-3.0.

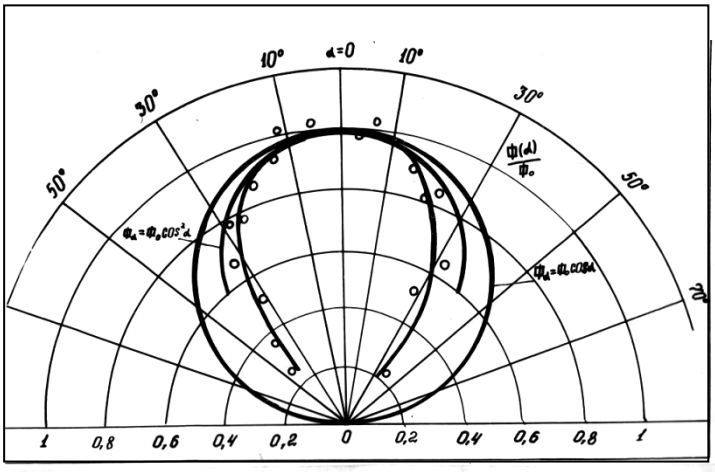

Fig. 3.28. Evaporation diagram for electron beam evaporation of fluorine–containing polymers.

Curve 1 corresponds to the $\Phi_a = \Phi_0 \cos\alpha$ dependence.

Curve 2 corresponds to the $\Phi_a = \Phi_0 \cos^2\alpha$ dependence

Curve 3 –results of experiments.

Thickness of the coating *h* at a fixed angle depends on the distance *R* as follows:

$$h \approx R^{-2.11}, \tag{3.8}$$

This ratio allowed to use the technique described in [69] to determine the utilization rate of the material. The material utilization factor [69] was understood as the ratio of the fragments mass condensing on the substrate located above the crucible in the form of a hemisphere to the mass of the

evaporated material. Table 3.4 presents the dependence of the utilization factor calculated by the method [69] on the voltage of the high-frequency signal. The table shows that the utilization rate of PCTFE is lower than that of PTFE and less than the material in [69]. This difference can be explained by different experimental conditions, as well as by the fact that the electron beam bombardment and PCTFE leads to more active release of the volatile fraction, which was not condensed at room temperature.

Table 3.4

Dependence of the coefficient of use of the polymer on the voltage of the high-frequency sinusoidal signal

Material	Voltage, V										
	0	20	40	60	80	100	120	140	160	180	200
PCTFE	0.42	0.42	0.30	0.27	0.19	0.12	0.05	0.02	0	0	0
PTFE	0.57	0.57	0.53	0.47	0.43	0.36	0.28	0.16	0.11	0.06	0.04

To determine the lines of the equal thickness, two mutually perpendicular axial lines were drawn on the samples before deposition. The film thickness was

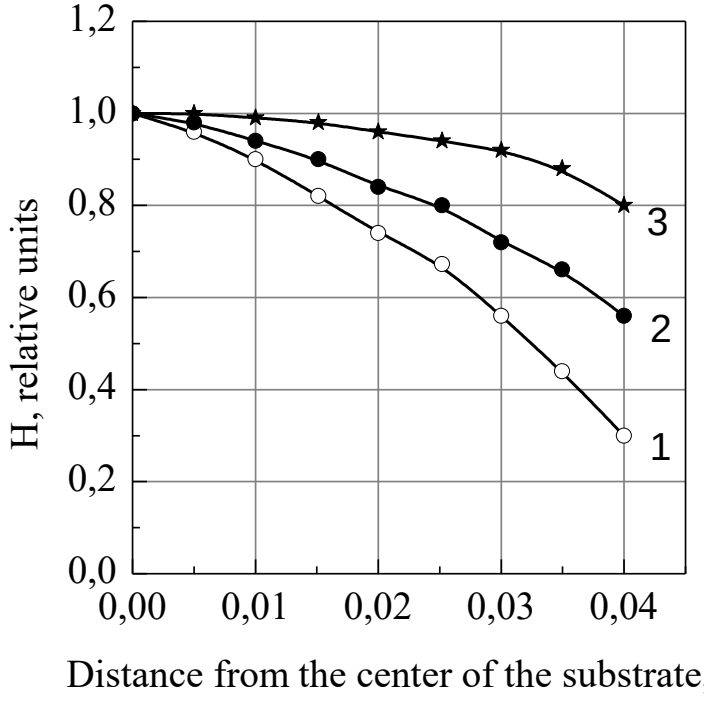

Fig. 3.29. Distribution of the coating thickness on a flat substrate on the "crucible-substrate" distance: 1 – 0.1 m; 2 – 0.15 m; 3 – 0.20 m.

then determined along these line using an interference microscope. The distribution of the coating thickness on the flat substrate is shown in Fig. 3.29. The ratio of the film thickness at a given point to the thickness at the center of the substrate was determined. As can be seen from the Fig. 3.29, the greater the “crucible-substrate” distance, the more uniform is the coating thickness. This indicates that the directional sputtering of the electron beam bombardment products occurs. The optimal distance should be chosen, given that the growth rate of the coating is inversely proportional to the distance from the substrate to the crucible (Fig. 3.30).

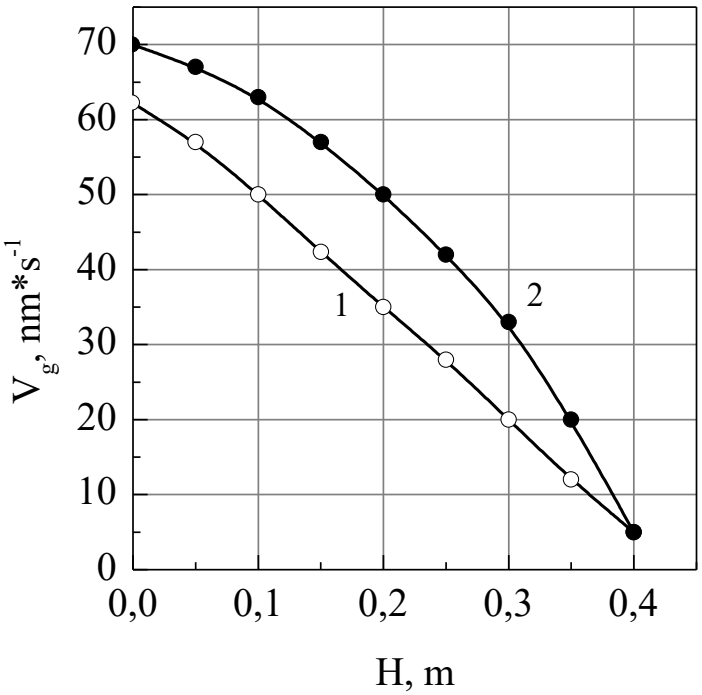

Fig. 3.30. Dependence of the growth rate of the PCTFE and PTFE coatings on the "crucible-substrate" distance. 1 – PCTFE; 2 – PTFE.

3.4. Optimization of the main parameters of the high-frequency glow discharge

The main parameters of the high-frequency glow discharge are the operating frequency and power. These values are interrelated according to research results. It is known from [138-141] that the activation of polymers, in particular PTFE, can be carried out by excited inert gases in the electrodeless space. Inert gas passes through the chamber, in which the electrical discharge exists. The gas excited by the electric current is fed with a certain speed into the vacuum chamber in which a polymer sample is placed. Thus, the surface of the polymer

was activated by bombarding it with the excited gas. Helium, neon, argon, krypton, xenon or mixtures of these gases are used as working gases.

The Japanese company Nitto Electric [84] processed molded products from fluoropolymers at a pressure of 0.5-50 Pa and the discharge energy of at least 0.75 mJ/m^2. The minimum distance between the electrodes should be proportional to $\frac{1}{\sqrt{p}}$, where p is the pressure. In [142], the magnitude of the high-frequency voltage varied from 100 to 1000 V, and the frequency changed from several hundred kilohertz to tens of megahertz. In the work of Goodman [54], the operating voltage was also several hundred volts during the polymerization of monomers, but there was no unambiguous dependence on the oscillation frequency of the generator.

A clear connection of the breakdown voltage with the frequency of glow discharge was established by Hale in 1939 [143]. Fig. 3.31 presents the calculated breakdown voltage (amplitude value) versus frequency at different pressures of argon.

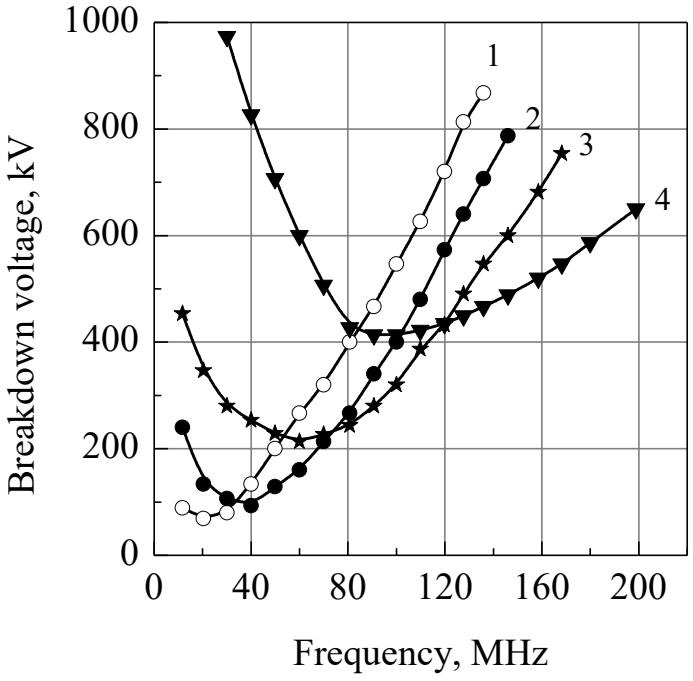

Fig. 3.31. Calculated curves of argon breakdown voltage versus frequency at different pressures.
1 – 1.5·10^{-2} mm Hg.; 2 – 3·10^{-2} mm Hg. v .; 3 – 6·10^{-2} mm Hg.; 4 – 12·10^{-2} mm Hg.

The calculated curves of the argon breakdown voltage versus frequency at various pressures are shown in Fig. 3.32. The experimental results of the dependence of the breakdown voltage of argon on the frequency at different

pressures are compared with the calculated values. The author initiated the breakdown in Pyrex tubes with the diameter of 22 mm and 41 mm and the length of 220 mm. The electrodes were located outside the tube and were 10 mm wide copper strips. The distance between the electrodes was 50 and 100 mm. Hale's theory has shown satisfactory agreement with the experiment.

Main provisions of the Hale theory for pressure above 10^{-3} Pa and frequencies in the range of 1-200 MHz were considered in [144]. If we neglect

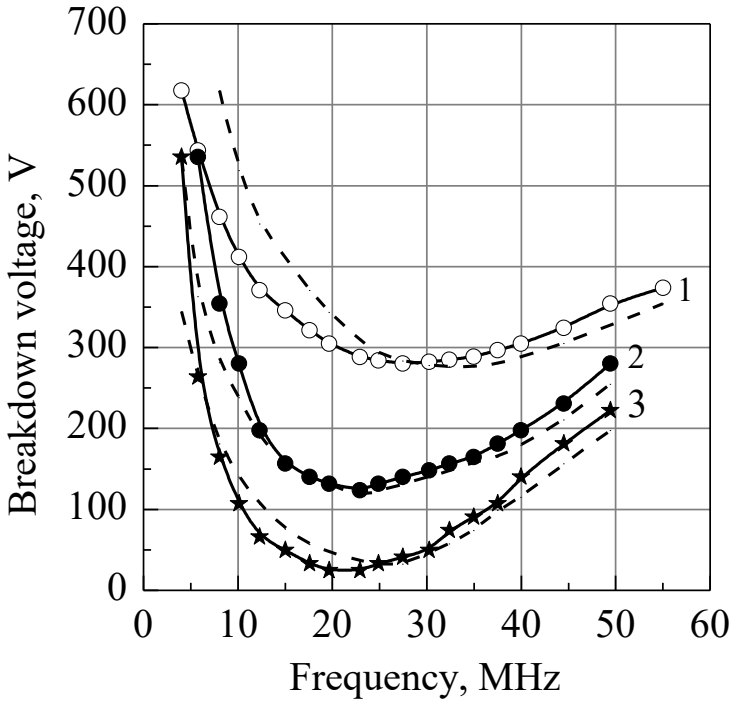

Fig. 3.32. Experimental dependences of the argon breakdown voltage on frequency at different pressures

1 – $4.9 \cdot 10^{-2}$ mm Hg.; 2 – $3 \cdot 10^{-2}$ mm Hg.; 3 – $3 \cdot 10^{-2}$ mm Hg;

The distance between the electrodes for 1 and 2 is 0.10 m, for 3 – 0.05 m. The calculated curves are shown by the dotted line.

the influence of space charges, then the motion of an electron in gas under the action of the electric field for the considered range of frequencies and pressures can be described by the following differential equation:

$$m\frac{d^2x}{dt^2} = eE_o \sin \omega t\,, \tag{3.9}$$

where m is the electron mass, x is the distance from the emitting electrode, e is the electron charge, E_o is the amplitude of the applied field, $\omega/2\pi$ is the frequency of the applied field. From here we get

$$\frac{dx}{dt} = \frac{eE_o}{m\omega}\cos \omega t + C_1 \tag{3.10}$$

$$x = \frac{eE_o}{m\omega}\sin\omega t + C_1 t + C_2 \qquad (3.11)$$

If $x = 0$ at $t = 0$, then $C_2 = 0$. To determine the constant C_1, we will assume that $dx/dt=0$ at the moment t_0 when the electron starts to move. It is the electron in the gas gap due to the operation of the gas-discharge gun, but not the secondary electron dislodged from the cathode. Then

$$C_1 = \frac{eE_o}{m\omega}\cos\omega t_o \qquad (3.12)$$

Regarding this

$$\frac{dx}{dt} = \frac{eE_o}{m\omega}(\cos\omega t_o - \cos\omega t), \qquad (3.13)$$

$$x = \frac{eE_o}{m\omega}(\omega t\cos\omega t_o - \sin\omega t).$$

If $\omega t_o = (2n+1)\frac{\pi}{2}$, where n is an integer, the electron motion is a simple harmonic oscillation, since $\cos\omega t_o = 0$. The electron motion for all other values of t_o consists of the oscillatory motion with frequency ω and the

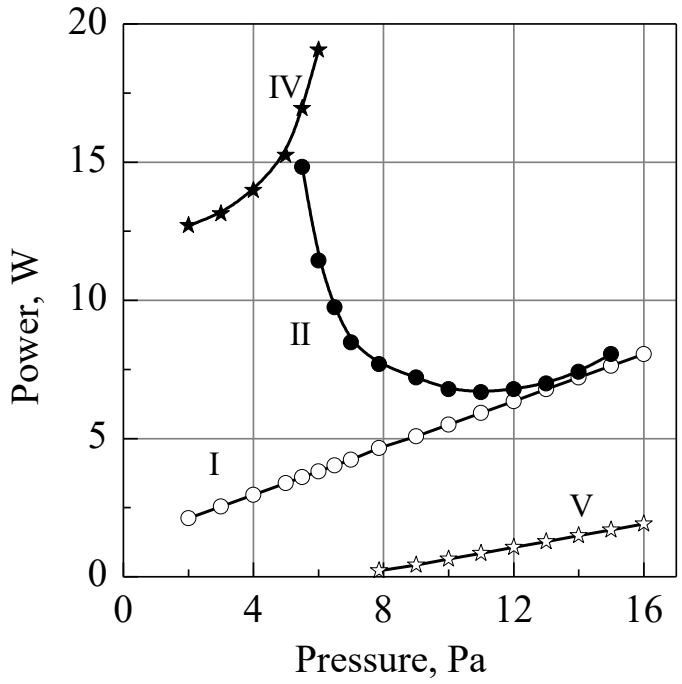

Fig. 3.33. Dependence of the appearance of the PTFE coating on the pressure and power of the RF discharge. The distance to the crucible is 0.11 m; evaporation rate is 0.011 kg/m^{2}s; evaporation time is 1200 s.

translational motion, the speed of which is maximal at $\omega t_o = n\pi$ and is equal to $V_{\max} = \pm\frac{eE_o}{m\omega}$ in this case.

Hale's breakdown criterion is formulated as follows: breakdown occurs at such the electric field strength, at which electrons during the free path have time to receive energy from the applied field equal to the ionization energy of the neutral gas molecule. In accordance with this position, the breakdown occurs when the values of E_o and $f = \frac{\omega}{2\pi}$, where ℓ is such that $x = \ell$, where ℓ is the electron mean free path in a given gas at a given pressure, and the electron energy at the end of the free path is equal to the ionization energy, i.e.

$$\frac{\mathrm{mV}^2}{2} = \mathrm{eU_i}, \tag{3.14}$$

where U_i is the gas ionization potential.

For simplicity, we assume that $t_o = 0$, with the time counting beginning at the moment of the electric field application. Then by using equalities (3.13) we get

$$\begin{aligned} \sqrt{\frac{2l}{m}}U_i &= \frac{eE_o}{m\omega}(1-\cos\omega t) \\ l &= \frac{eE_o}{m\omega^2}(1-\sin\omega t) \end{aligned} \tag{3.15}$$

where time t corresponds to the moment of the electron collision with the neutral molecule and it is a part of the field period. Equations (3.13) contain three unknown quantities: E_o, ω, and t. By eliminating t, one can obtain the dependence of E_o on the frequency of the external field ω. The electrons mean free path can be determined, since it depends on the gas composition and pressure. Fig. 3.31 presents the thus obtained curves of E_{break} for argon versus frequency at various gas pressures. As can be seen from Fig. 3.32, the curves of the breakdown voltage dependence on the frequency of the master oscillator have a minimum in the frequency range of 10-20 MHz. Intention to have the lowest possible breakdown voltage is proved by the fact that decrease in this voltage expands the range of operating potentials and pressures. Taking into account the requirements set by the commission on television and radio broadcasting for frequencies used for industrial purposes, one of the allowed frequencies was chosen, namely 13.56 MHz.

It was found in the experimental study that the high-frequency discharge can be ignited at voltages of several volts during the operation of the electron gun,

which greatly expands the range of operating voltages. As noted earlier, the majority of researchers carried out gas discharge polymerization of monomers with high-frequency discharge powers of 10-100 kW/m^2 and pressure of 13-133 Pa. From this power level, studies were started of the polymerization process of the electron-beam sputtering fluoropolymers products. However, the specific powers above 1 kW/m^2 lead to termination of the condensation process as the experiment has shown under our conditions. When studying the dependence of the film formation rate on the discharge power, it was found that the film growth rate depends on the power. With increase of the high-frequency discharge power, the growth rate of polymer films decreases. This phenomenon is explained by the fact that reactions occur in the following several directions under the action of the electric discharge in the chamber:

a) Disintegration of the molecules fragments of the original substance with the formation of stable compounds of lower molecular weight.

b) Formation of compounds of higher molecular weight from low molecular weight fragments than molecules of evaporated fragments

c) Bombardment of the fragments deposited on the substrate with charged particles that leads to their sputtering at high powers

3.5. Influence of the high-frequency discharge parameters on the polymer coatings formation

A major impact on the formation of fluorine-containing polymer coatings in our proposed method has the following: pressure, the sputtering rate, the high-frequency discharge power and the location of intra-chamber devices. The change in the appearance of PTFE coatings is shown in Fig. 3.33.

The lack of coverage in the IV region is explained by the breakdown of the condensation process under influence of the intense ion-electron bombardment. The boundary of the coverage absence is shifting to the region of increased high-frequency power with increasing pressure. This is explained by increasing proportion of the passing power of the discharge is released on the substrate with increase of pressure. Similar effect occurs in the near-electrode plasma leading to the re-evaporation. With ionization and under pressure of more than 6 Pa, the brown coating is formed on the substrate indicating presence of a large number of double bonds. The coatings obtained in this parameters area are fragile, porous, and they can be easily peeled off the substrate.

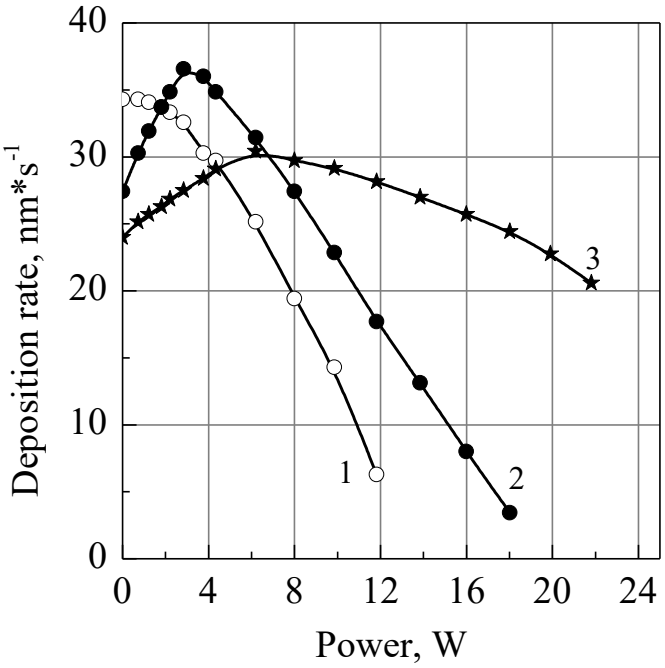

Fig. 3.34. Dependence of the deposition rate of PTFE films on the power of the RF discharge

1–3 Pa; 2 – 5.5-6.5 Pa; 3 – 10-12 Pa;

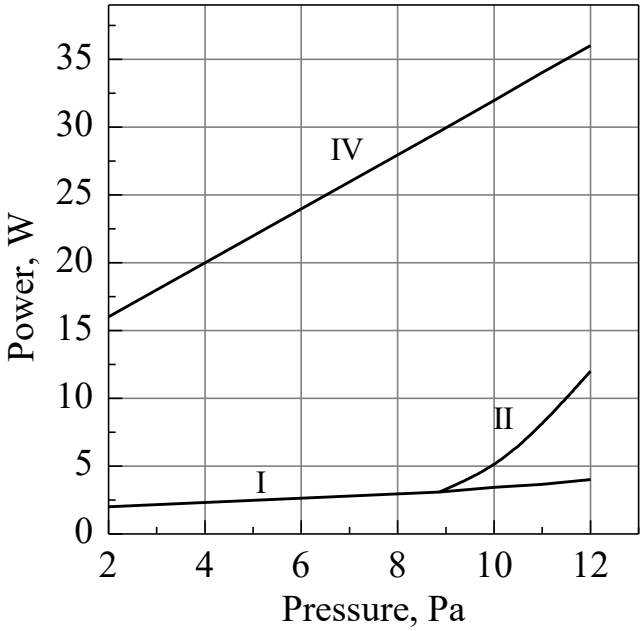

Fig. 3.35. Dependence of the appearance of PCTFE coatings on the pressure and discharge power. The distance to the crucible is 0.11 m; sputtering rate is 0.011 kg/m^{2}s; evaporation time is 1200 s.

The region V is characterized by very low high-frequency power, or its absence, and increased (from 8 Pa and above) pressure. The coatings have a

characteristic white matte color, and they are non-uniform in thickness. The bottom layers are dense, and the top layer is loose and powdered.

The coatings obtained in the region I have the white milky color. This area includes the entire range of operating pressures and characterized by a narrow band of high frequency power values. With increase in film thickness to more than 5 μm, they easily crack.

In the region II, transparent coatings are formed. The ductility of coatings increases with increasing power. Increasing the pressure leads to narrowing of the high-frequency discharge power range. The optimum area of coatings formation is in the pressure gap of 2-5 Pa.

Dependence of the PTFE films deposition rate on the power of the high-frequency discharge is shown in Fig. 3.34. At low pressures (3 Pa), the growth rate curve monotonously drops to zero at powers of 12-14 W. This dependence of the coating growth rate on the discharge power is explained by the fact that the increase in power increases the number and energy of the bombarding particles capable of sputtering fragments of polymer molecules deposited on the substrate. In the pressure range of 5.5-6.5 Pa (curve 2), the dependence of the growth rate has a pronounced extremum. The maximum growth rate in the 1-4 W power range is easily explained if we recall that both the surface polymerization of the polymer chain fragments and the monomer polymerization occur in the gas discharge. The decrease in the growth rate at the power higher than 4 W is explained by the fact that the re-evaporation rate of the settled fragments grows faster than the deposition rate with increasing of the discharge power.

The maximum growth rate is less pronounced at the pressure of 10-12 Pa (curve 3), since the fraction of power released in the discharge plasma, and not on the substrate, increases at high pressures. This means that the effect of the plasma cloud on the polymer fragments passing through it to the substrate is added. With increase of the discharge power, ever larger part of the polymer fragments is crushed to fragments of low molecular weight to a monomer dispersed in the gas and is not condensed on the substrate.

The diagram of the coatings appearance from decomposition products of PCTFE is presented in Fig. 3.35. In contrast to PTFE, the film-free limit passes at high-frequency discharge powers. This is explained by the greater resistance of the PTTFE condensate to ion bombardment and increased adhesion compared

to PTFE. Another feature of the gas-discharge films from PCTFE is their stickiness in the entire pressure range at very low values of the high-frequency

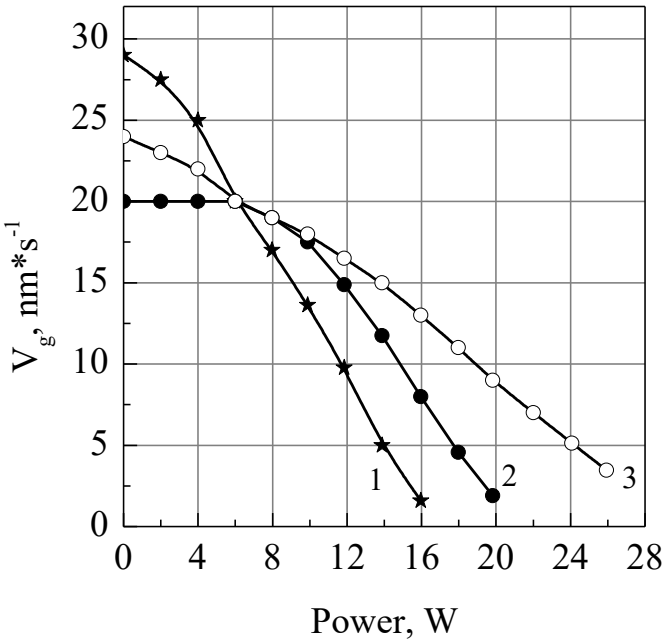

Fig. 3.36. Dependence of the growth rate of PTFE coatings on the power of the high-frequency discharge at different pressure in the chamber
1–3 Pa; 2 –5-5.6 Pa; 3 – 10-12 Pa.

discharge power (region I). This difference is explained by the specific structure of the PTFE and indicates to a low molecular weight of the condensate. Increase in the power of the high-frequency discharge from 2 W leads to the formation of turbid coatings of a brown tint (region III) starting with pressures of 8.3-8.5 Pa.

Transparent, non-adhesive coatings of PCTFE are formed in the much wider range of pressure and RF power as compared to PTFE (region II).

Fig. 3.36 shows the dependence of the PTFE coatings growth rate on the power of the high-frequency discharge at various pressures in the vacuum chamber.

Dependencies at different pressures have a monotonic decrease for all curves. Such behavior can be explained by increase in the sputtering rate of precipitated polymer fragments with increase in the power of the high-frequency discharge. Thus, the trifluorochloroethylene monomer cannot form a coating in the high-frequency glow discharge.

CHAPTER 4
THERMAL AND ELECTRON-BEAM DEPOSITION OF POLYETHYLENE FILMS

4.1 The process of decomposition of polyethylene (PE) in a vacuum

During the thermal heating of a crucible with PE, a significant amount of gaseous products is formed including low-molecular-weight hydrocarbons as a result of intensive destruction in the lower part of the material. Gas, gathering in bubbles, diffuses to the surface. The gas pressure in the bubbles is balanced by pressure in the melt. When the gas bubble evaporates, the volume occupied on the surface of the melt collapses resulting in splashing with the release of melt drops from the surface.

With electron beam evaporation, energy is supplied from above. Therefore, heating and destruction occur mainly in the upper layer of the sample. The possibility of gaseous products formation in the underlying layers is minimized when evaporation mode is properly selected.

However, in the case of the electron beam evaporation of PE, in contrast to PCTFE, along with the destruction of the polymer chains, they are intensively crosslinked. This is evidenced by the insolubility in organic solvents of the polymer residue after the electron-beam evaporation. The cross-linking of polymer chains increases melt viscosity and makes evaporation difficult. As a result, the residence time of polymer chains fragments under the beam increases and, accordingly, the degree of the polymer chains destruction increases. This leads to decrease in the molecular weight of the evaporating fragments. In addition, there is increase in the intensity of gas evolution compared with the thermal evaporation [69].

The depth of the electron penetration into PE when the electron energy changes from 3 to 1 keV varies from $33.3 \cdot 10^{-8}$ to $4.4 \cdot 10^{-8}$ m. The frequency of ionization acts increases with decreasing electron energy from the “string of beads” at energy above 1 keV to narrow continuous bands at the lower energy. Given this, it can be assumed that the region of maximum ionization and heating is not on the surface of the polymer, but at a certain distance from it. In this case, the greatest ionization and heating of the polymer occur the deeper, the higher the irradiation energy. In addition, even with the same degree of ionization along

the track of the primary electron, the surface heating is lower than the underlying layers due to energy removal during evaporation. If the surface temperature of the melt is low, then the proportion of cross-linking reactions is higher than in the more heated underlying layers. Some of the cross-linked molecules destruct and evaporate. However, the intensity of evaporation from the surface of initially formed fragments of linear chains is probably much higher [69]. Over time, a dynamic equilibrium is established on the surface between stitched fragments that have been decomposed and evaporated, and the newly formed fragments.

Thus, under the action of an electron beam, competing cross-linking and destruction reactions proceed. In addition, there is an uneven distribution of energy across the thickness in the surface layers. This leads to the formation of increased concentration of the cross-linked fragments of PE chains on the surface of evaporating PE. Therefore, the evaporation process and the release of gaseous products from the surface layers are impeded. As a result, the pressure in gas bubbles diffusing to the surface is sufficient to emit droplets of the melt after collapse of the bubbles. The analysis of the sputtering mechanisms explains why the selection of evaporation parameters in thermal and electron-beam methods does not remove the sputtering of PE.

Many authors propose to use a system of heated inclined screens to prevent splashing, precluding direct contact of melt drops on the substrate. The disadvantage of using such a screen design is the significant destruction of polymer chain fragments due to their repeated collisions with heated screens and a sharp decrease in evaporation rate compared to evaporation without screens.

To reduce the number of collisions with heated screens, and accordingly, to reduce the degree of their destruction, and to increase the growth rate of the film, we propose to use two side screens having the shape of the evaporation pattern, as well as a horizontal screen (Fig.4.1) [69]. The location of the screens prevents direct drops of the melt on the substrate and reduces the number of collisions of polymer chain fragments with heated screens. Thus, the degree of destruction of fragments falling on the substrate is reduced.

Consider the motion of a particle in which it experiences the least amount of collisions with heated screens. It is necessary to take into account that evaporation occurs at pressure below 0.13 Pa, at which the mean free path of the particle is of the same order, as the evaporator dimensions. In this case, collisions between evaporated particles practically do not occur.

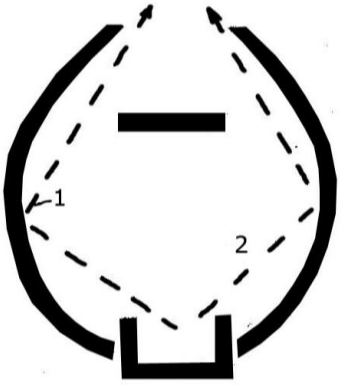

T_{ev} =680 K; T_{sc} = 790 K; $V_{c\,max}$ =7·10^{-9} m/s

Fig. 4.1. Evaporator in the form of the radiation pattern.

As seen in Fig. 4.2, the least number of collisions when using the evaporator with inclined screens is equal to three, while in the proposed version of the evaporator only one collision is possible along path 1 or 2.

It was established in [145], and this corresponds to our data [69], that the maximal growth rate of a PE film while using the evaporator with inclined screens is achieved at temperature of 690 K. If the temperature of the screens is lower, then they are contaminated with polyethylene. When the temperature is above 690 K, intense destruction of the evaporated fragments occurs when they

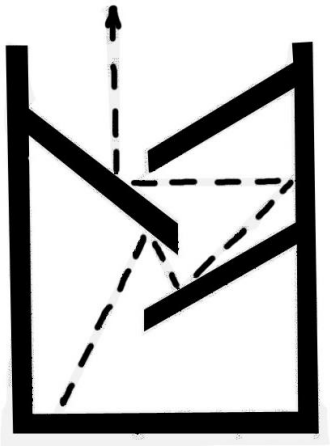

T_{ev} = 680 K; T_{sc} = 680 K; $V_{c\,max}$ =1.7·10^{-9} m/s

Fig. 4.2. Evaporator with side screens.

collide with heated screens. As a result, the film growth rate on the substrate decreases. In the proposed evaporator, when PE is evaporated by the electron beam or by the thermal method, the minimum temperature at which screen contamination does not occur is 750 K [69]. The maximum film growth rate on

the substrate is observed at 800 K. Further increase in screen temperature leads to decrease of the film growth rate.

Fig. 4.3 shows dependence of the condensation rate on the temperature of the screens in the proposed evaporator [69]. There are three areas on the graph:

1. The condensation rate on the screens is higher than the rate of evaporation from them. Screens are dirty.

2. The condensation rate is equal to or less than the evaporation rate from the screens.

3. The temperature of the screens is such that the intensive destruction of the polymer chain fragments begins.

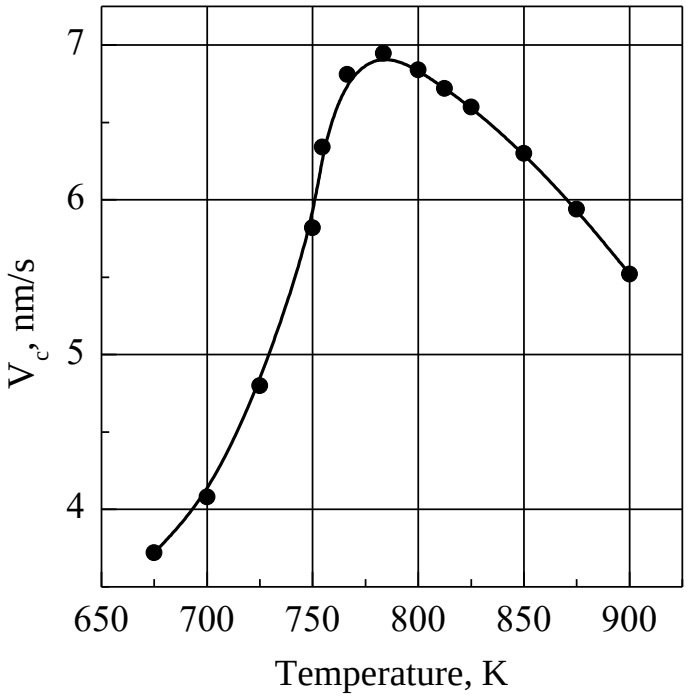

Fig.4.3. Dependence of the condensation rate on the screens temperature. Screens have the shape of the evaporation pattern. T_{ev}= 680 K; T_c=278 K.

The arrangement of the side screens in the shape of the evaporation pattern provides the same ratio of the condensation rate to the evaporation rate at any point on the side screen. In this case, the ratio of the evaporation rate to the condensation rate is a function of only screens temperature. When using the evaporator shown in Fig. 4.2, the condensation rate in the lower parts of the screen is significantly higher than in the upper parts. To avoid contamination of the lower parts of the screen, it is necessary to increase the temperature of the evaporator. Then, at the top of the screen, the destruction of polymer fragments begins to run more intensively. As a result, for the evaporator shown in Fig. 4.4,

the temperature of the screens at which the maximum evaporation rate is

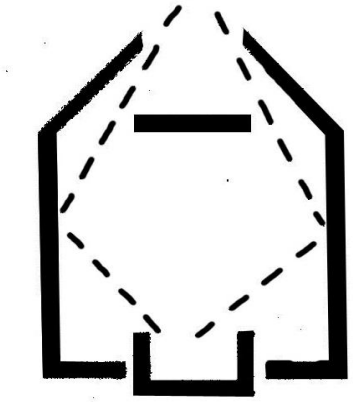

T_{ev} = 680 K; T_{sc} =860 K; $V_{c\,max}$ =$5\cdot10^{-9}$ m/s

Fig. 4.4. Evaporator with a horizontal screen.

reached, increases to 870 K, and the film growth rate decreases [69].

Thus, the use of side screens having the shape of the evaporation pattern has advantages over the inclined screens. The design of these screens allows evaporation to be carried out using both the thermal method and the electron beam one. The evaporation rate and the film growth rate during thermal evaporation is higher than with the electron beam evaporation. As follows from Fig. 4.5, this pattern is observed when the screens are used. The dashed line in the graphs shows the evaporation regimes with the same gas emission.

It was established that the effect of the condensation temperature T_c and electron irradiation of the substrate on the condensation rate was determined not by the method of evaporation, but by the concentration of volatile fragments of the PE chains near the substrate [69].

In cases of electron beam and thermal evaporation, the kinetic laws of condensation are similar. Therefore, we consider them on the example of the thermal evaporation. To assess the effect of substrate temperature on the rate of condensation at various temperatures of PE evaporation, which causes different concentrations of polymer chain fragments near the substrate, let us consider the relative rate of condensation. The relative condensation rate is the ratio of the condensation rate at a given substrate temperature T_s to the condensation rate at the substrate temperature of 278 K ($V_{c\,278}$) (Fig. 4.5).

For the curve 1 (Fig. 4.6) T_s = 680 K and $V_{c\,278}$= $7\cdot10^{-9}$ m/s, while T_s= 750 K and $V_{c\,278}$ = $38\cdot10^{-9}$ m/s for the curve 2. Naturally, the concentration of the polymer chain fragments on the substrate is much higher in the second case.

As follows from Fig. 4.6, this determines a slower decrease in the rate of condensation with increasing substrate temperature. Thus, at substrate

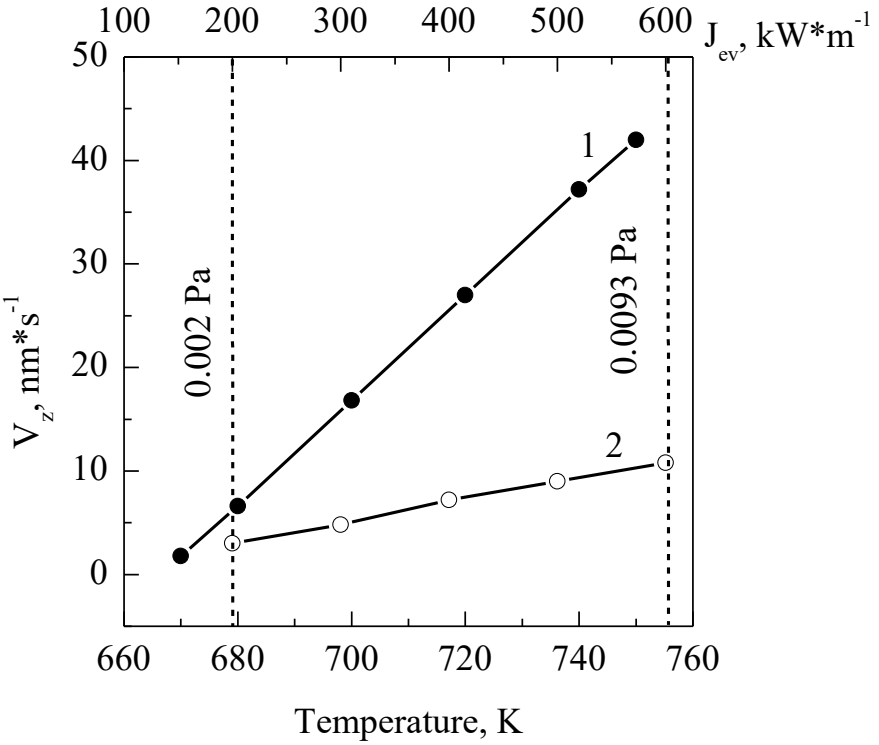

Fig.4.5. Dependence of the condensation rate on decomposition conditions during evaporation with screens T_c=278 K; T_{sc}=793 K;
1 – thermal evaporation; 2 – electron beam evaporation; U_c = 2 kV, dashed line corresponds to the modes with the same gas emission.

temperature exceeding 350 K, the condensation rate is determined by the temperature of the substrate and the concentration of fragments of polymer chains near the substrate.

The above-considered films have low molecular weight and poor adhesive properties. To improve the quality of PE coatings during condensation of polymer chain fragments on a substrate, they were irradiated with the electron beam [69]. Electron irradiation leads to cross-linking of fragments, as well as to increase in the molecular weight of the film and, accordingly, to improvement in its properties.

The energy transferred to the matter during radiation exposure is distributed very unevenly. The higher energy of a charged particle, the deeper it penetrates into the substance. In addition, the higher energy, the more discrete is distribution of the ionization and excitation energy in the bulk of the sample. The increase in molecular weight of condensable fragments under the action of the electron irradiation should take place mainly on the surface of the growing

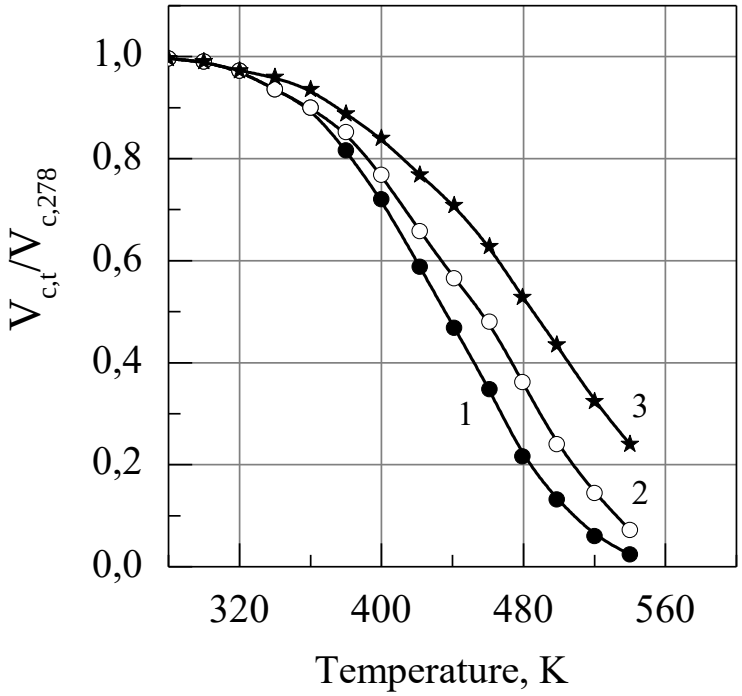

Fig. 4.6. Dependence of the condensation rate on the substrate temperature. 1,2 – condensation without irradiation: 1 – $V_{c\,278}$= 7·10^{-9} m/s; 2 – $V_{c\,278}$= 38·10^{-9} m/s; 3 – condensation with irradiation (U = 600 V; J=0.7 A/m^2 ; $V_{c\,278}$= 7·10^{-9} m/s;)

film. To achieve this, we determined experimentally the minimum energy of electrons, under the influence of which the cross-linking of the fragments of polymer chains occurs in the process of their condensation on the substrate. This obtained energy is about 200-250 eV. When irradiated with electrons having energies above 1 keV, the quality of the film deteriorates. This is probably due to the fact that most of the electron energy is spent not on stitching condensed fragments of chains, but on the transformation of already formed structures in the bulk of the film.

As can be seen from Fig. 4.6, the relative condensation rates of the irradiated and non-irradiated films are similar at room temperature. As T_c increases, the rate of condensation decreases more slowly when the substrate is irradiated than in the case of non-irradiated films. This indicates that the ability of fragments condensing on the substrate to re-evaporation decreases during the electron irradiation.

It has been established that the effect of electron irradiation parameters on the condensation rate is practically absent at room temperature of the substrate.

CHAPTER 5
STRUCTURE, PHYSICAL AND CHEMICAL PROPERTIES OF THIN POLYMER FILMS AND COATINGS

5.1. Infrared spectra of fluoropolymer condensates obtained by electron beam initiation

The study of infrared (IR) spectra of films in the wavelength range from 2 to 20 μm was carried out at the two-beam automated IR spectrophotometer in transmitted and reflected light [69]. All IR absorption spectra of PTFE films obtained under different deposition conditions are shown in Fig. 5.1-5.9.

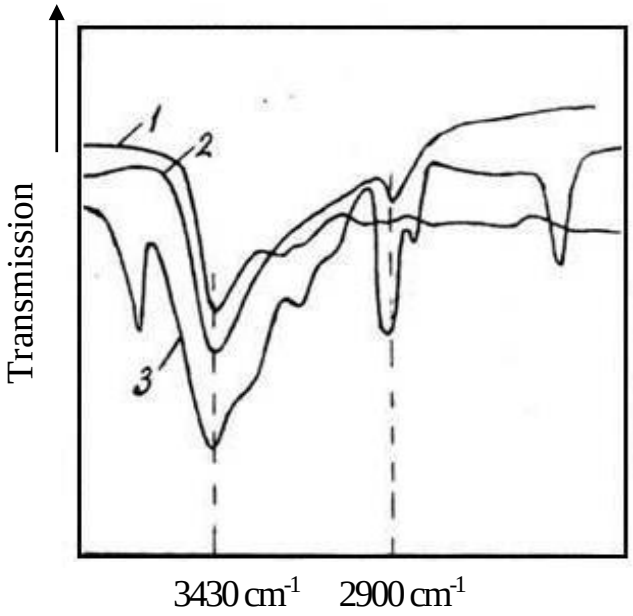

Fig. 5.1. IR absorption spectra of PTFE films obtained under different deposition conditions: 1 – 400 eV; 0.2 mA/cm^2; 2 – 700 eV; 0.2 mA/cm^2; 3 – 400 eV; 0.1 mA/cm^2.

However, some conditions were the same in all experiments. The film thickness was 10-20 μm. The spectra were taken in parallel using at least five samples. Scanning speed was 64 cm^{-1}/min with a linear scan. The spectral width of the slit device was 3 cm^{-1}. Such conditions for recording spectra ensured an accuracy of ± 3 cm^{-1} when measuring the wave numbers in the region of 1600-1800 cm^{-1}, and ± 10 cm^{-1} in the region of 3000 cm^{-1}, and in determining the transmittance up to 1%.

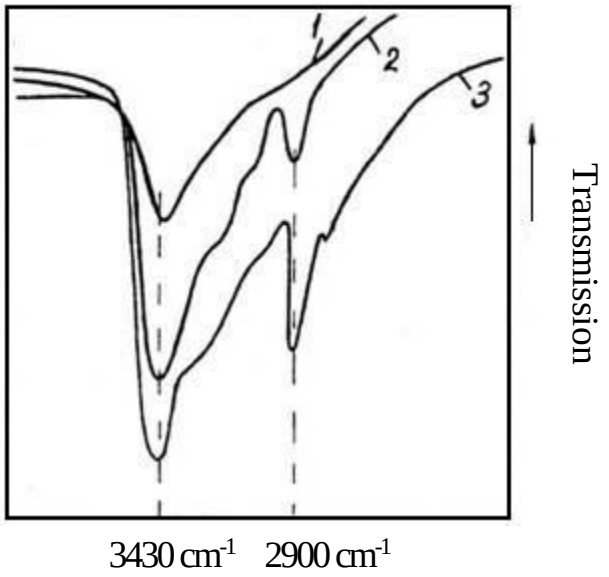

Fig. 5.2. IR absorption spectra of PTFE films obtained under different deposition conditions, as well as industrial films:
1 – T_c = 240 °C; 2 – industrial film; 3–200 eV, 0.5 mA/cm^2.

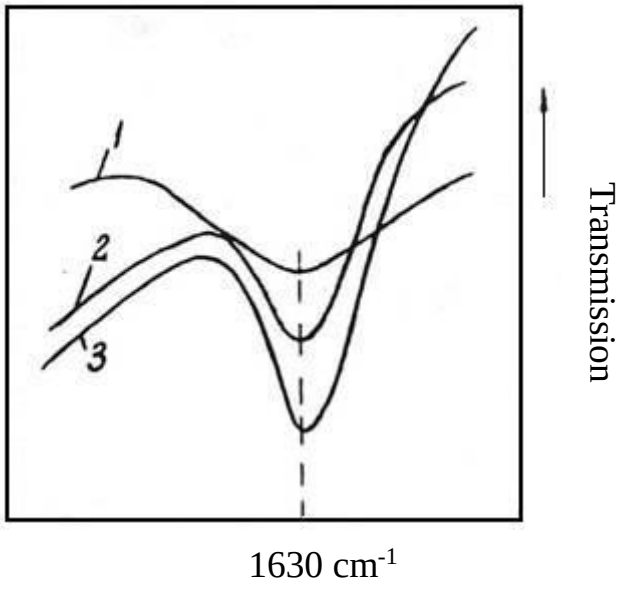

Fig. 5.3. IR absorption spectra of PTFE films obtained under different deposition conditions:
1– 200 eV, 0.3 mA/m^2; 2 – T_c = 25 °C; 3 – 200 eV; 0.45 mA/cm^2

The intensity of the absorption bands was characterized by the magnitude of the optical density, reduced to a unit film thickness

$$D = \frac{100}{l} \lg \frac{J_o}{J}, \qquad (5.1)$$

where 100 is the weight of the basic mole of the macromolecule, μm^{-1}; l is the film thickness (in μm); lg(J_o/J) is the optical density at a given wave

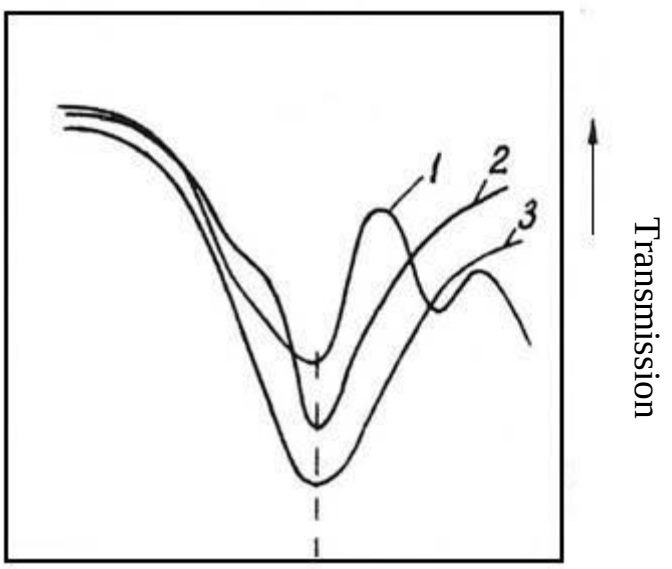

Fig. 5.4. IR absorption spectra of PTFE films obtained under different deposition conditions: 1 – 400 eV, 0.2 mA/cm^2; 2 – 400 eV, 0.2 mA/cm^2, annealed film; 3 – 400 eV, 0.1 mA/cm^2.

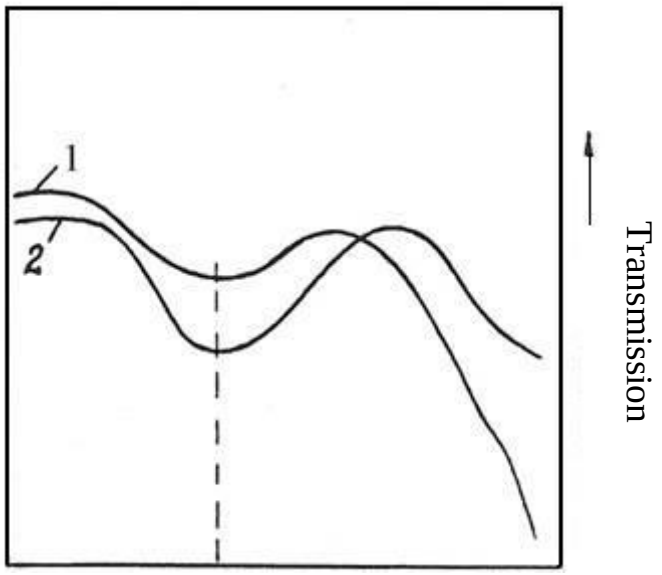

Fig. 5.5. IR absorption spectra of PTFE films obtained under different deposition conditions: 1 – 700 eV, 0.1 mA/cm^2; 2 – 700 eV, 0.35 mA/cm^2

number.

To eliminate the effect of the sample thickness and improve the accuracy of determining the degree of crystallinity, a band at 2330 cm^{-1} was chosen as the internal standard.

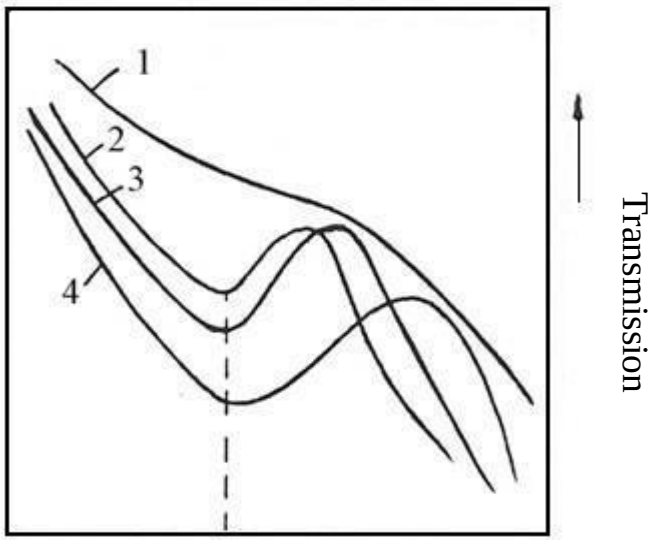

Fig. 5.6. IR absorption spectra of PTFE films obtained under different deposition conditions:
1 – 400 eV, 0.2 mA/cm^2, annealed film; 2–200 eV, 0.4 mA/cm^2; 4 – 400 eV, 0.1 mA/cm^2;
3 – industrial film.

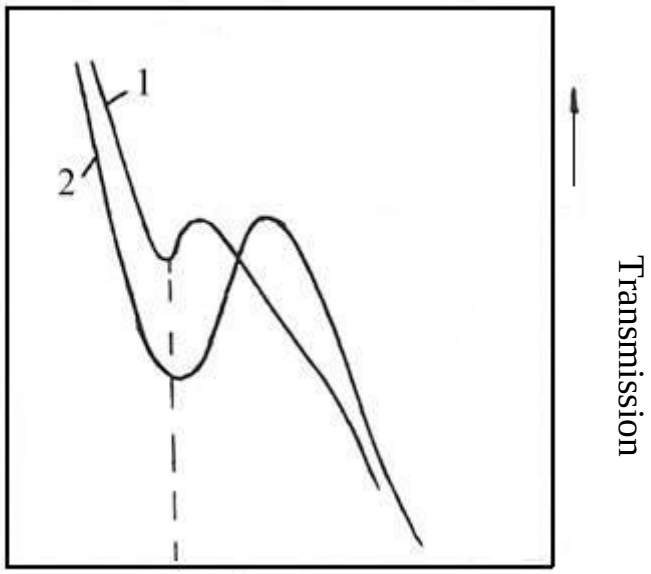

Fig. 5.7. IR absorption spectra of PTFE films obtained under different deposition conditions:
1 – 400 eV, 0.2 mA/cm^2; 2 – 200 eV, 0.6 mA/cm^2

In the infrared spectrum of ordinary PTFE, an intense and wide absorption band is observed in the region of 1300-1100 cm^{-1} attributed to stretching vibrations of the C–F bond [179]. In its spectrum, three less intense bands, 775,

745, and 714 cm^{-1}, are also observed. The absorption in the 775 cm^{-1} region

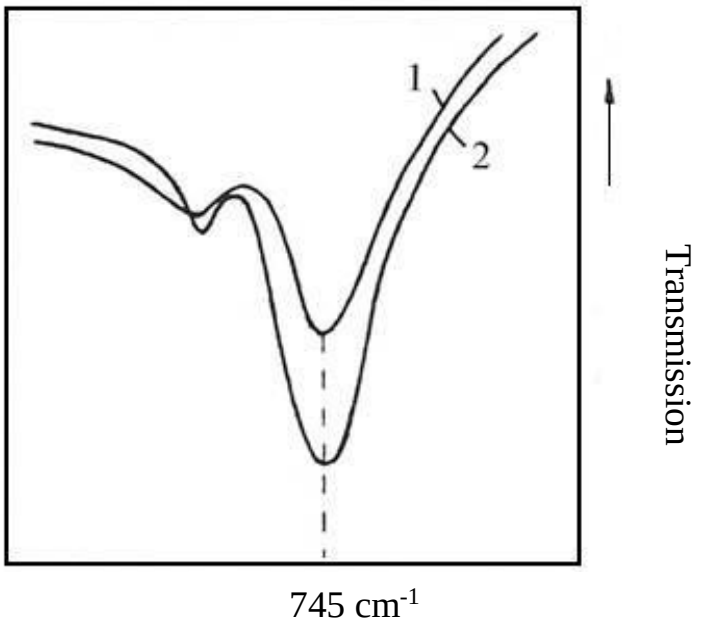

Fig. 5.8. IR absorption spectra of PTFE films obtained under different deposition conditions:
1 – 700 eV, 0.1 mA/cm^2; 2 – 700 eV, 0.1 mA/cm^2, annealed film.

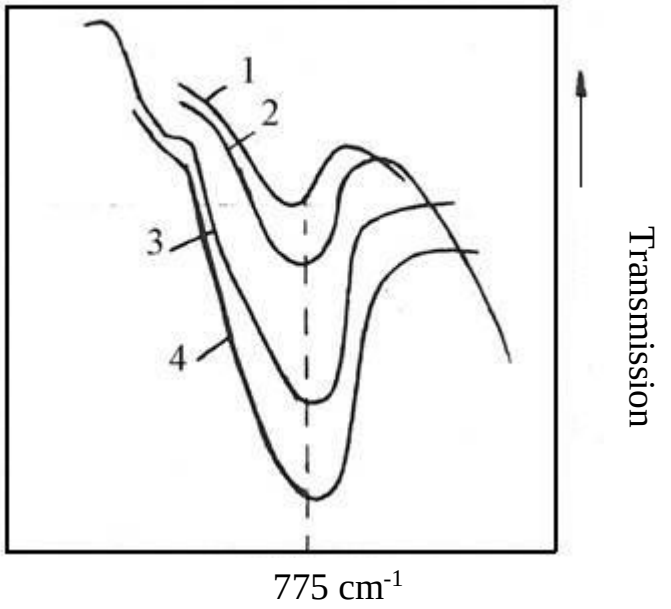

Fig. 5.9. IR absorption spectra of PTFE films obtained under different deposition conditions: 1 – 400 eV, 0.2 mA/cm^2; 2 – industrial film;
3 – T_c = 25˚C; 4 – 400 eV, 0.4 mA/cm^2.

refers to the stretching vibrations of the C–C bond in the fluorocarbon chain, the absorption band of cm^{-1} corresponds to the – CF_2 – CF_3 groups and = CF – CF_3 [146].

The 715 cm^{-1} band is observed in the presence of the CH_3 group in fluorocarbons. It has been found that during the melting of PTFE, i.e. when it

goes from crystalline to amorphous state, the intensity of these three bands decreases sharply.

Thus, according to the intensity of these bands, one can judge, in which state (crystalline or amorphous) PTFE is located. In the spectrum of vacuum PTFE condensates obtained by electron-beam initiation of polymerization, a sharp decrease

in the intensity of these bands is observed with increasing current density *j* of the electron beam and reaches a minimum at j = 0.25 mA/cm^2, which indicates amorphous films produced at such a current density. With an increase in current density to 0.4-0.7 mA/cm^2, the absorption intensity in the 745-725 cm^{-1} region begins to grow again, which indicates an increase in the number of CH_3 groups in PTFE, in other words, an increase in the branching of the polymer, which indicates a decrease in its molecular weight (Fig. 5.8-5.9).

The formation of free radicals under the influence of ionizing radiation in PTFE can proceed according to the following schemes:

$$R_F CF_2 - CF_2 - R_F^{'} - \sim \rightarrow R_F CF_2 - CFR_F^{'} + F \qquad (5.2)$$

$$R_F CF_2 - CF_2 - R_F^{'} - \sim \rightarrow R_F CF_2 + R_F^{'} CF_2 \qquad (5.3)$$

Study of the paramagnetic resonance of irradiated PTFE showed that free fluorocarbon radicals in the films obtained by us can exist for a long time. Such relative stability of the fluorocarbon radicals is explained by the fact that the unpaired electron of the radical is not localized on carbon and interacts with neighboring fluorine atoms.

Free radicals formed upon electron irradiation may further interact with the formation of molecules with double bonds

$$R_F CF_2 - CF_2 + F_2 CR_F^{'} - \sim \rightarrow R_F CF = CF_2 + F_3 CR_F^{'} \qquad (5.4)$$

$$R_F CF_2 - CFR_F^{'} + F - \sim \rightarrow R_F CF = CFR_F^{'} + F_2 \qquad (5.5)$$

Indeed, in the spectrum of PTFE irradiated in vacuum with γ - radiation of Co^{60}, two weak bands are observed, corresponding to terminal double bonds of the type: RFCF = CF_2 (1790 cm^{-1}) [69] and conjugate types RFCF = CFR′F (1733 cm^{-1}) [69].

The study of films obtained by thermal and electronic initiation of secondary polymerization showed that the concentration of terminal double bonds is high at low condensation temperatures (50-150 °C) and low electron current densities (<0.15 mA/cm^2). This indicates a low molecular weight of the obtained films. Increase in the condensation temperature to 240 °C or the electron beam current

density up to 0.25-0.3 mA/cm^2 leads to a sharp decrease in the intensity of these bands (they are almost absent). This indicates increase in the molecular weight of the films under these condensation modes. A further increase in the electron beam current density (> 0.3 mA/cm^2) leads to increase in intensity of these bands. This indicates that the two processes compete during the formation of films: polymerization and destruction with the formation of double bonds.

A band is observed in the region of 1720-1640 cm^{-1} in the spectrum of the obtained films, which corresponds to the appearance of conjugated double bonds. The intensity of this band largely depends on the conditions of the secondary polymerization of the films. Thus, for the films obtained by thermal initiation (T_c = 240 °C), the intensity of this band is low. Decrease of T_c leads to a sharp jump in the intensity, as well as to increase in the conductivity of the obtained films. The current density of electrons irradiating the substrate in the course of the condensation of coatings also significantly affects the intensity of this band.

As follows from Fig. 5.4 and 5.5, the lowest concentration of conjugated double bonds is contained in the films obtained at J = 0.25-0.3 mA/cm^2. In addition, a comparison of the positions of this band and the absorption band at 1790 cm^{-1}, the corresponding double bond at the end of the chain, shows that as a result of the conjugation, a shift by 100-150 cm^{-1} to the long wavelength occurs. Such a strong shift to the long-wavelength region of the absorption band observed in the spectrum of vacuum PTFE films indicates that the number of conjugated double bonds in this substance is more than two. In addition, the relatively large width of this band is probably associated with different length of the formed chains of conjugated double bonds. It should be noted that, in the general case, double bonds can be formed in relatively distant parts of the polymer molecule. The subsequent migration of the double bonds along the chain, as well as energy transfer in a macromolecule can occur with the help of free radicals according to some authors [69].

The presence of double bonds in PTFE is also indicated by the absorption band in the region of 1350 cm^{-1} in its spectrum. This band corresponds to the vibrations of the CF group in the double bond [69]. It should be noted that the absorption bands in the spectra of molecules containing CF_3 groups, as well as perfluorinated four-membered and five-membered rings, lie in the same region. However, according to some authors [69], the main contribution to the absorption in the 1350 cm^{-1} region is made by the vibrations of the CF group in

the double bond.

An analysis of the spectra of the obtained films showed that the regime of secondary polymerization during thermal and electronic initiation methods significantly affects the concentration of terminal double bonds, and therefore the molecular weight of PTFE films. As mentioned above, incomplete polymerization of the active fragments on the substrate occurs at low T_c and low current density of electrons. Under these conditions (T_c = 50-150 °C and J < 0.15 mA/cm^2), the radical disproportionation reaction takes place, and, what is less likely, the depolymerization reaction of radicals. Both of these reactions lead to the appearance of double terminal bonds and do not contribute to the growth of the molecular weight of the film formed on the substrate. Increase of T_c to 250 °C and at the current density on the substrate up to 0.25-0.3 mA/cm^2 leads to the following alternative reaction of polymer radicals

$$R_{F^-}CF_2 + CF_{2^-}R_F^{'} - \sim \rightarrow R_{F^-}CF_2 - CF_{2^-}R_F^{'} \qquad (5.6)$$

and increase in the molecular weight of the polymer film on the substrate. Further increase in T_c leads to destruction and re-evaporation (breakdown of condensation) of fragments. The increase in current density above 0.35-0.4 mA/cm^2 leads, as mentioned above, to the destruction of the film during its growth. The concentration of double bonds increases again, and the molecular weight of the films decreases.

In the spectra of PTFE films obtained at low T_c and low electron energy, as well as at J > 0.4 mA/cm^2, absorption bands are observed in the region of 1550-1450 cm^{-1} (Fig. 5.5-5.7). It is known that in the region of 1560-1410 cm^{-1} there is an intense broad absorption band in the spectrum of $CF_3 – CH = CH – CF_2$ attributed to the vibrations of CH - groups bound by a hydrogen bond to CF. In the region of 1510-1490 cm^{-1}, an intense absorption band is also observed in the spectrum of $CF_2 = CFH$. Sometimes it shifts to the region 1400-1420 cm^{-1}.

Thus, we can conclude that in the spectra of the films obtained according to these modes, there are absorption bands characterizing the presence of CH bonds in the fluorocarbon. The appearance of these bands is associated with the replacement of fluorine atoms by hydrogen in the process of electron irradiation with the formation of CH bonds. It is known from the literature data [69] that OH fluoroform radicals were found in the reaction products of perfluoroalkyl radicals with water. Consequently, the bonds of OH and CH could appear in the spectrum of the films obtained only as a result of the resulting free radicals

interaction with atmospheric water vapor. According to this, the formation of CH and OH groups in the films can be represented by the following scheme:

$$R_F CF_2 + H_2O \rightarrow R_F CF_2 H + OH \quad (5.7)$$

$$R_F CF_2 + OH \rightarrow R_F CF_2 OH \quad (5.8)$$

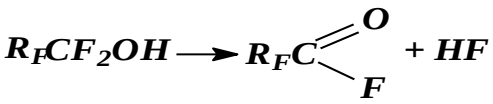

(5.9)

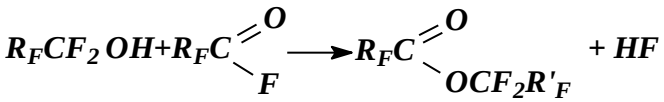

(5.10)

Further oxidation resulting from the reaction of (5.10) alcohols can lead to formation of molecules with carbonyl and carboxyl groups. The presence of absorption bands in the spectrum of the films characteristic of the products obtained by the reactions (5.7-5.9) confirms this scheme. Oxygen absorbed by the film directly interacts with free radicals formed in the film:

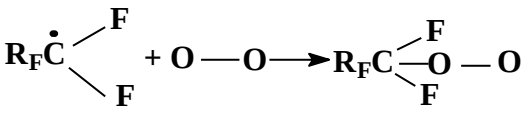

(5.11)

Subsequent reactions of such oxygen-containing radicals, most likely, lead to the formation of molecules with carbonyl groups, as follows from the spectra of the films. It is obvious that in our case the formation rate of free radicals significantly exceeded the rate of absorption of oxygen or vapors of molecular water by the film (in a vacuum their concentration is low). Therefore, most of the film growth process interacts with the formation of molecules with double bonds, according to schemes (5.4) and (5.5), and only a small part of the radicals was consumed in reactions (5.6) and (5.10).

Since the concentration of free radicals in unannealed films obtained by the worst regimes is great, the concentration of oxygen-containing groups in the film is greater due to the occurrence of reactions (5.7-5.10) and (5.11) in air. Films produced under the best conditions (T_c = 240 °C and J = 0.25-0.3 mA/cm^2) contain a significantly lower concentration of free radicals. Annealing of the films further reduces the radicals concentration. Therefore, the absorption in the region of 1550-1450 cm^{-1} in these films is practically absent.

The intensity of the absorption band extending from 3600 cm^{-1} to 2600 cm^{-1} is also insignificant in such films. There are absorption bands in this area

characteristic of free and bound groups of OH- molecules of alcohols and acids with fluorocarbon radicals (Fig. 5.1, 5.2) [69]. This suggests that the films should have good dielectric properties in a wide frequency range. The intensity of these bands sharply increases in the films obtained at low T_c <160 °C and current densities of 0.1 mA/cm^2 > J > 0.35 mA/cm^2. This can be explained by interaction of free radicals in the reactions (5.2-5.5) and (5.7-5.11). Films obtained according to these modes must have poor dielectric properties.

5.2. Infrared spectra of fluoropolymer condensates obtained by gas-discharge evaporation

It is known [69] that the intensity of absorption in the IR spectrum of PTFE decreases sharply when PTFE converts from a crystalline state to an amorphous state in the region of 775, 745 and 715 cm^{-1}. By intensity of the bands, one can evaluate the predominance of the crystalline or amorphous phase in the coating.

Fig. 5.8 and 5.9 show the dependence of the 745 cm^{-1} and 775 cm^{-1} band intensity from the conditions of the coating formation. Increasing the power of the high-frequency discharge from 2 to 4 W leads to increase in the degree of crystallinity. It is clearly seen that the treatment in the 10 W glow discharge further increases the absorption in this band. This phenomenon can be explained by the fact that with the increase of the high-frequency discharge power, the molecular weight of the condensate decreases due to increase in the electron-ion bombardment intensity and, as a result, the degree of crystallinity increases.

A further increase in the power of the high-frequency discharge leads to increase in the intensity of this band indicating increase in the branching of PTFE or its degradation.

In the spectrum of PTFE coatings obtained in glow discharge at powers up to 2 W and above 8 W, intense bands are observed in the region of 1790 cm^{-1} corresponded to the presence of terminal double bonds of the $R_fCF = CF_2$ type and 1733 cm^{-1}, which corresponds to conjugated bonds of the type $R_fCF = CFR_f'$.

This indicates that low-molecular films are obtained under these conditions.

When the discharge power is less than 3 W, the polymerization reaction is not so pronounced, and the process of destruction begins to prevail at the power higher than 8 W.

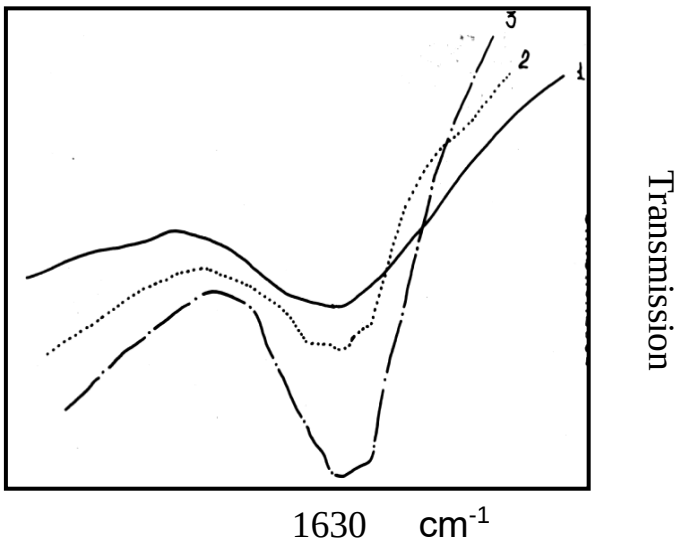

Fig.5.10. IR absorption spectra of PTFE films obtained in a glow discharge of different power. 1 – 2 W; 2 – 4 W; 3 – 10 W.

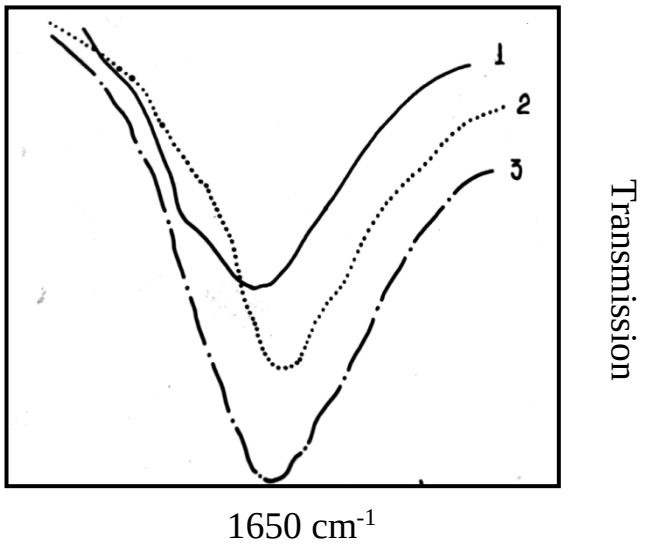

Fig. 5.11. IR absorption spectra of PTFE coatings obtained in a glow discharge of different power. 1 – 2 W; 2 – 4 W; 3 – 10 W.

In the power range of 3-8 W, the intensity of these bands decreases indicating existence of the polymerization process and increase in the molecular weight of the condensate.

A band is observed in the region of 1720-1640 cm^{-1} in the spectra of the obtained coatings, which corresponds to the appearance of conjugated double bonds. The intensity of this band significantly depends on the deposition conditions. The intensity of this band is rather low in the films produced at discharge powers of 4–6 W.

A decrease in power below 3 W or an increase above 8 W leads to increase in the absorption intensity. In addition, a comparison of the positions of this band and the 1790 cm^{-1} absorption band, the corresponding double bond at the end of the chain, shows that a shift in the long wave region of 150-200 cm^{-1} occurs as a result of the conjugation. A shift in the long wave region is such that the number

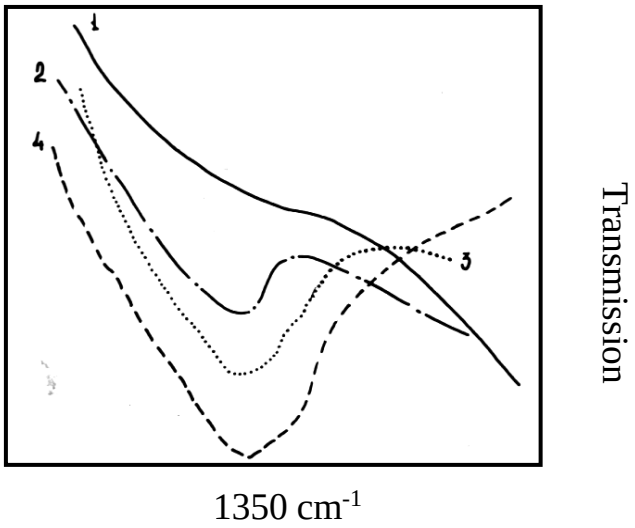

Fig. 5.12. IR absorption spectra of PTFE films obtained in a glow discharge of different power
1 – industrial film with a thickness of 10 μm; 2 – 4 W; 3 – 2 W; 4 – 10 W.

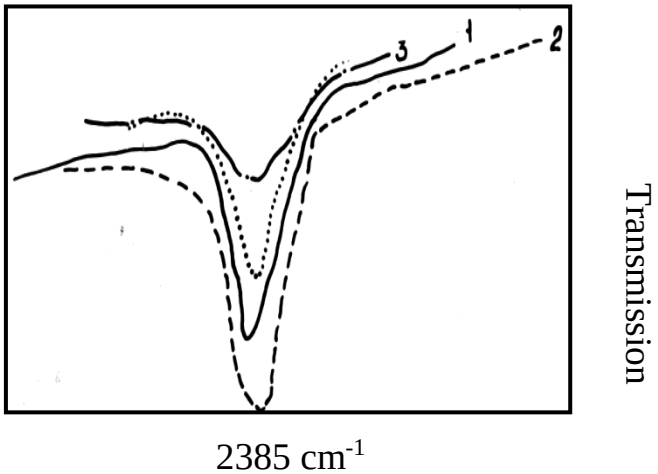

Fig. 5.13. IR absorption spectra of PTFE films obtained in a glow dıscnarge of different power. 1 – initial polymer; 2 – without treatment with high-frequency discharge; 3 – 2 W; 4 – 12 W.

of mates in the condensate is more than two. In addition, such a large bandwidth may be associated with different lengths of the formed chains of conjugated double bonds. The presence of double bonds in the PTFE vacuum condensates is also indicated by the absorption band in the region of 1350 cm^{-1} (Fig. 5.12). This

band corresponds to the vibrations of the CF group near the double bond [69].

Analysis of the PTFE coatings IR spectra shows that the treatment of the electron-beam destruction products of the starting PTFE significantly affects the concentration of terminal double bonds and, therefore, the molecular weight of the condensate. At low power of the high-frequency discharge, incomplete polymerization of the active fragments on the substrate occurs. Under these conditions, the radical disproportionation reaction and depolymerization of the radicals occur. Both of these reactions lead to the appearance of double terminal bonds and do not contribute to the growth of the molecular weight of the films.

In the range of high-frequency discharge powers of 3-6 W, an alternative reaction of polymer radicals occurs:

$$R_f - CF2 + CF2 - R'_f \longrightarrow R_f - CF2 - CF2 - R'_f$$

and the molecular weight of the polymer film increases. Further increase in the power of the RF discharge leads to destruction and fragments re-evaporation. In this case, the concentration of double bonds increases again meaning that the molecular weight of the films decreases.

In the band of 2600-3600 cm^{-1}, there is a very wide range in which the absorption bands lie characteristic of free and bound OH groups and molecules of acids and alcohols with fluorocarbon radicals [69]. From Fig. 5.12-5.15 it is seen that the intensity of these bands is insignificant.

PCTFE

The infrared absorption spectrum of PCTFE is more complex than the absorption spectrum of PTFE. A number of intense absorption bands are observed in the spectrum with maxima at 495, 505, 577, 592, 657, 970, 1125, 1195, 1280 and 2400 cm^{-1}. Absorption bands at 505 and 592 cm^{-1} are observed only as projections of the absorption bands at 495 and 577 cm^{-1}.

It is known [69] that the bands at 438, 490, and 580 cm^{-1} grow with an increase in the degree of crystallinity of PTFE. These bands are practically absent in films obtained at RF discharge powers of less than 2 W, i.e., these films are amorphous. To calculate the degree of crystallinity, a pronounced band of amorphousness of 755 cm^{-1} was used along with the 438 cm^{-1} band. The results are shown in Table. 5.1. It can be seen that the degree of crystallinity of PTFE films obtained at discharge powers of < 2 W is zero.

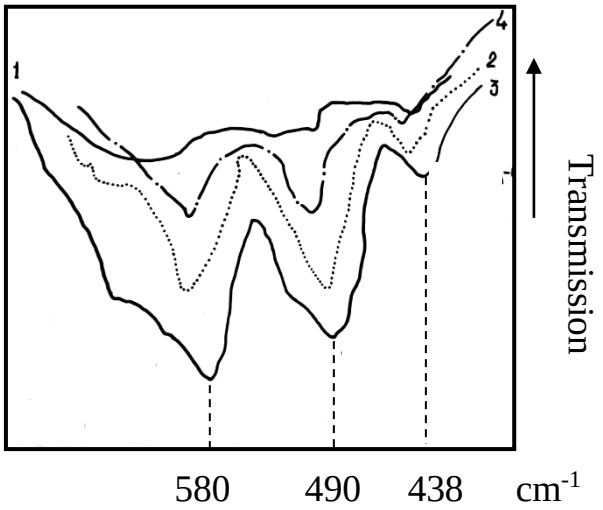

Fig. 5.14. IR absorption spectra of PCTFE films obtained in a glow discharge of different power.
1 – 2 W; 2 – initial polymer; 3 – without RF treatment; 4 – 4 W.

Table 5.1.

Degree of crystallinity of PTFE condensates obtained in high-frequency discharge

Sample	λ		$C_f = \frac{\lg(I_o / I)438}{\lg(I_o / I)755}$	S_{cc}.(%)
	438 cm^{-1}	755 cm^{-1}		
Commercial powder	0.038	0.006	6.33	33
W_p = 2 Вт	0.010	0.006	1.67	0
W_p = 10 Вт	0.042	0.006	6.47	42
W_p = 4 Вт	0.022	0.006	3.92	15

The unsaturation in the spectrum of PCTFE is characterized by absorption bands at 1767 and 1360 cm^{-1}, which are due to the formation of terminal double bonds – $CF = CF_2$ [69]. It should be noted (Fig. 5.15) that the intensity of these bands is minimal in films obtained at the high-frequency discharge power range of 2-4 W, which indicates increase in the molecular weight of the films as a result of the secondary polymerization reaction.

Polymerization reaction occurs if the power is less than 2 W. When power is higher than 6 W, the process of destruction begins to affect, as in the case of PTFE, leading to decrease in molecular weight and increase in the concentration of terminal double bonds.

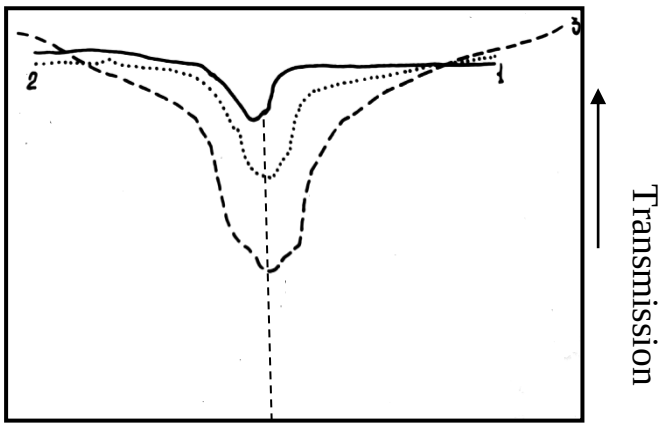

Fig. 5.15. IR absorption spectra of PCTFE films obtained in a glow discharge of different power: 1 – 2 W; 2 – without treatment; 3 – 10 W.

5.3. Infrared spectra of polyethylene (PE) films

The IR spectra were measured at the temperature of 300 K. A 30 μm thick film was deposited in vacuum directly on a potassium bromide tablet. To control the film thickness on the tablet, deposition of the similar film was carried out on the "witness" substrate. The film thickness was determined by the profilograph - profilometer and was equal to the film thickness on the potassium bromide tablet.

The standard deviation of the film thickness from the specified value did not exceed ±1 μm. To obtain the film required for measuring the IR spectrum of the original material, PE granules were pressed in vacuum under the specific pressure 24.5 MPa.

The degree of the polymer chains branching in the original PE and in the vacuum condensates was determined by the absorption band intensity at 1378 cm^{-1} responsible for deformation vibrations of C – H bonds in methyl groups. A number of double bonds was determined by 880, 910 and 965 cm^{-1} absorption bands, related to the non-plane deformation vibrations of C – H bonds in vinyl R = CH_2, vinylidene $\begin{matrix} R\backslash \\ R/ \end{matrix} C = CH_2$ bonds, and $R - CH = CH - R'$ trans-vinylidene groups. The extinction coefficients for these bands were taken from [4]. The applicability of this technique for determining the degree of unsaturation and branching under the experimental conditions was checked while taking the IR spectra of the original PE. Table 5.2 presents the averaged data and the mean square error (for five samples) of films of both the initial PE and the vacuum

condensate with the confidence level of 0.95. The obtained data are in satisfactory agreement with the literature data. Increase in the number of vinyl bonds in the initial PE film is probably due to mechanical destruction of the sample during pressing.

Competing reactions of cross-linking and destruction of macromolecules proceed when PE is irradiated. The cross-linking reaction is due to breaks in C – H bonds, while the destruction reaction is due to breaks in C – C bonds in the main chain of the macromolecules. If there is no significant heating of PE during irradiation, then the mobility of macroradicals formed when the C – C bonds are broken, is small, and a significant part of the broken bonds recombines (the "cell" effect of Franklin-Rabinovich). In the case of homolytic cleavage of the C – H bond, the hydrogen atom diffuses easily from the point of the bond cleavage. As a result, cross-linking reactions of polymer chains prevail at low radiation intensities.

If the electron beam intensity is more than 200 kW/m^2, the number of C – C bond breaks increases and significant radiation of the PE occurs, as a result of which the probability of recombination of broken C – C bonds decreases. The resulting fragments of polymer chains continue to break up until the kinetic energy of the fragment is sufficient for its evaporation. Simultaneously with the degradation reaction, the cross-linking reaction occurs. The resulting cross-linking between the polymer chains prevents evaporation of the gaseous decomposition products formed in significant quantities during the PE irradiation.

Gaseous products, collecting in bubbles, diffuse to the surface. The collapse of the bubbles on the surface of the melt leads to the sputtering of PE. To eliminate this drawback, deflecting screens have been installed between the crucible and the substrate, precluding the dropping of the macrodroplets of the melt on the substrate. As can be seen from the Table 5.2, the degree of unsaturation of polymer chains in vacuum condensates is significantly higher than in the original PE.

It is known that the formation of trans-vinylidene bonds is associated with intense release of hydrogen during irradiation and this occurs when two radical centers interact in neighboring polymer chains. This is accompanied by transfer of a hydrogen atom, or during a relay migration of an unpaired electron along the chain before meeting another unpaired electron.

Table 5.2

Results of the analysis of unsaturated groups and the degree of branching in the studied samples

Sample	Total number of double bonds per 1000 C atoms	Number of double bonds of the type			Number of CH_3 groups per 1000 C atoms
		vinyl	vinylidene	trans-vinylidene	
		per 1000 C atoms divided by the total number of double bonds,%			
LDPE [7]	0,3-0,7	- / 50-70	- / 20-30	- / 10-25	3-5
LDPE (our data)	0.719 ± 0.0054	0.593 ± 0.006 / 82.5	0.084 ± 0.002 / 11.7	0.042 ± 0.004 / 5.8	5.11 ± 0.04
Condensate	19.37 ± 0.772	16.2 ± 0.8 / 83.6	1.42 ± 0.03 / 7.3	1.75 ± 0.03 / 9.1	$23. \pm 0.5$

Destruction of polymer chains in the process of evaporation causes an increase in the terminal bonds of $R = CH_2$ and $R - CH_3$ type

$$-CH_2 - CH_2 - CH_2 - CH_2 - CH_2 - CH_2 - \xrightarrow{e} -CH_2 - CH = CH + -CH_2 - CH_2 - CH_3$$

A simple calculation of methyl and vinyl groups content in the original PE and in the vacuum condensate shows that the reaction 1 does not provide increased content of the methyl groups in the vacuum condensate. The additional formation of CH_3 groups indicates that not only loss of hydrogen occurs in the process of evaporation, but also its interaction in the atomic state with evaporating fragments of the polymer chains takes place:

$$-CH_2 - CH_2 - CH_2 - CH_2 - CH_2 - CH_2 - \xrightarrow{e} 2 - CH_2 - CH_2 - CH_2$$

$$2 - CH_2 - CH_2 - CH_2 + \psi 2H \longrightarrow 2 - CH_2 - CH_2 - CH_3$$

Naturally, the reaction 2 is possible only with high content of atomic hydrogen in the reaction zone, and this condition is satisfied in the case of PE

evaporation by the proposed method. The increase in the number of vinyledene bonds can be explained if to assume that the terminal and middle radicals are cross-linked during the irradiation process:

$$CH_2-CH-CH_2-CH_2-CH_2-CH_2-CH_2 \xrightarrow{e} -CH_2- \underset{\underset{CH_2}{I}}{C} H-CH_2-$$

One can see the break up with the formation of chains fragments, one of which contains a methyl group, and the other contains a vinylidene group:

$$CH_2-CH-CH_2- \xrightarrow{e} -CH_2-CH-CH_3 + --CH_2- \underset{\underset{CH_2}{II}}{C} -CH_2$$

It is known that the average vinyl group accounts for one macromolecule in linear PE. Therefore, knowing the number of vinyl groups in the initial PE per 1000 carbon atoms, one can estimate the length of the polymer chain. In this case, the carbon chain of the original PE contains approximately 1700 carbon atoms. In the vacuum condensate, there are 62 per vinyl group, and 42 methyl atoms per methyl group. The minimum chain length with CH_3 groups at the ends is 42 carbon atoms. If there is one vinyl group at the end of the chain, then the chain should contain about 62 carbon atoms and one or two methyl groups.

Thus, in the vacuum condensates obtained by the electron evaporation of LDPE, the significant decrease in the molecular weight of polymer chains was established by IR spectroscopy methods, as well as increase in the degree of unsaturation and branching compared with the original polyethylene.

5.4. Crystallinity of the polyethylene thin films obtained in a vacuum

The authors of [147] studied the effect of the decomposition method (thermal and electron beam), as well as the rate and temperature of condensation on the crystallinity of the resulting coating. Thin films of non-polar polyethylene (PE) with good dielectric characteristics were chosen as the object of research.

Calorimetric studies were performed using the differential scanning calorimeter. The degree of crystallinity χ of films was determined by:

$$\chi = \frac{\Delta H_m}{\Delta H_m^o} \tag{5.12}$$

where ΔH_m is the enthalpy of the film melting; ΔH_m^o is the enthalpy of the equilibrium crystal melting in kJ/kg determined by using the equation proposed by Wunderlich [148]

$$\Delta H_m^o = 227.14 + 0{,}786 \cdot T - 1.066 \cdot 10^{-3} \cdot T^2 - 0.51 \cdot 10^{-6} \cdot T^3, \tag{5.13}$$

where T is the temperature in Celsius degrees.

IR spectra of thin PE films were recorded on the Specord 75 IR spectrophotometer. The absorption band at 1303 cm^{-1} was used to determine the degree of PE crystallinity.

According to the Beer-Lambert law [149]

$$D = \varepsilon \cdot C_a \cdot d\,, \tag{5.14}$$

where D is the optical density of the absorption band at 1303 cm^{-1}; ε is the molar absorption coefficient; C_a is the amorphous factor; d is the sample thickness.

C_{a1} = 1 in a fully molten state. If D_1 is the optical density of this band for PE in a fully molten state and D_2 is the optical density at a certain temperature below the melting point, then

$$\frac{D_1}{D_2} = \frac{\varepsilon \cdot C_{a1} \cdot d}{\varepsilon \cdot C_{a2} \cdot d} = \frac{C_{a1}}{C_{a2}}\ ; \qquad C_{a2} = \frac{D_2}{D_1} \tag{5.15}$$

Thus, by knowing the optical absorption densities at a given temperature and in a fully molten state, one can determine the coefficient of PE crystallinity at a given temperature.

$$\chi = 1 - C_{a2}\,. \tag{5.16}$$

Films deposited in vacuum on potassium bromide tablets were used for research. The difficulty of determining the crystallinity of the films is that the tablet is positioned vertically, so when the film is heated to high temperature, polymer is draining from the tablet, and intensity of the absorption peaks decreases due to the decrease in the film thickness. To increase the adhesion of the film to the tablet, the tablet was treated with glow discharge before depositing the film. In addition, to reduce the polymer runoff, two tablets of potassium bromide with 15 μm thick films produced in the same mode were placed in one holder with the films contacting each other and pressed using the spring. As a result, it was possible to be sure that the intensity of the 1303 cm^{-1}band practically did not decrease at temperatures above the melting point

corresponded to 418 K [150]. Thus, the films were deposited simultaneously on 8 tablets and 4 spectrums were studied in parallel. The deviation error of the absorption intensity at the wave number of 1303 cm^{-1} was no more than 4%. Temperature fluctuations during the measurements were less than 0.5 K. For more accurate determination of the temperature, above which the optical absorption does not change, the spectrum of the film was measured every 1 K near the melting point.

When studying the process of crystallization of PE films obtained by evaporation in vacuum, one should take into account that chemically inactive fragments rather than macroradicals are condensed on the substrate according to our unpublished data. The molecular weight distribution (MWD) of the condensable polymer chains fragments M_w/M_n is rather narrow with M_w ranging from 1.1 to 1.83, and M_n from 1500 to 7500 depending on the method of evaporation and the condensation rate. M_n and M_w are the number average and weight average molecular weights, respectively.

Table 5.3 shows results of IR - spectroscopic studies of crystallinity of the films obtained by the thermal and the electron beam evaporation.

It can be seen from the table that measuring the degree of crystallinity of films obtained by thermal and electron-beam evaporation methods gives comparable results at the same substrate temperatures T_c and condensation rates V_c.

At the same condensation rates and substrate temperatures, the crucible-substrate distance and change in the evaporation mode (evaporation temperature T_e, electron energy U and current density J) do not affect the degree of the films crystallinity. The degree of the films crystallinity increases with decreasing substrate temperature and increasing the condensation rate.

Results of measyrements by the method of the differential scanning calorimetry (DSC) are presented in Table 5.4.

By using the DSC method, it was established that increasing the condensation temperature during thermal and electron beam evaporation reduces the melting point of films by 0.5 and 2 K, respectively. It should be noted that the preparation of the substrate surface before deposition has a significant effect on the formation of the coating. Surface treatment of the substrate with glow discharge before deposition of the coating reduces the degree of crystallinity in the PE film from 90.7 to 72.5% and lowers the melting point by 1.5 K.

Table 5.3

Results of IR-spectroscopic studies of films obtained by evaporation of PE in vacuum. Influence of the deposition conditions on MWD of PE thin films

No.			$V_c \cdot 10^3$, μm/s	T_c, K	H_{m-n}, cm	χ
	Evaporation method		Thermal method			
	T_e, K					
1	663		2.65	278	20	0.74
2	678		5.0	278	20	0.82
3	663		5.2	278	15	0.85
4	663		2.65	343	20	0.44
5	663		5.0	343	20	0.52
	Evaporation method		Electron beam method			
	U, V	j, mA/cm^2				
6	2	10	2.6	278	20	1.70
7	2	20	6.0	278	20	0.82
8	3	12	5.8	278	20	0.83
9	2	10	2.6	343	20	0.45
10	2	20	6.0	343	20	0.54
11	2	10	5.8	343	10	0.56

Table 5.4

Results of the crystallinity study of the films obtained by thermal and electron beam evaporation of PE (DSC method)

Evaporation mode	$V_c \cdot 10^3$, μm/s	T_c, K	T_m, K	ΔH_m, kJ/kg	χ	Note
Thermal evaporation	2.65	278	388	263	0.91	Without glow discharge
	2.65	278	386.5	210	0.73	With glow discharge
	38.0	278	388	282	0.97	
	2.65	343	386	177	0.61	
	5.0	343	386	194.6	0.67	
Electron beam evaporation	2.6	278	383	196.4	0.68	
	2.6	343	381	175	0.61	
	6	343	381.5	210	0.73	

The melting point of polymers obtained by crystallization from solution and melt depends on the molecular weight of the crystallizing chains and conditions of crystallization. In Fig. 5.16 it is shown how the melting point of equilibrium crystals changes in the case of elongated chains of relatively narrow PE

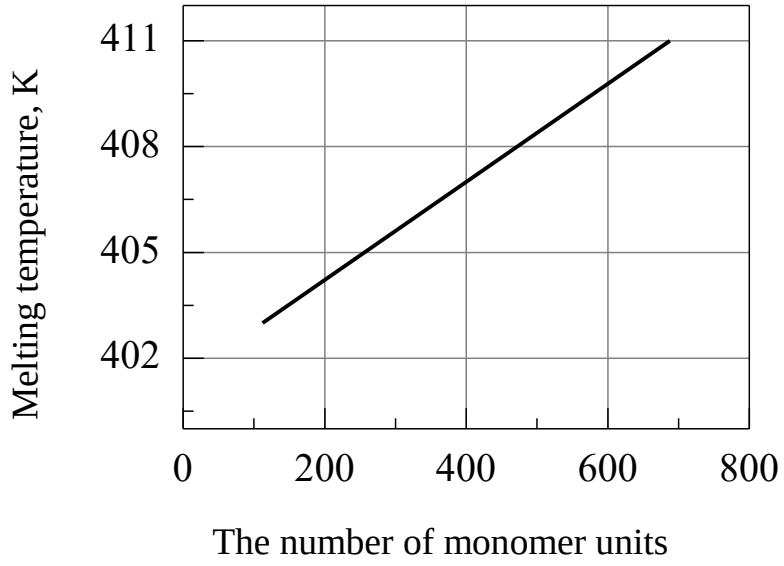

Fig. 5.16. Dependence of the melting point of equilibrium PE crystals on the number of monomer units in the chain

fractions. The straight line in the figure is described by the following equation

$$T_m = T_m^o - \frac{2071}{p}, \tag{5.17}$$

where T_m^o = 414.1 K is the melting point of polymer crystals with an infinitely large molecular weight. The melting point of PE films obtained by condensation in a vacuum is significantly lower than that indicated on the graph for the same molecular weight. One would assume that in accordance with the formula

$$m_m = \chi \cdot T_m^o, \tag{5.18}$$

where χ is the degree of crystallinity, the films obtained have a low degree of crystallinity.

However, the calculation of the degree of crystallinity by the formula (5.12) shows that in some cases (see Table 5.4) the degree of crystallinity is more than 0.9.

The melting point of the polymer is determined by the formula

$$m_m = \frac{\Delta H_m}{\Delta S_m}, \tag{5.19}$$

where ΔS_m is the entropy of melting.

The observed decrease in ΔT_m at high values of ΔH_m indicates that the value of the melting point according to (5.19) is more determined by the entropy of melting than by the enthalpy. By definition, the melting entropy ΔS_m is a quantitative measure of the disorder resulting from the volume increment during a crystal-melt transition. ΔS_m of the polymer is determined by the difference in the enthalpy of the melt S_1 and the enthalpy S_2 that the polymer had before the melting process starts.

$$\Delta S_m = S_1 - S_2 . \tag{5.20}$$

The entropy of the film obtained by crystallization in the process of condensation in a vacuum in a completely molten state S_2 differs little from the entropy of the melt previously crystallized from the solution or the melt. Therefore, increase in ΔS_m and accordingly decrease in T_m in PE films is due to low S_2 values. It is explained by the specific crystallization conditions in the process of condensation in a vacuum.

The authors concluded that the most probable conformation is a statistical coil during the free movement of a polymer chain fragment in a vacuum. The degree of crystallinity of the obtained PE films does not depend on the method of evaporation and is determined by the condensation rate and the condensation temperature. The degree of crystallinity of the films increases with increase in the rate or decrease in the condensation temperature.

5.5. Molecular weight and polydispersity of thin films of polyethylene obtained in a vacuum

The most common characteristics of a mixture of polymer homologists are three types of average molecular weight [124]. Depending on the method of determination, the number average molecular weight M_n, the weight average molecular weight M_w and the average molecular weight M_z can be obtained. The more the average molecular weights defined in different ways differ, the wider the molecular weight distribution of the polymer. The ratio $\frac{M_w}{M_n}$ or $\frac{M_z}{M_w}$ determines the statistical width of the MWD expressed by the distribution function of the degrees of polymerization or molecular weights, which in some cases can be represented in the analytical form. There are $q_n(M)$ numerical and

$q_w(M)$ weight distribution functions for molecular weight M.

The value of $q_n(M)$ is determined by the ratio of the numerical fraction of polymer chains dw enclosed in the range from M to $M + dM$ to the width of this interval

$$q_n(M) = \frac{dn}{dM}, \tag{5.21}$$

Similarly, $q_w(M)$ is determined by the ratio of the weight fraction of polymer chains dw enclosed in the range from M to $M + dM$, to the width of this interval

$$q_w(M) = \frac{dw}{dM}, \tag{5.22}$$

interconnected by the relation [124]: MWD of the obtained films is determined mainly by conditions of the course of the PE destruction.

Let the process evolve over time. By the selected moment t, the number of decays is so large that the degree of degradation w is already finite and it is equal to the ratio of the number of decay events to the number of bonds in the original chain, although small compared with I. If the probability of all bonds breaking is the same, then w at this stage of degradation is the probability that some arbitrarily selected bond in the original chain at time t is broken. Since only two events can occur with a connection (it either breaks or remains), the probability that this connection is maintained is equal. Therefore, the probability $\chi \cdot p$ that the p adjacent links separated as a single fragment from the original chain is the product of the probabilities of three independent events: 1) the breaking of some connection r; 2) rupture of the bond $r + p$ (r and $r + p$ denote the numbers of the corresponding bonds in the original infinite chain; r = 1, 2, 3, 3) preservation of the intact p-1 bonds between the connections r and $r + p$. Consequently,

$$\chi_p = w^2 (1 - w)^{p-1}. \tag{5.23}$$

The product $\chi_p \cdot p$ gives the relative number of monomer units contained in all fragments of the degree of polymerization p. According to the definition [124], this number is the weight (discontinuous) distribution function for the degrees of polymerization $q_w(p)$:

$$q_w(p) = pw^2 (1 - w)^{p-1} \tag{5.24}$$

After some transformations [6] and considering that $\omega << 1$, expression (5.24) reduces to the following continuous distribution

$$q_w(M) = M \cdot L^2 \cdot e^{-LM}. \tag{5.25}$$

where $L = \frac{w}{m_o(1-w)} = \frac{1}{M_n}$; m_o is the molecular weight of the monomer. The numerical function of this distribution will be, as follows:

$$q_n(M) = L \cdot e^{-LM} \tag{5.26}$$

Formula (5.26) is the most probable Flory distribution.

The actual process of the polymers destruction (but not chain depolymerization) is statistically equivalent to the random disintegration of an endless chain [151]. The actual destruction can be likened to the "continuation" or "resumption" of the decay process that leads to the most probable distribution (5.26). Thus, regardless of the type of the original MWD, as a result of the destruction, it is precisely this distribution that is obtained. Experiments show that this is indeed the case [151]. Traces of the initial distribution are lost after 5-10 cycles of destruction, which correspond to increase in the number of macromolecules in the system by 5-10 times. From [124, 151], it follows that the most probable distribution corresponds to the ratio $M_z : M_w : M_n$=3 : 2 : 1. Information on reactions occurring during the formation of the initial PE, as well as about reactions during its destruction and condensation is summarized in the MWD of the obtained films. From the statistical point of view, it makes no difference how the process of the polymer chains formation proceeded in time [151]. The nature of the distribution depends ultimately on the ratio of reaction rates resulting in dead chains. If the chains become inactive as a result of a quasi-monomolecular breakage, i.e., termination of chain growth is not associated with its attachment to another chain, the MWD is described by the form function (5.26). The concept of the quasi-monomolecular breakage also applies to disproportionation, although this is a bimolecular reaction. If recombination reactions take place simultaneously with the quasi-monomolecular breakage, the MWD is described by the Schulz distribution [151]:

$$q_n(M) = \frac{L^{K+1}}{r(K+1)} M^K e^{-LM}, \tag{5.27}$$

where K corresponds to the average number of recombinations resulted in the formation of the dead chains.

It was shown [151] that for distribution (5.27)

$$\frac{M_w}{M_n} = \frac{K+2}{K+1}, \tag{5.28}$$

$$\frac{M_z}{M_w} = \frac{K+3}{K+2}, \qquad (5.29)$$

The sign by which the Schulz distribution differs in experience from any other, is that $M_z - M_w = M_w - M_n = 0.5 = const$

It follows from (5.28) and (5.29) that the Flory distribution (5.13) is a special case of the Schultz distribution. In this case $M_z : M_w : M_n = 3:2:1$ [151].

It can be seen from formulas (5.28), (5.29) that the statistical width of the MWD decreases with increase in the number of recombinations that the chain undergoes. The data on the molecular weights of vacuum condensates obtained by the thermal evaporation of PE in a vacuum is very limited [4,152], and those obtained by the electron beam evaporation have not been found at all. The effect of the pyrolysis temperature on the molecular weight of the vacuum condensates was studied most thoroughly in the work of Madorsky [4]. To prevent splashing and dropping of the melt droplets on the substrate, Madorsky carried out the pyrolysis of small weights of 4-5 mg placed in the crucible in the form of a thin layer from the polymer solution. The molecular weights of the condensates obtained during the pyrolysis of PE and polymethylene in the temperature range from 653 to 473 K were studied. The number average molecular weight of the fraction volatile only at the pyrolysis temperature was determined by microscopy and amounted to 470-750. With increase in the pyrolysis temperature above 773 K, there was a tendency to decrease the molecular weight of the condensate. Madorsky suggested that M_n = 1200 represented the upper limit for molecules able to enter the gas phase.

To obtain polymeric coatings with a thickness of 0.5 μm and more, weights of 1-5 g were evaporated. Pyrolysis of such weights was accompanied by intense sputtering of PE and dropping of melt drops on the substrate that leads to violation of the homogeneity and continuity of the coating. The sputtering of PE was due to the fact that because of low thermal conductivity of the polymer during heating, a significant temperature gradient aroused directed from the bottom of the crucible to the free surface of PE. The destruction in the lower layers is much more intense than in the upper layers that leads to formation of a significant amount of monomer and other low molecular weight gaseous products. Gas, gathering in bubbles, diffused to the surface. The collapse of cavities with a gas on the surface led to the melt dropping from the crucible. With the electron beam evaporation, the mechanism for the formation of gas

bubbles is somewhat different, but the sputtering can also be explained by the collapse of cavities with gas in the surface layer. To prevent melt droplets from falling on the substrate, heated screens were used, on which additional destruction of evaporated fragments and melt drops occurred. Thus, the conditions for obtaining coatings from PE differed significantly from the conditions of the experiments described in [4].

Table 5.5 shows the results of chromatographic studies of the molecular weights of PE thin films obtained by evaporation in vacuum.

The number average molecular weights of the obtained films are 2 or more times higher than the M_n of the condensates obtained by Madorsky, who evaporated small weights.

The authors investigated the effect of the method and parameters of PE decomposition during thermal and electron beam evaporation on the molecular weight distribution (MWD) of the obtained vacuum condensates. We also determined activity of the polymer chains fragments.

Table 5.5

Influence of the deposition conditions on MWD of PE thin films

No.	Evaporation method	V_e mg/s	T_c K	M_n	M_w	M_z	K	$\frac{p}{p-1}$
1	Thermal	4	278	6317	7585	8918	4.0	-
2		4	343	7141	7979	8662	7.3	-
3		16	278	6104	7215	7944	4.6	-
4		1	278	2784	4748	6597	0.43	0.62
5	Electron-beam	4	278	1748	3161	5126	0.24	1.25
6		4	243	1594	2863	4790	0.25	1.20
7		4	413	1706	3122	4973	0.21	1.38
8		1	278	1340	2403	4308	0.27	1.09

MWD of the condensates were studied at the Dupont liquid chromatograph. Weight of the sample was 5-10 mg; orthodichlorobenzene was the solvent; the solution temperature was 383 K, and the flow rate was 0.7 ml/min. An IR sensor with a wavelength of 3.5 μm was used for the analysis. The scheme of the experimental setup for obtaining the vacuum condensates is shown in Fig. 5.17.

Low pressure PE granules were placed in the crucible 1. The crucible was heated by passing current in the case of the thermal evaporation. In case of the

electron beam evaporation, beam 4 from the electron gun 2 was guided into the crucible using the magnetic deflecting system 3. Heating of PE thermally or its electron irradiation led to the destruction of polymer chains into separate fragments and their evaporation. Fragments of the evaporated polymer chains condensed on the substrate 6, temperature of which was set by the thermostat 7. The system of deflecting screens 5 prevented the PE melt from dropping on the substrate. The residual pressure in the vacuum chamber 8 did not exceed $1.3 \cdot 10^{-3}$ Pa. The vapor pressure of PE fragments during its evaporation was no more than $6 \cdot 10^{-2}$ Pa.

Decrease in the weight of the sample during pyrolysis was determined by the loss of weight of the sample. The kinetic energy of the evaporating fragment can be increased significantly due to the energy of the collapse of bubbles on the surface of the melt, as a result of which the weight of the evaporating fragment increases. Increase in the molecular weight of the condensate may also be a consequence of the processes occurring during decomposition and evaporation of melt drops from the heated screens.

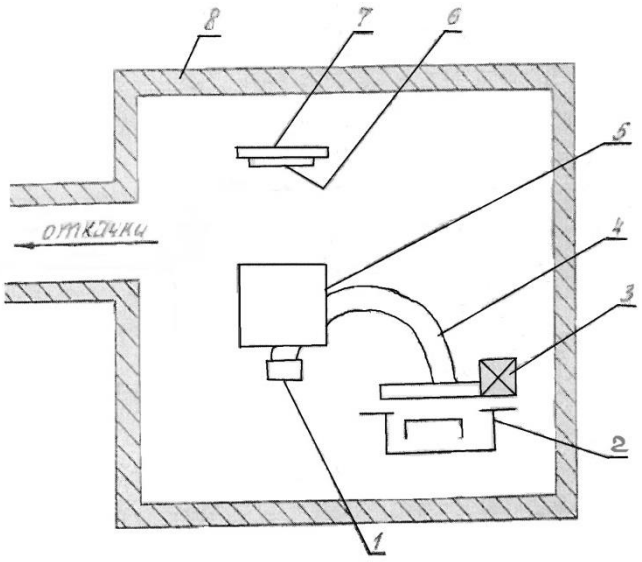

Fig. 5.17. The scheme of the experimental setup for obtaining PE vacuum condensates

It follows from chromatograms reflecting the general form of the MWD in the films under study that the distribution functions in all cases are unimodal. Therefore, it can be assumed that reactions that completely suppress the multimodality of the original MWD [151] occur during pyrolysis and condensation, and these reactions are homophasic in nature. In this case, the

analysis of MWD is reduced to the study of the relationship $\frac{M_w}{M_n}$ or $\frac{M_z}{M_w}$ for the case of radical polymerization [151]. From the table it can be determined that the MWD of films are described by the Schulz exponential formula (5.14). Moreover, *K* calculated by the formula (5.28) has positive values either greater, or smaller than one. Obtaining fractional values of $K > 1$ indicates the formation of dead chains as a result of recombination leading to the narrowing of the MWD. As shown in [151], such MWD obtained as a result of multiple recombinations and it becomes very difficult to describe it analytically. The *K* value between 0 and 1 means a fractional recombination number. It has no physical meaning, but if we talk about the average number of recombinations, this means that only a part of the chains recombined, and the rest ended their growth by a quasi-monomolecular mechanism. Therefore, the resulting distribution for $0 < K < 1$ can be represented by a linear combination of the Schulz distribution of zero and the first orders [124,151]:

$$q_n(M) = pLe^{-LM} + (1+p)L^2Me^{-LM}, \qquad (5.30)$$

where *p* and *l-p* are the relative concentrations of macromolecules resulting from quasi-mono-molecular breakage and recombination, respectively.

We introduce the following notation:

$$\beta = (1-p)L^2 \text{ and, } L\beta = \frac{p}{1-p}, \qquad (5.31)$$

then $q_n(M)$ can be rewritten as

$$q_n(M) = \beta(\beta + M)e^{-LM}. \qquad (5.32)$$

After simple transformations of [5.6] we get:

$$M_q = \frac{q}{2}\frac{(q+1)+L\beta}{q+L\beta}, \qquad \frac{M_q}{M_{q-1}} = \frac{q}{q-1}\frac{(q+L\beta)^2-1}{(q+L\beta)^2} \qquad (5.33)$$

where M_q is any *q* - average weight of the polymer.

Substituting the experimentally obtained values of M_n and M_w at $q = 2$ into the system of equations (5.33), we determine the values of *L* and β (calculations were performed on a PC using the program developed by us). Using the obtained values of *L* and β, we determine M_z^{theory} and compare it with M_z^{exper}. As follows from the table, the experimentally and theoretically obtained values are in the satisfactory agreement.

The primary destruction process of PE during heating or irradiation is the formation of free radicals [153]. As shown by the results of Electron

Paramagnetic Resonance (EPR), no radicals were detected in the obtained films. Radicals could disappear as a result of recombination and disproportionation reactions. The disproportionation occuring with the separation of hydrogen:

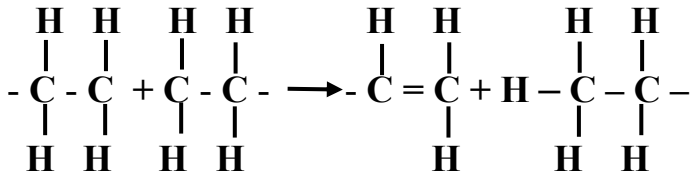

requires significantly more activation energy than the recombination:

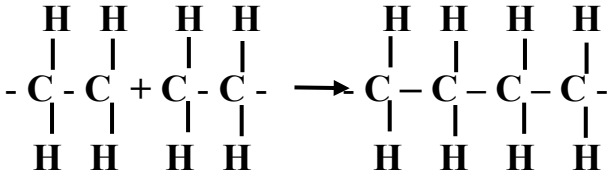

According to the available data [124], the activation energy of recombination does not exceed 0.3-0.4 kcal/mol, whereas the activation energy of disproportionation reaches values of the order of 4 kcal/mol. Therefore, the recombination rate constant hardly changes with temperature, while the disproportionation rate constant increases rapidly with increasing temperature. The ratio of the rates of these reactions determines the MWD form through the factor $\frac{p}{1-p}$ in equation (5.31). Thus, with increase in the reaction temperature, the MWD value should increase corresponding to increase in the number of low molecular weight chains in the film.

As follows from the table for films obtained by the electron-beam evaporation, $\frac{p}{1-p} > 1$ indicating a predominantly disproportionation reaction during formation of the dead chains. However, with increase of the condensation temperature T_c, the molecular weight of the film remains almost unchanged, although the ratio $\frac{p}{1-p}$ has a slight tendency to increase. With decrease in the evaporation rate V_e, the molecular weight of the film decreases somewhat, but the nature of the MWD remains the same. During the thermal evaporation, the molecular weight of the polymer in the film is higher, and the average number of recombinations K calculated by formula (5.4) is greater than one indicating the disappearance of radicals by the recombination mechanism and the production of the narrow MWD. Increase in the rate of evaporation and increase

in the temperature of the substrate have virtually no effect on the method of forming of the dead chains and the nature of the distribution. At the same time, decrease in the evaporation rate leads to decrease in the molecular weight of the film and to broadening of the MWD.

The MWD of films obtained by thermal and electron-beam evaporation practically does not change with change in the condensation temperature from 278 to 413 K. This indicates that there is no disproportionation in the condensate. It is unlikely that the formation of dead chains occurs only when free radicals recombine in such a wide range of condensation temperatures. Therefore, it is natural to assume that the radicals formed during the destruction disappear before condensation on the substrate. The MWD of condensates at a constant screens temperature is determined by the evaporation method and the deposition rate. The narrow MWD during thermal evaporation indicates that fragments of chains of approximately the same size evaporate from the crucible. With the low evaporation rate, decrease in the size of the evaporating fragments and broadening of the MWD are associated with deterioration of the evaporation conditions due to decrease of the destructive fragments kinetic energy with decrease of the evaporation temperature and decrease of the splashing phenomenon.

In the case of the electron beam irradiation, along with the destruction of the polymer chains, they are crosslinked that increases viscosity of the melt and complicates the evaporation process. Secondary reactions take place in the crucible and a more intense gas emission occurs. As a result, the broadening of MWD occurs as compared with the thermal evaporation of fragments and decrease in their average molecular weight.

As a result of the research, we made the following conclusions:

1. The evaporation of large portions of PE is accompanied by the passage into the vapor phase of larger fragments of polymer chains than during the pyrolysis of small portions [153].

2. The average molecular weight of the films during thermal evaporation is higher than that with the electron-beam evaporation, and the MWD is narrower.

3. With decrease in the rate of evaporation, there is a tendency for decrease of molecular weights and broadening of the MWD of condensable fragments.

4. At electron-beam and thermal methods of evaporation, mainly neutral fragments of polymer chains are condensed on the substrate.

5.6. Electron microscopic studies of fluoropolymers obtained with their initiation by an electron beam

With the development of industry, requirements for polymer films are

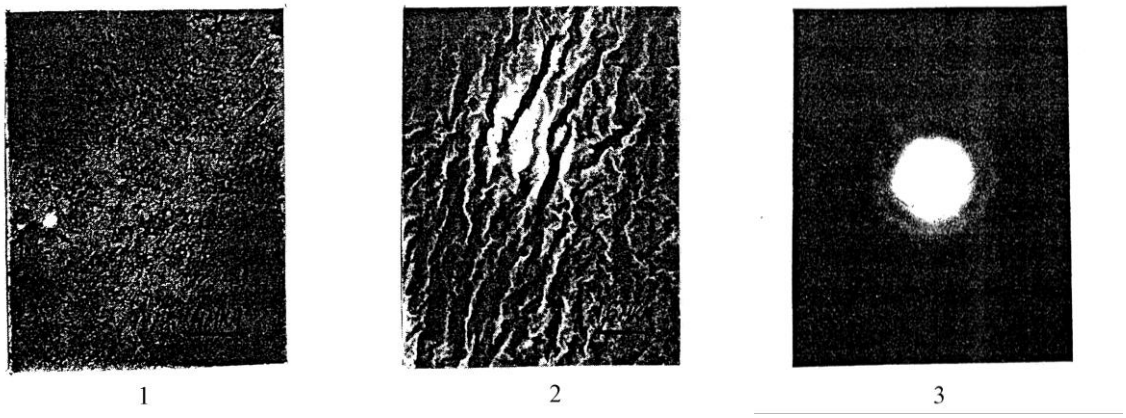

Fig. 5.18. Structure (1,2) and diffraction pattern (3) of PTFE films obtained in the following mode:
E = 400 eV, j = 0.25 mA/cm^2.

continuously increasing. One of the main requirements is the combination of high resistance to external mechanical, thermal and chemical influences in one material. If we confine ourselves to thermomechanical and chemical properties, they are set at the level of the macromolecular structure, but realized at the level of the supramolecular structure [147]. This structure can be “organized” in many ways depending on the state of macromolecules that are packaged in the polymer. Therefore, the term “supramolecular organization” is preferable to the physically non-strict term “supramolecular structure”. Each variant of the supramolecular organization has its own complex of physical and chemical properties. This applies equally both to crystallizing and to amorphous polymers.

It is known [154] that macromolecules in any crystalline formations can be either straightened or folded several times. Folding leads to the lack of strength, especially in the case of films and fibers. This deficiency is due to the fact that the areas neighboring to crystalline regions of the polymer are amorphous and do not provide a sufficient degree of the crystals coherence. The lack of the coherence is not due to the amorphousness of the intermediate sections, but due to the lack of the total number of macromolecules that pass from one such area to the neighboring section (feed-through or connecting chains). Only a part of these chains is tight enough to prevent deformations. The rest makes an

insignificant contribution to the resistance to deformations.

In our case, when films are used as dielectric spacers, the supramolecular organization should significantly influence the dielectric properties of the films. To obtain good dielectric properties, films must be continuous with the increased packing density of macromolecules. This can be achieved when macromolecules are combined into bundles forming fibrils or more complex supramolecular formations like spherulites. They are the main structural units during the crystallization of PTFE. With increase in the packing density, the electrical strength of the films increases and their conductivity decreases. In this regard, we investigated the effect of decomposition and condensation on film growth and the ability to "intervene" in a controlled way in the morphological kinetics of crystallization in the process of the secondary polymerization with

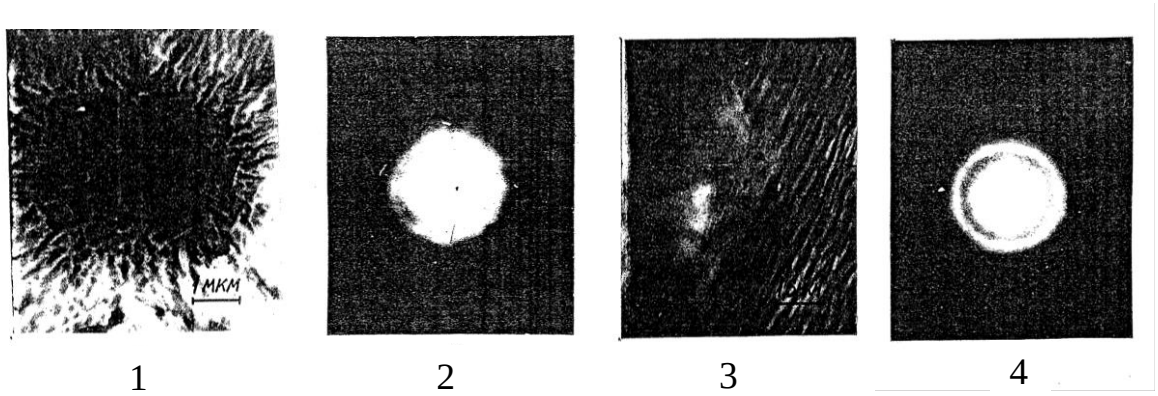

Fig. 5.19. Structure (1,3) and diffraction pattern (2,4) of PTFE films obtained under the following modes:
1, 2 – E = 400 eV, j = 0.15 mA/cm^2; 3, 4 – E = 700 eV, j = 0.5 mA/cm^2

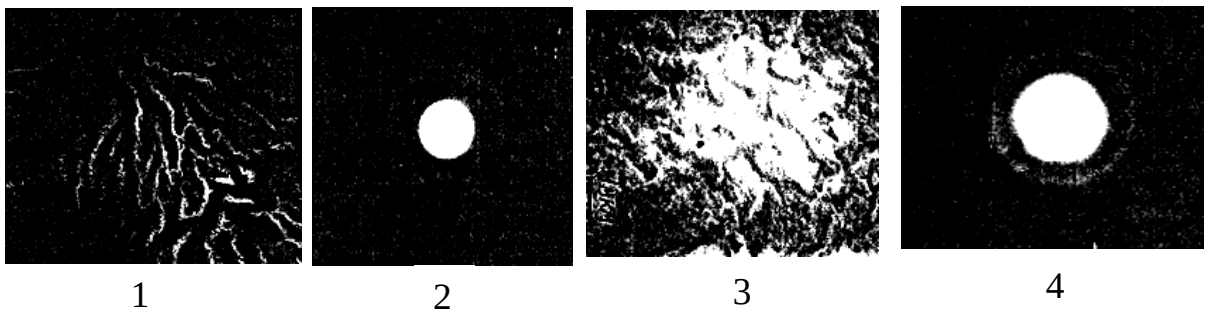

Fig. 5.20. Structure (1,3) and diffraction pattern (2,4) of PTFE films obtained under the following modes:
1, 2 – E = 400 eV, j = 0.3 mA/cm^2; 3, 4 – E = 800 eV, j= 0.6 mA/cm^2.

the ultimate goal of obtaining the desired supramolecular organization.

During the thermal initiation of the secondary polymerization process in the interval of T_c = 50-250 °C, the supermolecular organization of the films

significantly changes with increasing of T_c. Thermodynamically advantageous structure can be obtained at T_c = 200-250 °C. In this case, the films consist of thin ribbons (fibrils having different widths) combined into more complex formations: spherulites (Fig. 5.21-1). After annealing of the films in vacuum at T

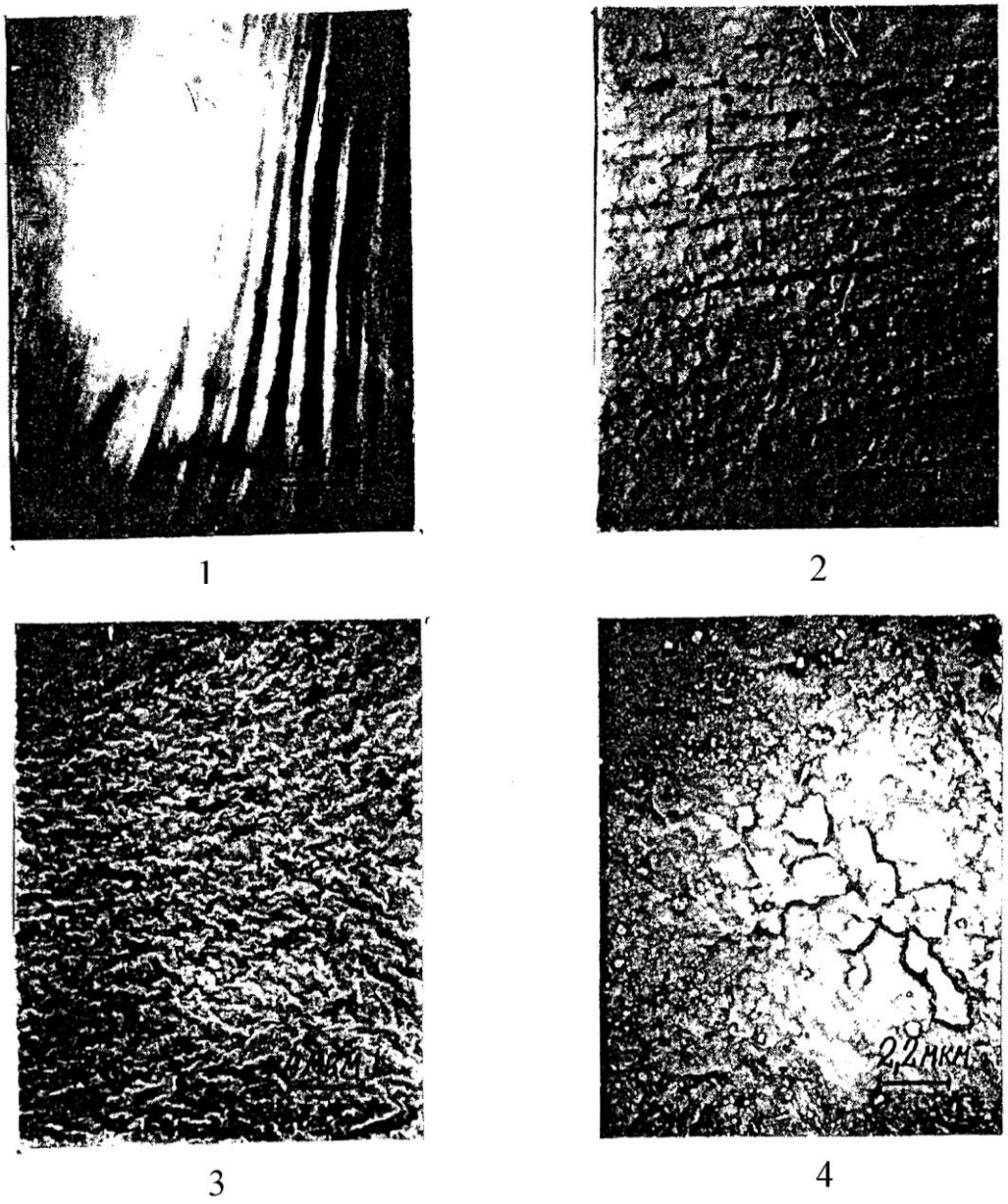

Fig. 5.21. The structure of PTFE films obtained in the following modes:
1 – T_c = 240 ˚C; 2 – E = 450 eV; j = 0.3 mA/cm^2, annealed film,
3 – Tc = 240 C, annealed film, 4 – E = 600 eV, j = 0.6 mA/cm^2

= 250–350 °C, the supermolecular organization of the films changes and the films consist of various kinds of spherulites (Fig. 5.21-3). Sharp rings appear on the electron diffraction patterns indicating that crystallization and increase in density occur during annealing. In this case, the volume resistivity of the films increases sharply. A substantial influence on the supramolecular organization

and the degree of crystallinity is exerted by the electron energy and their density during the electronic initiation of the secondary polymerization in the process of PTFE coatings condensation. For films obtained at low current densities of up to 0.1-0.15 mA/cm^2 a globular structure with spherulitic inclusions was found. This is due to the fact that the films are low molecular and can form ordered regions with the greater mobility (Fig. 5.18-5.21). In the range of current densities of 0.25-0.35 mA/cm^2, the best films with the fibrillar-burst structure are obtained. They are free from defects and their crystallinity is low. Even at small thicknesses (0.03-0.05 μm), the obtained films have good continuity at such current densities. Annealing in vacuum at 250-350 °C for 1.5-2.5 hours leads to the appearance of orderliness and increase in the specific volume resistance.

Further increase of the current density during the electron beam irradiating the substrate leads to deterioration of the films quality, despite the fact that the degree of crystallinity increases. The films are brittle and their molecular weight is small.

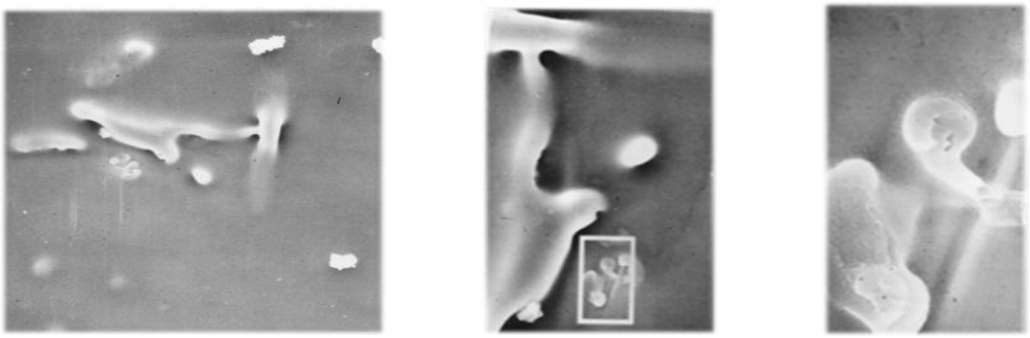

Fig. 5.22. Micrograph of PCTFE coating. Substrate temperature 150 ˚C;
a – 1000^x; b – 2000^x; c – 10 000^x.

Results of the electron diffraction decoding (Table. 5.6) show that we can get the required supramolecular organization by changing the deposition conditions.

5.7. Supramolecular organization of PCTFE and PTFE films obtained by the gas discharge deposition

Amorphous coatings has a translucent wax appearance that indicates their low M if thermally initiated the PCTFE secondary polymerization is performed at the substrate temperature of up to 50 °C. The surface structure of such objects was poorly distinguishable. Increase in temperature above 50 ˚C leads to appearance of the primary structural formations (Fig. 5.22)

When the substrate is irradiated with the RF discharge of 3-4 W, a close packed structure is observed in the PCTFE film (Fig. 5.23). Increase in power of the high-frequency discharge does not change the supramolecular formations, but only increases the size of the packs. With the high-frequency discharge power of 10 W, the type of films is shown in Fig. 5.24. No more complex supramolecular organizations were found during the PCTFE condensation.

Table 5.6

Interpretation of electron diffraction patterns and the structure of PTFE films obtained by electron-beam initiation of the secondary polymerization process

<table>
<tr><td colspan="9">The current density of the electron beam</td><td rowspan="2" colspan="2">Literary data</td></tr>
<tr><td colspan="3">0.15 mA/cm^2</td><td colspan="3">0.3 mA/cm^2</td><td colspan="3">0.6 mA/cm^2</td></tr>
<tr><td>d, nm</td><td>I</td><td rowspan="10">Clearly expressed globules</td><td>d, nm</td><td>I</td><td rowspan="10">Well-defined fibrils</td><td>d, nm</td><td>I</td><td rowspan="10">Separate spherulites on the background of the fibrillar structure</td><td>d, nm electron diffraction</td><td>d, nm X-ray analysis [69]</td></tr>
<tr><td>0.494</td><td>very weak</td><td>0.506</td><td>very weak</td><td>0.498</td><td>very weak</td><td>0.490</td><td>0.484</td></tr>
<tr><td></td><td></td><td></td><td></td><td></td><td></td><td>0.283</td><td>0.285</td></tr>
<tr><td>0.230</td><td>middle</td><td>0.23-</td><td>middle</td><td>0.234</td><td>weak</td><td>0.242</td><td>0.244</td></tr>
<tr><td></td><td></td><td>-0.24</td><td></td><td></td><td></td><td>0.197</td><td></td></tr>
<tr><td></td><td></td><td></td><td></td><td></td><td></td><td>0.183</td><td></td></tr>
<tr><td></td><td></td><td></td><td></td><td></td><td></td><td>0.163</td><td></td></tr>
<tr><td>0.128</td><td>very weak</td><td>0.128</td><td>very weak.</td><td>0.129</td><td>middle</td><td>0.138</td><td></td></tr>
<tr><td></td><td></td><td></td><td></td><td></td><td></td><td>0.131</td><td></td></tr>
<tr><td></td><td></td><td></td><td></td><td></td><td></td><td>0.124</td><td></td></tr>
</table>

It was noted above that the main structural formations during crystallization of PTFE are spherulites. This is due to the simplicity of the structure of individual molecules, which makes it possible to combine the PTFE

macromolecules in bundles, and the bundles in spherulites

a) 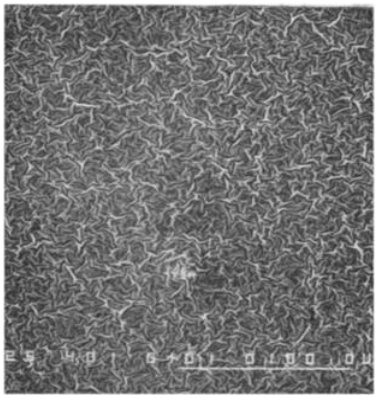 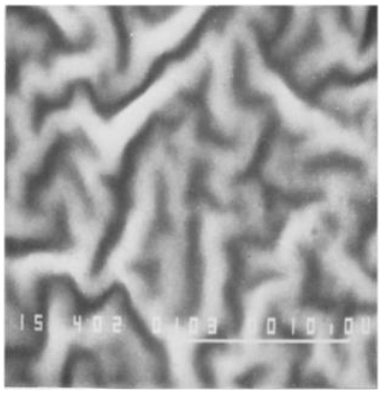 b)

Fig. 5.23. Micrograph of PCTFE coating. The substrate was treated in a high–frequency discharge with a power of 2 W; a – 500^x; b – 7000^x

Fig. 5.24. Micrograph of PTFE coating. 2000^x. The substrate was treated in a discharge of 10 W power

Fig. 5.25 Micrograph of PTFE coating. 4000^x. The substrate was not treated in HF discharge.

Fig. 5.27 is a micrograph of the PTFE film obtained without initiating the substrate with high-frequency discharge. Due to the low molecular weight, individual fragments are able to migrate on the substrate and combining with each other they prevent the final crystallization. Therefore, there are disordered regions between the crystals (amorphous regions). When irradiated with a high-frequency discharge of 2-3 W, the most acceptable structures are formed (Fig. 5.26, 5.27).

Further increase in the power of the RF discharge to more than 8 W leads

to the destruction of the film. Internal stresses arise in it leading to its cracking (Fig. 5.28). In addition, increase in power leads to the appearance of film breakdowns and to appearance of pores (Fig. 5.29).

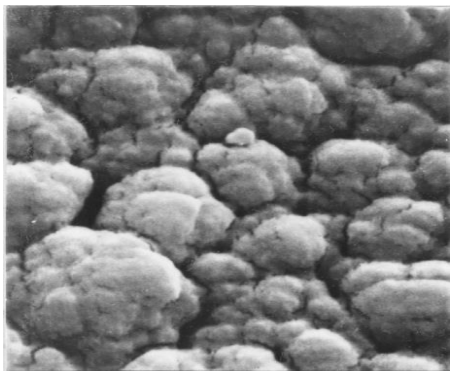

Fig. 5.26.Micrograph of PTFE coating. 25 000^{x}. The substrate was treated in 2 W discharge.

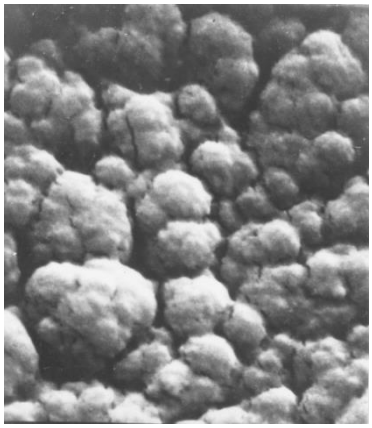

Fig. 5.27. Micrograph of PTFE coating. 25000^{x}. The substrate was treated in 3 W discharge.

a) b)

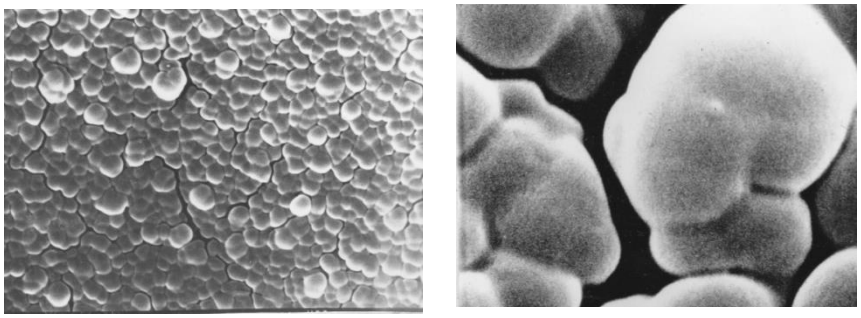

Fig. 5.28. Micrograph of PTFE coating.
The substrate was treated in a 9 W discharge; a – 5 000^{x}; b – 50 000^{x}

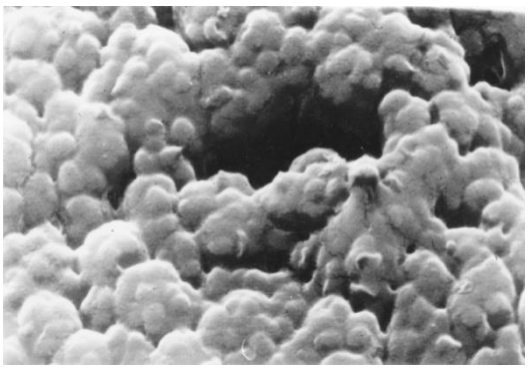

Fig. 5.29. Micrograph of PTFE coating.
The substrate was treated with a 10 W high-frequency discharge. 20 000^{x}.

Thus, it has been established that films with different supramolecular organization can be obtained by varying the power of the RF discharge.

5.8. Differential thermal and thermogravimetric analysis of PTFE condensates

5.8.1. Initiation of polymerization by the gas discharge

From experimental curves of the thermogravimetric analysis (TGA), it is possible to calculate the kinetic parameters of equations for changing the weight of the films obtained under increased temperature.

Let temperature T vary linearly with time. Then

$$T = T_o + \beta t \,. \tag{5.34}$$

where T_o is the initial temperature; β is the coefficient; t is time. If the polymer is split according to monomolecular kinetics, then consumption rate equations can be derived directly from the TGA curve. In this case $\beta \cdot t << T_o$.

Denote by w_n the initial weight of the polymer, and by w_f the final weight, by w_t the weight over time t from the beginning of the heating. If there is a residue, then $w_f \neq 0$, and if the polymer decomposes completely, then $w_f = 0$.

Assume that the active weight w is given by

$$w = w_t - w_k \,,$$

and it varies following the first order kinetic equation. Then

$$-\frac{dw}{dt} = kw = Zw \exp\left(\frac{E}{RT}\right), \tag{5.35}$$

where k is the rate constant of the consumption; Z is the statistical factor; E is the activation energy of the process.

Multiplying equation (5.35) by $\frac{dt}{dT} = \frac{1}{\beta}$, we obtain the expression for the tangent of the TGA curve slope:

$$\frac{dw}{dT} = \frac{dw}{dt} \cdot \frac{dt}{dT} = -\frac{Zw}{\beta} \exp\left(-\frac{E}{RT}\right). \tag{5.36}$$

Differentiating (5.36) by T, we get

$$\frac{d^2w}{dT^2} = \left[-\frac{Z}{\beta}\exp\left(\frac{E}{RT}\right)\right] \cdot \left(\frac{dw}{dt} + \frac{wE}{RT^2}\right). \tag{5.37}$$

The second derivative (5.37) is zero at the inflection point of the TGA curve. Equating the right side (5.37) to zero, we get:

$$E = -\left(\frac{RT_i^{\,2}}{w_i}\right)\left(\frac{dw}{dT}\right)_i .$$

Here T_i and w_i are the temperature and weight at the inflection point.

Statistical factor

$$Z = -\left(\frac{\beta}{w_i}\right)\frac{dw}{dT_i}\exp\left(\frac{E}{RT_i}\right). \quad (5.38)$$

and active weight

$$w = \left(\frac{\beta}{Z}\right)\left(\frac{dw}{dT}\right)\exp\left(\frac{E}{RT}\right). \quad (5.39)$$

For materials with high activation energy of the destruction process, the TGA curve is steeper. The results of processing the TGA curves are presented in Table. 5.7. It follows from the table that in films obtained in high-frequency

Table 5.7

Control parameters for the weight reduction rate of PCTFE and PTFE condensates obtained at different deposition modes

Sample	Production mode	T, K	W, mg	V_w, mg/deg	E, kcal/mol	Z, s
PTFE	Commercial powder	850	80	-4.1	72	$2.4\cdot10^{16}$
	$P_{discharge}$ = 4 W	700	90	-5.0	54	$4.6\cdot10^{16}$
	$P_{discharge}$ = 0	660	90	-3.5	36.8	$6.3\cdot10^{16}$
PCTFE	Commercial powder	613	71.3	-4.84	56	$2\cdot10^{18}$
	$P_{discharge}$ = 3 W	600	70	-4.80	52	$2.2\cdot10^{18}$
	$P_{discharge}$ = 0	580	70	-3.3	28	$4.1\cdot10^{18}$

glow discharge plasma, the transition temperature T_i is increased from 660 K to 700 K in PTFE and from 580 K to 600 K in PCTFE. Accordingly, the activation energy increases from 36.8 to 54 kcal/mol in PTFE and from 28 to 52 kcal/mol in PCTFE.

This changes the shape of the curves. They become flatter, and the phase transition is not sharp.

It follows from analysis of the DTA graphs that the films obtained by processing in glow discharge have the higher molecular weight. This conclusion

is confirmed by the shift of the melting peak of the crystalline phase with respect to the temperature of 327 °C for PTFE. It should be noted that the area of the endothermic melting peak of the crystalline phase in the DTA method is proportional to the degree of crystallinity of the polymer material.

Comparing areas of the obtained endothermic peaks, one can see that their area decreases with increasing power of the high-frequency discharge indicating the amorphization of PTFE condensates. As for PCTFE, the films are amorphous to such an extent that the melting peak of the crystalline phase curves is not visible on the DTA data.

5.8.2. Electron beam initiation of polymerization

The molecular weight and crystallinity of the obtained films can be judged by analyzing the graphs of the differential thermal analysis (DTA). It was shown that the area of the endothermic melting peak of the crystalline phase in the DTA method is proportional to the degree of crystallinity of the polymer material.

The displacement of the melting peak of the crystalline phase in films obtained by different regimes relative to 327 °C (the melting point of the crystalline phase of the initial PTFE) can be judged as the existence of defective formations and local disorienting processes in the crystals, and as the decrease in the average molecular weight of the films.

The modes and the method of the secondary polymerization in our case significantly affect the degree of crystallinity of the films and their molecular weight.

The molecular weight of the films is low at low T_c (thermal initiation of secondary polymerization) and current density $J < 0.15$ mA/cm^2 (electron beam initiation). It follows from the graphs (Fig. 5.30, 5.31) that the temperature offset reaches 20-35 ˚C. Increase of T_c to 200-250 ˚C and the current density up to 0.2-0.25 mA/cm^2 leads to the significant increase in the molecular weight. The difference from the molecular weight of the original PTFE becomes insignificant.

Indeed, if the decrease in the melting point is $1.05 \cdot 10^{-3}$ °C per unit mole fraction of the terminal groups [155] and if we take into account the presence of two such groups in the molecule, then:

$$\frac{M^{j=0.2}}{M^{j=0.1}} = \frac{100/(1.05\cdot 10^{-3}\cdot 5)}{100/(1.05\cdot 10^{-3}\cdot 30)} = 6. \qquad (5.40)$$

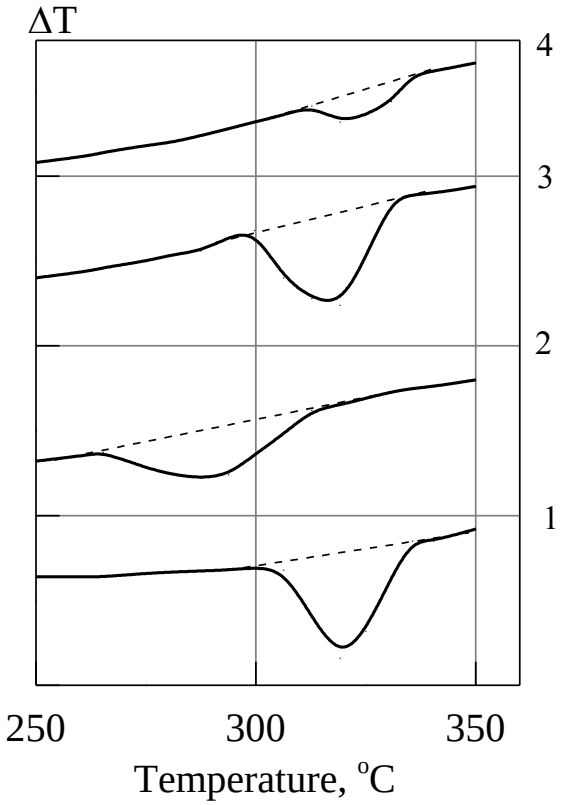

Fig. 5.30. DTA of PTFE films obtained under different deposition conditions and that of the industrial film: 1 – industrial film; 2 – T_c = 25 °C; 3 – T_c = 240 °C; 4 – T_c = 240 °C, annealed film. 4 – T_c =240°C, annealed film

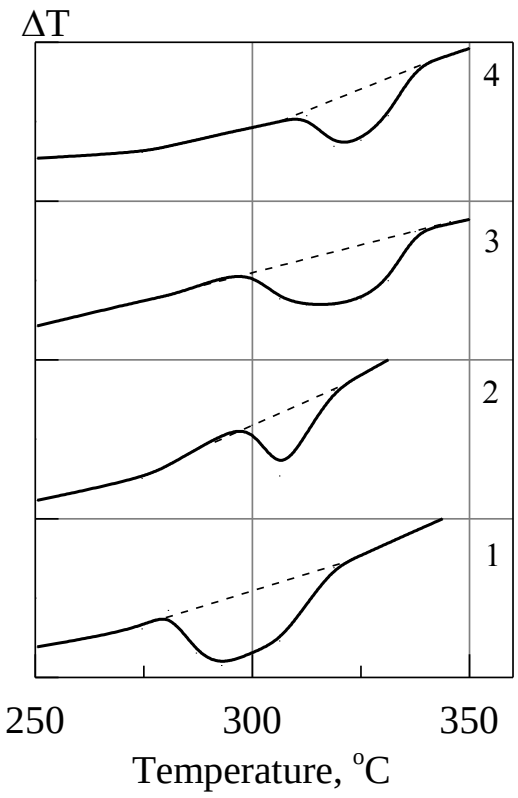

Fig. 5.31. DTA of PTFE films obtained under different deposition conditions: 1–700 eV; 0.1 mA/cm^2; 2–700 eV; 0.1 mA/cm^2, annealed film; 3 – 600 eV; 0.2 mA/cm^2; 4–600 eV, 0.2 mA/cm^2, annealed film

This means that the molecular weight of the films obtained in the best mode (J = 0.2 mA/cm^2) is 6 times greater than that of the films obtained at J = 0.1 mA/cm^2. It must be taken in mind that the defectiveness of the crystal structure contributes to the displacement of the endothermic melting peak.

Analyzing the area of the obtained endothermic peaks, one can see that the crystallinity of the films substantially depends on the initiation method. Annealing of films in vacuum at the temperature of 250-350 °C leads to a certain decrease of crystallinity (for films obtained by the thermal initiation). The degree of crystallinity almost does not change with the electronic initiation of the secondary polymerization reactions on the substrate. To confirm the results of DTA, we used the data of thermogravimetric analysis (TGA), since

this method allows us to determine the kinetic parameters in the equation of the consumption rate directly from the decomposition curve of the polymeric substance.

Table 5.8

Parameters of the equation for the weight reduction rate of PTFE films obtained by thermal and electronic initiation and various deposition modes, as well as the parameters of the industrial PTFE

Method of initiation	Deposition mode: T_c is the condensation temperature, °C; E is the electrons energy, eV; J is the electron current density, mA/cm^2	T_i, ˚C	W_i. mg	$(\frac{dW}{dT})_i$. mg/K	E_a, kJ/mol
Thermal	T_c=30	700	80	-2.5	132.3
	T_c =240	700	90	-5	226.8
	T_c =240, annealed film	710	90	-5.3	242.8
Electronic	E = 700, J = 0.1	660	100	-3.8	142.8
	E=700, J=0.1 annealed	720	90	-3.5	154.6
	E = 600, j = 0.2	660	90	-5.4	218.4
	E = 600, J=0.2 annealed	670	80	-6.0	285.6
Commercial PTFE		850	80	-4.1	302.4

Kinetic parameters of the equations for the change in the weight of films were calculated from experimental curves of the thermogravimetric analysis. These parameters are presented in Table. 5.8.

T_i is the temperature at the inflection point of the TGA curve; w_i is the weight at the inflection point of the TGA curve; $\left(\frac{dw}{dT}\right)_i$ is the tangent of the angle of the TGA curve inclination at the inflection point; E_a is the activation energy.

With increase of T_c, the transition temperature T_i increases from 427 ˚C for the films with T_c = 30 °C to T_i = 437 ˚C for the films with T_c = 240 °C. Similarly, T_i increases with increasing J from 0.1 mA/cm^2 to 0.2 mA/cm^2 from 387 °C to 397 °C. Accordingly, the activation energy increases from 132 kJ/mol to 285 kJ/mol. The shape of the curves changes: they are flat and the phase transition is less sharp due to increase in M of the films obtained in the best mode.

5.9. Study of the films by the Electron Paramagnetic Resonance (EPR)

Aging processes of thin polymer films obtained in vacuum are largely associated with the presence of free radicals [156], which can be detected by absorption signals in the EPR spectrum. Study of the radicals' stability is of undoubted interest in finding out the decomposition mechanism, as well as the polymerization mechanism and the degree of polymerization.

In the study of PTFE films by the EPR method, intense absorption signals were detected, the width and amplitude of which fluctuated depending on the conditions of decomposition and polymerization. The fact of the radicals' formation during decomposition under action of the electron beam cannot indicate that the radical mechanism was predominant [157]. To prove this position, it is necessary to show that the number of radicals formed under the action of irradiation is commensurate with the total number of molecules of the original substance that have turned under the same conditions.

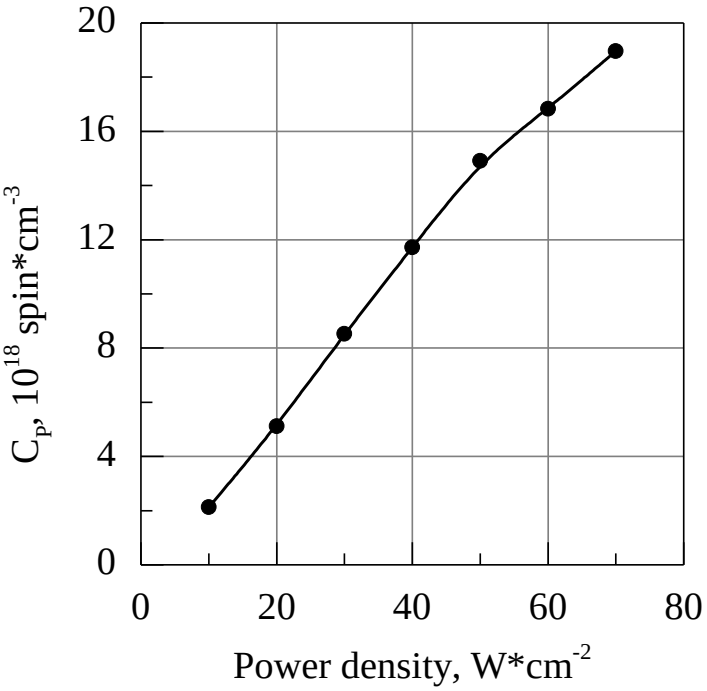

Fig. 5.32. Dependence of the concentration of free radicals (C_f) in PTFE films on the power of the electron beam decomposing PTFE at T_c = 25 °C.

The quantum theory of the free radicals structure is mostly developed in relation to aromatic radicals. The results of quantum mechanical calculations for these systems correlate well with the EPR data obtained from measurements in solution, i.e. at high resolution. This theory is less developed for unsaturated systems.

The situation is complicated for irradiated polymers by the fact that the EPR spectra in most cases are measured in the solid phase, the exact structure of which is unknown. The lines are broadened in the spectra of polymers due to the inhomogeneity of local fields acting on unpaired electrons. Accordingly, the resolution is low. Typically, polymers are a mixture of macromolecules with different steric configurations. It can be assumed that the groups adjacent to the radicals in such systems are not the same.

In the case of amorphous compounds, namely for the majority of free radicals, only complete cleavage is observed, summarized in all directions. The electron or nuclear spin-spin interaction in this case leads not to the splitting of the line, but to its broadening.

The author of [69] studied the dependence of the concentration of free radicals on the conditions for the preparation of polymer films from PTFE. The concentration of free radicals, as follows from Fig. 5.32, increases with increasing power of the electron beam, which decomposes the PTFE in the crucible. This is because, the degree of PTFE destruction increases with increasing the beam power and the number of evaporated fragments increases that subsequently polymerize and participate in the film formation.

It follows from Fig. 5.32 that the highest concentration of free radicals is observed at the electron beam power of P = 80 W/cm^2. The lowest concentration of free radicals was found in the films obtained with the power of the electron beam 10 W/cm^2 decomposing the polymer. However, the concentration of free radicals in the films depends not only on the power of the beam decomposing PTFE. Studies have shown that presence of paramagnetic centers (PMCs are free radicals) depends on the type of initiation of the secondary polymerization on the substrate (thermal, electronic), the substrate temperature, the current density of the electrons irradiating the substrate, their energy, and the heat treatment of the film after its deposition.

The concentration of free radicals in films obtained by the thermal initiation of polymerization is equal to $16 \cdot 10^{18}$ spin/cm^3. It decreases with increase of the substrate temperature and reaches a minimum (Fig. 5.33) at the temperature of 220-240 °C corresponding to $(3\text{-}4) \cdot 10^{18}$ spin/cm^3. For the films annealed in vacuum after their deposition, the concentration of free radicals is fewer and equal to $6 \cdot 10^{17}$ spin/cm^3. This is due to the fact that a significant part of the radicals recombines at the annealing temperature.

The presence of radicals in the films obtained by the electron initiation

method depends on the current density of the electrons bombarding the substrate and the energy of the electron beam. The minimum concentration of radicals is observed with increasing of the current density and with increasing the energy of electrons bombarding the substrate.

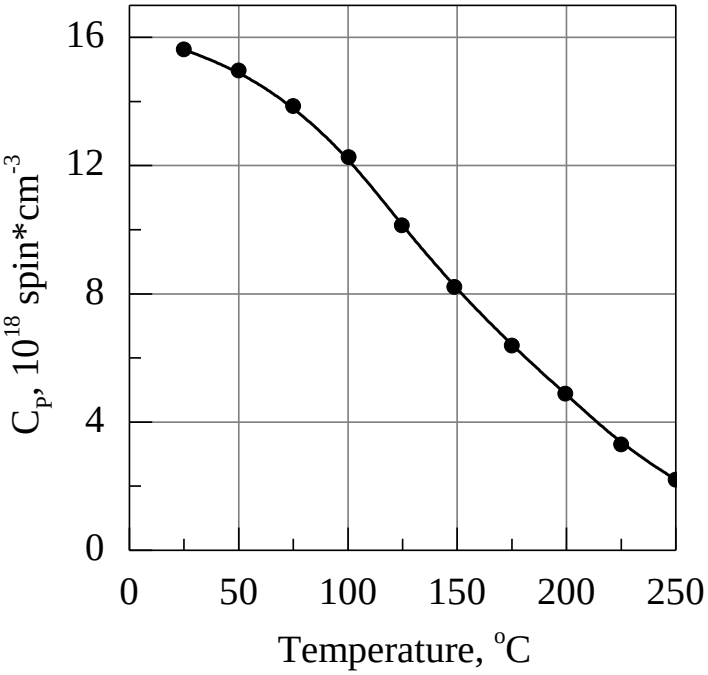

Fig. 5.33. Dependence of the spin concentration C_p in PTFE films on the condensation temperature T_c at the power of the electron beam 40 W decomposing PTFE.

As follows from the graph in Fig. 5.34, the concentration of radicals in films obtained at the electron beam energy of ~ 400 eV and the electron current density of 0.2-0.25 mA/cm^2 is of the order of $6 \cdot 10^{18}$ spin/cm^3, while in the films obtained with the electron energy less than 100 eV and the current density of about 0.1 mA/cm^2, the concentration of free radicals is approximately equal to $15 \cdot 10^{18}$ spin/cm^3. This is obviously due to the incomplete polymerization of the active fragments deposited on the substrate. With increasing the energy of the electrons irradiating the substrate, and with increasing the density of the electron current, the degree of polymerization increases meaning that the molecular weight of PTFE also increases. The increase in the molecular weight can also be judged by the infrared spectroscopy.

It should be noted that when analyzing the line shape of the EPR spectra of PTFE films, it can be seen that the line is asymmetric that may be due to peroxide-type radicals [158]:

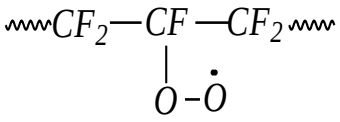

It is possible that the radicals of the type:

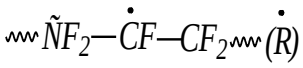

turn into peroxide-type radicals at temperatures of 25-100 °C in presence of oxygen.

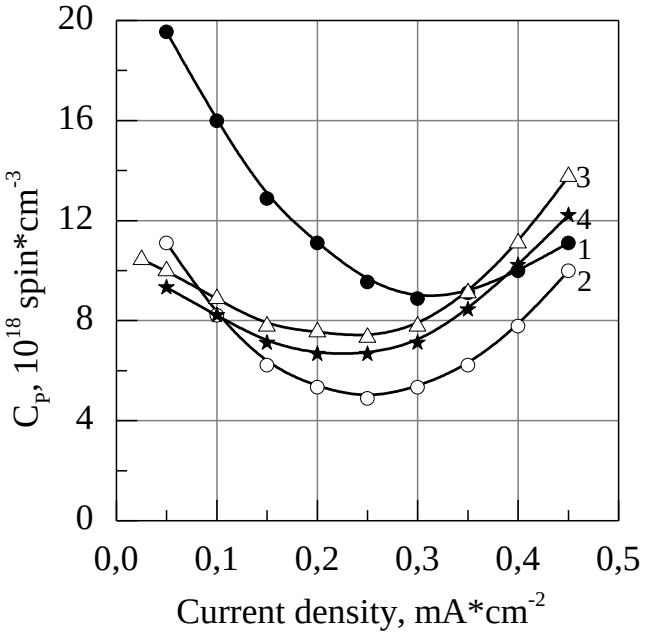

Fig. 5.34. Dependence of C_p in PTFE films on J of electrons bombarding the substrate, at different E of electrons:
1 – 100 eV; 2 – 400 eV; 3 – 600 eV; 4 – 800 eV.

From the point of view of practical application, it is of interest to study changes in the radicals' concentration in air and in vacuum in the films obtained in various modes.

It follows from the graph in Fig. 5.35 that the concentration of free radicals in the vacuum films remains almost unchanged. The concentration of PMC films in the air decreases in the first 3-4 days. Moreover, recombination proceeds faster in the films obtained at large values of the electron current density (up to 0.3 mA/cm^2). This may be due to the direct interaction of oxygen with radicals. In films obtained at the current density of 0.3 mA/cm^2, the radicals' concentration decreases by 80% after 3 days, and for films obtained at the current density of 0.1 mA/cm^2, it decreases by 80% after 5-6 days.

It follows from the above results that two different effects can be observed in the spectra of electron paramagnetic resonance upon absorption of molecular

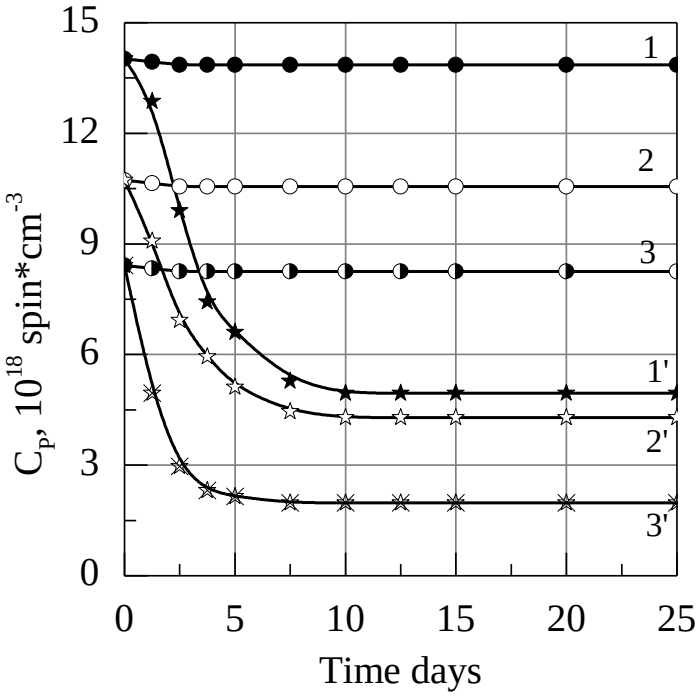

Fig. 5.35. C_p change in PTFE films obtained in different modes:
1 – E = 300 eV, j = 0.1 mA/cm^2; 2 – E = 400 eV, j= 0.2 mA/cm^2;
3 – E = 400 eV, j = 0.3 mA/cm^2; • – in vacuum, **x** – in air.

oxygen. In the first case, an intermediate radical compound $R-O-\dot{O}$ is formed, which then turns into a radical or other radicals that can react and produce saturated products. As a result, the intensity of the observed spectrum gradually decreases to zero under the action of oxygen. However, the intensity does not decrease and it can be assumed that a radical $R\text{-}O\text{-}\dot{O}$ is formed when interacting with oxygen. In this case, the unpaired electron is strongly localized at the oxygen atoms and the hyperfine structure of the spectrum due to delocalization of the unpaired electron is absent. As a result, a relatively wide line is observed, which may be asymmetric due to anisotropic factor or electronic splitting.

To study the possibility of aging and the use of films in a wide range of temperatures, we studied the dependence of the radicals concentration in films obtained under different conditions on the temperature in the range of 0-200 °C. It has been established that concentration of radicals decreases in films obtained at current densities of up to 0.2 mA/cm^2 . Almost all radicals recombine at the temperature of 200 °C.

The concentration of radicals decreases sharply with increasing temperature from 70 to 150 °C. The most rapid decrease in the concentration of radicals is

observed in films obtained at current densities of less than 0.15 mA/cm^2 and the electron energy less than 100 eV. This is due to the fact that a larger number of active fragments than in other modes did not react, and the degree of polymerization is correspondingly lower. With increase of the electron current density to 0.25 mA/cm^2 and their energy up to 400 eV, films with a smaller number of radicals are obtained and their concentration decreases with increasing temperature not so fast. This indicates on the high degree of polymerization in the films.

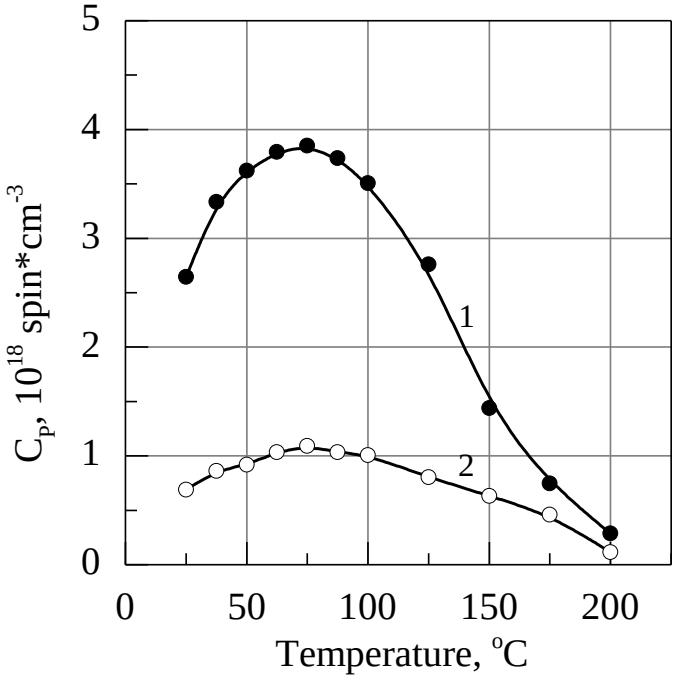

Fig. 5.36. Temperature dependence of C_p in PTFE films obtained by the thermal initiation of the secondary polymerization.
1 – T_c = 240 °C; 2 – T_c = 240 °C; annealed film.

As will be shown below, films produced in this mode are less susceptible to aging.

For films obtained at an electron current density of more than 0.25 mA/cm^2 and energy above 400 eV, the radical concentration increases with increasing temperature from 20 °C to 70 °C and then decreases. Increase in the concentration of radicals with increasing temperature from 20 °C to 70 °C may be due to the decomposition of peroxide radicals. A further decrease in the concentration of radicals with increasing temperature from 70 to 200 °C can be explained by partial recombination of the most active radicals. A slight broadening of the EPR spectra lines is caused by the due to increase of

temperature, and their further narrowing occurs due to disappearance of the spin-spin interaction, since concentration of free radicals decreases. This can be

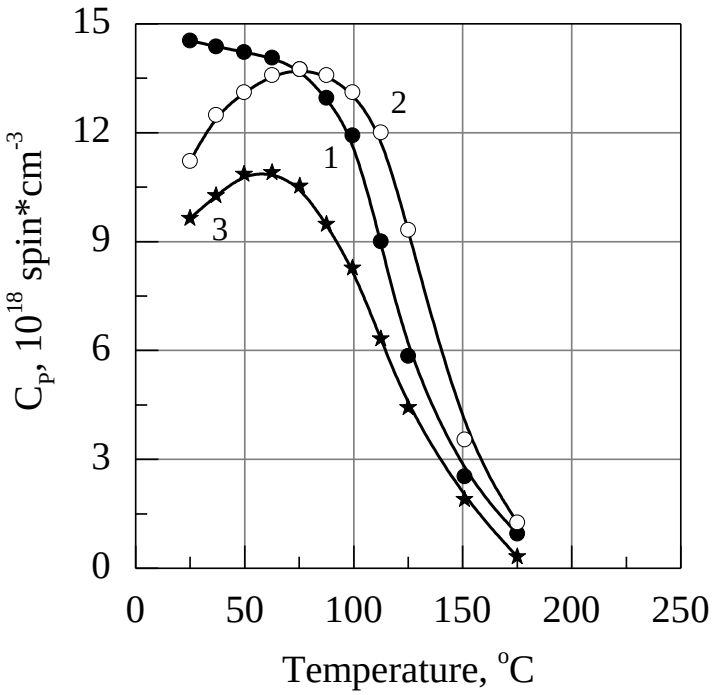

Fig. 5.37. Temperature dependence of C_p in PTFE films obtained by the method of electronic initiation of the secondary polymerization with J of electrons 0.1 mA/cm^2 and different E:
1 – 100 eV; 2 – 400 eV; 3 – 800 eV.

clearly seen from Fig. 5.36-5.39.

An interesting feature of PTFE films is that the oxygen effect is reversible in them. The EPR spectrum is restored if the films are cooled to room temperature after 6-10 hours, and the presence of peroxide radicals is again recorded.

This interaction is considered as a special case of the line broadening due to collisions. It is assumed that the oxygen molecule can come close to the radical center and then move away from it again, or vice versa. An electron of the free radical can quickly “slip” near a fixed oxygen atom. At the same time, the electron lifetime in the excited state will decrease due to the perturbation of the electron energy when interacting with the O_2 bi-radical that will lead to a broadening of the line.

A significantly lower concentration of free radicals is found in annealed films (about 10^{16} spin/cm^3). In this case, PTFE films were kept at a temperature of 250-350 °C for 1.5-2.5 hours.

The lowest concentration of radicals is obtained in the films produced with the beam power of about 40 W/cm^2 and with the current density of electrons

irradiating the substrate and initiating polymerization of 0.25 mA/cm^2 and their energy of 400 eV. These films were then annealed at the temperature of 250-350

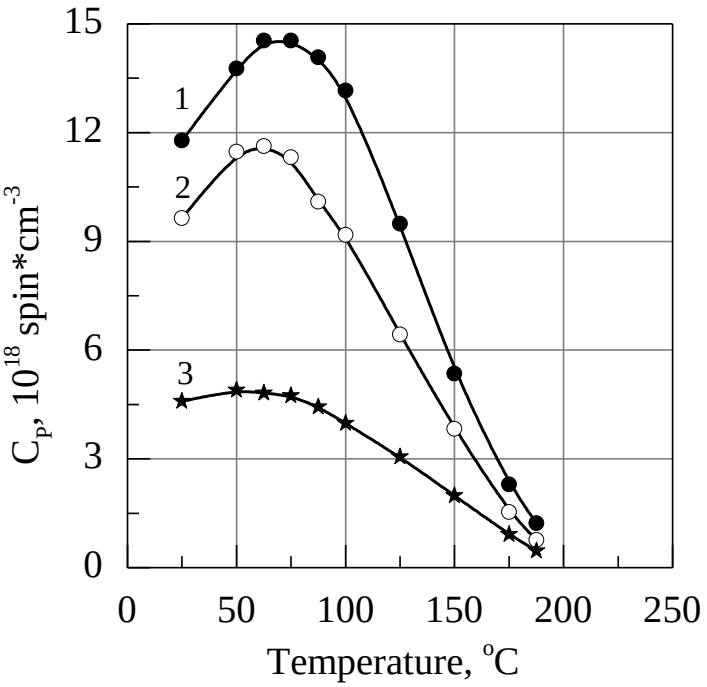

Fig. 5.38. Temperature dependence of C_p in PTFE films obtained by the method of the electronic initiation of the secondary polymerization with J of electrons equal to 0.2 mA/cm^2 and different E:
1 – 100 eV; 2 – 400 eV; 3 – 800 eV.

°C for 1.5-2.5 hours. Such films possess the best dielectric characteristics. They resist aging and other destabilizing factors well.

It follows from the experimental spectra that they coincide with the theoretical ones for the case of $K \parallel \mu$ (where K is the axis of the chain, μ is the axis of the paramagnetic center).

It can be concluded that the axis of the peroxide radical in the PTFE film is parallel to the axis of the polymer chain at room temperature. When using the gas discharge deposition, intense absorption signals were detected in the EPR spectra of PTFE and PCTFE that confirms the radical polymerization mechanism on the substrate.

The concentration of free radicals significantly depends on the processing modes of the growing film in the high-frequency discharge, as one can see from the Table 5.9.

The shape of the signals corresponds to the stable peroxide radicals.

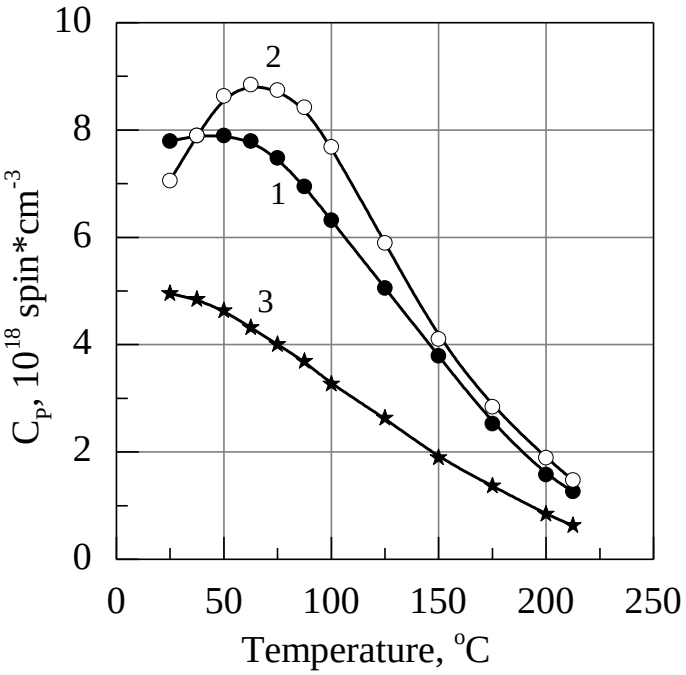

Fig. 5.39. Temperature dependence of C_p in PTFE films obtained by the method of electronic initiation of secondary polymerization at j of electrons 0.3 mA/cm^2 and different E:
1 – 100 eV; 2 – 400 eV; 3 – 800 eV.

Table 5.9.

Dependence of the free radicals concentration on the deposition mode

Material	Deposition mode	Free radical concentration, 1/g
PCTFE	initial	No signal
	without processing	$1.7 \cdot 10^{16}$
	optimal	$0.6 \cdot 10^{16}$
	power above 8 W	$9.0 \cdot 10^{17}$
PTFE	initial	No signal
	without processing	$1.8 \cdot 10^{18}$
	optimal	$8.0 \cdot 10^{16}$
	power above 10W	$2.0 \cdot 10^{18}$

CHAPTER 6
DIELECTRIC PROPERTIES OF THIN PTFE FILMS

Microminiaturization of electronic equipment through creation of thin-film passive and active elements is largely associated with the problem of producing films with good dielectric properties. These properties essentially depend on the nature of used materials and their manufacturing technology.

Thin polymer films used in electronics and microelectronics must meet the following requirements: to have a large resistivity ρ_v, low dielectric loss tanδ, high dielectric strength E_{br}, small or large dielectric constant ε depending on the purpose, and to keep these characteristics stable over time in a wide range of frequencies, temperatures and other external conditions.

Most authors, who studied polymer films obtained in glow discharge and under action of the electron beam, make a note of good dielectric properties of these films. The dielectric constant of the films approaches the values of the initial polymer. Analysis of the literature data [69,159] shows that thin polymer films obtained under action of the electron irradiation or in a glow discharge usually have a dielectric constant corresponding to the bulk polymer, while the dielectric loss tangent is significantly higher than that of the original polymer.

Influence of polymerization conditions on the dielectric properties of thin polymer films, as well as their temperature and frequency dependences have been studied in some works [69,161]. The films were obtained by polymerization of monomeric molecules adsorbed on a substrate either in the gas phase, or in the glow discharge, or under action of electron or UV irradiation.

The author of [69] obtained PTFE films with a thickness of the order of 0.5-4 μm and investigated dependences of the dielectric characteristics on conditions of obtaining these films, such as temperature and frequency. Porosity of PTFE films was also investigated. The porosity is one of the main parameters characterizing the dielectric properties, since presence of pores in the films is one of the main causes of the electrical strength weakening, as well as reduction of resistance and appearing defects in manufactured integrated circuits. Adhesion is also an important characteristic. The film production mode and surface pretreatment methods before deposition of coatings have a significant effect on adhesion.

Our studies were carried out with the aim of obtaining practical recommendations on the modes under which non-porous films were obtained with good adhesion to the surface and stable dielectric characteristics.

6.1. Porosity and adhesion of PTFE films obtained by deposition in vacuum

Porosity. We studied dependence of porosity on the following conditions of the PTFE films preparation: 1) method of initiating the secondary polymerization reactions of active fragments on the substrate; 2) condensation temperature; 3) current density of electrons bombarding the substrate and their energy, as well as film thickness. The porosity of the films was determined by the method described in [69]. Data on the results of the porosity measurement are given in Table 6.1.

Table 6.1

Dependence of the number of pores per 1 cm^2 in PTFE films on the film thickness and the deposition mode

Deposition mode	*E*, eV	100			400				700		Condensation temperature, T_c, ˚C		
	j, mA/cm^2	0.2	0.3	0.4	0.1	0.2	0.3	0.4	0.1	0.2	50	100	200
Thickness													
1 μm		-	2.3	-	-	0.5	1.8	-	-	1.5	-	1.7	0,4
3 μm		1.0	0.6	1.5	1.3	0	0.2	0.8	1.8	0.3	1.9	0.8	0
5 μm		0.5	0	0.7	1.0	0	0	0.4	1.2	0	1.3	0.5	0

It has been found that the largest number of pores is present in thin films (0.5 μm) at condensation temperatures up to 50 °C with thermal initiation and with electron current density less than 0.15 mA/cm^2 and more than 0.35 mA/cm^2 and electron energy smaller than 200 eV and more than 500 eV. The number of

pores per unit surface area decreases with increasing thickness. During thermal initiation, the number of pores decreases with increase of the condensation temperature. Thus, 3 μm thick PTFE films deposited on the substrate at the temperature of 200 °C are practically non-porous.

The smallest number of pores was in the films obtained by the best mode (j = 0.25 mA/cm^2; E = 400 eV), if the electronic initiation method was used. With increase or decrease of the electrons current density and their energy, the number of pores increased, as can be seen from Table 1. This is due to the low degree of polymerization if the current density was smaller than 0.2 mA/cm^2 and the electron energy was smaller than 300 eV, or due to the processes of destruction, which predominated over polymerization processes at the electrons current density of more than 0.4 mA/cm^2 and energies of more than 500 eV.

It follows from the table data that the number of pores per unit surface area decreases with increasing thickness of the films obtained by the electronic method of initiating the polymerization. The films having thickness of more than 3 μm were practically non-porous.

The porosity is also affected by pretreatment of the surface before deposition the film. The effect of surface treatment regimes by glow discharge was also studied. It was established that treating the substrate in glow discharge in air at pressure of 10 Pa and the discharge current density up to 2 mA/cm^2 for 20-30 s resulted in decrease of the number of pores per unit surface area. The films with the thickness of 1.5-2 μm become virtually non-porous after the electronic initiation.

The decrease of porosity after treatment of the substrate by glow discharge is explained by the fact that the surface is amorphized during the ion bombardment that leads to increase of the number of nucleation centers in the coating [69]. The formation of the film depends not only on the interaction of the active fragments with each other, but also on the condensation conditions.

Adhesion. PTFE is a non-polar polymer and it has poor adhesion to metals. PTFE coatings are often obtained by melting the original powder or as a film on the metal substrate deposited in air at temperature of about 400 °C. This leads to thermo-oxidative degradation of PTFE with releasing a monomer. Therefore, it is difficult to achieve good adhesion of the PTFE film to metals.

In our case [69], the deposition occurs in a vacuum at a pressure of $5 \cdot 10^{-3}$ Pa. The nature and degree of interaction between the coating and the substrate is determined by the state of the substrate surface. There can be various oxide

films and different types of pollution on the surface, which prevent the formation of strong bonds between the polymer coating and the substrate in different ways. The most common contaminants on the surface of metals and non-metals are: 1) corrosion products; 2) organic and inorganic pollution; 3) adsorbed vapors and gases.

The corrosion products of metals can be removed by machining (sandblasting or shot blasting). Organic and inorganic contaminants must be removed by solvents. However, a special final treatment is required to remove adsorbed vapors and gases. The oxide films located on the metals surface have a significant effect on the adhesion. There are different opinions on the effect of oxide films on the adhesion of polymer films to metals. Some researchers believe that a complete removal of the oxide film is necessary for obtaining good adhesion, while others think that oxide films with a thickness of up to 10 nm do not affect the adhesion.

Surface treatment by ions bombardment in a glow discharge has become widespread operation in the case of the vacuum coatings deposition [130]. There are several points of view regarding the effect of the glow discharge on the surface. On the one hand, the cleaning effect is explained by the fact that the metal surface being treated is heated to a high temperature under the action of ions and therefore the surface is degassed, while water layers and other volatile contaminants are also removed. Another point of view is that the glow discharge activates chemical processes on the surface and creates the high density of condensation centers, which grant good adhesion.

We investigated the influence of the surface treatment method (heating of the substrate in vacuum with subsequent cooling or processing in the glow discharge) of the substrate materials and the secondary polymerization mode on the adhesion of the coatings to glass, iron, copper, and aluminum. It was established that the substrate material had slight effect on the PTFE coatings adhesion. The adhesion depended mainly on the state of the substrate surface before deposition of the coating. The best ways to prepare the substrate surface before deposition of the coating are:

1. Heating of the substrate in vacuum $5 \cdot 10^{-3}$ Pa to the temperature of 600 °C for 1 min. In this case, the surface degassing appears, as well as evaporation of volatile oxides and formation of stable oxides with good adhesion to the base.

2. Surface treatment by the glow discharge with the current density of 2 mA/cm^2 for 20-30 s.

Improvement of adhesion during the surface treatment in the glow discharge is due to removal of surface impurities and adsorbed layers, as well as due to activation of various chemical reactions on the substrate surface. In particular, polymerization of silicone oil molecules on a substrate occurs that leads to formation of a monomolecular polymer layer with high concentration of radicals. The radicals can react with the growing polymer film to form a blocking copolymer. This leads to improved adhesion with the PTFE film.

Mode of the film deposition also significantly affects the adhesion of the film to the substrate. PTFE films obtained with irradiation by electrons with energy of 350-450 eV and the current density of about 0.2-0.25 mA/cm^2 have the best adhesion. In this case, high-molecular-weight films with a low degree of crystallinity are obtained (according to infrared spectrometry studies, the X-ray spectrometry; the differential thermal analysis and the thermogravimetric analysis). It is also possible that organometallic bonds of the Me–C or Me–O–C type are formed [161]. At the same time, a metal atom on the surface is connected both to the crystal lattice and to the PTFE macromolecule. Grafting of the polymer to the metal crystal lattice is not excluded in the case of a metal having thin oxide layers on the surface. The grafting is carried out not by the organometallic, but by the alcoholic bond.

The tests showed that the PTFE coatings deposited according to the best conditions on steel, glass-ceramic, C, and Al had good adhesion. Coatings do not peel off after boiling in water for half an hour. They withstand repeated heating and cooling cycles from -198 °C to +100 °C. When the coating is on a flexible substrate, it does not peel off when the substrate is bent at ± 180° until the substrate has completely fractured. When testing the adhesion by the normal avulsion method, the load, at which the gap occurred, was 950 N/cm^2, however, the gap occurred in the glue layer, but not at the film-substrate interface.

6.2. Dielectric constant ε' and dielectric loss tangent tanδ of PTFE films

The dielectric constant of the polymer can be represented as:

$$\varepsilon' = n_D^2 + \Delta\varepsilon_{res} + \Delta\varepsilon_{dip.or},$$

where $\Delta\varepsilon_{res}$ and $\Delta\varepsilon_{dip}$ are contributions of resonant and dipole orientational polarizations to the dielectric constant; n_D is the refractive index. $\Delta\varepsilon_{res} = 0$, $\Delta\varepsilon_{dip}$

= 0 and $\varepsilon' = n^2_D$ in non-polar polymers, in which the monomer units of macromolecules do not possess a dipole moment.

Electronic polarization is established in a time of the order of 10^{-13} s, so the dielectric constant is independent of the electric field frequency. It should be noted that there are various kinds of disruption of the electrical symmetry in the macromolecule of polymer films depending on the conditions of their manufacturing. There can be double bonds, carbonyl and hydroxyl groups, as well as bound oxygen. Therefore, it was necessary to study the dependences of ε' and tanδ of PTFE films on the conditions of their manufacturing and the effect of temperature and frequency changes on these characteristics.

6.3. Dependence of ε' and tanδ of PTFE films on the manufacturing conditions

The study was conducted of the dependence of ε' and tanδ on conditions of decomposition and polymerization of PTFE [69]. The initiation of the polymerization was carried out by either UV irradiation, or thermal method, or electron irradiation. The decomposition was carried out by the electron beam.

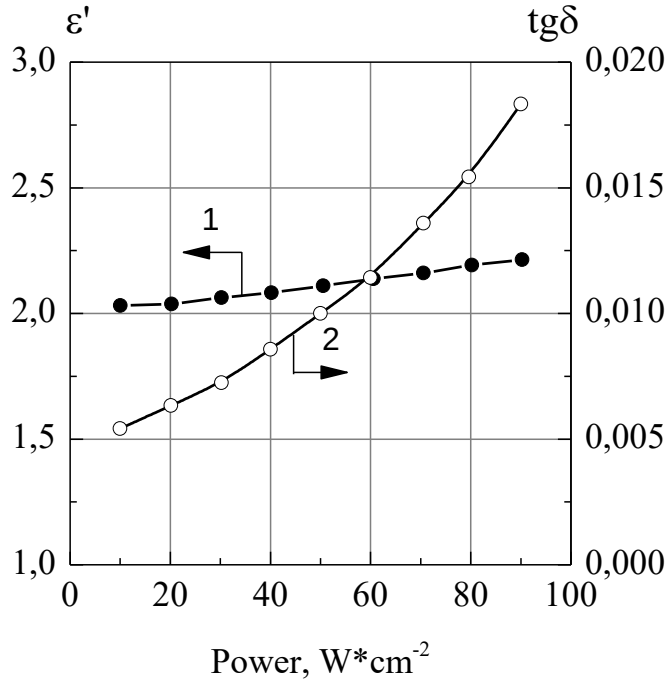

Fig. 6.1. The dependence of the dielectric constant (1) and the tangent of the dielectric loss angle (2) on the power of the electron beam decomposing PTFE at room condensation temperature.

The variable parameters were the power of the electron beam, the intensity of

UV light, the condensation temperature, the current density of the electrons bombarding the substrate, and the energy of the electrons.

A plot of ε' dependence on the power of the electron beam decomposing the polymer is shown in Fig. 6.1. With increase of the power from 10 to 80 W/cm^2,

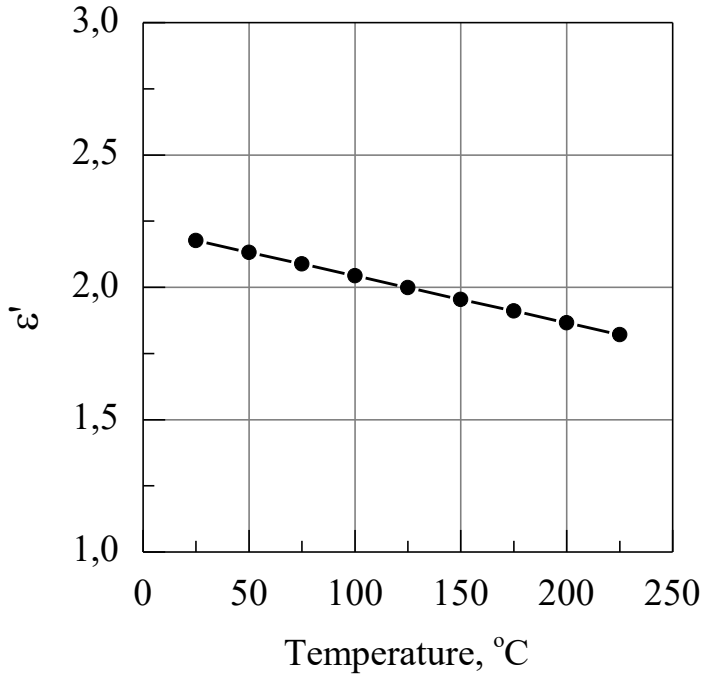

Fig. 6.2. Dependence of the dielectric constant of PTFE films on the condensation temperature.

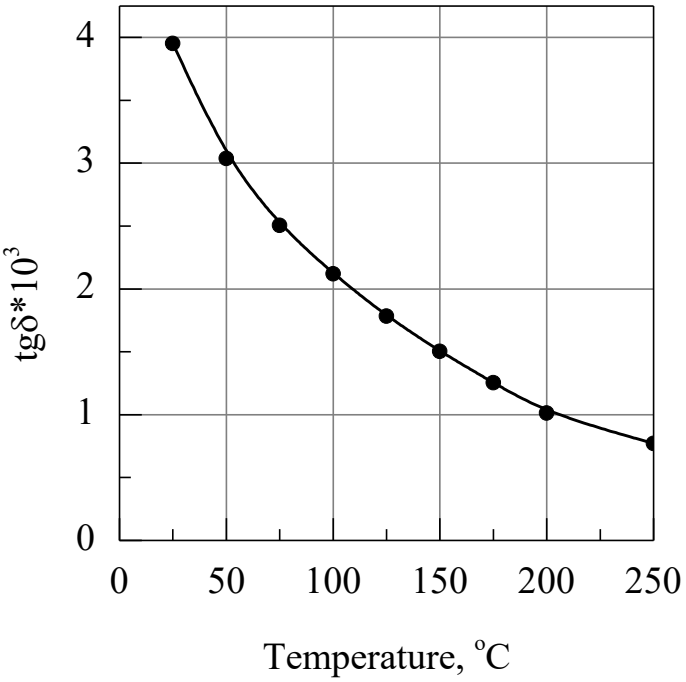

Fig. 6.3. Dependence of the dielectric loss tangent of PTFE films on the condensation temperature.

ε' slightly increased from 2.1 to 2.3. The condensation temperature was room

temperature. Large losses ($\tan\delta \approx 6\cdot10^{-3}$) also increased to the value of (10-20) 10^{-3}. Some increase in ε' and $\tan\delta$ was caused by increase of the double bonds concentration, as well as by the presence of bound oxygen and stable radicals in PTFE films, which can react with oxygen. Heating the films in vacuum led to insignificant decrease of the dielectric constant ($\varepsilon' = 2.2$) and to significant decrease of the dielectric loss tangent ($\tan\delta = 4\cdot10^{-3}$) associated with the recombination of free radicals. In the case of the films heating in air, ε' and $\tan\delta$ increased, respectively, to 2.4 and $4\cdot10^{-2}$ due to the film oxidation. The presence of oxygen-containing polar groups in the film caused increase of the dielectric constant ε' and the dielectric loss tangent $\tan\delta$. The concentration of free radicals increases with increasing power due to the deeper destruction of the irradiated polymer [162].

To reduce the concentration of the free radicals and double bonds, it is necessary to polymerize the fragments on the substrate. The polymerization was initiated by heating the substrate to various temperatures from room temperature to 250 °C or by bombarding the substrate with electrons of different energies from 50 to 700 eV with different current densities from 0.1 to 0.5 mA/cm^2.

Graphs of ε' and $\tan\delta$ as functions of the condensation temperature are presented in Fig. 6.2 and 6.3. The dielectric constant $\varepsilon' = 2.2$ and the dielectric loss tangent $\tan\delta = 5\cdot10^{-3}$ decreases with increasing the substrate temperature. This is associated with increase in the degree of polymerization and decrease in concentration of free radicals confirmed by the EPR studies. Decrease of the double bonds concentration is also confirmed by the X-ray studies. The highest molecular weight of the films was obtained at the condensation temperature of about 200-250 °C. The dielectric constant decreases to $\varepsilon' = 1.9$ and $\tan\delta$ decreases to (8-10) 10^{-4} at this temperature. As studies by the EPR method showed, a significant amount of free radicals ($4\cdot10^{18}$ spin/cm^3) still remained in the films. The concentration of free radicals decreased to $0.5\cdot10^{18}$ spin/cm^3 after annealing in vacuum at the pressure of $6.6\cdot10^{-3}$ Pa and the temperature of 250-350 °C for 1.5-2.5 hours. There was a slight decrease of ε', while $\tan\delta$ decreased to (6-8) 10^{-4}. There was a slight increase of ε' and increase of $tan\delta$ to 10^{-2} after annealing in air due to significant thermal oxidative destruction.

In the case of the electronically initiated secondary polymerization reactions on the substrate, it is important to determine the conditions under which the most complete polymerization of the active fragments occurs while the destructive action of the initiating particles has not yet begun to affect.

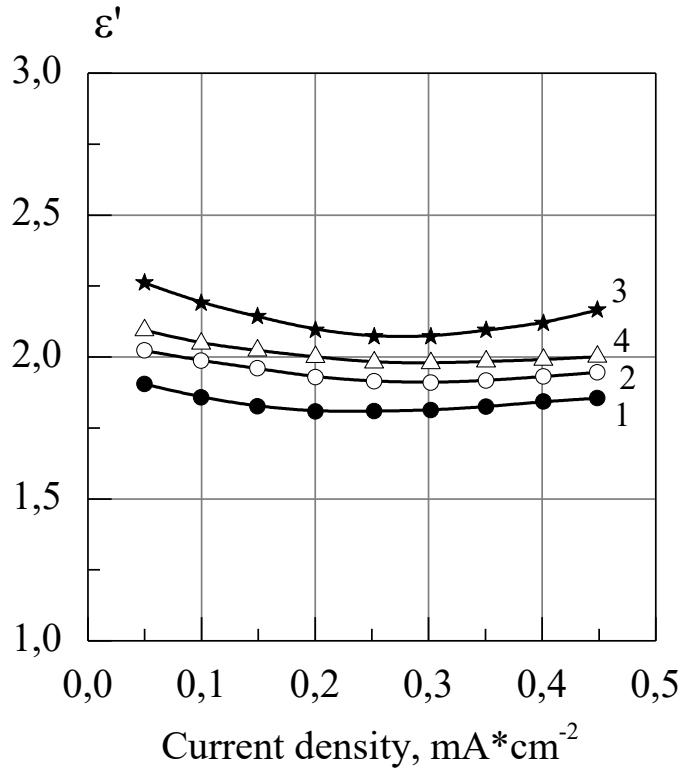

Fig. 6.4. Dependence of the dielectric constant of PTFE films on the current density of electrons irradiating the substrate at different electron energies:
1 – 100 eV; 2 – 400 eV; 3 – 600 eV; 4 – 800 eV.

The graphs of ε' versus the current density of electrons bombarding the substrate are shown in Fig. 6.4. The minimum of ε' corresponds to the electron current density of 0.2-0.25 mA/cm^2 at an energy of 40-60 eV. With increasing the electron energy, the minimum shifts to lower current densities, while the minimum of the dielectric constant corresponds to the current density interval of 0.15-0.2 mA/cm^2 at electron energies of 600-700 eV. The studies were carried out with the beam power of 40-50 W/cm^2, since the deposition rate of PTFE was low at smaller values of the power. A sharp increase in pressure and a significant decrease in the evaporation rate of PTFE occurred at high rates. The minimum dielectric constant of PTFE films is shifted to lower values of the current density with decrease of the electron beam power. The minimum value of tanδ is more pronounced on the graph of the tanδ dependence on the electron current density. At low current densities (up to 0.1 mA/cm^2), as shown by studies using DTA, TGA, X-ray and EPR methods, the films are low-molecular. They contain a large number of double bonds and free radicals that leads to increase of the dielectric losses. The degree of polymerization of the films increases with increasing the current density. Therefore, molecular weight of the

film increases and concentration of unsaturated double bonds decreases. The

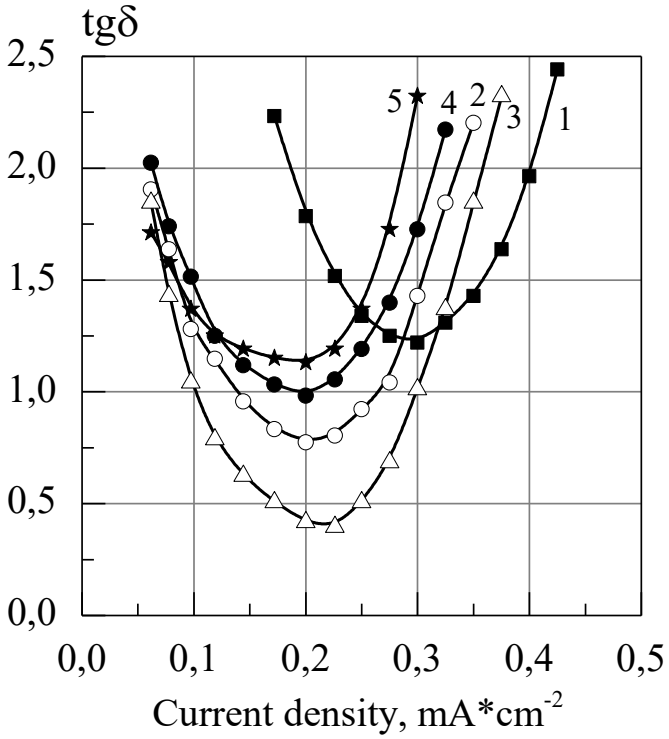

Fig. 6.5. Dependence of the dielectric loss tangent of PTFE films on the current density of electrons irradiating the substrate at different electron energies: 1 – 100 eV; 2 – 400 eV; 3 – 600 eV, annealed: 4 – 600 eV;
5 – 800 eV.

concentration of free radicals also decreases being confirmed by EPR studies.

This leads to decrease of tanδ. With further increase of the current density of the electrons bombarding the substrate (> 0.3 mA/cm^2), the losses again increase significantly (tan$\delta > 3 \cdot 10^{-3}$). This is explained by the fact that the destruction of active fragments deposited on a substrate begins to predominate over the formation of intermolecular chemical bonds under action of the bombarding electrons. This is evidenced by increase of the double bonds concentration [69], and decrease of the free radicals concentration [69]. It is known that the free radicals and unsaturated bonds serve as active sorption sites for water vapor.

The high-energy electrons used in the electron bombardment method to initiate polymerization result in deep cleavage of active fragments that condense on the surface. This process is less selective compared to the action of UV.

We obtained films that were irradiated by UV light during deposition. However, the tanδ was (8-12) 10^{-3} and $\varepsilon' = 2.4$ of films with a thickness of more than 2.5 μm, while $\varepsilon' < 1.7$ was in the films having the thickness of less than 1.5 μm. This was apparently due to the large porosity of the films comparing to the films obtained by other initiation methods. The values of ε' and tanδ of such a

film significantly increase after annealing in air ($\varepsilon' = 2.8$, $\tan\delta = 12 \cdot 10^{-3}$) that is associated with the formation of polar C = O groups and increase of the double bonds concentration, as well as with thermal oxidative destruction proceeding by the mechanism:

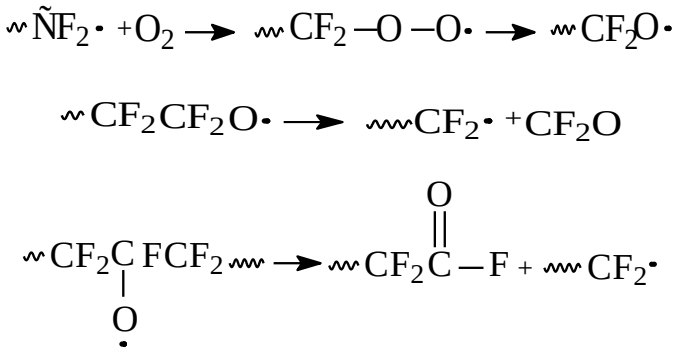

According to some authors [163], the increased dielectric losses of thin polymer films are due to presence of polar groups and free radicals. The smallest losses ($\tan\delta = 7 \cdot 10^{-4}$) possess PTFE films obtained at current densities of electrons bombarding the substrate of the order of 0.2 mA/cm^2 and energy 300-400 eV.

Heat treatment of the samples in vacuum leads to improvement of the dielectric characteristics [69], while treatment in air leads to deterioration of the properties. This is explained by the fact that heating of the films in vacuum leads to recombination of free radicals presented in the polymer. In this case, polar carbonyl and hydroxyl groups are removed from the films. Heat treatment of the films in air leads to oxidation of the polymer and formation of additional polar groups.

6.4. Capacitance of a flat capacitor with a PTFE spacer and the dielectric loss tangent of the spacer: temperature dependence

Stability of the dielectric parameters in a wide temperature range opens up the possibility of using polymer films in devices operating in a wide temperature range, particularly in capacitors.

WE studied dependence of the capacitance of a flat capacitor (C) with a PTFE film and the dielectric loss tangent of this film ($\tan\delta$) on temperature in the range of 100-200 °C. The dielectric constant of PTFE decreases with increasing temperature. This is consistent with the decrease in the density of PTFE when it is heated. In films of PTFE obtained with different initiation methods (thermal, UV irradiation with light or electrons), there is a slight

decrease of ε′ up to 10% at 200 °C. The decrease of ε' with increasing temperature is in accordance with the Clausius-Mosotti-Debye formula for non-polar dielectrics:

$$\frac{\varepsilon'-1}{\varepsilon'+2}=R\frac{\rho}{M}, \tag{6.1}$$

where ε' is the dielectric constant of the polymer; ρ is the polymer density; M is the molecular weight of the mono link; R is a constant.

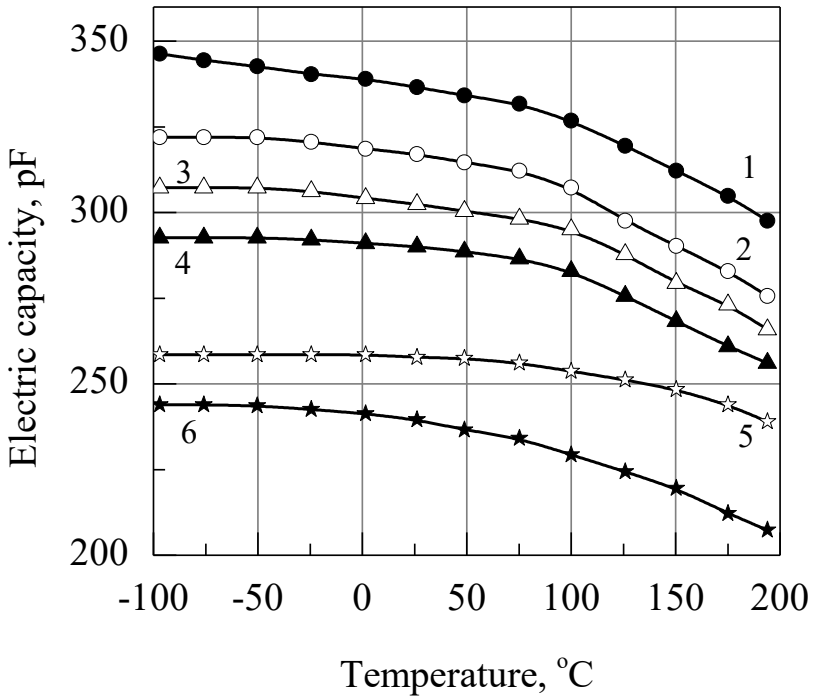

Fig. 6.6. Temperature dependence of the capacitance of PTFE films obtained by irradiating a substrate with electrons. E = 100 eV at different current density (mA/cm^2): 1 – 0.2; 2 – 0.2, annealed film; 3 – 0.4; 4 – 0.3; 5 – 0.3, annealed film; 6 – 0.2, annealed film.

It follows from (6.2) that with decreasing density caused by the temperature increase, the dielectric constant decreases. The dielectric constant of PTFE polymer films obtained by different deposition modes was calculated by the following formula:

$$\varepsilon'=\frac{C\cdot l}{\varepsilon_o\cdot a}, \qquad C=\frac{\varepsilon'\varepsilon_o\cdot a}{l}, \tag{6.2}$$

where a is the surface area of the electrodes; l is the distance between them; ε_o is the permittivity of vacuum. Capacitance was measured during continuous change of temperature. Graphs of the capacitance C as functions of temperature are presented in Fig. 6.6 and 6.7.

It follows from the graphs that capacitors have a negative temperature coefficient of capacitance (TC_C). Data on TC_C are given in Table 6.2 and in [69].

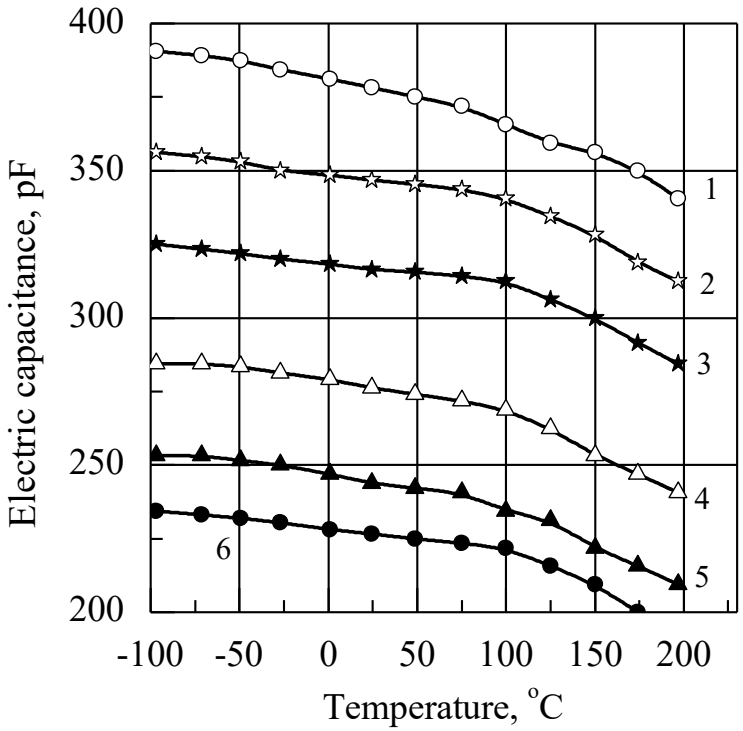

Fig. 6.7. Temperature dependence of the capacitance of PTFE films obtained by irradiating a substrate with electrons. E = 400 eV at different current density of electrons (mA/cm^2): 1 – 0.2; annealed film, 2 – 0.2; 3 – 0,3; 4 – 0.4; 5 – 0,1; 6 – 0.3, annealed film.

Differentiation of equation (6.2) gives:

$$TK_{c+} = \frac{1}{C}\frac{dC}{dT} = \frac{1}{\varepsilon}\frac{d\varepsilon}{dT} + \frac{1}{a}\frac{da}{dT} - \frac{1}{l}\frac{dl}{dT}. \qquad (6.3)$$

From Clausius-Mosotti's equation for non-polar materials, we can find:

$$\frac{1}{\varepsilon}\frac{d\varepsilon}{dT} = -\frac{(\varepsilon-1)(\varepsilon+2)}{\varepsilon}\alpha, \qquad (6.4)$$

where α is the linear expansion coefficient presented as follows:

$$\alpha = \frac{1}{l}\frac{dl}{dT}. \qquad (6.5)$$

Two cases can be distinguished for the second term of the TC_c:

a) Following Cockbein and Harrop [164], it can be assumed that a increases with expansion of the polymer. In this case, the second term is $+2\alpha$.

b) It can be assumed that the surface area is constant because α is small comparing to that of the PTFE film. Hence, the second term is almost zero.

Table 6.2

Temperature coefficient of capacitance (TC_C) and glass transition temperature (T_g) of PTFE films obtained under different deposition modes, and the Commercial PTFE film

	Deposition mode													
TC_c, °C^{-1};	E, eV	100			400				700			T_c, °C		Commercial film
T_g, °C	j, mA/cm^2	0.2	0.3	0.4	0.1	0.2	0.3	0.4	0.1	0.2	0.3	25	240	
-$TC_{c1}\cdot 10^5$		10	13	18	28	16	26	26	22	19	27	34	9	7
T_g		87	97	95	83	93	97	90	83	87	80	83	87	105
-$TC_{c2}\cdot 10^5$		98	88	95	94	81	85	91	104	87	117	142	49	48
Heat treated (annealed) films														
-$TC_{c1}\cdot 10^5$		16	8	20		22	24			16	31		6	
T_g		87	103	97		100	97			93	83		93	
-$TC_{c2}\cdot 10^5$		100	56	98		71	109			81	128		43	

Given the inhomogeneity of the films, such as defects and disorders, it is necessary to add a term equal to $0.05\tan\delta$ associated with the temperature change of the dielectric constant. Then, we obtain the temperature coefficient of capacitance for two cases:

a) $TK_c = -\dfrac{(\varepsilon'-1)(\varepsilon'+2)}{\varepsilon'}\alpha + \alpha + 0.05tg\delta$

b) $TK_c = -\dfrac{(\varepsilon'-1)(\varepsilon'+2)}{\varepsilon'}\alpha - \alpha + 0.05tg\delta$

We calculated linear expansion coefficients α_1, (below the T_g temperature) and α_2 (above T_g) taking into account the expansion of the electrodes and without expansion for the films obtained in different deposition modes. Data for α_1 and α_2 are given in Table 6.3. It follows from the table that the T_g temperature

depends on the deposition mode and for all samples at temperatures below T_g the coefficient of linear expansion is smaller than at the temperature higher than T_g.

Table 6.3

The coefficient of linear expansion (α) and the glass transition temperature (T_g) of PTFE films obtained by different deposition modes, and Commercial PTFE film

	Deposition mode													
α, °C^{-1}; T_g, °C	E, eV	100			400				700			$T_к$, °C		Commercial film
	J, mA/cm^2	0.2	0.3	0.4	0.1	0.2	0.3	0.4	0.1	0.2	0.3	25	240	
$\alpha_1 \cdot 10^5$		5	7	9	11	7	9	11	12	9	13	15	6	7
T_g		87	97	95	83	93	97	90	83	87	80	83	87	105
$\alpha_2 \cdot 10^5$		35	32	35	33	27	30	33	40	31	43	52	19	20
Heat treated (annealed) films														
$\alpha_1 \cdot 10^5$		7	7	9		8	10			7	13		4	
T_g		87	103	97		100	97			93	83		93	
$\alpha_2 \cdot 10^5$		35	23	37		24	38			29	45		16	

This is typical for amorphous polymeric materials. The T_g temperature is called the glass transition temperature and corresponds to the appearance of joint motion of relatively long molecular chains segments. Below T_g, the polymer is in a glassy state, but it is in the highly elastic state at the temperature above T_g.

It can be seen from the data in the table that the highest glass transition temperature corresponds to the films annealed in a vacuum and deposited at the current densities of 0.2-0.3 mA/cm^2 and electron energies of at least 200 eV. As shown by X-ray, DTA and TGA studies, these films have the highest molecular weight. The Commercial film has $T_g \approx 110$ °C.

Simha and Boyer [165] suggested the following relation:

$$(\alpha_1 - \alpha_2) \cdot T_g = \rho \cdot K\,, \qquad (6.6)$$

where T_g is the glass transition temperature in Kelvins; ρ is the polymer

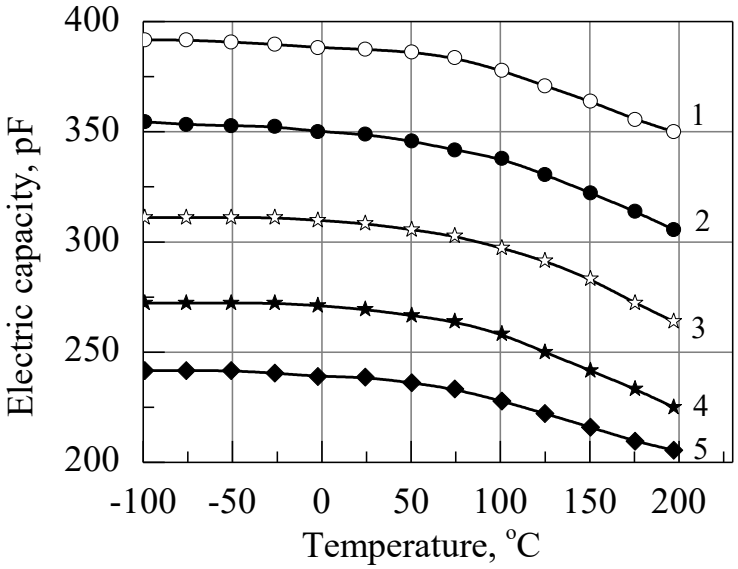

Fig. 6.8. Temperature dependence of the capacitance of PTFE films obtained by irradiating the substrate with electrons (E = 700 eV) at different current density of electrons: 1 – 0.2 mA/cm^2; annealed film, 2 – 0.2 mA/cm^2; 3 – 0.1 mA/cm^2; 4 – 0.3 mA/cm^2; 5 – 0.3 mA/cm^2, annealed film.

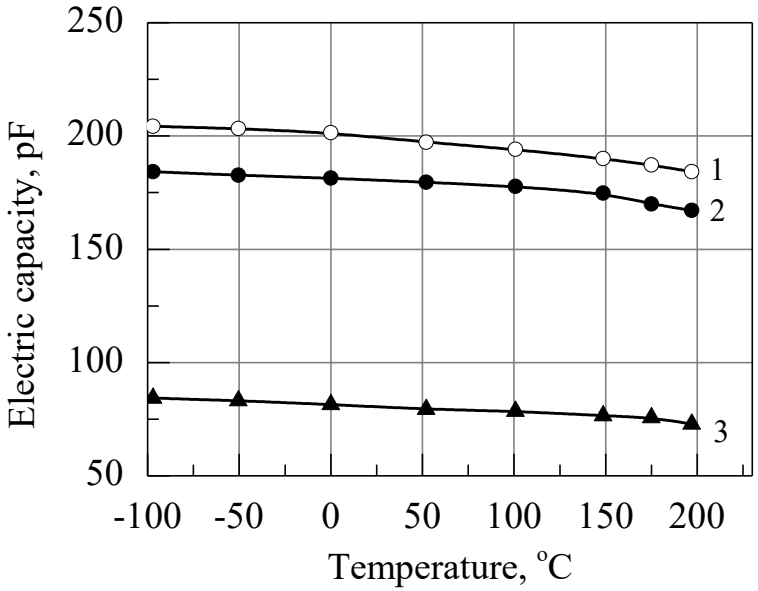

Fig. 6.9. Temperature dependence of the capacity of PTFE films obtained by the method of thermal initiation of secondary polymerization:
1 – T_c = 240 °C; 2 – T_c = 240 °C, annealed film; 3 – industrial film.

density ρ = 2.1 g/cm^3; K is a constant that has been found for 16 polymers.

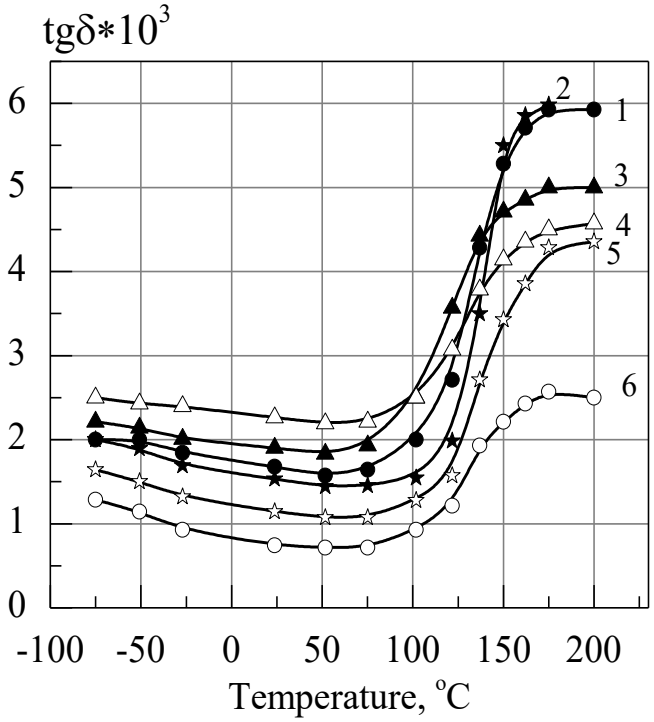

Fig. 6.10. Temperature dependence of the dielectric loss tangent of PTFE films obtained by irradiating the substrate with electrons E = 100 eV at different electron current density (mA/cm^2): 1 – 0.1; 2 – 0.3; 3 – 0.4; 4 – 0.3, annealed film; 5 – 0.2; 6 – 0.2 mA/cm^2, annealed film

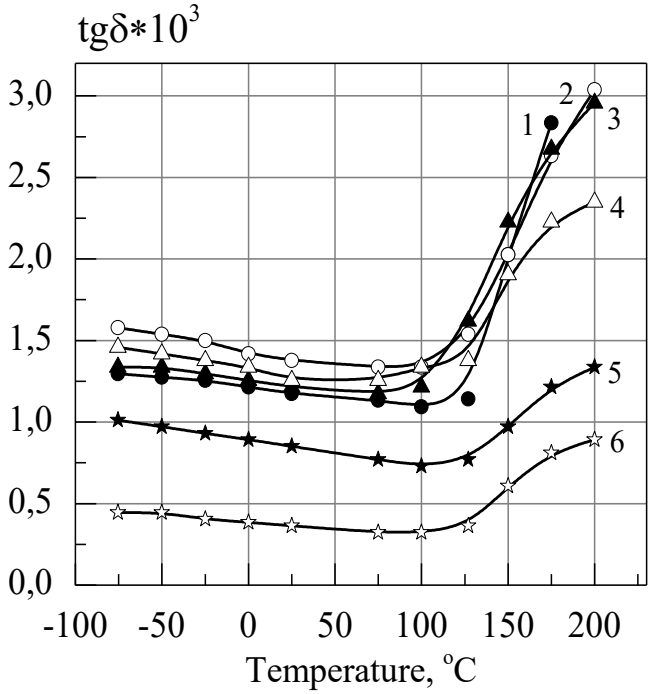

Fig. 6.11. Temperature dependence of the dielectric loss tangent of PTFE films obtained by irradiating a substrate with electrons E = 400 eV at different electron current density (mA/cm^2): 1 – 0.1; 2 – 0.4; 3 – 0.3; 4 – 0.3, annealed film; 5 – 0.2; 6 – 0.2, annealed film

$T_g \approx$ 125 °C for PTFE from literature data [166]. The highest T_g temperature of our samples was 110 °C.

The end of the chain is less connected than the segment in the center of the

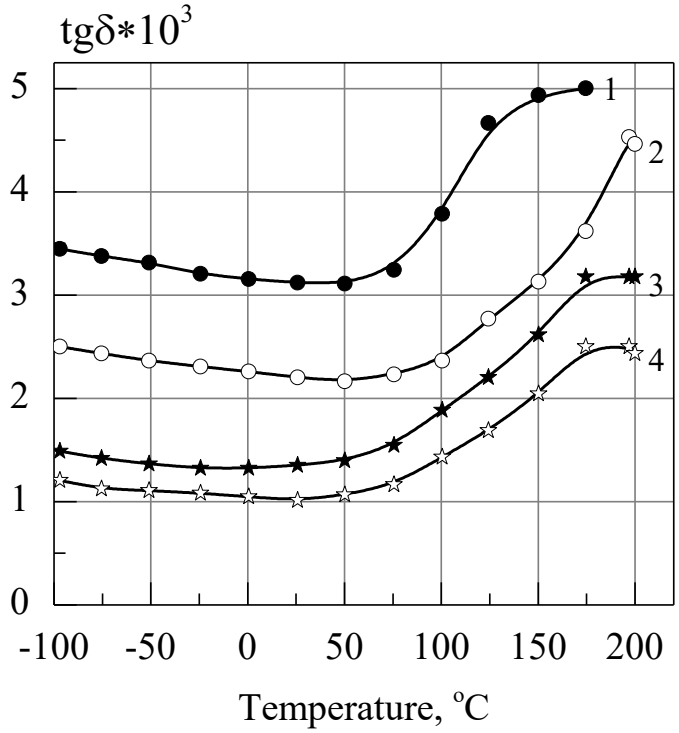

Fig. 6.12. Temperature dependence of the dielectric loss tangent of PTFE films obtained by irradiating a substrate with electrons E = 700 eV at different electron current density (mA/cm^2): 1 – 0.1; 2 – 0.3; 3 – 0.2; 4 – 0.2, annealed film

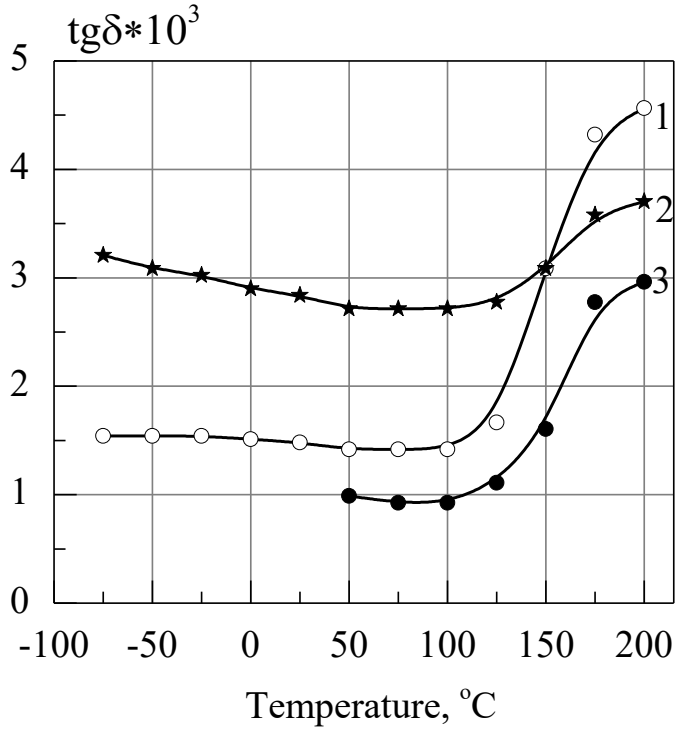

Fig. 6.13. Temperature dependence of the dielectric loss tangent of PTFE films obtained by the method of thermal initiation of secondary polymerization: 1 – T_c = 240 °C; 2 – industrial film; 3 – T_c = 240 °C, annealed film.

chain. In order to facilitate the rapid movement, the mass of material adjacent to the end of the chain must tend to expand creating a free volume. However, it can be expected that the greater concentration of the chain ends (double bonds), the greater degree of freedom at a given temperature.

This gives the chain more freedom to move and less energy is needed to move the segments. The value of α_1 for PTFE is smaller than the linear expansion coefficient that we found for the precipitated polymer in the glassy state. This can also be explained by increase in free volume due to increase in the number of the chain ends.

A study was carried out on the temperature dependence of the dielectric loss tangent of the PTFE films. The tanδ of all films decreases slightly with increase of temperature from room temperature to 100 °C (Fig. 6.10-6.13). This is due to the evaporation of adsorbed water vapor and cleavage of hydroxyl groups, which are centers of the moisture sorption. With further increase of temperature, increase of tanδ is observed. A significant increase in dielectric loss tangent was found in the films obtained with the current density less than 0.1 mA/cm^2 and more than 0.4 mA/cm^2 and electron energies less than 100 eV and more than 600 eV. The tanδ value of such films increases by one order of magnitude at temperatures of 120-150 °C and reaches the value of $(8\text{-}10)\cdot10^{-3}$. The smaller increase of the dielectric loss tangent ($\tan\delta \leq 15\cdot10^{-4}$) is observed in the films deposited at the electron current densities of 0.15-0.25 mA/cm^2 and energy of about 350-450 eV.

The increase of tanδ in films obtained under these conditions begins at the temperature of ~140 °C. With increase of the current density more than 0.25 mA/cm^2, a rapid increase of tanδ to $(6\text{-}8)\cdot10^{-3}$ is again observed. The increase of tanδ with increasing temperature is due to the increase the electrical conductivity of PTFE films. Values of ε' and tanδ decrease to 1.9 and $3\cdot10^{-4}$, respectively, in the films subjected to heat treatment in vacuum. Their increase with temperature is slower than in the films not subjected to annealing in vacuum. In addition, the increase of the dielectric loss tangent begins at the temperature of about 150 °C. This is apparently due to the fact that evaporation of low molecular weight fractions occurs after annealing in vacuum, as well as the elimination of oxygen-containing groups and decrease of the polar double bonds concentration, and decrease of the sorption centers of water vapor concentration. The higher molecular weight fractions in films contribute to losses at the higher

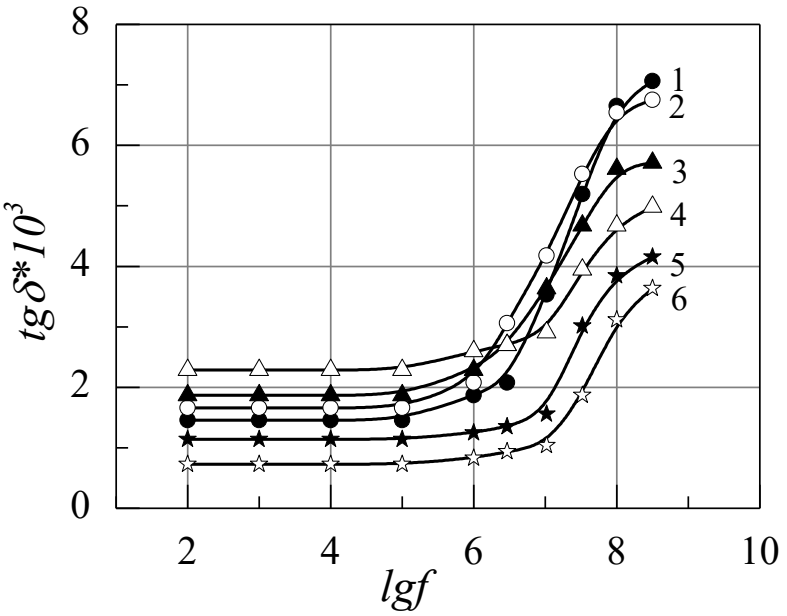

Fig. 6.14. The frequency dependence of the dielectric loss tangent of PTFE films obtained by irradiating the substrate with electrons E = 100 eV at different electron current density (mA/cm^2): 1 – 0.1; 2 – 0.4; 3 – 0.3; 4 – 0.3, annealed; 5 – 0.2; 6 – 0.2, annealed film.

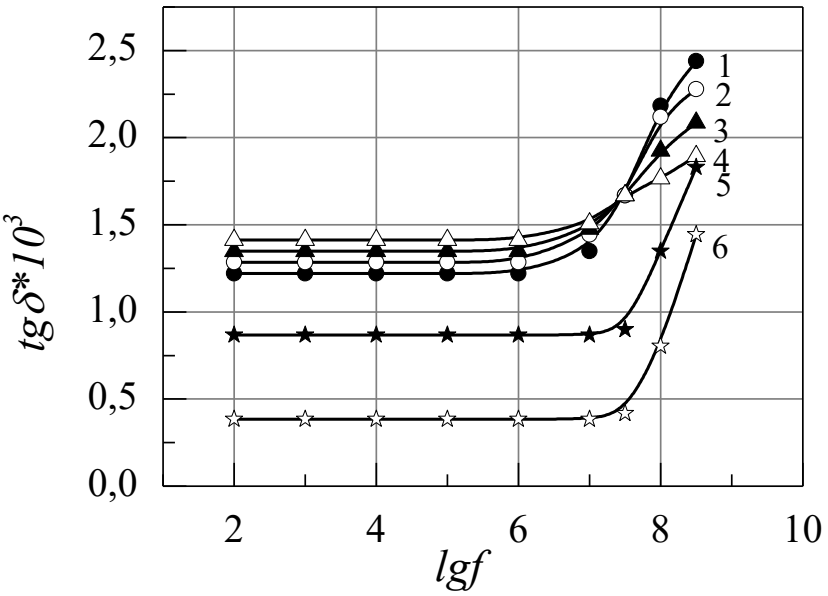

Fig. 6.15. Frequency dependence of the dielectric loss tangent of PTFE films obtained by irradiating a substrate with electrons E = 400 eV at different electron current density (mA/cm^2): 1 – 0.1; 2 – 0.4; 3 – 0.3; 4 – 0.3, annealed film; 5 – 0.2; 6 – 0.2, annealed film.

temperatures. With increase of the polymerization degree, the molecular weight of the films increases and, accordingly, the tanδ decreases.

The degree of polymerization (according to of X-ray, DTA and TGA methods) is greatest at the electron current densities of ~0.2 mA/cm^2 and their energy of about 400-450 eV with the electronic initiation. The films deposited

on the substrate having the temperature 220-240 °C behave similarly during the thermal initiation of the secondary polymerization reactions of the fragments.

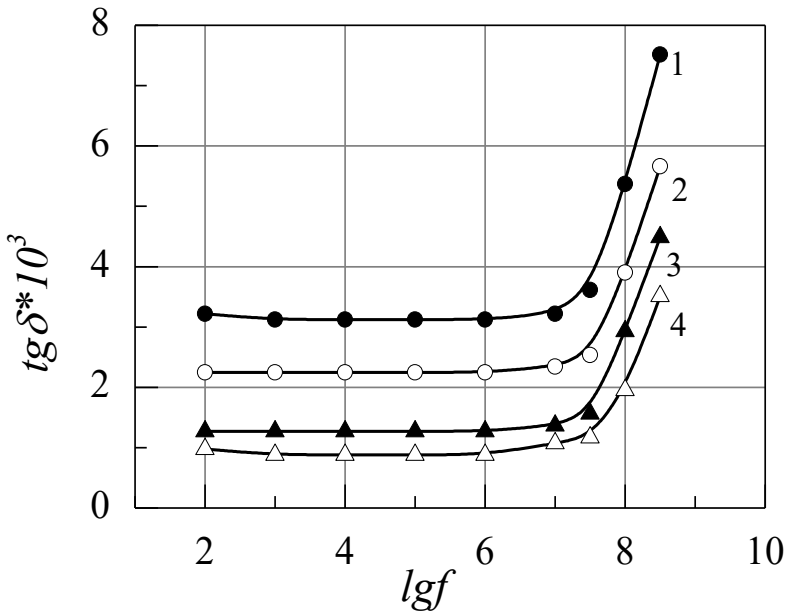

Fig. 6.16. The frequency dependence of the dielectric loss tangent of PTFE films obtained by irradiating the substrate with electrons E = 700 eV at different electron current density (mA/cm^2): 1 – 0.1; 2 – 0.3; 3 – 0.2; 4 – 0.2, annealed film.

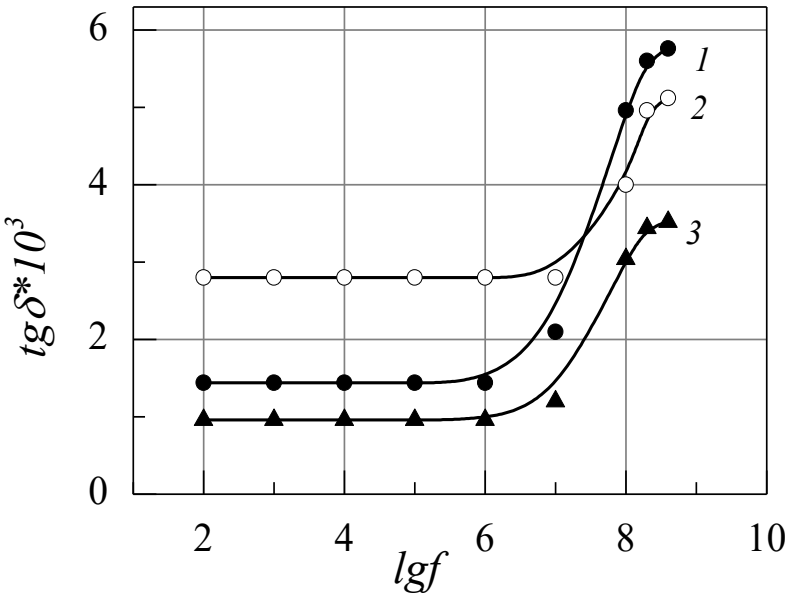

Fig. 6.17. The frequency dependence of the dielectric loss tangent of PTFE films obtained by the method of thermal initiation of the secondary polymerization: 1 – T_c = 240 °C; 2 – industrial film; 3 – T_c = 240 °C, annealed film.

6.5. Frequency dependence of the dielectric properties of PTFE films

Stability of the dielectric parameters in a wide frequency range opens up the possibility of using polymer films in high-frequency devices. An important feature of the dielectric properties of polymers in the microwave range determining their practical application is presence of the losses “background”, i.e. absorption weakly dependent on frequency and temperature [163].

Insignificant information can be obtained about dispersion regions in PTFE from the measurements of the dielectric constant ε', since the changes of ε' are too small and difficult to observe. The change of ε' at any dispersion is proportional to the value of ε'' ($\tan\delta = \varepsilon''/\varepsilon'$) maximum [80]. In PTFE ε'' does not exceed 10^{-3}, so a noticeable change of ε' cannot be observed.

In view of the above, a study was made of the tanδ dependence of PTFE films obtained at different deposition modes on the applied electric field frequency. It follows from the graphs in Fig. 6.14-6.17 that the tanδ does not change in all films with increasing frequency in the range of 10^2-10^7 Hz.

With further increase of frequency, tanδ increases too. The tanδ increases by one order of magnitude to $7\cdot10^{-3}$ at a frequency of $2.8\cdot10^8$ Hz in films deposited by electronically initiating polymerization at electron current densities lower than 0.15 mA/cm^2 and greater than 0.4 mA/cm^2 and their energies up to 50 eV and more than 700 eV. This is due to the presence of polar groups ($-\overset{|}{\underset{|}{\mathrm{C}}}=\mathrm{O}$ and $-\overset{|}{\underset{|}{\mathrm{C}}}-\mathrm{OH}$), as well as terminal double bonds.

A lower degree of polymerization under these conditions is associated with a high concentration of the end groups, and a high concentration of free radicals with the presence of peroxide radicals and oxygen. A smaller increase in tanδ is observed in films deposited at electron current densities of 0.2-0.25 mA/cm^2 and their energies of about 350-450 eV during electronic initiation of polymerization, as well as at condensation temperatures of about 220-240 °C during thermal initiation of the polymerization. This is due to a decrease in the concentration of the end groups. For films obtained in the best regimes and heat-treated in vacuum at a pressure of 10^{-3} Pa at 250-350 °C for 1.5-2.5 hours, tanδ at a frequency of $2.8\cdot10^8$ Hz decreases to the values of $1{,}4\cdot10^{-3}$-$2\cdot10^{-3}$. The decrease of tanδ is associated with decrease in the concentration of terminal double bonds due to evaporation of the low molecular weight phase, cleavage of

oxygen, oxygen-containing groups, which are polar and, therefore, sorption centers of water vapor. After annealing, the structure of PTFE films changes.

Strictly speaking, the nature of dielectric losses in PTFE is unclear [41]. However, the correlation of the data obtained in the study of molecular relaxation by dynamic, mechanical, and dielectric methods indicates that the relaxation process of the dipole polarization is associated with the thermal motion of the kinetic segments of macromolecules in which there are polar groups. In cases where the concentration of these groups is low, the method of the dielectric loss cannot detect relaxation losses.

6.6. Electrical conductivity of PTFE polymer films

The resistivity of polymer films is an important dielectric characteristic, the magnitude of which makes it possible to estimate the leakage currents, and hence, the loss of energy and information in thin-film capacitors.

According to their electrical properties, polymers are divided into dielectrics, semiconductors and conductive materials. Dielectrics include polymers whose molecules do not contain groups dissociated into ions and conjugated double bonds along the macrochain. The conductivity of such polymers at room temperature does not exceed $\gamma = 10^{-8}$ Sm/m. Polymeric semiconductors ($\gamma = 10^{-8}$-10^{-1} Sm/m) are characterized by presence of the conjugated double bonds.

Polymer films obtained from the initial monomers by polymerization in vacuum or from polymers by decomposition and polymerization in vacuum contain low molecular weight fractions. They contain more unsaturated bonds, oxygen-containing groups, terminal double bonds and free radicals than the original polymer. The presence of these components lowers the resistivity of the films. Since these films can serve as dielectric capacitor layers, charge carriers injection from capacitor plates is possible. However, as Adamets [167] showed, the injection of electrons into the polymer film is either absent or so insignificant that it does not affect the resistivity. The structure of macromolecules, as well as their thermal motion, the physical structure of the polymer, the presence of low molecular weight fractions or special additives in it affects the concentration and mobility of carriers. Low molecular weight fractions presented in the polymer films reduce intramolecular interaction that leads to increase of the macromolecules mobility.

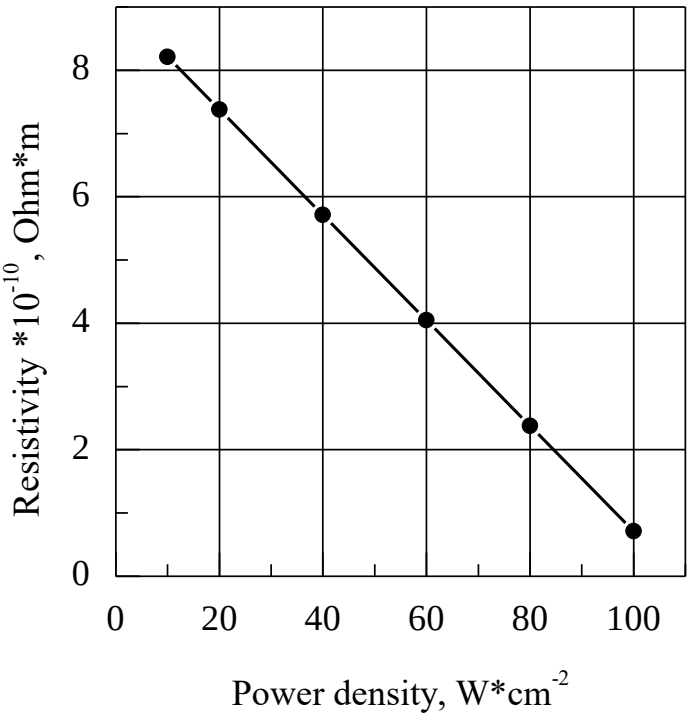

Fig. 6.18. The dependence of the specific volume resistance of PTFE films on the power of the electron beam decomposing PTFE at T = 25 °C.

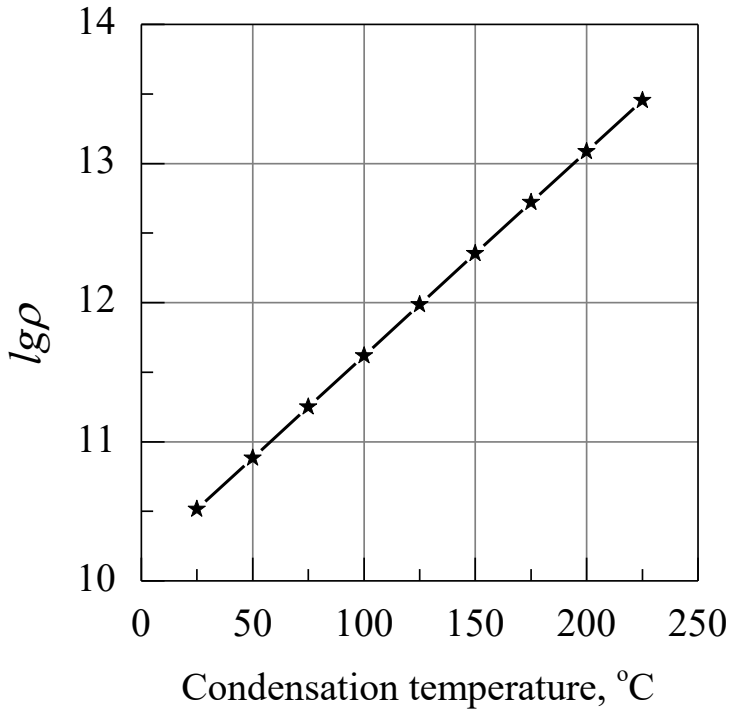

Fig. 6.19. Dependence of the specific volume resistance of PTFE films on the condensation temperature.

6.7. Dependence of the specific volume resistance (ρ_v) of PTFE films on conditions of their preparation

The dependence of the specific volume resistance of the films (ρ_v) of PTFE on the conditions of their preparation has been studied and the temperature dependence of the resistance was investigated.

Fig. 6.18 shows a plot of the PTFE film ρ_v as a function of the beam power decomposing the polymeric material followed by deposition of evaporated fragments on the substrate at room temperature. It is seen that ρ_v decreases with increasing the electron beam power from 10 W/cm^2 to 100 W/cm^2.

The decrease from $8 \cdot 10^{10}$ Ω·m to $2 \cdot 10^{10}$ Ω·m is due to the low molecular weight of the films obtained at high power of the electron beam, and also with a higher concentration of free radicals and double bonds. This is confirmed by studies using DTA, TGA, EPR and X-ray methods [69].

Increase of the molecular weight of the PTFE films should lead to the growth of ρ_v. Therefore, a study was conducted on PTFE films, upon deposition of which secondary polymerization was initiated on the substrate by: 1) the heating to the temperature of 220-240 °C; 2) the electron bombardment, while changing the current density of electrons in the range from 0.05 to 0.5 mA/cm^2 and their energy from 40 to 600 eV.

Fig. 6.19 shows plots of PTFE film ρ_v versus condensation temperature T_c. It follows from the graph in Fig. 6.19 that ρ_v of the PTFE films increases significantly with increasing T_c (by 2-3 orders of magnitude). The low resistivity of the films at room temperature of the substrate is explained by the insufficient degree of polymerization, as well as by the high concentration of the low molecular weight phase, which deteriorates the insulating properties of the film. As the condensation temperature increases, the molecular weight of the PTFE films increases too due to the re-evaporation of low molecular weight fragments and polymerization of the heavier active fragments. The films are more stable after annealing in vacuum (10^{-3} Pa) at a temperature of 250-350 °C for 1.5-2.5 hours.

Films obtained at the temperature of 220-240 °C lost up to 6% of their weight after annealing, while the films obtained at room temperature lost up to 30%. This also confirms presence of the low molecular weight phase in the films obtained at room temperature.

Fig. 6.20 shows dependence of the PTFE films ρ_v from the mode of their

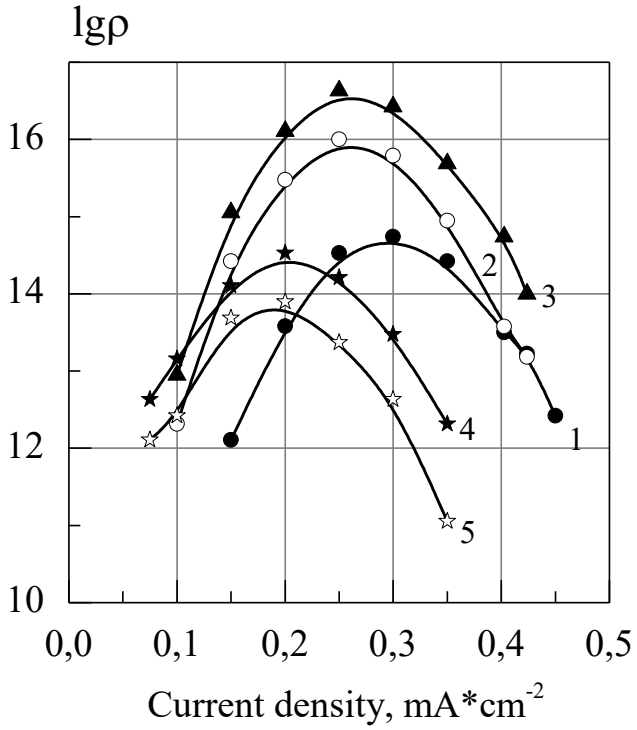

Fig. 6.20. Dependence of the specific volume resistance of PTFE films on the energy of electrons irradiating the substrate at different electron energies: 1 – 50 eV; 2 – 200 eV; 3 – 200 eV, annealed film; 4 – 400 eV; 5 – 600 eV.

production with the electronic initiation of the secondary polymerization. It follows from the graphs that the resistivity is equal to $\rho_v = 10^{11}$ Ω·m at current densities of up to 0.1 mA/cm^2. Then the resistivity reaches a maximum of $\rho_v = 10^{16}$ Ω·m with increase in the electron current density to 0.2-0.25 mA/cm^2, and then a decrease is again observed with the specific resistance $\rho_v = 10^{14}$ Ω·m at the current density of J = 0.4 mA/cm^2. A similar pattern of change is also observed when the energy of electrons bombarding the substrate varies from 40 to 600 eV.

At first, the growth of ρ_v is observed and it reaches a maximum of $\rho_v = 10^{16}$ Ω·m at the electron energy of 150-200 eV, and then ρ_v decreases. However, it should be noted that the maximum of the specific resistance with a change of the electron energy is more pronounced than with a change in the electron current density.

The presence of a maximum can be explained by the fact that the degree of polymerization is low at low current densities. At low electron energies, the degree of polymerization is also low, as evidenced by the increased

concentration of the double bonds and the free radicals. Presence of the low molecular weight phase is also confirmed by the fact that the films after annealing lost up to 22% of their weight if they were deposited at the electron current densities up to 0.1-0.15 mA/cm^2 and energies up to 150 eV. After annealing, the films lost up to 12% of the mass if they were obtained at current densities above 0.35-0.4 mA/cm^2 and electron energies above 500 eV. This indicates to the presence of a lower molecular weight phase in the smaller amount. In the smallest amount, the low molecular weight phase is present in films obtained at the electron current density of 0.2-0.25 mA/cm^2 and energies of about 150-200 eV, as well as at the electron beam power of 40-50 W/cm^2 degrading the polymer.

This is due to the lower concentration of the double bonds and the free radicals discovered in X-ray and ESR studies. Under these conditions of the PTFE films preparation, the resistivity reaches the maximum of $\rho_v = 10^{16}$ Ω·m. Some increase is achieved after annealing the film in vacuum resulting in increase of 30-40% [69].

The weight loss of films obtained in the best mode after annealing in vacuum (10^{-3}Pa) at the temperature of 300 °C for two hours is no more than 6% confirming the low concentration of the low molecular weight phase.

6.8. Temperature dependence of the PTFE films volume resistance

As mentioned above, the constancy of the dielectric characteristics of films in a wide temperature range extends their applicability. Therefore, a study was conducted of the effect of temperature change on the specific volume resistance in the temperature range of 100-200 °C.

The change in resistivity as a function of temperature is characterized by the temperature coefficient of resistance determined by the following formula:

$$TK_{\rho_v} = \frac{1}{\rho_v}\frac{d\rho_v}{dT}$$

It follows from the graphs in Fig. 6.21-6.24 that there are two portions of the curve with different changes in resistivity on the temperature dependence of the resistivity of PTFE films.

The $TC_{\rho v}$ values of the films deposited in different modes and methods of initiation are presented in Table. 6.4.

Table 6.4

Temperature coefficient of specific volume resistance ($TC_{\rho v}$) and glass transition temperature (T_g) of PTFE films obtained under different deposition conditions and Commercial PTFE film

	Deposition mode													
$TC\rho$°C^{-1}	E, eV	50			200				400			$T_к$, °C		Commercial film
T_c, °C	j, mA/cm^2	0.2	0.3	0.4	0.1	0.2	0.3	0.4	0.1	0.2	0.3	25	240	
$-TC_\rho \cdot 10^4$		13	27	32	27	10	16	23	31	19	22	36	9	5
T_g, °C		93	97	95	93	100	97	87	83	93	97	83	90	105
$-TC_\rho \cdot 10^4$		41	52	61	55	37	42	58	75	40	48	81	35	31
Heat treated (annealed) films														
$-TC_\rho \cdot 10^4$		8	24			6	14			17	24		4	
T_g, °C		97	103			103	100			100	97		93	
$-TC_\rho \cdot 10^4$		30	47			27	42			42	73		29	

The table shows that the glass transition temperature T_g increases in the films

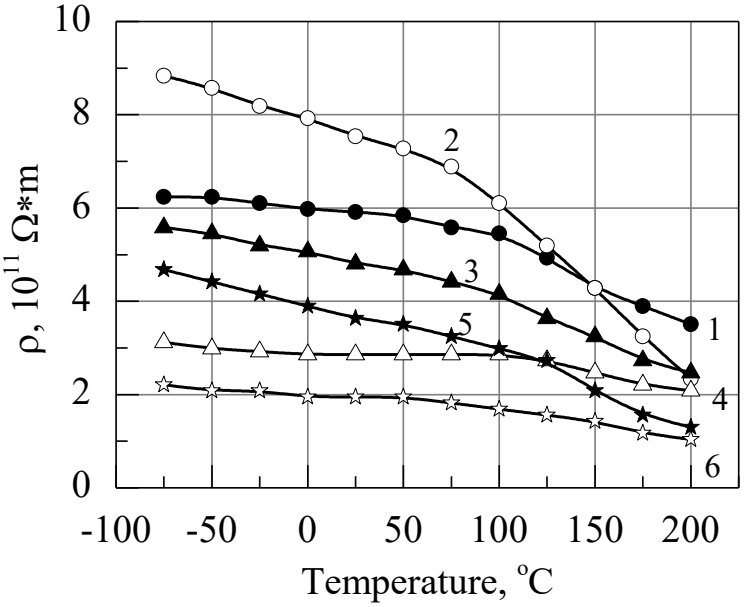

Fig. 6.21. Temperature dependence of the specific volume resistance of PTFE films obtained by irradiating a substrate with electrons E = 50 eV at the different electron current density: 1 – 13.2 mA/cm^2, annealed film; 2 – 14.3 mA/cm^2, annealed film; 3 – 14.3 mA/cm^2; 4 – 13.4 mA/cm^2; 5 – 13.2 mA/cm^2.

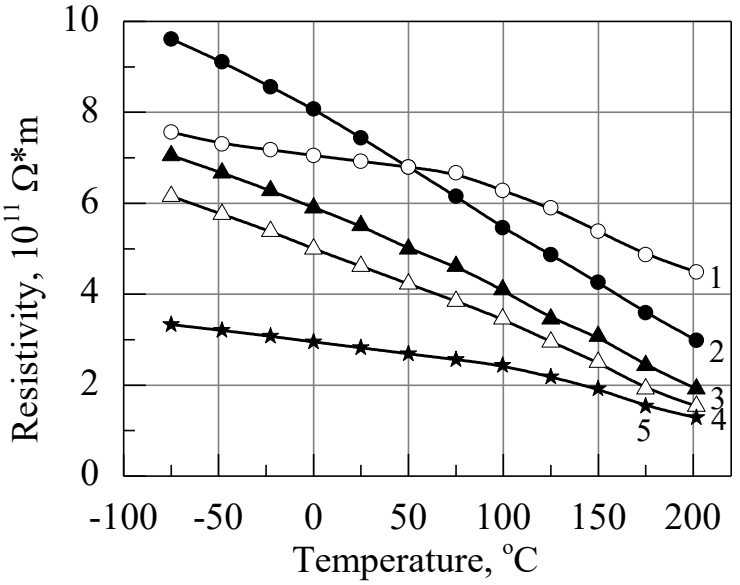

Fig. 6.22. Temperature dependence of the specific volume resistance of PTFE films obtained by irradiating a substrate with electrons E = 200 eV at the different electron current density: 1 – 15.2 mA/cm^2: 2 – 15.3 mA/cm^2; 3 – 13.4 mA/cm^2; 4 – 16.2 mA/cm^2, annealed film; 5 – 12.1 mA/cm^2; 6 – 16.3 mA/cm^2, annealed film.

deposited at the higher condensation temperatures during the thermal initiation

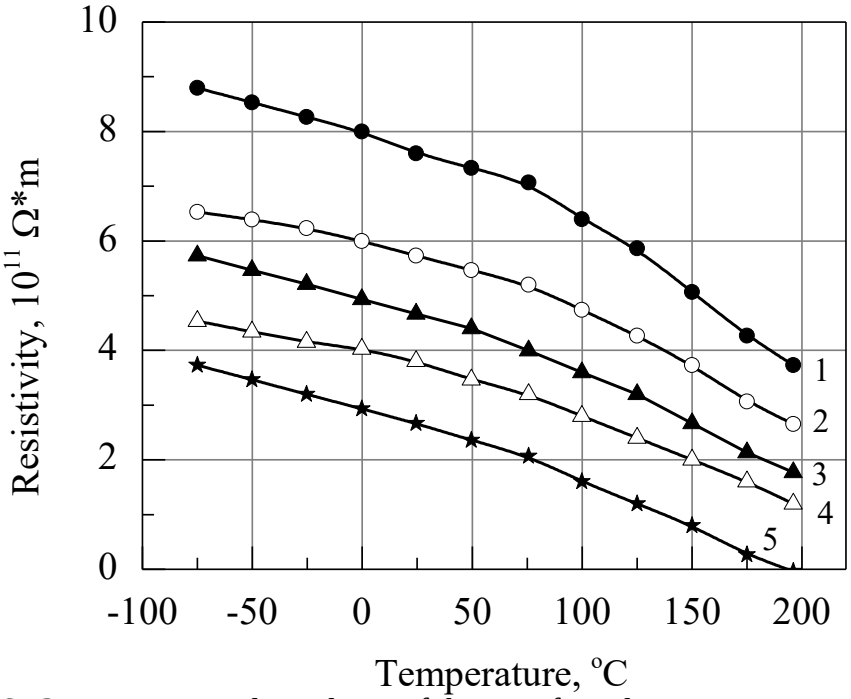

Fig. 6.23. Temperature dependence of the specific volume resistance of PTFE films obtained by irradiating a substrate with E=400 eV electrons at the different electron current density: 1 – 14.2 mA/cm^2 annealed film; 2 – 14.2 mA/cm^2; 3 – 13.3 mA/cm^2, 4 – 13.3 mA/cm^2, annealed film; 5 – 13.1 mA/cm^2.

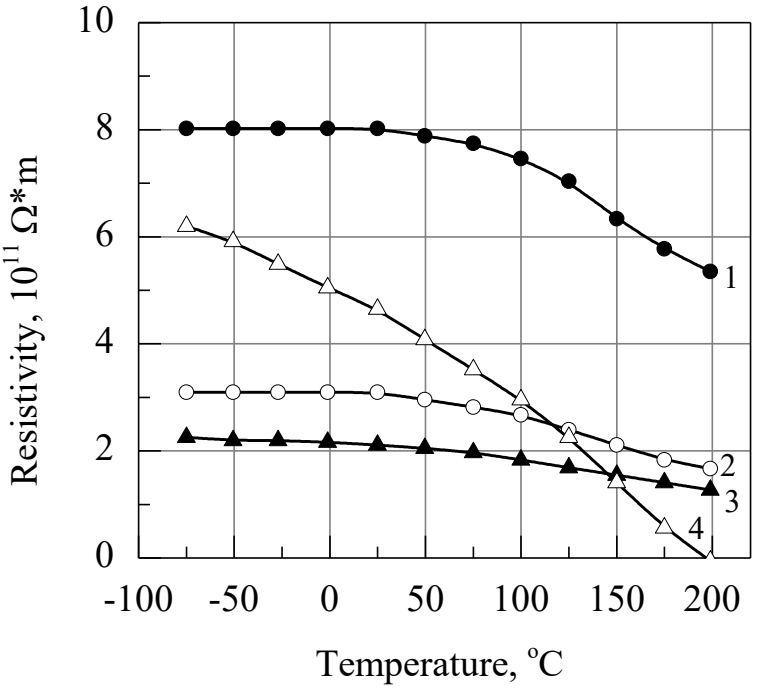

Fig. 6.24. Temperature dependence of the specific volume resistance of PTFE films obtained by the method of thermal initiation of secondary polymerization: 1 – T_c = 240 °C, annealed; 2 – T_c = 240 °C; 4 – T_c = 25 °C, 3 – industrial film.

of polymerization and T_g is maximum in the films deposited at the current densities of 0.2-0.25 mA/cm^2 and energy 150-200 eV. It should also be noted

that $TC_{\rho v}$ of all samples is negative, and it is the smallest in absolute value in the films prepared according to the above modes and subsequently annealed at the temperature of 250-350 °C for 1.5-2.5 hours in vacuum.

It follows from the graphs in Fig. 6.21-6.24 that the glass transition temperature is not clearly expressed, and its dependence on T can only be considered approximately as linear. The increase in the glass transition temperature occurs due to increase of the molecular weight. With increase of the molecular weight, not only the length of the molecular chains changes, but the degree of their branching also changes, as well as the type and size of supramolecular structural formations and the packing density of the polymer films.

The nature of such changes in ρ_v (Fig. 6.19, 6.20) depending on the molecular weight can be explained as follows. The viscosity of the system increases during polymerization due to a partial replacement of intermolecular forces by chemical bonds. In addition, the supramolecular organization of the polymer material changes. All this leads to decrease of the mobility of the electrically charged particles and their concentration. According to EPR studies, the concentration of radicals that serve as electron traps decreases with increasing the molecular weight. Therefore the conductivity of the polymer decreases.

It also follows from the table that the highest $TC_{\rho v}$ is observed in the films obtained at room temperature and in the films obtained at the electron current densities less than 0.1 mA/cm^2 and more than 0.4 mA/cm^2 and energies less than 100 eV and more than 300 eV.

The glass transition temperature, as follows from the graphs and tables, also increases with increasing condensation temperature to 220-240 °C and approaches 100 °C. The glass transition temperature also increases in the films obtained by using the best regimes with the electronic initiation and is equal to ~100 °C. The $TC_{\rho v}$ value of the films obtained at the best deposition mode (J = 0.2 mA/cm^2; E = 200 eV) is the smallest and is equal to $TC_{\rho v} = -10 \cdot 10^{-4}$ °C^{-1} at $T < T_g = 100$ °C and $TC_{\rho v} = 37\ 10^{-4}$ °C^{-1} at $T > T_g$.

$TC_{\rho v}$ decreases with increasing condensation temperature during thermal initiation of the secondary polymerization reactions on the substrate. $TC_{\rho v} = -9 \cdot 10^{-4}$ °C^{-1} at $T < T_g = 97$ °C and $TC_{\rho v} = -26 \cdot 10^{-4}$ °C^{-1} at $T > T_c$ at a condensation temperature of 220-240 °C. It can also be noted that the temperature coefficients

differ slightly at temperatures lower than T_c and at higher temperatures in the films obtained under the best conditions.

The decrease in the absolute value of $TC_{\rho v}$ is associated with a low concentration of free radicals in the films, as well as with increase of the PTFE film molecular weight confirmed by EPR and IR spectroscopy. It can be assumed that the stability of the specific volume resistance of PTFE films increases after their heat treatment. As follows from the table, the films obtained in the best mode (J = 0.2-0.2 mA/cm^2; E = 150-200 eV) and annealed in vacuum (10^{-3} Pa) at the temperature of 250-350 °C for 1.5-2.5 hours $TC_{\rho v}$ is smaller than in unannealed samples and $TC_{\rho v} = - 6 \cdot 10^{-4}$ °C^{-1} at $T < T_g$ = 103 °C and $TC_{\rho v} = - 27 \cdot 10^{-4}$ °C^{-1} at $T > T_g$. In the samples obtained in other modes, $TC_{\rho v}$ (in absolute value) also decreases after the heat treatment. This is explained by decrease of the free radicals concentration in the process of the films heat treatment due to recombination of radicals. The concentration of the free radicals is reduced by two orders of magnitude, as shown by studies using the EPR method [69]

6.9. Electric strength of thin PTFE films

During the operation of thin polymer films, even small operating voltages create electric fields in the volume of the film having the close to critical intensity of 10^5-10^6 V/m. In this regard, the study of the breakdown phenomena

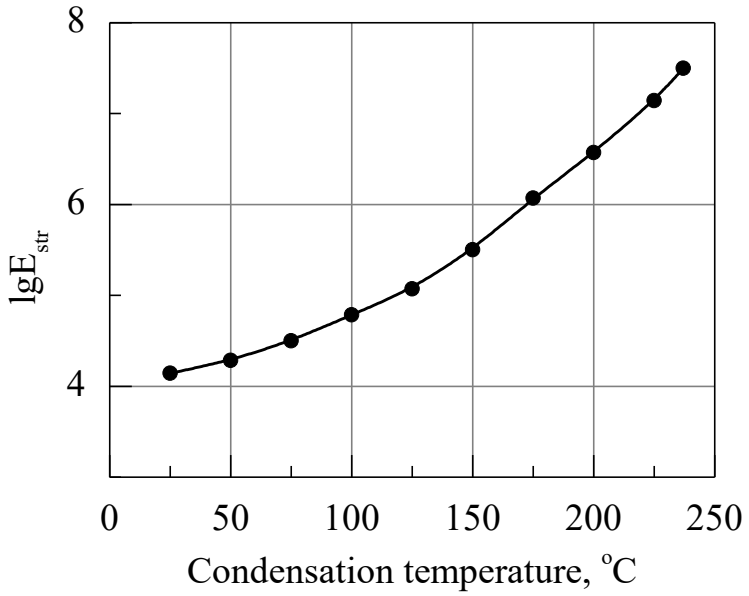

Fig. 6.25. The dependence of the electrical strength of PTFE films on the condensation temperature.

in thin polymer films is not only of theoretical interest, but is also of great practical importance.

The data on the electric strength of polymer films with a thickness of about 1 μm or less are not reliable enough, since defects in the films have a strong influence on the results. It is extremely important for practical use of the polymer films to know the nature and number of weak points, that is, areas with sharply reduced values of the electrical strength. One of the special cases of inhomogeneous dielectrics is a dielectric containing gas inclusions. The presence of the inclusions (pores, cracks) reduces the dielectric strength of the polymer film as a result of field distortion inside the sample, and as a result of the sharply reduced strength of the gas inclusions themselves.

Destruction of a polymer film can occur under the action of discharges developed in pores at the boundary between the polymer and the electrode, or near the electrode. Pores and cracks can appear as a result of the technology violation, as well as a result of poor surface preparation before deposition of the coating.

We investigated the electrical strength of PTFE films obtained with different initiation methods (thermal, electronic) and in various modes. Research results

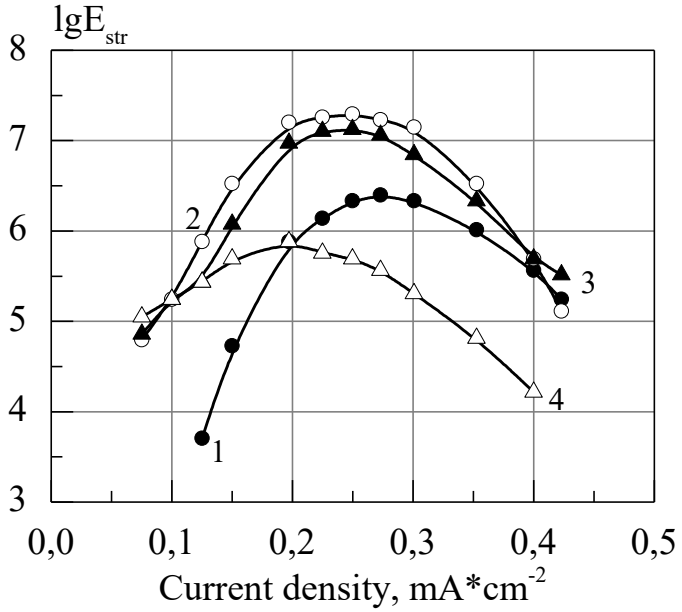

Fig. 6.26. The dependence of the electrical strength of PTFE films on the current density of electrons at different electron energies: 1 – 100 eV; 2 – 400 eV; 3 – 400 eV, annealed film; 4 – 700 eV.

are presented in Fig. 6.25 and 6.26. It follows from the graphs that during the

thermal initiation of polymerization, PTFE films formed at T_c = 220-240 °C have the greatest electrical strength $E_{br} = 5 \cdot 10^7$ V/m. This is due to the highest molecular weight of the films obtained under these conditions, as well as due to the low porosity.

A study was made of the dependence of the electrical strength of PTFE films obtained by the method of electronic initiation of the secondary polymerization on the current density of electrons bombarding the substrate and their energy. The results are shown in Fig. 6.26. Films deposited by using the best mode (J = 0.25 mA/cm^2, E = 400 eV) had the highest electrical strength. In this mode, as indicated above, the films were obtained with the highest molecular weight, as well as with the lowest number of pores per unit surface area. In other modes (J < 0.15 mA/cm^2, J > 0.35 mA/cm^2; E < 100 eV, E > 600 eV), the dielectric strength of the films decreased and the breakdown strength was $E_{br} \approx 10^4$-10^5 V/m. When assessing the effect of the molecular weight on the dielectric strength of a polymer film, it is also necessary to take into account the possibility of structural changes in the samples with the change of the molecular weight. With decrease of the thickness, the electrical strength of PTFE films decreases, which is associated with increase in the number of pores. After the heat treatment of the films in vacuum (10^{-3} Pa) at the temperature of 250-350 °C for 1.5-2.5 hours, the electric strength increases slightly in the films obtained under the best conditions. This is probably caused by the formation of voids in the places of evaporation of the low molecular weight fractions.

6.10. Stability of dielectric characteristics of PTFE films

Polymer films are characterized by change in the structure and dielectric properties with time. The aging processes of thin polymer films are largely associated with the presence of free radicals, carbonyl and hydroxyl groups, bound oxygen and absorbed water.

Studies have been conducted on how the dielectric characteristics, such as ε', tanδ in PTFE films change with time when stored either in vacuum, or in air, or in a humid chamber.

It should be noted that the stability of the dielectric properties (aging) of the samples does not depend on the electrodes material (Pb, Ag, Al, Zn, Cu). Change in the dielectric properties of the films is mostly associated with diffusion of oxygen molecules into the film through the electrodes.

6.10.1. Stability of the dielectric constant ε' and the dielectric loss tangent of PTFE films

Samples of PTFE were placed in a desiccator, in which 98% moisture was created, and were kept there for 60 days at 40 °C. Fig. 6.27 and 6.28 show the changes of the dielectric characteristics (ε' and tanδ) with time of the PTFE films obtained under different process conditions. It follows from the graphs in Fig. 6.27 and 6.28 that the greatest change in the dielectric constant is observed

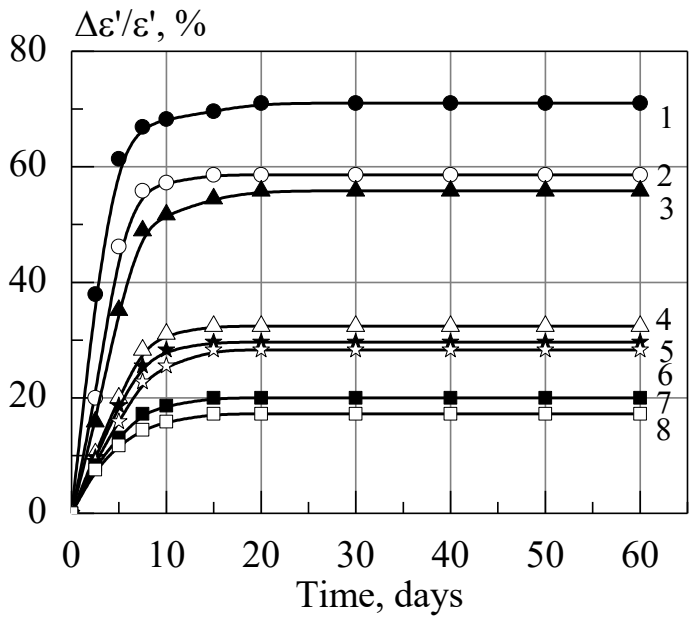

Fig. 6.27. The change of the dielectric constant of PTFE films obtained at different deposition regimes: 1 – T_c = 25 °C; 2 – 700 eV; 0.1 mA/cm^2; 3 – 700 eV, 0.1 mA/cm^2; 4 – 700 eV, 0.3 mA/cm^2, annealed film; 5 – 700 eV, 0.2 mA/cm^2; 6 – 700 eV, 0.2 mA/cm^2, annealed film; 7 – T_c = 240 °C; annealed film; 8 – industrial film in the humid chamber.

in films obtained at the electron current densities (J < 0.15 mA/cm^2; J > 0.35 mA/cm^2) and their energies of the order of (E < 100 eV, E > 600 eV). A significant increase of ε' (up to 60%) was found in the films deposited on the substrate at T_c from room temperature to 100 °C. The value of ε' stabilizes after 10-15 days and does not change over the entire remaining measurement time (up to 60 days). It should be noted that after 6 hours of vacuuming with heating to 100-120 °C, the dielectric constant of the films became 10-20% higher than the initial value (ε' = 2.1). It is possible that water vapor absorbed by the film and free radicals contribute to the change of this dielectric characteristic. There is

approximately the same change (up to 50-55%) in the films obtained at the electron current density $J > 0.3$ mA/cm^2 and energy $E > 500$ eV. However, this value comes back to its initial value after removing samples from the desiccator and evacuating the sample with heating to 100-150 °C for 5-6 hours. This indicates that the main contribution to the change in the dielectric constant is made by water vapor absorbed by the film.

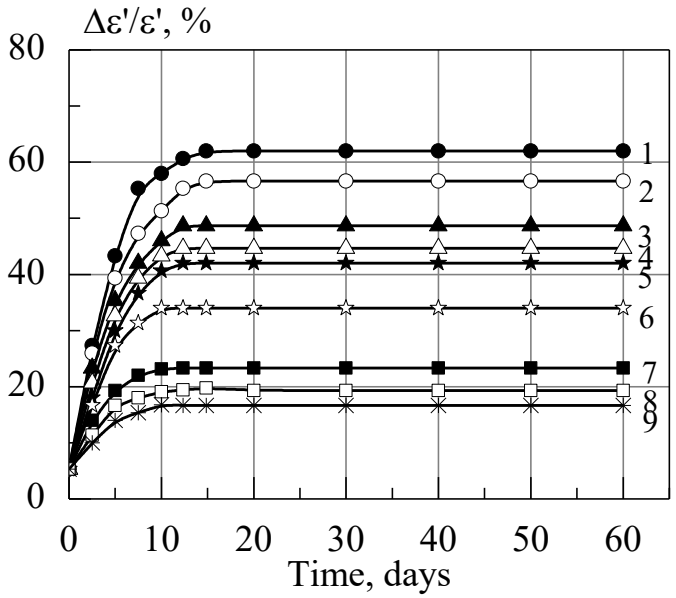

Fig. 6.28. Changes in the dielectric constant of PTFE films obtained at different deposition modes: 1 – 100 eV, 0.4 mA/cm^2; 2 – 400 eV, 0.1 mA/cm^2; 3 – 100 eV, 0.2 mA/cm^2; 4 – 100 eV, 0.4 mA/cm^2, annealed film; 5 – 400 eV, 0.3 mA/cm^{2}6 – 400 eV, 0.3 mA/cm^2, annealed film; 7 – 100 eV, 0.3 mA/cm^2, annealed film; 8 – 400 eV, 0.2 mA/cm^2; 9 – 400 eV, 0.2 mA/cm^2, annealed film in a humid chamber.

The smaller changes in the dielectric constant (up to 20%) in comparison with the above under conditions of high humidity are found in the PTFE films obtained at the electron current densities of the order of 0.2-0.25 mA/cm^2 and energy 350-450 eV, as well as in the films with the initiation of the secondary polymerization by heating to 220-240 °C. Moreover, the change in the dielectric constant is reversible. This is consistent with the fact that the concentration of free radicals, double bonds, which are the sorption centers of water vapor, is lower than that in the films obtained in other modes. Similar studies were carried out with samples in air. Changes of the dielectric constant are of the same nature (Fig. 6.29). The only difference is the amount by which the dielectric constant changes (up to 10%).

Similarly, the tanδ also varies. In air, this parameter practically does not change in the films deposited in the best mode, and it increases up to one order

of magnitude comparing to the same films in the humid chamber. As follows from the graphs in Fig. 6.30 and 6.31, when comparing the concentrations of free radicals in the films studied by the EPR method, it was found that the increase of tanδ and ε' is associated not so much with the concentration of free radicals, but with the presence of polar oxygen-containing groups serving as the water vapor sorption centers.

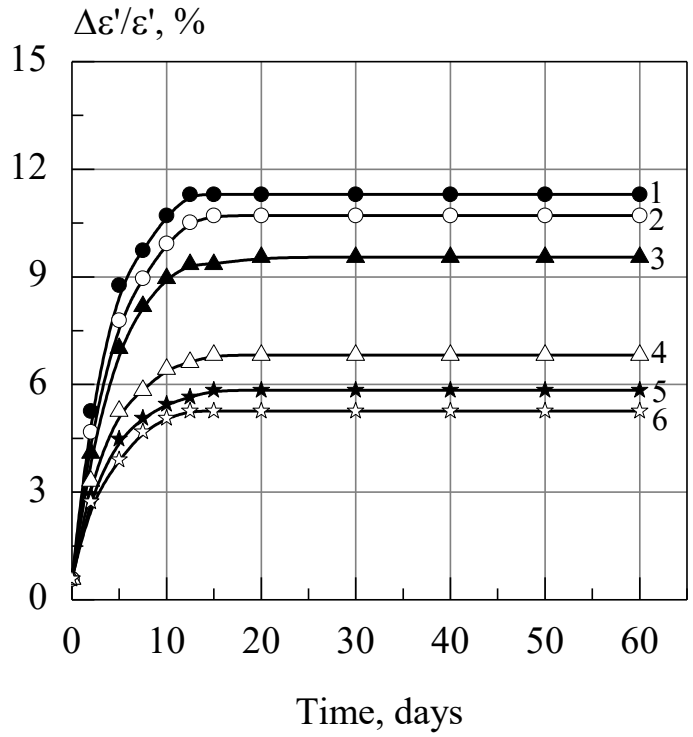

Fig. 6.29. The change in the dielectric constant of PTFE films obtained at different deposition regimes: 1 – T_c = 25 ° C; 2 – 700 eV; 0.1 mA/cm^2; 3 – 400 eV, 0.1 mA/cm^2; 4 – 100 eV, 0.3 mA/cm^2, annealed film; 5 – T_c = 240 °C; 6 – 400 eV, 0.2 mA/cm^2, annealed film in air.

To increase the stability of the dielectric characteristics, the films were heat treated. They were annealed in vacuum at the temperature of 250-350 °C for 1.5-2.5 hours. Under these conditions, the recombination of free radicals and the detachment of oxygen-containing polar groups occur. The studies have shown that the dielectric constant and the dielectric loss tangent of the films obtained at the electron current density of 0.2-0.25 mA/cm^2 and energy of 400-500 eV, and annealed in vacuum, do not change after 60 days storage in air. When the samples were held in the humid chamber, ε' increased by 20% and tanδ by 40%. These changes were reversible. The changes of ε' and tanδ in the samples obtained in other modes and annealed are somewhat larger and constitute 30% and 60%, respectively. When the samples were heated in air, there was a strong increase of ε' and tanδ associated with the processes of the oxidative destruction.

When the samples were kept in vacuum at the pressure of no more than 100 Pa, ε' and tanδ of all samples remained almost unchanged for 60 days.

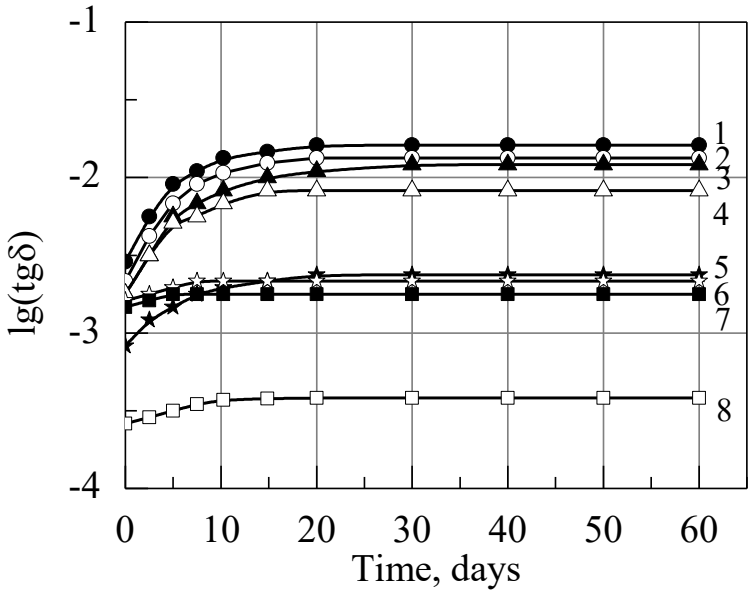

Fig. 6.30. Change of the of dielectric loss tangent of PTFE films obtained at different deposition modes: 1 – 700 eV, 0.1 mA/cm^2; 2 – 700 eV, 0.3 mA/cm^2; 3 – 400 eV, 0.1 mA/cm^2; 4 – 400 eV, 0.4 mA/cm^2; 5 – 400 eV, 0.3 mA/cm^2; annealed film; 6 – 400 eV, 0.2 mA/cm2; 7 – 700 eV, mA/cm^2, annealed film; 8 – 400 eV, 0.2 mA/cm^2; annealed film in the humid chamber.

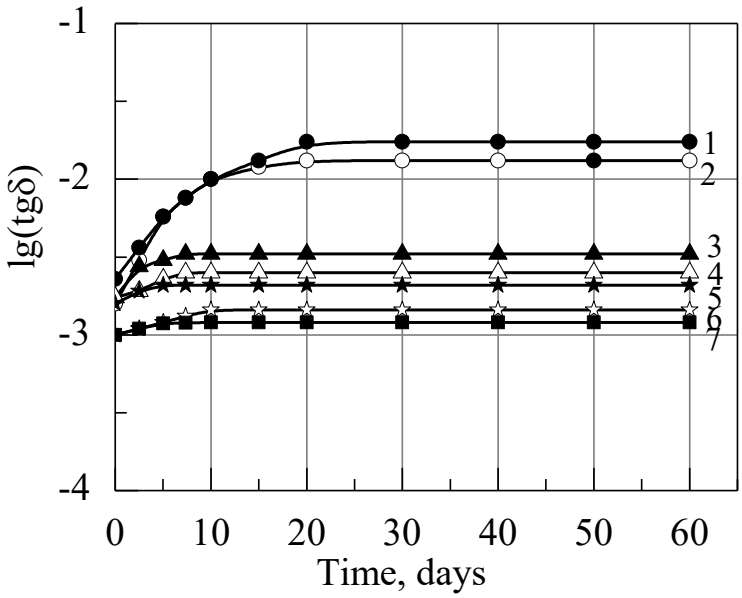

Fig. 6.31. Changes of the dielectric loss tangent of PTFE films obtained at different deposition modes: 1 – 100 eV, 0.1 mA/cm^2; 2 – 100 eV, 0.4 mA/cm^2; 4 – T_c = 240 °C; 5 – 100 eV, 0.3 mA/cm^2 annealed film; 6 – 100 eV, 0.2 mA/cm^2; 7 – T_c = 240 °C, annealed film; 3 – industrial film in a humid chamber.

Thus, we can conclude that instability of the dielectric parameters (ε' and

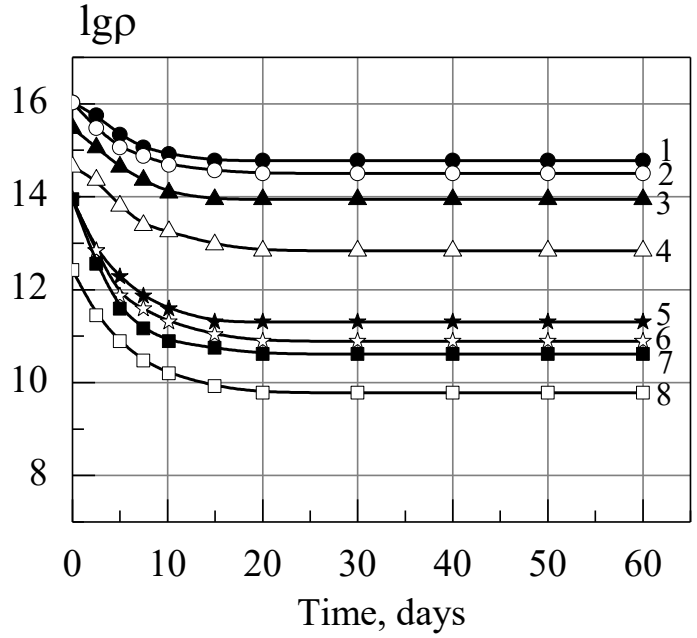

Fig. 6.32. Change of specific resistance of PTFE films obtained at different deposition modes: 1 – 200 eV, 0.2 mA/cm^2, annealed film; 2 – 200 eV, 0.3 mA/cm^2, annealed film; 3 – 200 eV, 0.2 mA/cm^2, 4 – 400 eV, 0.2 mA/cm^2, annealed film; 5 – 200 eV, 0.4 mA/cm^2; 6 – 400 eV, 0.3 mA/cm^2; 7 – 400 eV, 0.1 mA/cm^2; 8 – 200 eV, 0.1 mA/cm^2, in a humid chamber.

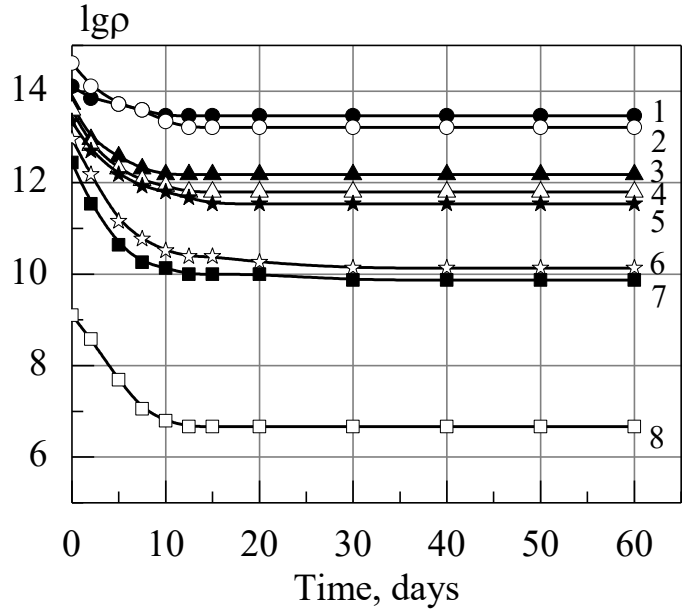

Fig. 6.33. Change in resistivity of PTFE films obtained at different deposition modes: 1 – industrial film in a humid chamber; 2 – 50 eV, 0.3 mA/cm^2, annealed film; 3 – T_c = 240 °C, annealed film; 4 – 50 eV, 0.2 mA/cm^2; 6 – T_c = 240 °C annealed film; 5 – 50 eV, 0.4 mA/cm^2; 6 – T_c = 240 °C; 7 – 50 eV, 0.2 mA/cm^2; 8 – T_c = 25 °C.

tanδ) is irreversible, if it is associated with the oxidation of films and reversible, if it is associated with sorption of water vapor by the films.

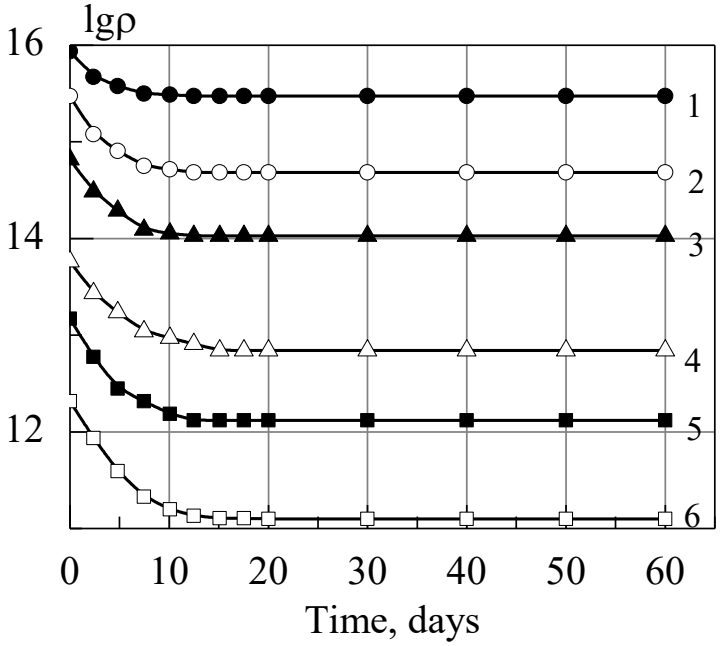

Fig. 6.34. Change in resistivity of PTFE films obtained at different deposition modes: 1 – 200 eV, 0.2 mA/cm^2, annealed; 2 – 200 eV, 0.2 mA/cm^2; 3 – 400 eV, 0.2 mA/cm^2, annealed film; 4 – 200 eV, 0.4 mA/cm^2; 5 – 400 eV, 0.1 mA/cm^2; 6 – 200 eV, 0.1 mA/cm^2, in air.

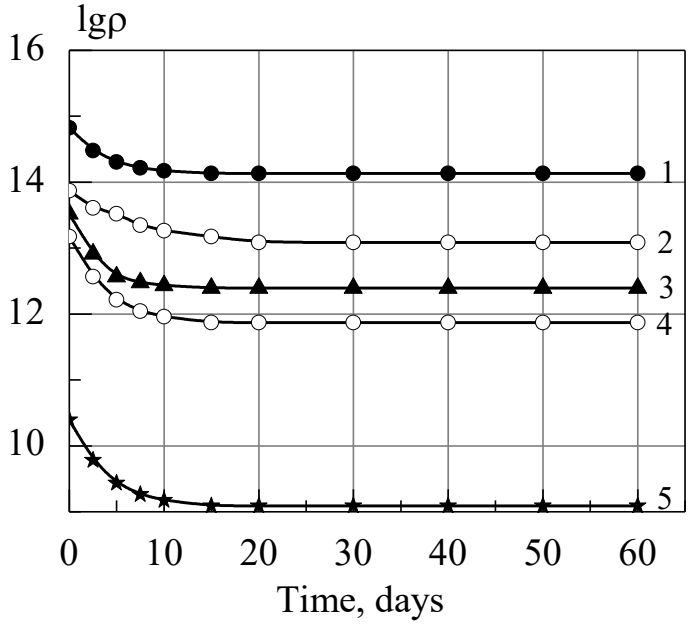

Fig. 6.35. Change in resistivity of PTFE films obtained at different deposition modes: 1 – 50 eV, 0.3 mA/cm^2, annealed film; 2 – T_c = 240 °C, annealed film; 3 – 50 eV, 0.4 mA/cm^2; 4 – 50 eV, 0.2 mA/cm^2; 5 – T_c = 25 °C, in air.

The moisture absorption and stability of the dielectric characteristics depend on the film production modes. Films obtained at the current density 0.2 mA/cm^2 and energy of 400-500 eV, subsequently annealed in vacuum at the pressure of 10^{-3} Pa and the temperature of 250-350 °C for 1.5-2.5 hours, have the most

stable dielectric properties. It was established that the determining factor of the moisture absorption was the structure and chemical composition of the films. The presence of terminal polar groups and polar groups in the main chain led to increasing of the moisture absorption and to instability of the dielectric properties of the PTFE films.

6.10.2. Stability of the specific volume resistance (ρ_v) of PTFE films

In order to determine the possibility of using films in various conditions, studies have been carried out on the stability of the specific volume resistance (ρ_v) of PTFE films in a humid chamber (humidity 98%), in vacuum (pressure 100 Pa) and in air for 60 days.

As studies have shown, the ρ_v increased in all samples, both in air and in the humid chamber (Fig. 6.32-6.35). The smallest change of ρ_v up to one order of magnitude after 10 days was observed in the films obtained in the optimal mode (J = 0.2 mA/cm^2; E = 200 eV and T_c = 240 °C) with exposure to air, and annealed in vacuum (pressure 10^{-5} Pa) at a temperature of 250-350 °C for 1.5-2.5 hours. The resistance did not change with time (after 10 days of exposure). The decrease in the resistivity by one order of magnitude was noted in the films obtained in the same mode, but not annealed in vacuum. For the films obtained in the modes other than the above, the decrease in resistivity was up to two orders of magnitude in 6-8 days of exposure to air.

The decrease of the specific volume resistance in the humid chamber in the films obtained by using the optimal mode reached 2-3 orders of magnitude (for annealed ones, up to two), and the decrease in all other samples was three orders of magnitude.

In order to determine the resilience of the specific resistance, the samples were kept in vacuum after their evacuation from air and from the humid chamber where they were stored for 60 days, and heated to 100-150 °C for 4-6 hours at a pressure of 10^{-3} Pa. During the measurements, almost complete recovery was found of the value of the samples obtained in the best mode and then annealed.

In unannealed films obtained in the optimal mode, the specific volume resistance differed from the initial value one order of magnitude. In the films obtained in other modes (T_c < 160 °C, J <0.15 mA/cm^2; J > 0.4 mA/cm^2 and E < 100 eV and E > 400 eV), the specific volume resistance differed from the

original value by 2 or 3 orders of magnitude, respectively, in samples aged in air and in the humid chamber.

It can be concluded that the samples obtained under the optimal conditions and annealed in vacuum, undergo physical sorption of oxygen and water vapor removed from the films when they were heated in vacuum. In the samples obtained under other conditions, the chemical sorption takes place along with the physical sorption leading to further destruction by the reactions [69] and irreversible changes of the dielectric characteristics. In the samples kept in vacuum at the pressure of not more than 100 Pa for 60 days, the maximum decrease of the specific resistance to one order of magnitude was found in the films obtained using the non-optimal conditions. In the films of PTFE obtained under the best conditions, no changes were found after keeping them in vacuum for 60 days.

6.11. Dielectric and electret properties of PTFE and PCTFE films obtained by the gas discharge deposition

Such dielectric characteristics, as the dielectric constant, the dielectric loss tangent, the specific volume resistance, and the breakdown voltage were investigated. We studied the dependence of these parameters on power, high-frequency discharge under identical other conditions (pressure, electron gun power, crucible-substrate distance, surface preparation method, substrate temperature, growth rate).

The 10 μm thick films were grown. The dependence of the dielectric constant on the power of the RF discharge is shown in Fig. 6.36. The change in the values of the dielectric constant increases monotonically with increasing the RF power. This dependence can be apparently explained by the change in the degree of the crystallinity, which, in turn, affects the conductivity.

The dependence of tanδ on the power of the RF discharge is shown in Fig. 6.37. In the range of 2-4 W, the minimum values of the dielectric loss tangent are observed for both PCTFE and PTFE films. With increasing the power above 8 W, a sharp increase in this parameter is observed. In Section 4, while describing the IR spectra, it was noted that the processing in the RF discharge of both PTFE and PCTFE films increases the degree of crystallinity and the saturation of double bonds. This leads to increase in crosslinks in the polymer and to degradation of the dielectric characteristics. The analysis of the given

dependences confirms the fact that the optimal power of the glow discharge is in the range of 2-4 W.

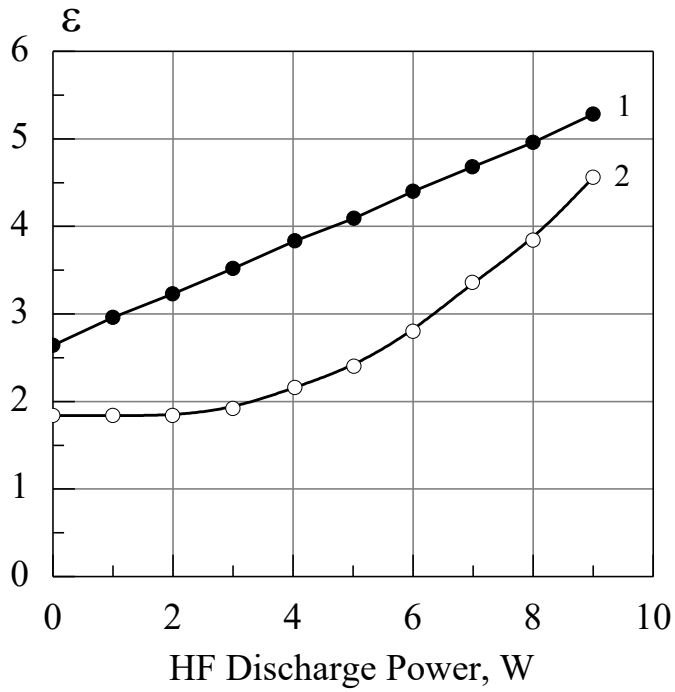

Fig. 6.36. Dependence of dielectric permeability of PTFE and PCTFE coatings on high-frequency discharge power

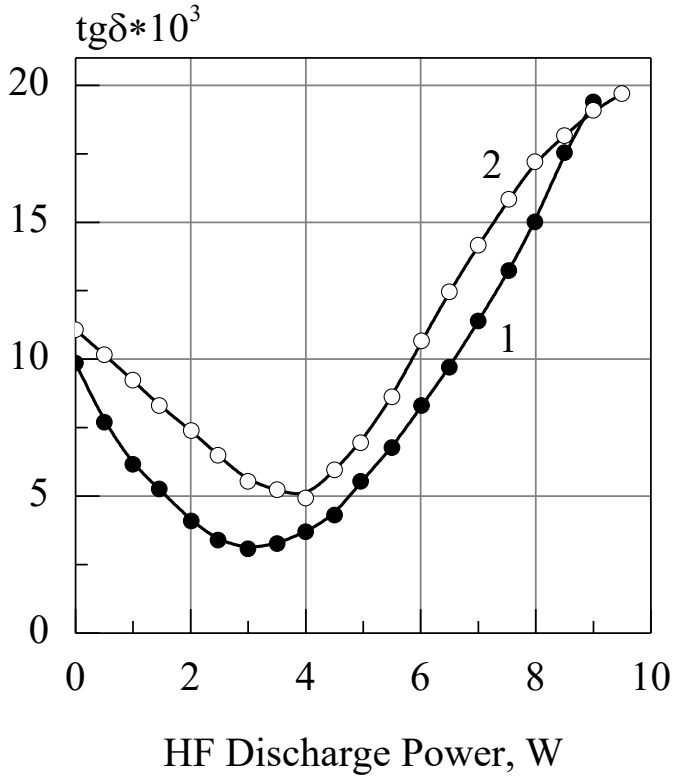

Fig. 6.37. Dependence of the tangent of the dielectric loss angle of PCTFE (1); PTFE (2) on the power of the glowing high-frequency discharge.

The electret properties of the fluoropolymers are the specific characteristics that can be used both as an independent parameter, taken into account in the

special-purpose devices (for example, in electrostatic microphones), and as a complementing phenomenon to the overall picture of the gas-discharge polymerization process.

PCTFE films obtained by the gas discharge deposition showed very low susceptibility to induced surface charge. The electret potential in these coatings did not exceed 55-70 V immediately after charging. After one day of storage, the electret potential was halved, and decreased to zero in a humid atmosphere. This behavior can be explained by the specific structure and changes in the surface layer caused by the electron-ion bombardment. It is also possible that charging of PCTFE should not be carried out in a corona discharge.

In contrast to PCTFE, PTFE films were charged in a corona to 120-130 V (Fig. 6.38). With increasing the RF power, the electret potential increases and the maximum value of 130 V (P = 10 W) is observed. However, despite the

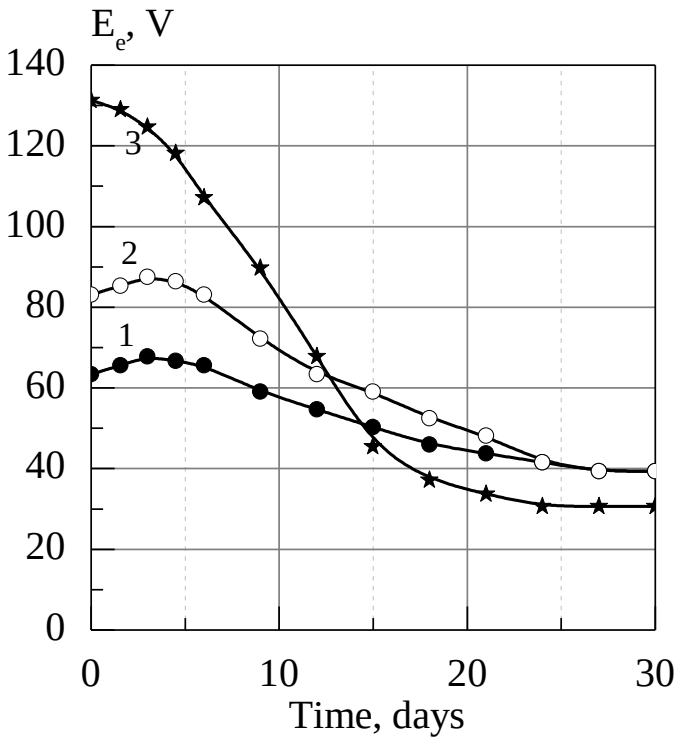

Fig. 6.38. Dependence of the electret potential difference on the exposure time at different power of the RF discharge: 1 – 2 W; 2 – 4 W; 3 – 10 W.

higher initial values, the films obtained at the power of 10 W lose their charge faster, and after stabilization it is lower than that of the samples obtained under more “mild” conditions. This is explained by decrease in the number of the electron vacancies on the film surface and by a rapid charge “draining” due to internal relaxation and neutralization by atmospheric charge carriers.

CHAPTER 7
PROTECTIVE PROPERTIES OF POLYMER FILMS OBTAINED BY DEPOSITION IN VACUUM

7.1. Influence of surface preparation methods and deposition modes on porosity and adhesion of the coatings

Since chemical properties of high-molecular compounds are mainly determined by chemical nature of the monomer unit, we studied vacuum coatings using the secondary ionization mass spectrometry (SIMS) method. Obtained results showed that chemical composition of the monomer unit of PCTFE and PTFE vacuum coatings were identical with composition of the initial polymers.

Porosity and adhesion are main factors affecting protective properties of PCTFE and PTFE coatings. An important characteristic affecting porosity and adhesion is purity of the substrate surface.

The following methods were used to prepare the substrate surface before deposition of films: 1) washing with ethyl alcohol, 2) chemical treatment [69], 3) thermal heating, 4) processing in a glow discharge.

Dependence of the polymer films porosity on the method of the surface preparation is presented in Table 7.1.

Table 7.1

Influence of the surface treatment method of the copper substrate on porosity of PCTFE and PTFE coatings (surface treatment class is Δ12, coating thickness is 2 μm)

Processing method	Ethyl wipe	Chemical treatment	Thermal heating up to 500˚C (5 min)	HF glow discharge (16 W, 2 min)
Porosity (pores/cm^2)				
PCTFE	20	9	1-3	1-3
PTFE	23	11	1-2	1-2

It was established that the smallest porosity was obtained after complex cleaning: first washing with ethyl alcohol, then heating to 500 °C in vacuum and

processing in a glow discharge with a capacity of 14-16 W. This is due to the fact that ethyl alcohol degreases the surface while thermal heating in vacuum helps to remove adsorbed gases and treatment in a glow discharge activates the surface helping to improve the adhesion of the coating and to form a continuous coating. However, such a set of cleaning methods is contrary to the goal of creating a gas-discharge polymerization of coatings method. Coatings should be formed without breaking the vacuum in the process lines for chemical cleaning or washing the samples with alcohol at low (preferably room) temperature. The time required to cool the samples after warming up extends the technological cycle duration. Therefore, it was decided to use only samples processing in a glow discharge. The main parameters of the discharge are power and processing time. Dependence of the coatings porosity on the power is given in Table 7.2.

The dependence of the number of pores on the power of the RF discharge shows a steady tendency to decreasing of the porosity with the increasing power. This phenomenon can be explained by increase in the degree of substrate surface activation, as well as by increase in the number of the crystal structure defects which then become centers of the polymer film nucleation and adhesive bonds. As a result, these centers improve continuity of the coatings.

Table 7.2.

Dependence of PCTFE and PTFE coatings porosity on the processing time in a glow discharge (treatment class of the copper surface is Δ12, coating thickness is 5 μm, discharge power is 16 W)

Processing time, s	20	40	60	80	100	120	140	160	180	200	220
Porosity (pores/cm^2)											
PCTFE	23	19	13	9	6	3	1-2	-	-	-	-
PTFE	30	26	15	11	7	5	1-3	1-2	-	-	-

Experimental data show that low RF discharge powers (ranging from 1 to 10 W) do not have a significant effect on porosity regardless of the processing time. For this reason we used more powerful processing modes, in particular P = 16 W. The dependence of porosity on the processing time is shown in Table 7.3

Table 7.3.

Dependence of the PCTFE and PTFE coatings porosity on the power of a glow discharge (processing class of the copper surface is Δ12, coating thickness is 5 μm, processing time 2 min)

RF discharge power (W)	2	4	6	8	10	12	14	16
Porosity (pores/cm^2)								
PCTFE	30	17	11	5	3-5	1-3	1-3	-
PTFE	43	29	16	9	5-7	3-5	1-3	-

Data of the Table 7.3 show that increasing of the electron-ion processing duration improves continuity of the coating. However, it should be remembered that irreversible changes occur on the surface of the substrate during prolonged irradiation by a glow discharge. Visually, it looks like the darkening of the coating color on copper, steel and aluminum substrates. The glassceramic surface after processing in the RF discharge with power of 14-16 W for 5-10 min acquires a light yellow tint that can be removed only by emery paper. Such a reaction suggests existing of the oxidative process due to presence of the residual oxygen in the chamber. During the experiment, it was found that the sufficiently clean surface of the substrates can be achieved by processing in a glow discharge with a power of 14-16 W for 2-3 min.

Adhesion of the coatings was determined in three ways: 1) bending until the substrate fracture, 2) thermal shock (periodic immersion in liquid nitrogen and boiling water, 3) using a lattice notch. Such a program of adhesion tests was due to the fact that adhesion to fluoroplastic materials, and in particular to PTFE, cannot be tested by the method of normal tearing-off.

The adhesion of the films was significantly affected by the conditions of surface preparation and deposition regimes. Films obtained in optimal deposition regimes had the best adhesion to the substrate. The tests have shown that the films obtained under these conditions on steel, copper, aluminum, or glass, had good adhesion. The films did not peel off after boiling in distilled water for half an hour. They withstand repeated “heating - cooling” cycles from -196 ° C to +98 ° C and did not peel off from the flexible substrate after numerous bending by ± 180° until the substrate fracture.

7.2. Electrochemical behavior of PTFE and PTFE protective coatings

In order to evaluate protective properties of coatings, the author of [69] carried out electrochemical studies. Effect of the coatings thickness and the kind of the substrate material on the corrosion resistance of the coatings has been studied.

The studies were carried out in a 3% solution of sodium chloride on samples of copper, aluminum and steel, coated with the polymer film with a thickness of 0.2; 0.5; 1.0 μm; 5 μm. Studies were conducted in the following areas:

– obtaining dependences of changes in the electrode potential on the exposure time in 3% NaCl;

– obtaining the dependence of the films conductivity on their thickness and substrate material;

– obtaining the polarization curves on samples with different coating thickness and determination of the corrosion rate.

The dependence of the electrode potential on the exposure time in a 3% solution of sodium chloride was obtained using a potentiostat. The values of the electrode potentials are given in Tables 7.4 - 7.6 for coating thicknesses of 0.4-4.5 μm. On samples with coatings of more than 7 μm thickness, the potentials cannot be measured indicating absence of pores in these coatings. Electrochemical studies were conducted to find the effect of the coatings thickness (up to 5 μm) on their protective properties.

From the data given in these tables, it is clear that displacement of electrode potentials relative to potentials of uncoated metal samples is observed on samples with the coatings. Stability of the samples electrode potentials with coatings indicates their significantly lower electrochemical activity compared to unprotected metals.

Comparison of the stationary potentials shows that the degrading of electrode potentials decreases with time with increasing the coating thickness. This was observed for different substrate materials.

Polarization curves were obtained using the potentiostat in a potentiodynamic mode with automatic recording of the corrosion current. A silver chloride electrode was used as a reference electrode.

To obtain comparative characteristics, initially clean metal surfaces were polarized. In order to determine the change in the protective properties of

coatings over time, the samples were kept for six days in a 3% sodium chloride solution before measuring the polarization curves.

Table 7.4.

Potential kinetics in 3% NaCl solution of aluminum samples with different thickness of PTFE coating

Coating thickness, μm	Potential, mV		Time of holding in solution				
	Days		Hours		Minutes		
	1	6	1	20	0	10	20
Without coating	810	770	875	890	800	860	870
0.5	850	800	760	780	730	755	765
1	700	700	600	720	480	500	560
1.8	720	700	666	725	560	600	620
5	720	720	720	740	660	630	700

Table 7.5.

Potential kinetics on steel samples with different thickness of PTFE coating in 3% NaCl solution

Coating thickness μm	Potential, mV		Time of holding in solution				
	Days		Hours		Minutes		
	1	6	1	20	0	10	20
Without coating	470	490	440	440	400	400	430
0.1	470	470	470	490	400	430	470
0.5	440	450	410	420	380	395	400
1	430	430	430	430	325	380	400
2	420	430	410	420	330	350	400
4,5	420	420	400	420	365	380	385

The results are shown in Fig. 7.1-7.6. It can be seen from the above data that

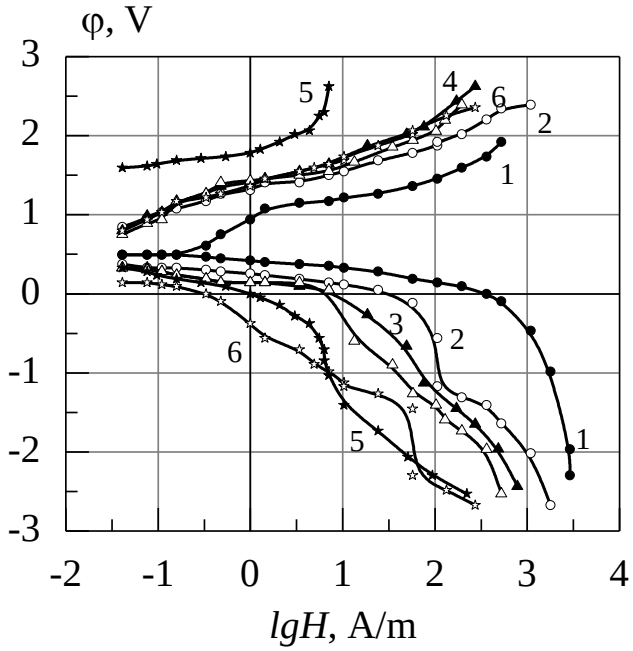

Fig. 7.1. Polarization curves in 3% NaCl solution of mild steel samples and PTFE coatings without prior exposure to corrosion: 1 – uncoated sample; Samples with a coating thickness: 2 – 0.1 μm; 3 – 0.5 μm; 4 –1.0 μm; 5 – 2.0 μm; 6 – 4.5 μm.

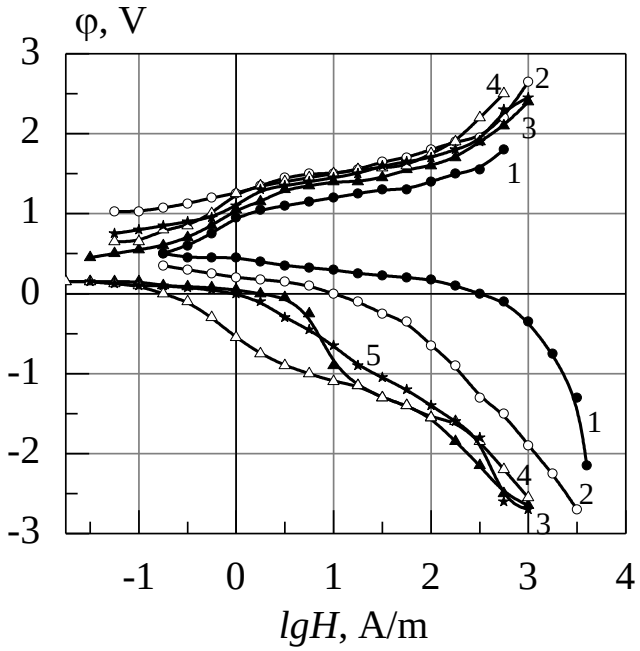

Fig. 7.2 Polarization curves in 3% NaCl solution of mild steel samples coated with PTFE of various thickness after preliminary exposure in solution for 6 days. 1 – sample without coating; Samples with a coating thickness: 2 – 0.1 μm; 3 – 0.2 μm; 4 – 1.0 μm; 5 – 2.0 μm.

even PTFE coatings with a thickness of up to 1 μm are slowing down the anodic

corrosion process. As the coating thickness increases, the inhibition of the

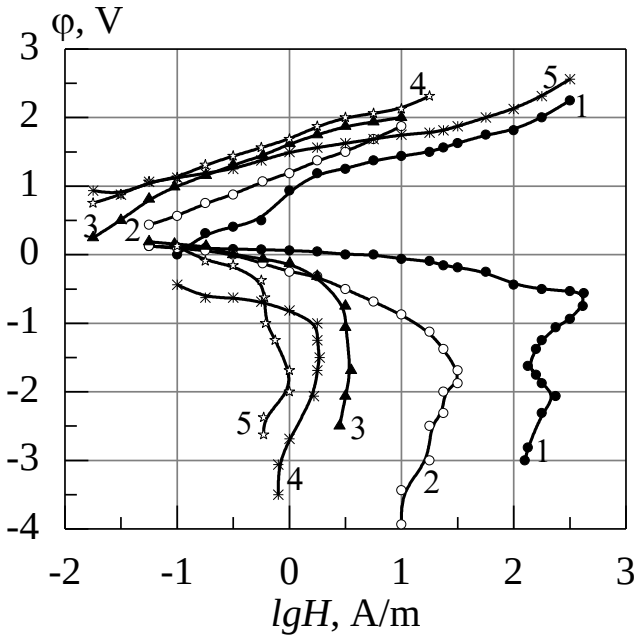

Fig. 7.3. Polarization curves in a 3% solution on copper samples coated with PTFE without preliminary exposure for corrosion. 1– uncoated sample; Samples with a coating thickness: 2 – 0.1 μm 3 – 0.2 μm; 4 – 1.0 μm; 5 – 2.0 μm.

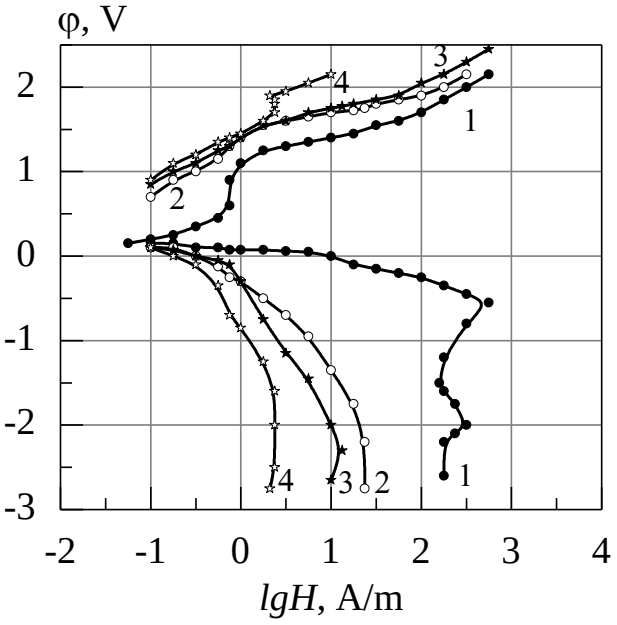

Fig. 7.4. Polarization curves in 3% NaCl solution on samples of copper coated with PTFE measured after preliminary aging for corrosion for 6 days. 1 – uncoated sample; Samples with a coating thickness of 2 – 0.1 μm; 3 – 0.2 μm; 4 – 1.0 μm

anodic process increases.

When a certain positive potential is reached, the coated sample is passivated

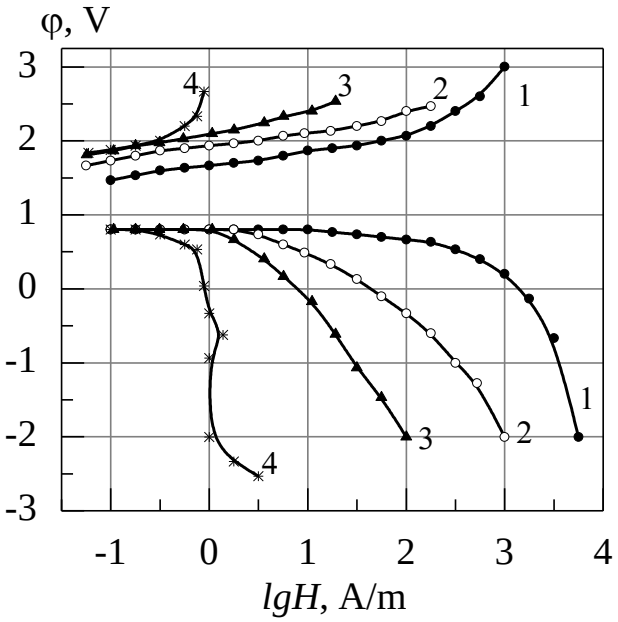

Fig. 7.5. Polarization curves in 3% NaCl solution on aluminum samples coated with PTFE without preliminary aging for corrosion. 1 – uncoated sample; Samples with a coating thickness: 2 – 0.5 μm; 3 – 1.0 μm; 4 – 2.0 μm

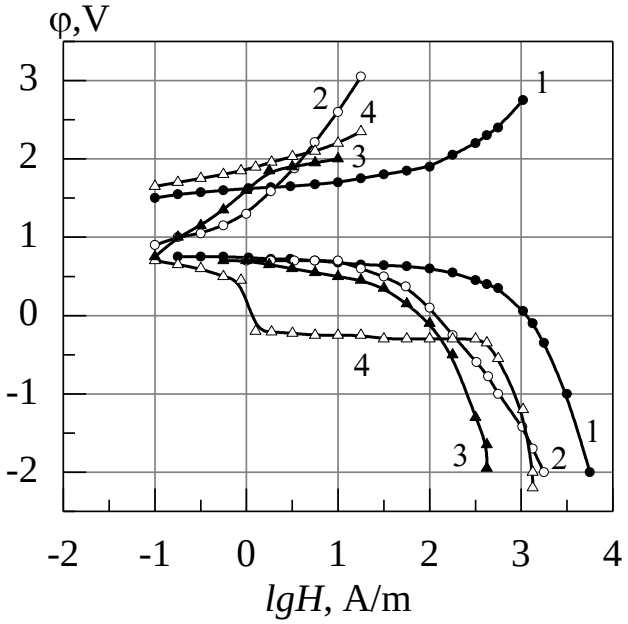

Fig. 7.6. Polarization curves in 3% NaCl solution on aluminum samples coated with PTFE taken after preliminary exposure in solution for 6 days. 1 – uncoated sample; Samples with a coating thickness: 2 – 0.5 μm; 3 – 1.0 μm; 4 – 2.0 μm.

despite the presence of Cl^- active depassivators, i.e. the anodic passivity occurs.

On samples of unprotected metals, an increase of the anode current density with a potential shift is observed. Further anodic loading of the coated electrodes

with a thickness of more than 1 μm occurs without a noticeable increase in the current density.

Moreover, with increase of the coating thickness, a shift towards lower current densities is observed. Consequently, the process of the metal transition to the ionic state, easily carried out in this solution on the surface of the uncoated metal, is significantly inhibited by the passivation of the electrode.

With further increase of the anodic polarization degree, the curves of coatings with a thickness of 0.2-0.5 μm are again become flat before a new stage of the anodic process. With increase of the coating thickness of more than 1 μm, no exit from the passive state is observed at the indicated polarization potentials.

The cathode polarization curves indicate the dependence of the depolarization process rate coupled with the process of metal dissolution on the film thickness. With increase in thickness, and, consequently, with decrease in the porosity of the coating, access of the depolarizer (oxygen) to the metal surface is difficult. The thicker the film, the steeper the cathodic polarization curve.

It should be noted that the deposition of PTFE coatings shifts the onset of polarization curves relative to their onset in the case of uncoated samples. The anodic curves are shifted towards positive potentials, and the cathode curves, respectively, toward negative potentials.

Table 7.6

Fe	Curve number	5	1	2	3	4
	Thickness, μm	Pure	0.1	0.5	1.0	2.0
lgDi	“Cold”	-1.7	-2.1	-2.34	-2.4	-3.0
A/m^2	HF	-1.7	-2.3	-3.2	-2.8	-1.8
	Powerful	-1.7	-2.0	-3.35	-4.0	-2.6

The data on the polarization curves were obtained on samples with coatings without preliminary aging for corrosion. Exposure to corrosion reduces the total shift of the polarization curves onset of the potentials. Based on the above, it can be concluded that the corrosion of samples with PTFE coatings is under a mixed control. From Tables 7.6-7.8 and graphs 7.7-7.9 it can be seen that the protective properties of PCTFE substantially depend on the thickness of the coating (and their porosity). As follows from the above data, the coatings with a thickness of 2 μm or more deposited in the optimal mode have the best protective properties.

Table 7.7

Cu	Curve number	5	1	2	3	4
	Thickness, μm	Pure	0.1	0.5	1.0	2.0
lgDi	“Cold”	-2.64	-1.9	-2.64	-3.12	-2.96
A/m^2	HF	-2.64	-2.3	-2.7	-3.2	-2.6
	Powerful	-2.64	-2.86	-2.7	-1.7	-5.0

Table 7.8

Al	Curve number	5	1	2	3	4
	Thickness, μm	Pure	0.1	0.5	1.0	2.0
lgDi	“Cold”	-2.86	-3.56	-4.2	-4.4	-4.52
A/m^2	HF	-2.86	-2.88	-3.15	-3.21	-3.38
	Powerful	-2.86	-2.0	-3.9	-2.5	-1.08

7.3. Accelerated corrosion testing in aggressive environment

Polymer coatings of PCTFE and PTFE deposited in a high-frequency glow discharge were tested in atmosphere with content of 0.1% SO_2, 3% solution of NaCl and in seawater with a salt content of 18 ppm. Tests for bio-corrosion were also carried out to determine the fungicidal properties of the coatings.

Tests on bio-corrosion were carried out in the Czapek-Doks medium with a spore suspension concentration of 12 million/ml. For the preparation of suspensions, cultures of fungi were used aged from 14 to 28 days from the time of subculture. Evaluation of the fungicidal properties of films using a five-point scale showed that PCTFE and PTFE corresponded to a score of 2-3. When examined under a microscope, 30% of the tested samples showed mycelium in the form of branching hyphae, which indicated a possible sporulation. As a result of accelerated corrosion tests, it was found that PTFE and PCTFE coatings formed in the glow discharge in the optimal deposition mode have good protective properties.

Tests on fungicidal properties have shown inertness of PCTFE and PTFE coatings to the reproduction of bacteriological cultures.

CONCLUSION

Peculiarities of thin polymer films and coatings obtained in vacuum are discussed in this book. The following polymers are investigated: polytetrafluoroethylene (PTFE), polychlorotrifluoroethylene (PCTFE) and polyethylene (PE). Among the discussed problems are mechanisms of decomposition, evaporation and condensation of the polymers in a vacuum, as well as their structure and physico-chemical properties. Considered are devices for producing the polymer films. The thermal heating and the electron beam evaporation of the polymers in the residual atmosphere of air and in an inert atmosphere are compared. Methods of the secondary polymerization on a substrate including treatment by UV irradiation and by electron beam are considered in detail.

It is shown that the selection of the evaporation method is determined by the structure of polymer chains and by kinetics of chemical reactions that occur under electron irradiation. The products of polymers decomposition in vacuum under action of the thermal heating and the electron beam irradiation are investigated. The optimal conditions for the decomposition process are determined, ensuring the maximal utilization rate of the initial polymer and transition to the vapor phase of fragments with the highest molecular weight.

It was found that neutral fragments are condensed on the substrate in the case of PE that are cross-linked under the electron irradiation, while a large number of free radicals remain in the films of PTFE and PCTFE. Their concentration slightly varies if they are kept in vacuum and significantly decreases in the atmosphere of air and water vapor.

The temperature dependence of changes in the concentration of free radicals in vacuum and in air has been studied. The studies have led to the conclusion about the radical mechanism of the secondary polymerization on the substrate under the action of electrons.

The features of the films structure formation on the substrate under the action of temperature, UV irradiation, the electron beam, and the RF discharge were determined. For each polymer, optimal parameters of electron irradiation of the substrate were found during film growth, at which the number of double bonds was minimal. The least defective structure was in the films obtained at the condensation temperature T_c = 100–200 °C and the energy of electrons irradiating the substrate 300–600 eV.

The influence of deposition conditions on the dielectric properties of the polymer films has been studied. The stability of the dielectric parameters of the films in the atmosphere of dry and humid air was investigated. It was established that there were two types of instability: irreversible one associated with the oxidation of films, and reversible instability associated with the absorption of water vapor. The presence of terminal polar groups in the main circuit led to increase in moisture absorption and instability of the dielectric characteristics.

The porosity of the coatings and their adhesion to the substrate have been investigated. The best surface preparation turned out to be the plasma treatment by a glow discharge in argon. It was established that high-quality adhesion of coatings with the substrate was obtained due to the formation of donor-acceptor bonds at the metal-oxide-polymer interface.

The electret properties of polymer films and the protective properties of polymer coatings in various aggressive media have been also studied.

REFERENCES

1. D. M. Mattox, *The Foundations of Vacuum Coating Technology* (Elsevier Science, 2013).

2. D. M. Mattox, *Handbook of Physical Vapor Deposition (PVD) Processing* (Elsevier Science, 2010).

3. Goodfellow, *Index of Materials – Polymers*, viewed 14 July 2019, <http://www.goodfellow.com/E/Polymers.html>

4. S. L. Madorsky, *Thermal Degradation of Organic Polymers* (Interscience, New York, 1964).

5. P. P. Luff and M. White, Thin Solid Films, **6,** 175 (1970).

6. M. White and P. P. Luff, U.K. Patent Appl. 393/69 (1969).

7. G. N. Jackson, Thin Solid Films, **5,** 209 (1970).

8. N. F. Jackson and P. J. Harrop, U.K. Patent No. 29059/67, (1967).

9. K. Lunkwitz, U. Lappan, U. Scheler, J. Fluorine Chemistry, **125** 863 (2004).

10. G. A. Hishmeh, T. L. Barr *et al*., J. Vac. Sci. Technol., **A14,** 1330 (1996).

11. H. Biederman, Y. Osada, Plasma Polymerization Processes (Elsevier, NY 1992).

12. J. M. Tibbitt, Thin Solid Films, **29,** L43 (1975).

13. G. Travot, Crit. Rev. Acad. Sci. Paris, **277,** B313 (1977).

14. N. Marechal and Y. Pauleau, J. Vac. Sci. Technol., A **10,** 477 (1992).

15. I. Sugimoto and S. Miyake, Thin Solid Films, **158**, 51 (1988).

16. T. Wydeven, M. Golub, N. R. Lerner, J. Appl. Polym. Sci., **37,** 3343 (1989).

17. H. Biederman, Vacuum, **59,** 594 (2000).

18. D. J. Morrison, T. Robertson, Thin Solid Films, **15,** 87 (1973).

19. R. Harrop, P. J. Harrop, Thin Solid Films, **3,** 109 (1969).

20. H. Biederman, S. M. Ojha, L. Holland, Thin Solid Films, **41,** 329 (1977).

21. H. W. Lehmann, K. Frick, *et al*., Thin Solid Films, **52,** 231 (1978).

22. Y. Yamada, K Tanaka, K.Saito, Surf Coat Technol., **43/44,** 618 (1990).

23. H. Biederman, *et al*., J. Non-Cryst Solids, **218,** 44 (1997).

24. H. Biederman, J. Jecek, *et al*. In: Schauer F. (ed). 3rd Conf. Proc. Phys. Chem. Molec. Syst., Brno, (1998).

25. S. Pedram, H. R. Mortaheb, *et al* Plasma Chem Plasma Process, **19** (2016).

26. Y. Zhang, G.H. Yang, E.T. Kang *et al*., Langmuir, **18,** 6373 (2002).

27. V. Stelmashuk, H. Biederman, J. Zemek, M. Trchova, Vaccum, **77,** 131 (2005).

28. M. Drabik, O. Polonskyi, O. Kylian *et al*., Plasma Process Polym., **7,** 544 (2010).

29. O. Kylian, M. Drabik, O. Polonskyi *et al*., Thin Solid Films, **519,** 6426 (2011).

30. Y. Suzuki, H. Fu, Y. Abe, M. Kawamura, Vacuum, **87,** 218 (2013).

31. S. Iwamori, N. Hasegawa, A. Uemura *et al*., Vacuum, **84,** 592 (2010).

32. C. Becker, J. Petersen, G. Mertz, *et al*., J. Phys. Chem., C **115,** 10675 (2011).

33. H. J. Biederman, Vac. Sci. Technol., **18,** 1641 (2000).

34. R. N. Wenzel, Ind. Eng. Chem. Res., **28,** 988 (1936).

35. A. B. D. Cassie, S. Baxter, Trans. Faraday Soc., **40**, 546 (1944).

36. H. J. Lee, S. J. Michielsen, Polym. Sci., Part B **45,** 253 (2007).

37. H. C. Barshilia, D. K. Mohan *et al*., Appl. Phys. Lett., **95,** 33116 (2009).

38. L. Gao, T. J. McCarthy, X. Zhang, Langmuir, **25,** 14100 (2009).

39. W. de Wilde, Thin Solid Films, **24,** 101 (1974).

40. P. White, Proc. Chem. Soc., **337** (1961).

41. B. V. Tkachyuk, V. M. Kolotyrkin *Obtaining of thin polymer films from gaseous phase*, (M.: Khimiya, 1977) (Russian).

42. R. W. Christy, J. Applied Phys., **31,** 1680 (1960).

43. M. A. Bruk, E. N. Zhikharev, A. V. Spirin, V. A. Kalnov, High-Molecular Compounds, Series A, **45,** 45 (2003) (Russian)

44. I. A. Volegova, M. A. Bruk, E. N. Zhikharev, *et al*., Vysokomolekularnye Soedineniya. Ser.A Ser.B Ser.C - Kratkie Soobshcheniya, **45,** 390 (2003) (Russian).

45. M. A. Bruk *et al*., Micro- and Nanoelectronics, **2005**, 62600J (2006).

46. K. P. Grytsenko, P. M. Lytvyn, J. Friedrich, *et al*., Materials Science and Engineering, C **27,** 1227 (2007).

47. Y. Gao, L. Wang, D. Zhang, *et al*., Appl. Phys. Lett., **82,** 155 (2003).

48. H. Yasuda, *Plasma Polymerization*, (Academic Press, NY, 1985).

49. K. P. Gritsenko, Ukr. Chem. J., **57,** 782 (1991).

50. K. P. Gritsenko, A. M. Krasovsky, Chem. Rev., **103,** 3607 (2003).

51. M. Moisan, M. R. Wertheimer, Surf. Coat. Technol., **59,** 1 (1993).

52. M. B. Wijesundara, Y. Ji, B. Ni, *et al*., J. Appl. Phys., **88,** 5004 (2000).

53. P. C. Painter, M. M. Coleman, and J. L. Koenig, *The theory of vibrational spectroscopy and its application to polymeric materials* (Wiley, New York, 1982).

54. J. Goodman, J. Polym. Sci., **44,** 551 (1960).

55. A. R. Denaro, P. A. Owends, A. Crawschaw, Eur. polym. J., **4,** 94 (1968).

56. E. M. da Silva , E. C. Miller, El. Chem. Technol., **2,** 147 (1964).

57. J. M. Brown and P. Hofmann (Eds), *Organometallic Bonding and Reactivity. Fundamental Studies,* (Springer-Verlag Berlin Heidelberg, 1999).

58. V. E. Fortov (ed). *Encyclopedia of low-temperature plasma. Introductory volume IV.* (M.: Nauka. 2000) (Russian).

59. K. Tanaka, T. Yamabe, T. Takeuchi, K. Yoshizawa, S. Nishio, J. Appl. Phys., **70,** 5653 (1991).

60. K. Yoshizawa, K. Tanaka, T. Yamabe, J. Chem. Phys., **96,** 5516 (1992).

61. H. Nishide, T. Kaneko, T. Nii, *et al*, J. Am. Chem.Soc., **118,** 1695 (1996).

62. R. Hernandez, *et al*, J. Phys. Chem., **88,** 3333 (1984).

63. M. W. MacKenzie *Advances in Applied Fourier Transform Infrared Spectroscopy* (John Wiley & Sons Ltd, 1988).

64. R. T. Morrison, R. N. Boyd, *Organic Chemistry*, 6th ed., (Rentlee-Hall of India, 2002).

65. C. H. Bartholomew, R. J. Farrauto *Fundamentals of Industrial Catalytic*

Processes, 2nd Edition, (John Wiley and Sons, Hoboken, NJ, 2006).

66. P. Sykes *A Guide book to Mechanism in Organic Chemistry*. (Academic Press,·2005).

67. M. N. Subramanian *Basics of Polymer Chemistry* (River Publishers, 2017).

68. B. N. Gorbunov, Ya. A. Gurvich, I. P. Maslova *Chemistry and technology of polymer materials stabilizers* (M.: Khimiya, 1981). (Russian)

69. V.G. Zadorozhniy, *Investigation of processes of structuring of thin polymer films in vacuum and creation of new technologies on their basis* (D.Sc. Dissertation, ONAFT, 1989).

70. V. A. Roginskiy, *Phenolic antioxidants. Reactivity and efficiency* (M.: Nauka, 1988). (Russian)

71. A. V. Rogachev, "*Vacuum technologies and equipment*". Kharkov: 123 (2003).

72. A. A. Rogachev, 5th Belarussian Seminar on Scanning Probe Microscopy: 41 (2002)

73. A. A. Rogachev, J. Appl. Chem., **77,** 285 (2004) (Russian)

74. V. P. Kazachenko, A. V. Rogachev, High Energy Chemistry, **33,** 270 (1999). (Russian)

75. M.A. Yarmolenko, Universities News. Physics, **51,** 124 (2008). (Russian)

76. H. S. Ahn, S. A. Chizhik, A. M. Dubravin, *et al*, Wear, **249,** 617 (2001).

77. M. A. Bruk, S. A. Pavlov *Polymerization on the surface of solids* (M.: Khimiya,1990). (Russian)

78. T. T. Kodas, P. B. Comit, Ace. Chem. Res., **23,** 188 (1990).

79. Y. Gnanou, M. Fontanille *Organic and Physical Chemistry of Polymers*, (John Wiley & Sons, Inc, 2008).

80. A. A. Rogachev, J. Appl. Chem., **79,** 1207 (2006). (Russian)

81. A. V. Rogachev, M. A. Yarmolenko, A. A. Rogachev, Proc. National Academy of Sciences of Belarus. Chemical Sciences **4** 38 (2005). (Russian)

82. M. White, Thin Solid Films, **118,** 157 (1973).

83. U.S. Patent. No. 3322565 (1967.

84. C. A. Hogarth and S. Golestanian, Intern. J. of Electronics, **77**, 351 (1994).

85. S. Fedosov, V. Zadorozhny, A. Sergeeva, Proceedings of International Symposium on Electrets; Berlin, 272 (1992).

86. S. Iwamori, Y. Yamada, Y. Ono, and K. Ikeda, in *Adhesion Aspects of*

Thin Films, ed. K. L. Mittal (VSP, Utrecht), **3**, 21 (2007).

87. Y. Ohnishi, R. Kita, *et al*, Jap. J. Appl. Phys., **55**, 02BB04 1 (2016).

88. S. Iwamori and K. Noda, Mater. Lett., **66,** 349 (2012).

89. R. Jędrzejewski, *et al*, Polymer, **62,** 743 (2017).

90. V. Chandra S. S. Manoharan, Applied Surface Science, **254,** 4063 (2008).

91. R. Henda, G. Wilson, J. Gray-Munro, *et al*, Thin Solid Films, **520,** 1885 (2012).

92. A. Rudawska, E. Jacniacka, Intern. J. Adhesion & Adhesives, **29,** 451. (2009).

93. V. Matias, *et al* (eds.), *Frontiers in Superconducting Materials*—New Materials and Applications, Mat. Res. Soc. Symp. Proc. EXS-3, EE1.8.1. (2004).

94. A. Goyal (Ed.) *Second-Generation HTS Conductors*, (Springer NY, 2005).

95. S. Wang, J. Li, J. Suo, T. Luo, Appl. Surf. Sci., **256,** 2293 (2010).

96. Y. Zhang, G.H. Yang, E.T. Kang, *et al*, Surf. Interface Anal., **34,** 10 (2002).

97. H. Usui, Thin Solid Films, **365,** 22 (2000).

98. H. Usui, H. Koshikawa, IEICE Transactions on Electronics, **E81,** 1083 (1998).

99. J. L. He, W. Z. Li, *et al*, Nucl. Instr. Meth. Phys. Res., B **135,** 512 (1998).

100. R. Schwodiauer, J. Heitz, E. Arenholz, *et al*, Journal of Polymer Science: Part B: Polymer Physics, **37,** 2115 (1999)

101. D. Bauerle, *Laser Processing and Chemistry*; (Springer: Berlin, 1996).

102. G. B. Blanchet, C. R. Fincher Jr. C. L. Jackson *et al*, Science, **262,** 719 (1993).

103. M. G. Norton, W. Jiang, J. T. Dickinson, Appl Surf Sci, **96,** 617 (1996).

104. Y. Hetzler, E. Kay, J Appl. Phys., 49, 5617 (1978)

105. S. T. Li, E. Arenholz, H. Heitz, Appl. Surf .Sci., **125,** 17 (1998)

106. R. A. Alawajji, G. K. Kannarpady, A. S. Biris Applied Surface Science **444**, 208 (2018).

107. H. Y. Kwong, M. H. Wong, Y. *et al* Applied Surface Science, **253,** 8841 (2007).

108. W. A. Daoud, J. H. Xin, Y. H. Zhang, C. L. Mak, Thin Solid Films, **515,** 835 (2006).

109. T. Smausz, B. Hopp and N. Kresz, J. Phys. D: Appl. Phys., **35,** 1859

(2002).

110. G. B. Blanchet and S. l. Shah, Appl. Phys. Lett., **62**, 1026 (1993).

111. M. A. Karnath, Q. Sheng, A. J. White, S. Muftu, Tribology Trans., **54**, 36 (2011).

112. S. J. Limb, C. B. Labelle, K. K. Gleason, Appl. Phys. Lett., **68,** 2810 (1996).

113. K. K. S. Lau, J. A. Caulfield, K. K. Gleason, Chem. Mater., **12,** 3032 (2000).

114. Limb, S. J. *et al*, Plasmas and Polymers, **4,** 21 (1999).

115. S. Schröder, T. Strunskus, S. Rehders, *et al*, Scientific Reports, **9,** 2237 (2019).

116. H. G. P. Lewis, J. A. Caulfield and K. K. Gleason, Langmuir, **17,** 7652 (2001).

117. K. K. S. Lau, S. K. Murthy, H. G. P. Lewis, J. Fluor. Chem., **122,** 93 (2003).

118. H. G. P. Lewis, *et al*, Thin Solid Films, **517,** 3551 (2009).

119. A. M. Coclite, *et al*., Adv. Mater., **25,** 5392 (2013).

120. D. W. Smith, S. T. Iacono, *S. S. Iyer Handbook of Fluoropolymer Science and Technology*, (Wiley, 2014).

121. R. E. Florin, M. S. Parker, L.A. Wall, J. Res. Nat. Bur. Stand. A. Phys. and Chem., **70A,** 115 (1966)

122. A. Charlesby, *Atomic Radiation and Polymers, International Series of Monographs on Radiation Effects in Materials*, (Pergamon Press, 1960).

123. P. J. Ozawa, IEEE Transactions PMP, **44,** 2848 (1969)

124. M. Dole, *The Radiation Chemistry of Macromolecules*, (Academic Press, 2013).

125. U.S. Patent No. 2932591, C23C 35/00 (1956).

126. U.S. Patent No. 3068510, C23C 35/04 (1959).

127. U.S. Patent No. 3309221, HO3 K3/53 (1967).

128. S. Schiller, U. Heisig, S. Panzer *Electron Beam Technology*, (Wiley, 1995).

129. D. S. Karpuzov *Vacuum Electron and Ion Technologies*, (Nova Science Publishers, Inc. 1996).

130. I. L. Roikh, L. N. Koltunova, S. N. *Fedosov Deposition of Protective Coatings in Vacuum* (M.: Mashinostroenie, 1976). (Russian)

131. E. C. Moly, I. Litton Intern. Conf. on Electron and Ion Beam Science and Technologes, No 14, 133 (1963).

132. T. Makabe, Z. L. Petrovic, *Plasma Electronics: Applications in Microelectronic Device Fabrication*, 2nd Edition, (CRC Press, 2016).

133. H. L. L. van Paasen, E. C. Moly, R Allen, Bull. Am. Phys., **7,** 69 (1962).

134. Yu. A. Ilyin, V. D. Khomichev Electronic Engineering. Ser. 8 "Radio components", **1** 29 (1967) (Russian)

135. H. Ibach, *Electron Spectroscopy for Surface Analysis*, (Springer Berlin Heidelberg, 2012).

136. A. Fridman, *Electric Discharges in Plasma Chemistry*, Ch. 4 in "*Plasma Chemistry*", (Cambridge University Press, 157-258 2008).

137. M. I. Kushner, J. Appl. Phys., **4,** 212 (1982).

138. U.S. Patent No. 3462335, HO3 K3/53 (1969).

139. Patent of France No. 492598, G0IL 27/16 (1967).

140. Patent of France No. 2307838, R0I 3128 (1976).

141. Japan patent No.22108, R0I 5/20 (1978).

142. UK Patent No. 890466, C08 B15/06 (1962).

143. C. Yuan, A. A. Kudryavtsev and V. I. Demidov *Introduction to the Kinetics of Glow Discharges,* (Morgan & Claypool Publishers 2018).

144. B. V. Tkachuk, V. V. Butin, V. M. Kolotyrkin, N. P. Smetankina, Visokomolekulyarnie soedinebiya, Ser., A **9,** 2018 (1967) (Russian)

145. UK patent No. 890466, C08 B15/06 (1962).

146. H. Lobo, J. V. Bonilla, *Handbook of Plastics Analysis*, (CRC Press, 2003).

147. J. M. G. Cowie, V. Arrighi, *Polymers: Chemistry and Physics of Modern Materials*, 3rd Edition, (RC Press, 2008).

148. B. Wunderlich, *Macromolecular Physics, V1*, (Elsevier, 2012).

149. H. Frey, H. R. Khan *Handbook of Thin Film Technology*, (Springer-Verlag Berlin Heidelberg, 2015).

150. M. V. Russo, *Advances in Macromolecules: Perspectives and Applications* (Springer-Verlag Berlin Heidelberg, 2010).

151. K. Matyjaszewski, T. P. Davis, *Handbook of Radical Polymerization* (John Wiley & Sons: Hoboken, 2002).

152. T. T. Tson, *Atom-Probe Field Ion Microscopy* (Cambridge University Press, 2005).

153. C. L. Beyler, M. M. Hirschler, *Thermal Decomposition of Polymers. SFPE Handbook*, Section 1, Chapter 7, 111-131 (2002).

154. L. Mandelkern, *An Introduction to Macromolecules* (Springer-Verlag, New York, 2012)

155. V. P. Privalko, V. V. Novikov, *The Science of Heterogeneous Polymers: Structure and Thermophysical Properties* (Wiley, 1995).

156. M. Hakkarainen (ed.), *Mass Spectrometry of Polymers – New Techniques*, Series: *Advances in Polymer Science*, **248,** (Springer Berlin Heidelberg, 2012).

157. V. Chechik, *Electron Paramagnetic Resonance*, Series: Oxford *Chemistry Primers*, (Oxford University Press, 2016).

158. S. A. Dikanov, Y. Tsvetkov, *Electron Spin Echo Envelope Modulation Spectroscopy* (CRC Press, 1992).

159. Yu. A. Ilyin, V. D. Khomichev, Electronic Engineering. Ser. Radio components, **1,** 11 (1967).

160. V. G. Zadorozhniy, A. E. Sergeeva, J. Nano- Electron. Phys., **10,** 05010 (2018).

161. T. Willliams, M. W. T. Hayes, Nature, **209,** 769 (1966).

162. P. Singh, R. Kumar, *Radiation Physics and Chemistry of Polymeric Materials*, in "*Radiation Effects in Polymeric Materials*" (Springer 35-68, 2019).

163. S. M. Haque, J. A. A. Rey *et al*, *Electrical Properties of Different Polymeric Materials and their Applications*, in "Properties and Applications of Polymer Dielectrics", Du Boxue (ed.), 41-63 (2017).

164. A. G. Cockbain, P. J. Harrop, Brit. J. Appl. Phys., **1,** 1109 (1968).

165. R. Simha, R. F. Boyer, J Chem Phys., **37,** 1003 (1962).

166. G. Calleja, A. Jourdan, B. Ameduri, J.-P. Habas, European Polymer Journal, **49**, 2214 (2013).

167. V. Adamec, Zeitscrift fur Angewandte Physik, **29**, 291 (1970).